Development of a microfluidic atmospheric - pressure plasma reactor for water treatment

L Patinglag

PhD 2019

Development of a microfluidic atmospheric - pressure plasma reactor for water treatment

LAILA PATINGLAG

A thesis submitted in partial fulfilment of the requirements of Manchester Metropolitan University for the degree of
Doctor of Philosophy

Faculty of Science and Engineering
Manchester Metropolitan University
in collaboration with the
School of Mathematics and Physical Sciences
University of Hull, UK

2019

Abstract

Conventional water treatment methodologies are often incapable of eliminating chemical and biological pollutants from water sources leaving residual contaminants in treated water. These contaminants are of growing concern due to their potential for adverse health effects from chronic exposure. Non-thermal plasma generated in a dielectric barrier microfluidic plasma reactor, operated at atmospheric pressure, was studied for its potential to treat organic contaminants and pathogenic microorganisms in water. In this thesis, non-thermal plasma generated in a microfluidic reactor was investigated for the degradation of contaminants in water. The overall aim of this thesis is to optimize treatment efficiency of an organic contaminant, i.e. methylene blue, and biological contaminants, i.e. *E. coli* and *P. aeruginosa,* in non-thermal plasma by investigating the key process parameters. The microfluidic device in this work incorporated a dielectric barrier discharge generated in a continuous gas flow stream of a two-phase annular flow regime generated in the microchannel of the device. Using air as the carrier gas, low concentrations of long-lived chemicals generated in plasma such as nitrates were detected in plasma treated water. The relative degradation rates of MB were influenced by the residence time of the sample solution in the discharge zone, type of gas applied, channel depth and flow rate. Increasing the residence time inside the plasma region led to higher levels of degradation. Using a 100 μm deep device, oxygen was found to be the most effective gas for promoting MB degradation and by reducing the channel depth to 50 μm, the highest results were obtained, achieving more than a 97% level of degradation with air as the applied gas at a flow rate of 4 ml/min. Effective disinfection of water was achieved using air as the carrier gas. Full inactivation of both bacteria (10^8 CFU/mL maximum number of each bacteria treated) as monocultures and mixed cultures in water was achieved after 5 seconds of residence time in the plasma zone. The microfluidic system presented here demonstrates proof–of-concept that plasma technology can be utilised as an advanced oxidation process for water treatment, with the potential to achieve total mineralization of organics and hence eliminate water treatment consumables such as filters and disinfectants. A summary of the findings of this work is presented in Chapter 7 including further works.

Table of Contents

List of Figures

List of Tables

Declaration

I hereby declare that the contents of this thesis are original and has not been submitted in whole or in part for consideration for any other degree or academic award in any University. To the best of my knowledge, this thesis contains no material written or distributed previously by any other parties, apart from where specifically stated.

List of publication and presentations

Publication

- Patinglag, L., Sawtell, D., Iles, A., Melling, L.M. and Shaw, K.J., 2019. A microfluidic atmospheric-pressure plasma reactor for water treatment. Plasma Chemistry and Plasma Processing, pp.1-15.

Oral and Poster Presentation

- An evaluation of a microfluidic plasma reactor for water treatment., Laila Patinglag, David Sawtell, Alex Iles, Louise Melling, and Kirsty Shaw, 1st UK Microfluidics for Analytical Chemistry Conference, 2018, University of Southampton, UK.

- An evaluation of a microfluidic plasma reactor for water treatment., Laila Patinglag, David Sawtell, Alex Iles, Louise Melling, and Kirsty Shaw, Man Met PGR Conference (Provoking Discourse), 2018, Manchester Metropolitan University, UK.

- Degradation of methylene blue using non-thermal plasma generated in a microfluidic reactor., Laila Patinglag, David Sawtell, Alex Iles, Louise Melling, and Kirsty Shaw, 11th International symposium on non-thermal/thermal plasma pollution control technology & sustainable energy, 2018, University of Padova, Italy.

- Microfluidic atmospheric-pressure plasma reactor for water treatment., Laila Patinglag, David Sawtell, Alex Iles, Louise Melling, and Kirsty Shaw, 22nd International Conference on Miniaturized Systems for Chemistry and Life Sciences, 2018, Kaohsiung, Taiwan

- Microfluidic atmospheric-pressure plasma reactor for water treatment and disinfection., Laila Patinglag, David Sawtell, Alex Iles, Louise Melling, Katherine Whitehead and Kirsty Shaw, 2019, STEM for BRITAIN, Westminster, UK

Acknowledgement

This thesis would not have been possible without the help, support and guidance of many people who in one way or another have extended their assistance in the preparation and completion of this study.

First and foremost, I would like to thank Father God in Heaven who has made it possible to complete this work.

I would like to thank my supervisors Dr Kirsty Shaw, Dr David Sawtell, Dr Louise Melling and Dr Kathryn Whitehead for all the support, encouragement and understanding throughout my PhD. Their kindness and patient teaching contributed to a rewarding experience by giving me intellectual freedom in my work, supporting my attendance at various conferences, engaging me in new ideas and demanding a high quality of work in all my endeavours. I also would like to thank my supervisor Dr Alex Iles from the Lab-on-a-chip Fabrication Facility at the University of Hull for his support, availability and constructive suggestions, which were determinant for the accomplishment of this work.

Special thanks go to colleagues and lab technicians from the Department of Chemistry, Engineering, Microbiology and Environmental Science, Manchester Metropolitan University for their technical support, laboratory assistance and providing a pleasurable and friendly working environment.

Thanks to the Faculty of Science and Engineering, Manchester Metropolitan University for the funding of this project.

Special thanks to my friends for the endless distractions that helped to keep me sane for the duration of my PhD.

Special thanks to Hope Leeds Community Church for their constant care, encouragement and support.

Finally, I would like to thank my Dad, Mum, brother and sister for their unconditional support and love, and without would I not have come this far.

List of abbreviations

AC	Alternating Current
AOP	Advanced Oxidation Processes
AP-DBD	Atmospheric Pressure Dielectric Barrier Discharge
ARB	Antibiotic Resistant Bacteria
CAD	Computer-Aided Design
CFU	Colony Forming Units
CT	Concentration x Contact Time
DBD	Dielectric Barrier Discharge
DBP	Disinfection By-Product
DC	Direct Current
DNA	Deoxyribonucleic acid
DoH	Department of Health
DWI	Drinking Water Inspectorate
E/N	Electric field to neutral particles density ratio
EPS	Extracellular Polymeric Substances
EurEau	European Federation of National Associations of Water & Waste Water Services
HCAI	Health-care Associated Infection
HPSC	Health Protection Surveillance Centre
HV	High Voltage
IC	Ion Chromatography
LC/MS	Liquid Chromatography-Mass Spectroscopy
LTE	Local Thermodynamic Equilibrium
MB	Methylene Blue
MGW	Molecular Grade Water
MIC	Minimum inhibitory concentrations
MP	Micropollutant
MPR	Microfluidic Plasma Reactor
NICU	Neonatal Intensive Care Unit
NHS	National Health Service
PAH	Polycyclic Aromatic Hydrocarbon
PAW	Plasma-Activated Water
PBS	Phosphate Buffered Saline
PCR	Polymerase Chain Reaction
PDMS	Polydimethylsiloxane
PMMA	Poly (methyl methacrylate)
PTFE	Polytetrafluoroethylene
PWT	Plasma-based Water Treatment
RNS	Reactive Nitrogen Species
ROS	Reactive Oxygen Species
SCV	Small Colony Variant
SEM	Scanning Electron Microscope
TBE	Tris/Borate/EDTA
TCU	True Colour Unit
THM	Trihalomethane
UV	Ultraviolet
VBNC	Viable but nonculturable
WHO	World Health Organization

List of nomenclatures and symbols

k	Rate constant
η	Degradation efficiency
ε_r	Dielectric constant
c	Concentration
Cl	Chlorine
ClO_2	Chlorine dioxide
e^-_{aq}	Solvated electron
HNO_3	Nitric acid
HF	Hydrofluoric acid
H	Hydrogen
HO_2^-	Hydroperoxyl
H_2O_2	Hydrogen peroxide
I	Input current
k_H	Henry's law constant
N_2	Nitrogen
NH_3	Ammonia
NH_4^+	Ammonium
NO_2^-	Nitrite
NO_3^-	Nitrate
O	Atomic oxygen
$O_2^{\cdot-}$	Superoxide
O_3	Ozone
P	Partial pressure
P_t	Deposited power
SO_2^-	Sulphate radicals
t	Time
T_e	Temperature of electrons
T_h	Temperature of heavy particles
T_g	Temperature of gas
V	Applied voltage

Chapter 1 Introduction

1.1 Overview

This research focuses on investigating an atmospheric pressure dielectric barrier discharge (AP-DBD) generated in a miniaturized plasma reactor and its potential application for water treatment. Understanding and controlling the behaviour of fluids and AP-DBD under these conditions will aid in the development of reactors using plasma to treat contaminated water. The behaviour of the AP-DBD generated in a closed system miniaturized reactor (microfluidic reactor) and the chemical reactions initiated were investigated for treatment of water contaminated with organic chemicals or microorganisms. The main focus was determining the factors affecting the AP-DBD treatment processes using a miniature plasma reactor including voltage, barrier thickness, channel length, and residence time.

1.2 Research Motivation

Water is necessary for life, for the Earth's population and the planet's survival; the human body is made up of 60% water and nearly 70% of the planet's surface is covered with water, mainly saltwater and only 2.5% is freshwater. Of this, less than 1% of freshwater sources are available to feed the whole planet's population, nearly 7.8 billion as of 2019. This water is consumptively used for industry, agriculture and domestic purposes; the rest is inaccessible, either frozen as snow and ice or stored as ground water (Gleick and Schneider, 1996). Human activities lead to a depletion of water quality by leaching various synthetic and naturally occurring contaminants into freshwater sources, which can be increasingly aggravated in the future as populations grow, climate change and global sea level rise. Without action, this is expected to cause an imbalance of water demand and availability. Most dialogues about this topic have focussed on low-income and developing countries suffering the environmental, health, social and economic ramifications of depleting water quality. However, recent reports have shown that even wealthier countries suffer contamination and face water crisis, with new stricter requirements for drinking water reducing the availability of clean water supplies. In the UK, several reports in recent years have identified microbial and chemical contaminants in drinking water, linked to treatment failure and resulting in significant adverse health effects (Gray, 2008; Inspectorate, 2015; DWI, 2017). A recent survey has shown that one in two people in the UK

are concerned about contaminants in their tap drinking water and over 47% take additional precautions by buying bottled water or using a filter system. This is likely to be a consequence of water contamination reports (Danny et al., 2018).

Traces of contamination from various sources, chemical or biological, are still a problem if not treated efficiently by conventional physical, chemical or biological techniques and may require expensive methods to attain safe contaminant free water. The presence of these contaminants in treated water is a cause of growing concern of environmental consequences and potential adverse health effects from chronic exposure, prompting further investigation of novel methodologies to treat water sources effectively. Electrical discharge plasma technology has been widely investigated as a promising solution for water remediation driven by advanced oxidation process (AOP). Cold atmospheric plasma generated at room temperature and atmospheric pressure has produced encouraging results for disinfection and removal of contaminants in water through *in situ* generation of highly reactive species and physical processes (Anpilov et al., 2001; Foster, 2017; Miklos et al., 2018). In addition, the spectrum of contaminants for treatment can be extended to other pollutants and the efficiency of treatments improved by incorporating mediators such as catalysts (Lukes et al., 2012; Reddy et al., 2014). The ability to mineralize organic pollutants via plasma is an attractive feature for a fast and clean process with no toxic by-products formed and chemicals used during the process while simplifying the management of the process and reducing the toxicity of waste products (Sato et al., 2005). Generation of plasma at atmospheric pressure and room temperature reduces the operational costs required by other processes such as high temperatures and vacuum pumps. The application of plasma can be integrally modular and offers an alternative source for the chemical precursors and consumables operated in conventional AOPs and water treatment methods. Plasma-based Water Treatment (PWT) is predicted to be efficient and overcome current operational expenses since the treatment efficiency observed in plasma requires the synergetic combination of several conventional methods, AOPs and consumables to initiate the same reactions simultaneously for water treatment.

Review papers have studied various reactor geometries to generate plasma in contact with water and investigate the chemical and physical processes involved that are useful for its

application (Locke et al., 2006; Bruggeman and Leys, 2009; Vanraes et al., 2016; Malik, 2010). However, it has proven difficult to implement PWT at the macro-scale. This was mainly due to mass transfer limitations of plasma species in the gas phase into the liquid bulk at the gas-liquid interface. This leads to an unfavourable energy yield, the amount of pollutant degraded per kilowatt-hour (Locke et al., 2006; Malik, 2010; Jiang et al., 2014).

Recently, a number of studies on miniaturised reactors were investigated for plasma production in a continuous flowing system. Olabanji *et al* investigated the behaviour of plasma generated in a continuous flow microreactor (Olabanji and Bradley, 2011), Stauss *et al* investigated a continuous flow microreactor using plasma to synthesise diamondoids (Stauss et al., 2014). In both studies, the microreactors operated with AP-DBD systems, generating non-thermal plasma in a continuous gas flow. However, such reactors have yet to be further expanded as dual phase plasma-liquid microfluidic systems for studies in PWT.

In this thesis, a miniaturised AP-DBD reactor was adapted and designed to operate a continuous liquid-gas flow and investigate the efficiency of a miniaturised AP-DBD reactor to degrade organic contaminants and to reduce the viability of opportunistic pathogens in water, by exploiting the benefits of microfluidics.

1.3 Aim and objectives

The aim of this project is to develop a novel microfluidic plasma reactor (MPR) to degrade organic contaminants and reduce the viability of pathogens in water sources by using atmospheric pressure plasma. Production of plasma in proximity to water was investigated to improve the aforementioned limitations and enhance treatment efficiency with the purpose of developing a potential application for continuous in-line water feed systems. It is predicted that the microfluidic plasma reactor would act as a proof-of concept for the inclusion of plasma technology into water systems, replacing current water treatment consumables such as filters.

For the initial phase, an organic pollutant in the form of methylene blue (MB), an organic dye, was selected as a model compound to test the treatment efficiency using the AP-DBD reactor. Influence of applied voltage, residence time, liquid flow rates and gas composition with degradation of MB were investigated and optimised. Further optimisation of the physical parameters, dielectric barrier thickness and length of the serpentine channel, were

investigated to improve the efficiency of the discharge formed in the MPR. Optimised results were carried forward to chosen pathogens often detected in treated water; to test its potential to reduce the viability of *E.coli* and *P. aeruginosa* implicated in outbreaks of waterborne health-care associated infections (HCAIs). The results obtained were used to test the potential of an MPR to treat water in a continuous flowing system.

1.4 Structure of the thesis

This thesis starts with a literature review in **Chapter 2**, introducing the problems with conventional water treatment processes and considers the advantages of AOPs, specifically the significance of plasma technology, as a prospective remedy to current water treatment problems. The fundamental aspects of plasma chemistry in water and microfluidics are discussed. **Chapter 3** introduces the experimental set-up, the preparation of samples, analysis methods and calculations that were used in this study. **Chapter 4** presents the investigation of the influence of process parameters such as residence time, liquid flow rate, gas flow rate, reactor design and plasma properties on the ionic composition of water samples. **Chapter 5** then proceeds to investigate the degradation of MB and formation of possible products formed after plasma treatment. **Chapter 6** reports the investigation of applying the optimized parameters from Chapters 3 and 4 on the anti-microbial activity of plasma generated in the MPR with selected samples, i.e. antibiotic resistant *E. coli* and *P. aeruginosa*. **Chapter 7** presents the conclusions from results obtained from the investigations studied in this thesis, including future work.

Chapter 2 Literature review

This chapter begins with a general overview of water remediation by conventional water treatment processes and reviews the problems encountered, which emphasise the growing need for advanced water treatment processes. This is followed by an overview of the development of innovative advanced oxidation processes by plasma technology from several existing plasma reactor designs, leading to the introduction of a new plasma reactor design. An introduction and overview of the importance of microfluidics along with emerging plasma technology for water treatment is presented.

2.1 Conventional Water Treatment

With contaminants present in various forms in wastewater or water from source catchments, a single method of treatment is often inadequate to remove and process every contaminant (Hofman-Caris and Hofman, 2017). For example, the process of filtration is a common form of physical treatment that removes contaminants bigger than the perforation of the filter, yet contaminants of smaller size or those dissolved in water remain untreated. Thus, treating water to provide safe and clean water for consumption has relied mostly on the application of a multi-barrier water treatment approach, letting water flow through several stages and forms of treatment (Jackson et al., 2001; Dore, 2015). The barriers were selected and set-up to ensure that the removal capability of each step in the treatment process was maximized, in terms of removing contaminants that passed through untreated by preceding barriers, until drinking water quality is achieved. The treatment system occurs in serial steps and includes several conventional water treatment methods (Table 2.1). Each barrier was identified along with their limitations, such as treatment efficiency and risks of contaminants passing through the barrier untreated. Additional barriers to improve such limitations provide the support required to allow continuous operation in times of decline in performance of one or more barriers. In the event of failure of one or more of the barriers, the subsequent barriers can compensate thus limiting the possibility of contaminants left untreated.

Table 2.1: Common stages and examples of conventional water treatment methods and their effects. Adapted from (Vanraes, 2016).

Stages	Methods	Effects	Examples
1^0 treatment	Coarse screening, mechanical/ physico-chemical methods	Removal of large debris Settling of suspended solids and adsorbed pollutants Evaporation of volatile substances pH adjustment	Filtration Coagulation Flocculation Sedimentation
2^0 treatment	Biological treatment	Biodegradation of organic compounds Biological nutrient removal (e.g. nitrogen, phosphorous)	Aerated lagoons Activated sludge
3^0 treatment	Water polishing, chemical treatment	Removal of particulate material Sedimentation of non-degraded and degraded suspended particles Oxidation of compounds Photolysis of organic pollutants Sterilization	Distillation Chlorination Ultraviolet radiation Ozonation
4^0 treatment	Physico-chemical methods, biological treatment	Metabolic and co-metabolic reaction Vaporisation of volatile components Photolysis or hydrolysis of organic micropollutants	Reverse osmosis Ozonation Volatilization Adsorption Biotransformation Abiotic reaction

The primary treatment involves mainly conventional phase separation techniques, followed by chemical methods in the secondary and tertiary treatment. The quaternary treatment is carried out in response to contaminants of possible health concern that pass through untreated by prior conventional water treatment methods such as waterborne pathogenic microorganisms at low levels of 1 to 10 colony forming units (CFU) per 100 mL or micropollutants (MP), defined as organic contaminants of low levels in ng/L. For pathogenic microorganisms such as *E. coli* strains, regulators state 0 CFU/100 mL in water supplied for consumption (DWI, 2009). However, regulations for MP guidelines are still in the process of evaluation worldwide where political decisions and regulations concerning MP affecting the quality of water are driven by ambiguity and defended by precautionary and preventive principles (Metz and Ingold, 2014). To date, environmental quality standards for some MPs such as nonylphenol, bisphenol-A and diiron have been regulated by the European Parliament through Directive 2008/105/EC but other MPs are not listed (EU, 2008). The limited number of MPs regulated is a matter of concern due to the inability of conventional water treatment

methods to remove many MP compounds. In addition, current routine analytical technologies used in water treatment plants risk current and future MPs being undetected. So far, routine analysis is capable of detecting MPs up to the µg/Lrange, with ongoing studies on improving sensitivity of analytical methods to detect contaminants as low as 1 ng/L. This is based on precautionary principles and estimated risk (Schmidt, 2018). According to Metz *et al*, prohibiting substances or restricting authorization of substances that pose a significant health risk to humans and aquatic life may curb or reduce the presence of MPs in treated water (Metz and Ingold, 2014). Such a precautionary approach is inherent in risk management of contaminants not treated efficiently by water treatment (Hartmann et al., 2018). Hence it is essential to develop effective methods to remove contaminants where suspected adverse effects may arise.

Ideally, fewer barriers in treatment will benefit the total operational cost, reduce the use of chemicals and the associated carbon footprint with water-related energy use. The UK water industry consumes 8100 GWh per annum of energy and directly contributes to an estimated 4 million tonnes of the UK's greenhouse gases (Ainger et al., 2009). In addition, the burden of treating contaminants not treated efficiently by conventional methods have been reflected in drinking water demand and supply costs, which can be recovered through water bills. The choice and cost of additional treatment barriers leads to increased operational expenditure in terms of energy demand and disposal of waste (Jones et al., 2007). According to a report of the EurEau summarizing treatment of MPs in several European countries, additional water treatment leads to an additional financial burden on the population and water treatment facility plants (EurEau, 2019). This includes 10% to 15% increase of total costs for water treatment in Switzerland, 20 to 30% increase of current wastewater charges in Finland, 10 to 35% increase of energy consumption using advanced treatment, i.e. ozone and activated carbon, in Denmark and an average increase of 14% in water bills in Germany. According to Logar *et al*, inclusion of new technology increases operational costs by 30% and 35% for activated carbon and ozonation, respectively, for treatment of MPs not removed efficiently by conventional methods (Logar et al., 2014). Thus, the attention of researchers is focused on viable, robust and resource-efficient methods with performance beyond conventional methods to treat water from source to point-of-use at lower cost, without jeopardizing life and the environment by the treatment itself. Table 2.2 shows a summary of described

disadvantages and issues with conventional water treatment methods such as those described in Table 2.1.

Table 2.2: Examples of challenges facing the water treatment process.

Examples	Description	References
Fouling in water systems	- Biofilm formation acts as a reservoir for subsequent spread of pathogens and microbial leaching in treated water - Influences the taste and odour of treated water - Increased localised pipe corrosion and release of iron particles in water	(Herzberg and Elimelech, 2007; Nguyen et al., 2012; Bagheri and Mirbagheri, 2018)
Water treatment plant residuals	- Toxicity problems, even at low concentration, in treated water (e.g. chlorates and chlorites by-products) - Concentrated levels of co-occurring contaminants (e.g. heavy metals, ions) that require advanced processing and disposal methods - Difficult recovery of added reactants (e.g. homogenous catalyst) during regeneration (e.g. iron in water softener resin bed) - Replacement frequency of water consumables (e.g. filter, adsorbents, regeneration chemicals, ion exchange resins, reverse osmosis membranes)	(Fawell and Nieuwenhuijsen, 2003; WHO, 2004; Ippolito et al., 2011; De Gisi et al., 2016)
Selective removal and further reaction/treatment	- Rising problems of resistant pollutants, i.e. anti-microbial resistant pathogens with conventional disinfectants (e.g. chlorine) - New/emerging MPs and resistant microorganisms - Further reactions of disinfectants with other organic and inorganic compounds in untreated water forming potential toxic substances	(Council and Council, 2006; Rajasulochana and Preethy, 2016; Lood et al., 2017; Krzeminski et al., 2018)

2.2 Water Quality

Water readily dissolves a variety of chemicals and accumulates microorganisms from various sources such as the underground strata and anthropogenic pollution (Table 2.3).

Table 2.3: Sources and examples of water contaminants (Fawell and Nieuwenhuijsen, 2003; Margot et al., 2015).

Major Sources	Contaminants	Examples
Hospital effluents	Biological contaminants (antibiotic resistant bacteria)	Bacteria, viruses, protozoa, parasites
Industrial wastewater Agricultural runoffs Domestic wastewater	Chemical contaminants	Pharmaceuticals, dye, pesticides, heavy metals, industrial chemicals
Underground source leakage (i.e. from soil, oceans)	Physical contaminants	Sediment, suspended organic matter
	Radiological contaminants	Radon, radium, uranium, lead

Ideally, potable water should not contain any of these contaminants capable of causing adverse effects. The adverse effects of many of these contaminants to public health and the environment are known and regulated by their level of risk/hazard. This provides an ideal standard of clean and safe water. In accordance to the Water supply (Water Quality) Regulations of 2018 (England and Wales), water supplied via a consumer's tap must not contain any microorganisms or substances at concentration values that can cause potential danger to human health (Table 2.4) (DWI, 2018).

Table 2.4: The microbiological and chemical parametric values of treated water provided in consumer's taps. Adapted from (DWI, 2018).

Microbiological parameters		
Parameters	Concentration or value (maximum)	Units
Enterococci	0	Number/100 mL
Escherichia coli	0	Number/100 mL
Coliform bacteria	0	Number/100 mL
Chemical Parameters		
Acrylamide	0.10	µg/l

Antimony	5.0	µg/l
Arsenic	10	µg/l
Benzene	1.0	µg/l
Benzo(a)pyrene	0.010	µg/l
Boron	1.0	mg/l
Bromate	10	µg/l
Cadmium	5.0	µg/l
Chromium	50	µg/l
Copper	2.0	mg/l
Cyanide	50	µg/l
1, 2 dichloroethane	3.0	µg/l
Epichlorohydrin	0.10	µg/l
Fluoride	1.5	mg/l
Lead	10	µg/l
Mercury	1.0	µg/l
Nickel	20	µg/l
Nitrate	50	mg/l
Nitrite	0.50	mg/l
Pesticides (Aldrin, Dieldrin, Heptachlor, epoxide,	0.030	µg/l
other pesticides	0.10	µg/l
Pesticides: Total	0.50	µg/l
Polycyclic aromatic hydrocarbons	0.10	µg/l
Selenium	10	µg/l
Tetrachloroethene and Trichloroethene	10	µg/l
Trihalomethanes: Total	100	µg/l
Vinyl chloride	0.50	µg/l

Failing to meet these criteria reduces the quality of water, which generally makes the water unacceptable for consumption and introduces a need for the water to undergo some type of treatment. So far, conventional water treatment processes such as filters and chemical treatments are inadequate for the effective removal of resistant contaminants such as microorganisms that get to re-enter water sources (Sousa et al., 2018; Gogoi et al., 2018). These contaminants can cause undesirable effects even at low concentrations (mg/L to ng/L), leading to adverse ecological impacts and interference with the use of water for domestic, recreational or critical applications due to short- and long-term toxicities (Richardson, 2009; Ratola et al., 2012; Bayen, 2012; Stuart et al., 2012). The public's recognition of water quality and acceptability is derived on the general aesthetic properties such as turbidity, taste, odour, hardness and colour. In general, the aesthetic of water for public satisfaction and perception

of water free from contamination is often associated with colourless, odourless and tasteless qualities. However, water free from aesthetic problems is not necessarily safe for consumption, with contaminants such as pathogenic microorganisms, even at low levels, can lead to devastating consequences for health or even death. In response, environmental and public health concerns continue to increase in parallel with industrial development, climate change and population growth, which are the chief sources of these pollutants (Fawell and Nieuwenhuijsen, 2003; Margot et al., 2015).

With an increasing number of emerging contaminants detected at low levels, lack of epidemiological studies and regulation and the uncertainty of their long-term consequence compromises the confidence of people in the safety and quality of their water supply. Other effects may be indirect, such as health decline and economic constraints caused by increasing morbidity rate, mortality rate and a combination of multiple water treatment process that lead to expensive remediation and cost inflation of safe water (WHO, 2004). Contaminated water sources are already prevalent in developing countries where water treatment process are either inefficient or absent. The World Health Organization (WHO) estimates that diseases sourced from poor quality drinking water supplies and/or scarcity of water treatment infrastructure, cause 4.0 % of deaths and 5.7 % of disability or ill health worldwide, with children and those on a low income bearing more of the burden of outbreaks by waterborne diseases, such as dysentery (WHO, 2012). In addition, poor water quality was not only limited to an impact on health but is now also closely associated with economic and social implications on a country. The World Bank estimated an economic loss of US $9 billion a year in Southeast Asia from poor sanitation that significantly contributed to polluted water sources, an increasing cost of safe water production and environmental losses such as decline in fish populations and a reduction in agricultural growth (Hutton et al., 2008).

2.1.1 Chemical Contaminants

Chemical contaminants in water are mainly the products of waste from natural and anthropogenic sources. In terms of their effect on health and the environment, it is important to destroy contaminants that are resistant to conventional water treatment, resist biodegradation and can accumulate in the environment. The average removal rates of some

of these contaminants by conventional water treatment processes is variable but they are generally low, down to 5% in some cases (Table 2.5). This results in an increased risk of chronic toxicity upon exposure through drinking water and to aquatic life.

Table 2.5: Examples of chemical substances and average removal rates using conventional water treatment methods. Adapted from (Margot et al., 2015).

Substance	Examples (including ingredients)	Average removal rate (%)
Surfactants	Soaps, alkylbenzene sulfonates, alcohol ethoxylates, alcohol ether sulfates, alkane sulfonates	< 95 %
Pharmaceuticals	Analgesic, anti-inflammatory, antibiotics, antihistamines, synthetic metabolites	> 70%
Fragrances	Polycyclic musks galaxolide, tonalide	< 85%
Preservatives,	Parabens	< 95%
Antimicrobials	Triclocarban and triclosan, chloroxylenol	< 95%
Insect repellants	*N,N*-diethyl-*m*-toluamide	62%
UV filter	Oxybenzone, octorylene, octyl-triazone	50 − 95%
Additives	Aspartame, acesulfame, sucralose	90 − 95%
Plasticizer, plastic additive	phthalate, bisphenol	60 − 95%
Anticorrosives	Benzotriazole	20 -30 %
	Benzothiazole	0 - 80%
Synthetic chelating agent	Ethylendiamine tetracetic acid	> 10%
Flame retardants	Brominated flame retardant	~ 90%
	Organophosphorous flame retardant	50 -75%
	Chlorinated paraffins	> 99%
Perfluorinated compound	Perfluorooctane sulfonic acid	< 5%
Biocides and pesticides	Diazinone, diuron , irgarol	< 50%
	Aldrin, diedrin, hexachlorobenzene	<90%
	Triclosan	90 %
Heavy Metals	Zinc, copper, cadmium	> 75%
	Mercury	2-10%
Polycyclic aromatic hydrocarbons	Fluorence, pyrene, naphthalene	< 90%
Volatile organic compound	Benzene, toluene, ethylbenzene, xylene	< 97%
Illicit drugs	Amphetamine	98%
	Cocaine	79%
	Ecstasy	15%
Hormones	Estrone	76%
	Progesterone	97%

17 α-ethinyl estradiol	60%

Around 28 organic and inorganic compounds are required to be monitored by tap water providers (DWI, 2018) (Table 2.4). The limited number of compounds monitored is a matter of concern due to the likelihood of contaminants such as in Table 2.5 passing through treatment processes untreated or undetected. Topics that address the risk-based nature of some emerging contaminants at low concentrations in drinking water, in terms of bioaccumulation and cooperative effects, are currently being studied to establish the limits regarded safe for consumption (Virkutyte et al., 2010; Burkhardt-Holm, 2011; Cizmas et al., 2015; Verlicchi et al., 2017). For example, polycyclic aromatic hydrocarbons (PAHs) found in petroleum-based products such as coal tar are regulated to a collective standard concentration of 0.1 µg/L for all substances (DWI, 2009); some PAHs are known carcinogens and mutagens, hence they are strictly monitored in water intended for consumption (Abdel-Shafy and Mansour, 2016). Some chemicals such as pharmaceuticals in water, which have been linked to toxic biological effects including estrogenicity, genotoxicity and mutagenicity (Elliott et al., 2018), are also routinely monitored for and detected below or above the regulated value of 0.05 µg /L in treated water. So far, studies on the potential health risk of chronic exposure to pharmaceuticals at trace concentrations in drinking water are limited; current observations suggest improbable adverse effect from trace values less than 1000 fold below the clinical active dosage (Benson et al., 2017; Wee and Aris, 2017). However, each pharmaceutical has a different clinical active dosage and thus, the general consensus of 1000 fold may not apply for all pharmaceuticals with low active dosages, such as 0.05 mg for Beclomethasone, against high active dosage pharmaceuticals such as 52 mg for Tamiflu (Watts et al., 2007). In addition, these observations may not apply to children and vulnerable immunocompromised populations (H. Wang et al., 2016; Kamba et al., 2017).

2.1.2 Microbial Contaminants

The most common and widespread health risk linked to treated water is microbial contamination. The importance of clean and uncontaminated water is critically highlighted in various fields, such as the major role it plays in immunocompromised hosts at risk of exposure to waterborne pathogens in settings such as healthcare. Most of these microorganisms are

harmless, but some opportunistic pathogens such as *P. aeruginosa* are extremely virulent, especially among the most vulnerable patients, and can lead to outbreaks of HCAIs (Cristina et al., 2013). In the UK, HCAIs represent an important patient safety challenge and economic burden upon the NHS, with approximately 1,000,000 cases reported annually from acute care hospitals (Hopkins et al., 2011). The burden imposed by HCAIs includes unnecessary deaths, prolonged hospital stays, financial strains for both the health system and family and increased resistance of pathogens to anti-microbial therapy (Plowman et al., 2001; Stone, 2009; Wiegand et al., 2012). Table 2.6 provides examples of microorganisms linked to water-borne HCAIs.

Table 2.6: Examples of waterborne and persistent microorganisms affiliated with HCAIs. Adapted from (Decker and Palmore, 2013).

Microorganism	Example of organism(s)	Examples of reservoir
Legionella	*Legionella pneumophila, Legionella dumoffii*	Showers, ice machines, decorative fountains, humidifiers, plumbing systems, taps, water baths
Gram-negative bacteria	*Pseuodomonas, Stenotrophomonas, Klebsiella spp,*	Therapy pools, tubs, water baths, taps, intravenous lines, invasive devices, sinks, wash basins, aerators, drains
Gram-positive bacteria	*Methicillin-resistant Staphylococcus aureus, Staphylococcus aureus*	Invasive devices, sinks, wash basins, plumbing system
Mycobacteria	*Nontuberculous mycobacteria*	Plumbing systems, invasive devices, taps
Protozoa	*Cyclospora cayetanensis, Cryptosporidium parvum*	Plumbing systems, ice machines, taps, hospital water
Fungi	*Aspergillus, Fusarium, Phialemonium*	Plumbing systems, hospital water, wastewater lines, invasive devices,
Virus	*Norovirus*	Water contaminated by vomit or faeces

The risk of acquiring a water-borne HCAI depends on various factors including susceptibility of the host and infective dose, defined as the number of microorganisms required from exposure

through ingestion to cause an infection. Infective dose varies broadly depending on the type of microorganism, which has been associated with their pathogenicity and virulence (Leggett et al., 2012). Table 2.7 shows the minimal infective dose of various microorganisms of health concern, which have been linked to contaminated drinking water. However, these values are expected to be lower for immunocompromised patients compared to a healthy individual.

Table 2.7: Minimum infective dose of various microorganism. Taken from (Bitton, 2014).

Microorganism	Minimum infective dose (MID)
Salmonella spp.	10^4–10^7
Shigella spp.	10^1–10^2
Escherichia coli	10^6–10^8
Escherichia coli O157:H7	< 100
Vibrio cholerae	10^3
Campylobacter jejuni	about 500
Mycobacterium avium	10^4–10^7 (for mice)
Yersinia enterocolitica	10^6
Giardia lamblia	10^1–10^2 cysts
Cryptosporidium	10^1 cysts
Entamoeba coli	10^1 cysts
Ascaris	1–10 eggs
Hepatitis A virus	1–10 plaque forming unit

In addition to drinking water, water outlets, in particular taps and water supply pipes, are commonly recognized reservoirs for these water-borne pathogens (Decker and Palmore, 2013; Hutchins et al., 2017). This includes sludge and sediments in supply water, storage tanks, water distribution pipes and associated equipment such as different tap components such as valves, pumps and filters. The link between outbreaks with contaminated tap water and water systems for medical devices is well documented. However, it was not until 2013, after the most publicised fatal outbreak in a Northern Ireland Neonatal Intensive Care Unit (NICU) and several further outbreaks reported by paediatric and NICUs UK wide (Simon et al., 2008; Wise, 2012; Walker and Moore, 2015; Kinsey et al., 2017) that the Department of Health (DoH) and Health Protection Surveillance Centre (HPSC) issued guidelines regarding the prevention and control

of HCAIs from water systems (DoH, 2013; HPSC, 2015). Table 2.8 lists the recommended conventional water treatment processes in the healthcare water distribution systems. In such situations, improving the quality of drinking and tap water may reduce HCAI prevalence. Concerning water treatment, continuous disinfection rather than sporadic disinfection, for example with ultraviolet (UV) treatment, is primarily recommended (HSE, 2015).

Table 2.8: Secondary disinfection methods employed to healthcare water distribution systems. Adapted from (HSE, 2015).

Method	Examples	Remark	
		Advantages	Disadvantages
Cleaning	Descaling, deposit removal, water outlet replacement	- Reduces biofilms, chemical and inorganic deposits	- High financial liability from replacement and maintenance
	Chlorine dioxide	- More effective disinfectant than chlorine, greater penetration and removal of biofilms	- Difficult to control, insufficient to prevent contamination, additional disinfection required difficult to control, toxic DBPs produced
	Monochloramines	- Cheaper than chlorination, effective against biofilm formation	- Narrow microbiocidal activity, toxic DBPs
	Copper-silver ionisation	- Effective in controlling bacterial and biofilm formation	- Water parameters must be monitored to avoid going over the regulated value of 2.0 mg/L copper in drinking water
	Electrochemically activated water	- No toxic chemicals required, greater antimicrobial activity, effective removal of biofilms	- high power consumption, electrode corrosion

Systemic Intermittent	Thermal disinfection and shock hyperchlorination	- Effective antimicrobicidal activity	- Recommended short term solution, corrosive, high levels of trihalomethanes (THMs) and DBPs levels
	Silver catalysed hydrogen peroxide	- Effective in removing biofilms	- Recommended short term solution
Focal Continuous	Ultraviolet irradiation	- Inexpensive and effective against a wide range of microorganisms, no residual or little effect on established biofilms	-Inability to penetrate turbid water, ineffective for treatment of chemical contaminants in water
	Ozone	- Effective antimicrobicidal activity	- Expensive, low water solubility, stability and inability to oxidise some organic compounds
Filters	Filter with pore size 0.2 μm	- Easy to connect	- Blocked over time, must be replaced regularly, can cause retrograde contamination, pressure drop across filter
No longer recommended	Continuous chlorination		- Lack efficiency, corrosive effect on pipework, poor penetration into biofilm, chlorine residuals, formation of THMs

Unfortunately, even the presence of trace microbiological contaminants can cause significant financial, morbidity and mortality burdens. Public Health England reported an increase of incidence of *Pseudomonas* bacteraemia in England, Wales, and Northern Ireland per year between 2008 and 2015; the overall rates increased by 4.4% from 6.6 to 6.9 reports per 100,000 population (Public Health England, 2016). In 2015, the highest rates of patients affected were the older age group (more than 74 years) at 54.7 reports for male and 21.9 reports for female, as well as infants (less than 1 year old) at 8.8 for males and 8.7 for females

reports per 100,000 population. These results are expected to increase with the occurrence and spread of anti-microbial resistant pathogens if not treated effectively by current and new water treatment processes in the future.

Most treatment methods, such as filters, rely on preventing the downstream flow of biological contaminants present in water. Filtration fails to inactivate most microorganisms, especially those found in microbial biofilms, which continue to develop in filters, distribution systems, and purification equipment (Sala-Comorera et al., 2016). Biofilms are densely packed microbial communities enclosed in an extracellular polymeric matrix allowing bacterial adhesion to most surfaces, with studies showing their presence in many medical devices, water reservoirs and any surface water comes into contact (Percival et al., 2015). The complex bacterial community in biofilms is responsible for many obstructions in water distribution systems, leakage and downstream contamination that requires replacement of filters, resulting in additional costs and energy for their removal (Herzberg and Elimelech, 2007; Simoes and Simões, 2013; Hutchins et al., 2017). Even when water treatment facilities and equipment are well maintained, water quality can rapidly decline due to biofilm detachment in water distribution systems (Figure 2.1) (Zhang et al., 2018). Biofilm formation can be reduced by residual chlorine in water as a result of treatment and high wall shear stress that limits the deposition rate or thickness of the biofilm. However, such processes are insufficient with detached biofilms, which release microbial contents showing tolerance against antibiotics or disinfection by chlorine in water (Fux et al., 2004; Steed and Falkinham, 2006; Xi et al., 2009).
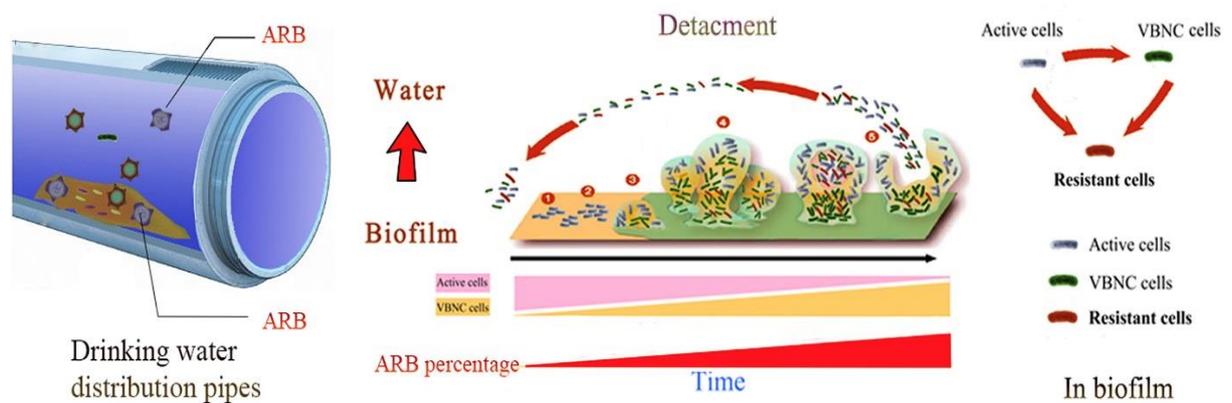
Figure 2.1: Schematic illustration showing biofilm formation in water pipes, formation of antibiotic resistant bacteria (ARB) with viable but nonculturable (VBNC) bacteria in the biofilm over time and detachment, releasing ARB, VBNC bacteria and active cells into treated water. Taken from (Zhang et al., 2018).

2.1.3 By-products of Water Treatment

The purpose of water treatment is to remove microbial and chemical contaminants so improving the quality of water to ensure that it is safe and accepted by the official regulatory body for consumption. Outbreaks associated with microbial contamination have raised concerns about the efficacy of water treatments, with viable microorganisms recovered from potable water distribution systems, maintaining residual disinfectant in the form of free chlorine (hypochlorous acid and hypochlorite ion) or combined chlorine (chloramine) at 0.5 mg/L or less. However, certain treatment processes such as chlorination can also lead to adverse effects due to their potential to react with naturally occurring organic matter and other constituents to form disinfection by-products (DBP) such as chlorinated organic compounds (Minear, 2017; Li and Mitch, 2018). Table 2.9 shows some examples of DBPs identified as potentially toxic.

Table 2.9: Examples of DBPs found in treated water (Minear, 2017).

Disinfectants	Examples of DBPs		
	Inorganic products	Organohalogen products	Non-halogenated products
Chlorine, hypochlorous acid	Chlorate	Trihalomethanes, haloacetic acid, N-chloramines, chlorophenols	Aldehydes, benzene, carboxylic acids, alkanoic acid, cyanoalakanoic acid
Chlorine dioxide	Chlorite, chlorate		
Chloramine	Chlorate, nitrite. Hydrazine, nitrate	Haloacetonitriles, cyanogens, haloketones, chloramino acids	Aldehydes, ketones
Ozone	Chlorate, bromate, iodate, ozonates, epoxides, hypobromous acid	Bromoform, monobromoacetic acid, dibromoacetic acid, cyanogen bromide	Aldehydes, ketoacids, carboxylic acids, ketones

Such chemical methods require a balance to be met between the ability to remove microorganisms and the potential hazards of DBPs produced. This is a major challenge because of the tendency to over use such treatments. Chemical treatment such as chlorine may require

high concentrations for full disinfection, depending on the level of water contamination, but can lead to significant DBP production. In response, additional steps are used after conventional treatment process to remove DBPs and pathogens resistant to normal doses of chlorine. Integrated techniques that involve a combination of different methods that match and improve the process efficiency aspect of conventional methods while averting the negative aspects are often employed. For example, combining ozone as primary disinfection with a secondary disinfection method listed in Table 2.8 such as chloramine to maintain a residual of chloramine in the distribution system can adequately remove microorganisms and reduce formation of DBPs (Robertson and Oda, 1983).

2.3 Advanced Oxidation Processes

Although several advanced water treatment technologies such as reverse osmosis and membrane filtration have been introduced to remove water contaminants from water reservoirs, AOPs are an attractive alternative for driving oxidation of contaminants resistant to conventional treatment methods. Literature reports regarding AOPs have demonstrated the effectiveness of oxidants to remove contaminants and deactivate pathogens in water (Mahamuni and Adewuyi, 2010; Oller et al., 2011; Oturan and Aaron, 2014; Miklos et al., 2018). AOPs, in general, utilize the simultaneous operation of more than one oxidation process and involve the generation and reaction of highly reactive species such as hydroxyl radicals *in situ* to remove contaminants or to inactivate and destroy microorganisms in water (Oturan and Aaron, 2014; Deng and Zhao, 2015). The non-selective nature of these highly reactive oxidative species (Table 2.8), reacting with various forms of contaminants in water upon generation forms the principle of a potential treatment system (Oturan and Aaron, 2014).

Most AOP methods utilize the production of hydroxyl radicals, a powerful non-selective oxidant with a high oxidation potential (Table 2.10). Hydroxyl radicals are capable of inducing cytotoxic effects on microorganisms leading to cell death and can oxidise organic matter to carbon dioxide and water, limiting the production of highly toxic and concentrated residues (Oller et al., 2011). The oxidation potential of hydroxyl radicals is higher than conventional chemicals such as chlorine; oxidation potential reflects the reactivity of the oxidant to induce an oxidation reaction and in this regard, degrade contaminants (Table 2.11). Li *et al* compared hydroxyl

radicals with chlorine and found that hydroxyl radicals disinfected more effectively, with lower CT (concentration X contact time) compared to chlorine, 33.5 and 1674 mg min L^{-1}, respectively (Li et al., 2011). The high reactivity of hydroxyl radicals, attributed to its oxidation potential, offers a potential solution for removing contaminants not treated effectively by conventional treatment process such as chlorine resistant pathogens and without the associated DBPs.

Table 2.10: Examples of AOPs used in water treatment (Oturan and Aaron, 2014; Deng and Zhao, 2015).

AOP	Reactive species formed
UV based AOPs	$\cdot OH$, $O_2^{\cdot-}$, H^+, $\cdot H$,
Ozone based AOPs	$\cdot OH$, HO_2^-, $O_2^{\cdot-}$, $O_3^{\cdot-}$
Fenton and photo-Fenton related AOPs	$\cdot OH$, $HO_2^{\cdot}$, OH^-, H^+
Photocatalysis	$\cdot OH$, H^+, $HO_2^{\cdot}$, e^-, $O_2^{\cdot-}$
Ultrasound and electronic-beam irradiation	$\cdot OH$, $\cdot H$, H_3O^+, e^-
Sulphate radical-based AOPs	$\cdot OH$, SO_4^{2-}, $SO_4^{\cdot-}$

Table 2.11: Oxidation potential of several reactive species used for water treatment. Taken from (Deng and Zhao, 2015).

Oxidant	Oxidation potential (V)
Hydroxyl radical ($\cdot OH$)	2.8 (pH 0) and 1.95 (pH14)
Atomic oxygen (O)	2.42
Ozone (O_3)	2.07
Hydrogen peroxide (H_2O_2)	1.77
Sulphate radicals ($SO^{2-)}$)	2.01
Chlorine dioxide (ClO_2)	1.50
Chlorine (Cl)	1.36

Among conventional methods employed in water treatment described in Chapter 2.1, oxidation through a combination of several AOPs or with other advanced treatment technologies appears as an attractive way of decomposing a wider spectrum of contaminants (Miklos et al., 2018). The most commonly applied and studied combined method includes hydrogen peroxide, ozone, Fenton process and/or UV radiation (Oturan and Aaron, 2014; Miklos et al., 2018). However, these methods require chemical precursors in conjunction with chemical storage and on site availability. With precursors such as catalysts needed to form reactive species or increase degradation rates, implementation at a large scale is still difficult. This requires the development of kinetic models to determine optimal operating conditions

when encountering fluctuating parameters such as pollutant content without leading to new waste problems such as DBPs (Oller et al., 2011).

The need for a cost-effective and efficient method for the production of highly reactive species in water while decreasing reliance on chemical or biological precursors has motivated research on the application of plasma for AOPs in water treatment. In general, high voltages applied in water induce chemical and physical process such as UV radiation and the generation of radical and molecular reactive species in water (Foster, 2017; Miklos et al., 2018).

2.3.1 Plasma

States of matter are generally described as solid, liquid and gas, with plasma widely referred to as the fourth state. Plasma is a gas that has been either partially or fully ionised. Plasma covers a wide range of pressures, temperatures and electron densities. The ionization degree of gases can vary from fully ionised plasma to very low values of $10^{-4} - 10^{-6}$ (partially ionised plasma) (Fridman, 2008).

Plasma either occurs naturally or can be made artificially. Figure 2.2 shows examples of plasma described in terms of electron density and temperature, under various pressure conditions. More than 99% of the universe is made up of plasma in various forms such as interstellar gas, solar corona and nebula while on Earth, plasma naturally appears as lightning and *aurora borealis*. Though naturally occurring plasmas are rare, artificial plasma is extensively used for industrial applications and academic research. The most commonly used method of generating artificial plasma for technological and technical application is by applying thermal energy or an electric field to a neutral gas (Fridman, 2008). Using various operational parameters, i.e. discharge type, pressure, operating temperature, gas species, power supply and magnitude, it is possible to modify the characteristics of plasma such as density, electric field and temperature. The difference in electron density and temperature distinguish artificial plasma into two types, thermal equilibrium plasmas and non-thermal or non-equilibrium 'cold' plasma. Both types are used in various applications such as chemical synthesis (Oehrlein and Hamaguchi, 2018; Peng et al., 2018a), surface coatings (Nikiforov et al., 2016; Chung and

Chang, 2016) and environmental remediation (Bruggeman et al., 2016; Zhang et al., 2017; Liao et al., 2017)
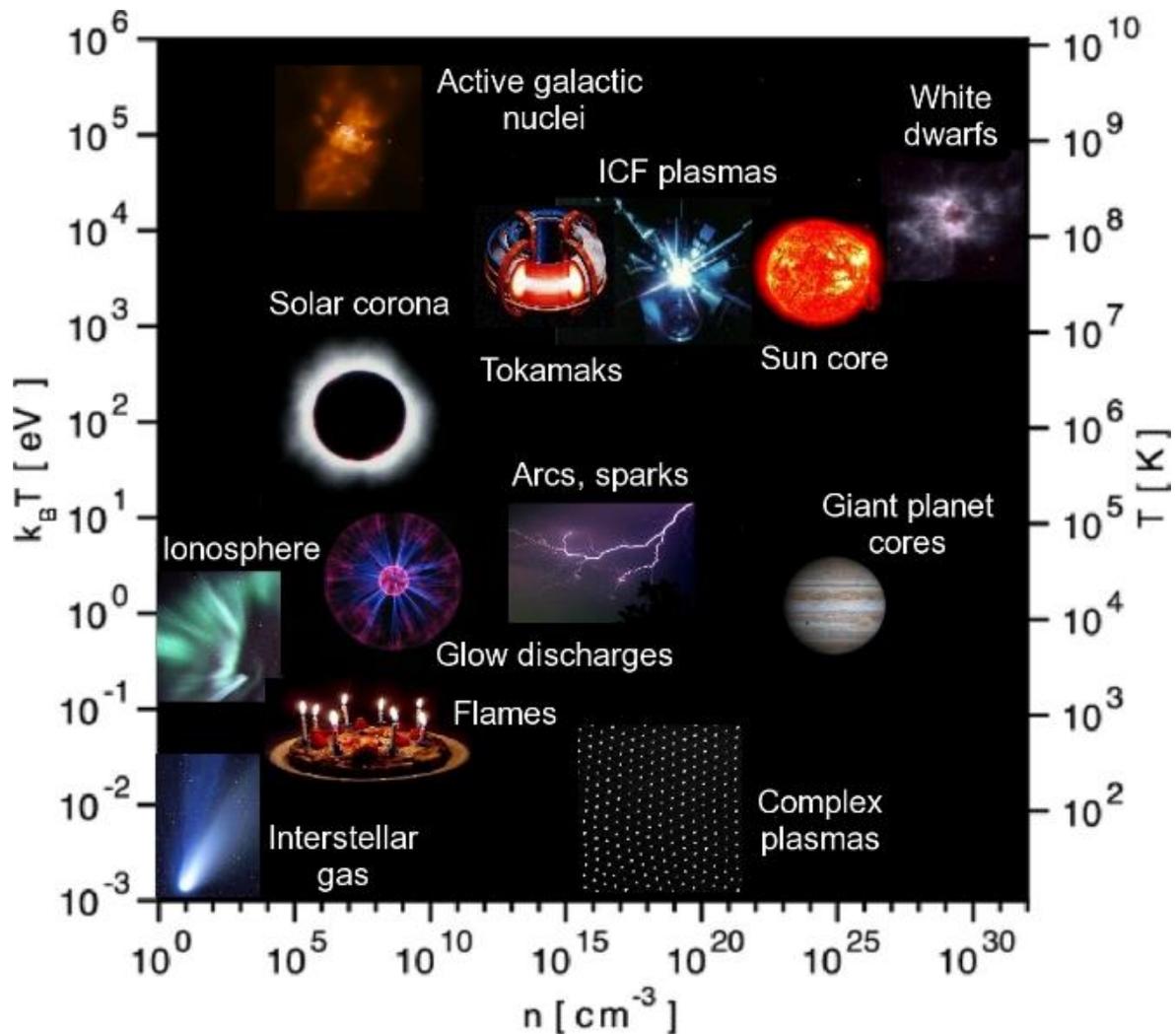
Figure 2.2: Examples of plasma found in nature and in the laboratory with different particle densities (unit: eV), temperature (unit: K) and wavelength (unit: cm^{-3}). Taken from (Donko, 2013).

Thermal plasma, also known as local thermodynamic equilibrium (LTE) plasma is generally operated at atmospheric or high-pressure conditions by means of high power plasma generators. Under these conditions, elastic collisions and high temperatures govern the ionization of the gas where LTE dominate ($T_e = T_h \approx 10\,000$ K); the temperature of electrons (T_e) in the plasma is equal or nearly equal to the heavy particles (atoms, ions and molecules) temperature (T_h). With high energy density ($0.1 - 10$ kW cm^{-3}) and a large number and variety of active species, thermal plasma is widely used in a variety of applications. Examples of thermal plasmas are spark and arc plasmas used for welding, plasma cutting and high temperature applications (Fridman, 2008). Recently, thermal plasmas have been used for

hazardous waste treatment and solutions with chemical and microbial contaminants due to its high energy densities and temperature (Gomez et al., 2009; Yuan et al., 2010). For water treatment, thermal plasma is unsuitable in most cases due to the high ion temperatures involved that will simply boil and evaporate the water.

Non-thermal plasma, commonly known as cold plasma, is non-LTE operated at atmospheric pressure or low-pressure reactors. With non-thermal plasma, the main constituent of energy deposition is transmitted to the electrons instead of the heavy particles. Thus, gas remains 'cold' and the energy of the electrons is in the range of 1 eV to 10 eV (1 x 10^4 to 1 x 10^5 K). The electron temperature is higher than the temperature of heavy particles, which ranges from 300 to 1000 K ($T_e \gg T_h$). Compared to thermal plasma, non-thermal plasma does not require extreme conditions and requires less power to transfer energy to electrons and not the whole gas bulk. The ability of non-thermal plasma to produce reactive species at atmospheric pressure and at ambient temperature is of interest and has led to a wide range of industrial, environmental and commercial applications (Nikiforov et al., 2016; Chung and Chang, 2016; Oehrlein and Hamaguchi, 2018; Peng et al., 2018a). For water treatment, non-thermal plasma is of greater interest compared to thermal plasma since the power supplied is simply used to generate plasma at ambient conditions rather than heating the water.

2.3.1.1 Non-thermal plasma generation

In general, the generation of non-thermal plasma occurs in a gap between parallel metal electrodes, one of which is connected to a high voltage power supply (cathode) and the other is grounded (anode). An electric field is formed between the two electrodes when a high voltage is supplied to the electrodes. The electric field strength increases with the input power until breakdown voltage of the employed feed gas is reached, generating a Townsend discharge and this is followed by the propagation of a streamer discharge (Figure 2.3). The threshold value for the electrical breakdown varies depending on the gas and electrode configuration (Fridman, 2008).
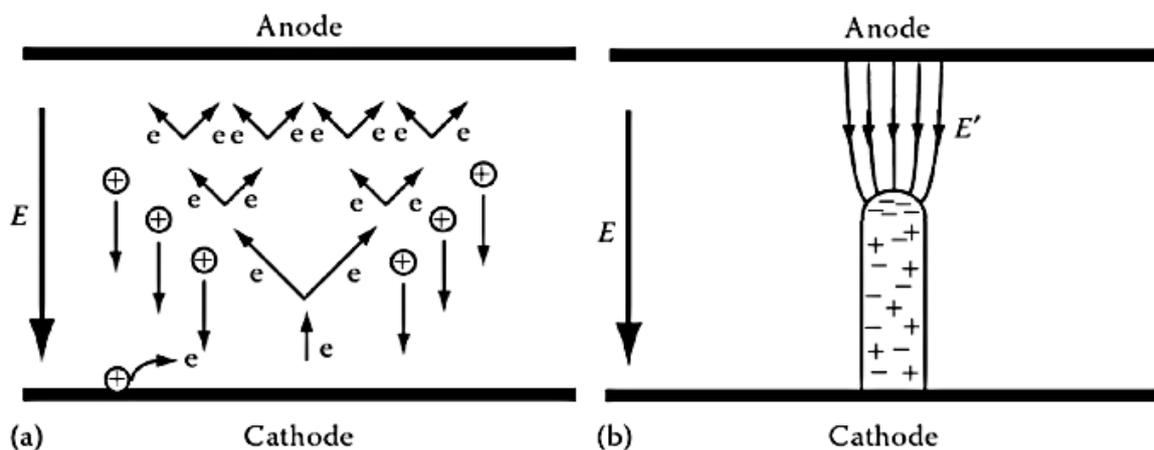
Figure 2.3: Schematic illustration of a) Townsend breakdown and b) streamer breakdown. Taken from (Chu and Lu, 2013).

Under the influence of the electrical field formed from application of high voltage across two electrodes, the free electrons in the discharge gap are accelerated towards the anode. The energetic fast moving electrons within the discharge gap collide with and ionize neutral atoms and molecules in the gas or on the surface of the electrodes, producing secondary electron-ion pairs (Fridman, 2008; Samukawa et al., 2012). These active species undertake subsequent secondary reaction processes in plasma to form the final plasma products. At very high currents and long durations of applied voltage, an irreversible transition into an arc or spark occurs. This transition from non-thermal ionization to arc or spark occurs when enough energy is dissipated in the discharge gap during the glow phase (Figure 2.4).
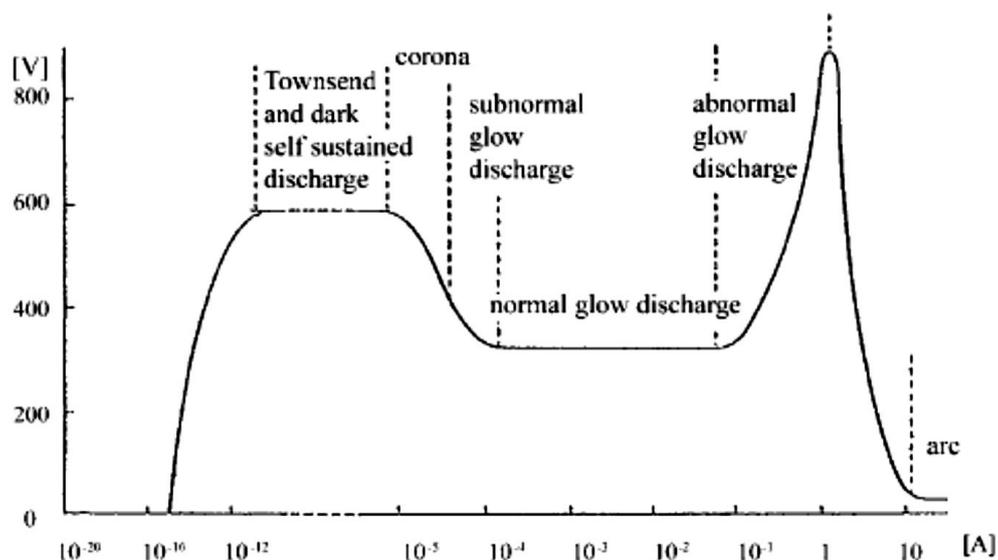
Figure 2.4: Current versus voltage characteristic of a typical DC low-pressure gas discharge. Taken from (Conrads and Schmidt, 2000).

The increased number of ionization collisions leads to increasing gas temperature (T_g) and reduction of the gas density, which is followed by increasing electric field to neutral particles density ratio (E/N). Transition from Townsend to corona, followed by subnormal to normal glow discharge occurs (Figure 2.4). The transition is marked by an increase in current and decrease in voltage. As E/N increases further, greater frequency of electron collision leads to electrons gaining energy, which is associated to an increasing T_e. As T_e increases, a runaway condition occurs where the high degree of collision between the electrons and other components of the plasma leads to equilibrium distribution of internal energy, i.e. kinetic, heat of dissociation and ionization, between electron and heavy particles (Heberlein, 1992). This ultimately leads to the formation of a thermal plasma arc, which occurs at low applied voltage and high discharge current.

Underwater thermal arc plasma have been studied for various applications such as nanocarbon synthetics and water treatment applications (Lange et al., 2003; Yamatake et al., 2006b). However, for water treatment, generation of thermal plasma arc involves high temperatures that can heat up and vaporise the bulk media, i.e. 4000 – 6500 K plasma temperature (Lange et al., 2003). In terms of water treatment, non-thermal plasma is ideal due to lower temperatures and power usage compared to thermal plasma. Several studies use various ways of preventing transition from non-thermal ionization to thermal plasma arc or spark for water treatment (Foster, 2017), i.e. ballasting (resistor), dielectric barriers, fast rise time limited duration (ns) voltage pulses, control of duty cycle, electron beams, modification of gas composition and increasing flow rate to enhance cooling. Water treatment using various types of non-thermal plasma and plasma reactors has been reported in the literature and has shown promising microbial inactivation for effective sterilisation and purification of various water sources, compared to conventional methods (Bruggeman et al., 2013; Vanraes, 2016). Based on water treatment by plasma, various types of discharge were described in the literature (Table 2.12).

Table 2.12: Different types of plasma used in water treatment. Adapted from (Malik et al., 2001; Romat et al., 2004).

Type	Electrode characteristic for plasma formation	Applied Voltage	Energy
Glow discharge electrolysis	Thin wire anode in contact with water while cathode dipped in water	DC ~ 0.5 kV	Maximum of 100 eV
Dielectric-barrier discharge (DBD)	Parallel electrode with at least one covered with a dielectric material, i.e. glass or quartz	AC ~15 kV	~1-10 eV
Corona discharges	Various configurations, I.e. needle-plate electrode, wire cylinder	DC ~15-100 kV	~5 eV
Arc discharge	Point to point electrode with a gap in-between	AC or DC	~1-5 eV

2.3.1.2 Plasma in contact with liquid

In general, the detailed mechanism of the complex processes involved with non-thermal plasma in contact with liquid is not yet fully understood (Fridman, 2008; Samukawa et al., 2012). However, numerous studies have proved plasmas as an effective source of oxidants and physical processes such as UV emission, heat, shockwaves and ultrasound that promote desirable chemical reactions in liquids and at the plasma-liquid interface (Bruggeman et al., 2016). The reactive species produced by plasmas are short lived (milliseconds and microseconds) and undergo subsequent reactions either with each other, chemical and biological species in water or directly with water. Table 2.13 provides examples of accounted particle interactions by electron impact and other reaction pathways of plasma with water to form these reactive species (Malik et al., 2001). In addition to radical and molecular products, plasma discharge can form solvated electrons (e_{aq}^-) (Richmonds et al., 2011; Rumbach et al., 2015a; Rumbach et al., 2015b). Solvated electrons have strong potential that can either react directly with water to form radicals or degrade electron-accepting pollutants in contaminated water (Sun et al., 2000). The formation of these oxidants in water was confirmed by various chemical probe measurements, reactive species scavengers and optical techniques (Sunka et al., 1999; Bruggeman et al., 2009; Kanazawa et al., 2011; Marotta et al., 2011). The synergistic

effects of these products and processes are considered to achieve higher water treatment efficiency than conventional methods.

Table 2.13: Examples of reaction that occur in the liquid phase and gas/plasma-liquid interphase (Malik et al., 2001).

Ionization	$H_2O + e^{-*} \rightarrow H_2O^+ + 2e^-$
Dissociation	$H_2O + e^{-*} \rightarrow \cdot OH + \cdot H + e^-$ $H_2O^+ + H_2O \rightarrow \cdot OH + H_3O^+$ $H_2O^{\cdot+} + H_2O \rightarrow \cdot OH + H_3O^+$ $H_2O^* + H_2O \rightarrow \cdot H + \cdot OH + H_2O$
Radiation pathway	$H_2O \xrightarrow{rad} H_2O^{\cdot+} + e^-$ $H_2O \xrightarrow{rad} H_2O^*$
Photolysis of water	$H_2O \xrightarrow{hv} \cdot OH + \cdot H$ $H_2O \xrightarrow{hv} H_2 + O$
Recombination reactions	$\cdot OH + \cdot OH \rightarrow H_2O_2$ $H_2O_2 + H \rightarrow HO_2 + \cdot OH$ $HO_2 + \cdot OH \rightarrow H_2O + O_2$ $O_2 + H \rightarrow \cdot OH + O$
Bulk reaction	$6H_2O \rightarrow 4H_2 + 2H_2O_2 + O_2$
Electron solvation	$H_2O + e^- \rightarrow e^-_{aq}$ $H_2O + e^-_{aq} \rightarrow \cdot OH + \cdot H$ $\cdot OH + e^-_{aq} \rightarrow OH^- + \cdot H$

* indicates a high-energy state.

Various indirect or direct methods are commonly employed to achieve interaction of plasma with liquid water. Indirect treatments by plasma generation in the gas phase above a liquid are typically considered similar to gas electrical discharge due to a similar breakdown strength in atmospheric gases. For plasma discharge that occurs in the gas phase, collision of plasma electrons initiates the chemical reactions in the bulk gas phase to produce reactive species (Samukawa et al., 2012). These reactive species produced in plasma rely on diffusion across the gas-liquid interface into the bulk liquid via Henry's law;

$$p = k_H \cdot c \qquad \qquad \text{Equation 2.1}$$

where p is the partial pressure above the liquid, c is the concentration in the liquid and k_H is the respective Henry's law constant. These oxidizing species, formed in the gas phase and then transferred into water, are reported in several studies (Hoeben et al., 1999; Petr Lukes et al., 2005; Dobrin et al., 2013; Lindsay et al., 2015). According to some authors, reactive oxidants

formed in close proximity to the liquid surface diffuse through the gas-liquid interface, initiate reactions within the liquid and by increasing the plasma-liquid contact area, higher treatment efficiency can be achieved. Others suggest that oxidation of some chemical pollutants takes place in the gas phase. Ognier *et al* reported that volatile pollutants, where pollutants that readily transitions from liquid to gas phase, react with the plasma species in the gas phase (Ognier et al., 2009).

With plasma discharge in the gas phase, the formation of the reactive species varies with different gases. For example, air is made up of around 79% N_2, 20% O_2 and a 1% mixture of other gases (Bruggeman et al., 2016)**.** Air under plasma drives the formation of other oxidants such as reactive nitrogen species (RNS), which are absent in other pure gases (Lukes et al., 2014; Lu et al., 2017; Tarabová et al., 2018). Several long-living species, such as O_3 and H_2O_2 can induce post reactions, increasing the cumulative oxidizability of plasma treatment, through the generation of subsequent ·OH products via processes such as catalytic reactions, dissociation and photolysis. Thus, by sealing such plasma reactors, (mainly reactors in static configuration), postreaction of long-lived species in the gas phase were confined and appeared to improve treatment efficiency (Yano et al., 2009; Cui et al., 2018). In addition, the surrounding water vapour in humid gases and the plasma-liquid interface can generate further reactive species following interaction with these long-lived species (Moreau et al., 2008).

Compared to indirect plasma discharge, direct discharge in a liquid requires a strong electrical field for breakdown to occur; it can also be achieved by using microwaves, laser pulses and sonoluminescent bubble implosions (Foster, 2017). In general, the electrodes are submerged in liquid and require ~1 MV/cm for electrical breakdown in water (dielectric constant (ε) ~80 for deionized water), forming filamentary streamers or bubbles (Figure 2.5) (Foster, 2017; Korobeynikov and Melekhov, 2016). Streamer discharges are a consequence of electron avalanche in liquids, similar to gas discharge, and occur in a relatively short period, i.e. nanoseconds, limiting the transfer of excessive heat to the heavy particles and the surrounding liquid medium (Locke et al., 2006). On the other hand, electrical breakdown in water can occur through bubble formation, a consequence of gas cavities formed by heating up the liquid, Joule heating, during discharge (Tachibana et al., 2011). When Joule heating between the electrodes

exceeds the threshold value for breakdown, instability occurs at the surface of the electrodes, resulting in phase transition and vapour voids, followed by thermal breakdown.
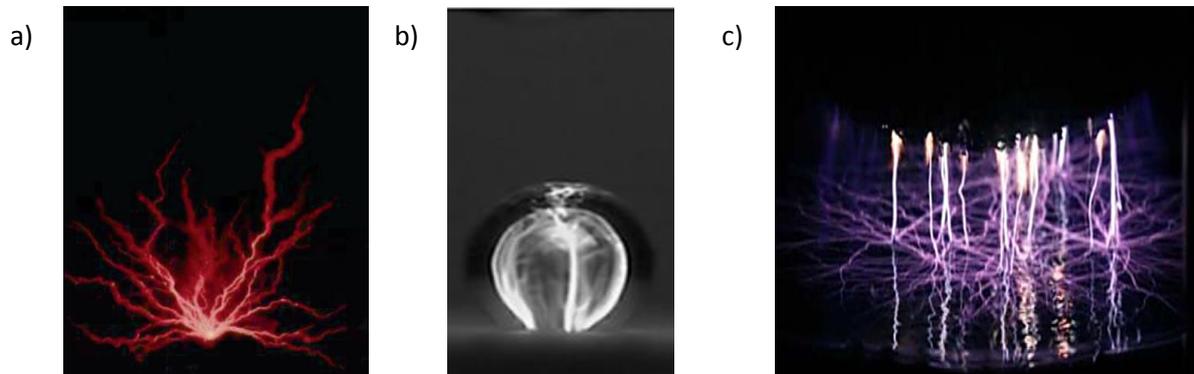
Figure 2.5: Example of plasma generation for water treatment: a) Streamer propagation in liquid, b) Bubble process in liquid and c) Gas phase discharge over liquid. Taken from (Sato, 2000) (a), (Tachibana et al., 2011) (b) and (Lukes et al., 2011) (c).

The overall plasma discharge directly formed in liquids is in general affected by additional factors such as electrode materials and solution parameters that influence plasma efficiency and the production of the reactive species (Jiang et al., 2014). The mechanism of this phenomenon in liquids is still not well understood and several theories have been suggested, i.e. thermal, bubble, crack and nanopore mechanisms (Bruggeman et al., 2016; Foster, 2017). These theories describe how breakdown in liquid occurs through phase transition to a low-density state or channels, i.e. water to vapour, bubbles or cracks, except for nanopore mechanisms that propose streamers are generated in nanopores, formed in water via electrostriction.

2.3.1.2.1 Non-thermal plasma application for chemical degradation

Several studies have studied degradation of dissolved chemicals in water using non-thermal plasma. The number of non-thermal plasma studies for treating various chemicals, organic and inorganic is continually expanding. The plasma-induced decomposition of organic compounds is well established but there are limited studies in regards to treating inorganic compounds. Conventional methods such as ion exchange transfers dissolved inorganic compounds to sludge, which requires safe post treatment and resin regeneration (Gunatilake, 2015). However, plasma has the potential to oxidize inorganic compounds to their less toxic form and enhance their potential for removal. Back *et al* reported treatment of arsenic with non-thermal

plasma, oxidizing As (III) to As (V), which is less toxic and has a higher affinity for surfaces, and thus, combined with coagulation and ultrafiltration leads to effective removal of higher levels of arsenic in water (Back et al., 2018).

The ability to mineralize organic pollutants by non-thermal plasma has raised interest for a fast and clean process for water treatment, involving no or few chemicals while also simplifying process management and reducing the toxicity of waste products. Numerous studies have investigated the degradation of organic contaminants such as phenols, pesticides, pharmaceuticals and organic dyes, which are contaminants not effectively removed by conventional methods. Several studies have shown effective degradation of organic contaminants using plasma as a stand-alone process or in combination with other components such as catalysts to enhance degradation. Non-thermal plasma as a stand-alone process is ideal in terms of limiting pre-or post-treatment costs, since components such as catalysts are expensive. Table 2.14 shows some examples of non-thermal plasma treatment of various organic contaminants with no pre-or post-treatment of solution.

Table 2.14: Treatment of organic contaminants dissolved in water using various types of non-thermal plasma. Publications including pre- or post-treatment of solution are not included.

Contaminants	Non-Thermal Plasma	Gas/ Voltage/ Energy	Treatment Results	Reference
Phenol / phenolic compounds	Corona discharge	Air/ 10-12 kV/ 0.2 - 3.6 W	Maximum of 90% degradation of **phenol** in mists	(An et al., 2011)
	Dielectric barrier discharge	Air/ 16.5 – 18 kV	80% degradation of **phenol** after 4 hours of treatment	(Marotta et al., 2011)
	Corona discharge	Air/ 0 - 30 kV	100% degradation of **phenolic compounds** after 60 minutes of treatment	(Cheng et al., 2012)
	Dielectric barrier discharge	Oxygen/ 2 kV	99% degradation of **phenol** with 45 mg/L hydroxyl radical concentration in solution	(Yang et al., 2009)
	Corona discharge	Air/ 40 kV/ 54 mJ per pulse	90% **phenol** degradation at pH 10.2	(Grabowski et al., 2006)

Pesticide	Dielectric barrier discharge	Air/ 80 kV	78.98%, 69.62% and 57.71% degradation for **dichlorvos**, **malathion** and **endosulfan** respectively after 8 min of treatment	(Sarangapani et al., 2016)
	Corona discharge	Oxygen/ 18 kV/ 11-13 W	> 90% degradation of **2,4-dichlorophenoxyacetic acid** after 60 minutes of treatment	(Bradu et al., 2017)
	Corona discharge	Air/ −9.5 kV/ 5.5 W	Degradation of **imidacloprid** and **thiamethoxam** after 5 hours of treatment	(Tampieri et al., 2019)
	Corona discharge	Air/ $15 - 25$ kV/ $26016 - 101.5$ W	100% degradation of **2,4-dichlorophenoxyacetic acid** after 6 minutes of treatment	(Singh et al., 2017)
	Dielectric barrier discharge	Air or oxygen/ 6 kV/	Higher degradation using oxygen, with 98% degradation of **oxadiazon** achieved after 30 minutes of treatment	(Ying et al., 2017)
Pharmaceutical	Dielectric barrier discharge	Air/ $40 - 44$ kV_{p-p}/ $5 - 33$ W	Maximum of 90% degradation of **2-naphthlol** after 2 minutes of treatment	(Krugly et al., 2015)
	Corona discharge	32 kV/ 30 mJ per pulse	91.7% degradation of **ibuprofen** achieved after 80 minutes of treatment	(Zeng et al., 2015)
	Dielectric barrier discharge	Oxygen/ 12 kV/ 1.2 W	92.5% degradation of **pentoxifylline** achieved after 60 minutes of treatment	(Magureanu et al., 2010)
	Dielectric barrier discharge	Air, argon or nitrogen/ 8 kV_{p-p}/ 1 W	81% degradation of **paracetamol** achieved after 60 minutes of treatment	(Baloul et al., 2016)
	Dielectric barrier discharge	Oxygen/ 17 kV/ 2 W	25%, 22.5%, 29% mineralization as carbon dioxide of **oxacillin**, **amoxicillin** and **ampicillin** after 120 , 120 and 30 minutes, respectively, of treatment	(Magureanu et al., 2011)
Organic dye	Corona discharge	Air/ 17 kV	50% degradation of **methylene blue** after 10 minutes of treatment	(Magureanu et al., 2013)
	Gas discharge	Oxygen/ 46 kV/ 5.67 W	92% degradation of **methyl orange** after 20 minutes of treatment	(Jiang et al., 2012)

Dielectric barrier discharge	Air, O$_2$/ 5 - 7 kV/ 18 W	99.98% degradation of **methylene blue** using oxygen plasma for 20 minutes and 85.3% degradation using air plasma for 100 minutes	(Wang et al., 2017a)
Dielectric barrier discharge	Air/ 14 kV/ 25 W	Complete degradation of **reactive black 5** after 5 minutes of treatment	(Dojčinović et al., 2016)

As shown in Table 2.14, degradation of the contaminant was achieved to at least an average of 90% but this does not mean complete mineralization was accomplished instantaneously. Oxidation of contaminants was indicated as the first step of degradation, which leads to formation of shorter intermediates rather than direct mineralization. This could be due to mineralization occurring at a slower rate compared to production of degradation products and may require longer treatment time for further oxidation of formed degradation products to mineralisation. Magureanu *et al* reported degradation of dissolved pharmaceuticals in water by non-thermal plasma yet to undergo mineralization took 120 minutes (Magureanu et al., 2011). In such conditions, energy consumption is high and not cost effective to achieve complete mineralization. Several papers have employed various factors such as using different gases, i.e. oxygen to increase reactive oxygen species concentration, increase plasma contact using mist or water films and increase plasma density by reducing the space gap where plasma is generated to increase degradation rate (Locke et al., 2006; Stratton et al., 2015; Foster, 2017; Yang et al., 2018). Thus, maximizing contact between plasma, contaminants and its degradation products may encourage early mineralization and reduce treatment time.

2.3.1.2.2 Sterilization by non-thermal plasma

Non-thermal plasma offers several strategies for developing antibacterial approaches that repel or kill bacteria. Previous studies with non-thermal plasma have demonstrated promising antimicrobial activity in surface sterilization, development of antimicrobial surfaces that prevent bacterial adhesion, food preservation and safety, anti-biofilm activity, water treatment and treatment of aerosolised and antibiotic resistant bacteria (Moreau et al., 2008; Misra et al., 2011; Liang et al., 2012; Isbary et al., 2013; Cha and Park, 2014; Prochnow et al., 2014; Liao et al., 2017; Bourke et al., 2017). For water treatment, various studies have investigated long-lived reactive agents generated in water after plasma treatment that can induce antimicrobial

activity, allowing plasma activated water (PAW) to be used for disinfection of equipment, sterilization and surface decontamination. Direct application of non-thermal plasma treatment on microorganisms in water, and indirect via PAW, added to contaminated water represent alternative methods of water disinfection rather than using chlorine with its associated toxic by-products and the growing number of microorganisms resistant to chlorine (Vanraes, 2016). Table 2.15 shows some studies that investigated the anti-microbial activity of plasma against various microorganisms in water responsible for diseases and HCAIs.

Table 2.15: List of examples of microorganisms in water treated with non-thermal plasma, with or without pre- or post-treatment of the bacterial suspension.

Type	Contaminant	Non-Thermal Plasma	Gas/ Voltage/ Energy	Treatment Results	Reference
Gram negative bacteria	*Escherichia coli*	Atmospheric pressure plasma jet	Nitrogen / 70 V / 7 W	5 log reduction after exposure to plasma combined with vapour systems (deionised water /HNO_3)	(Shaw et al., 2018)
		Gliding arc discharge	Air/ 3 kV/ 200 W	Total of 6 log reduction during 25 minutes of treatment and 2 hours after treatment	(Kim et al., 2013)
		Dielectric barrier discharge	Air/ 40 kV$_{p-p}$	7 log reduction after 20s direct or 45 s indirect treatment	(Ziuzina et al., 2013)
		Atmospheric pressure plasma jet	Argon/ 1-5 kV	7 log reduction after 15 minutes of treatment but after 45 minutes of treatment 12% remained alive	(Dolezalova and Lukes, 2015)
	Legionella pneumophila	Corona discharge	Air/ ±80 kV	5.4 log reduction after 12.5 minutes of treatment (+80 kV) and 2.54 log surviving population detected using -80 kV	(Banaschik et al., 2016)

	Legionella gratiana	Arc discharge	Air/ 1.12 kW	6 log reduction after 20 seconds of treatment	(Johnson et al., 2016)
	Acidithiobacillus ferrooxidans	Arc discharge	Air/ 1.06 kW	6 log reduction after 40 seconds of treatment	(Johnson et al., 2016)
	Pseudomonas aeruginosa	Dielectric barrier discharge	Air/ 7.4 kV$_{p-p}$	4.8 log reduction after 4 minutes of treatment	(Choudhury et al., 2018)
		Glow Discharge	Helium (98%), Oxygen (2%)/ 0.30 kV/ 0 - 80 W	8 log reduction after 6 minutes of treatment	(Zhang et al., 2012)
	Pseudomonas fluorescens	Microplasma jet	Air/ $1 - 5.5$ kV/ $0.1 - 2.3$ W	6 log reduction after 4 minutes of treatment	(Zhang et al., 2013)
Gram positive bacteria	*Staphylococcus aureus*	Plasma microjet	Helium (98%)-Oxygen (2%)/ 400 V	4 log reduction after 10 minutes of treatment	(Bai et al., 2011)
		Plasma microjet	Air/ 100 V	3 ~ 4 log reduction over 30 days period *after S. aerus* added to PAW and stored at -80 °C	(Shen et al., 2016)
		Dielectric barrier discharge	Air/ 7.4 kV$_{p-p}$	5.4 log reduction after 2 minutes of treatment	(Choudhury et al., 2018)
	Bacillus subtilis	Plasma microjet	Air/ $400 - 600$ V	97% inactivation rated after 6 minutes of treatment	(Sun et al., 2012)
	Bacillus thuringiensis	Dielectric barrier discharge	Oxygen, air, argon/ 6 kV/ 5 W	3 log reduction after 20 minutes of treatment	(Hayashi et al., 2013)
	Bacillus pumilus	Gas discharge	Air, oxygen/ 4.21 W cm^{-1}	4.54 log reduction after 30 minutes of treatment	(Purevdorj et al., 2003)
Yeast	*Saccharomyces cerevisiae*	Plasma microjet	Air/ 0.56 kV	51.9% apoptotic rate for no strain *S. cerevisiae* in comparison to nearly 30% for two strains of *S. cerevisiae*	(Ma et al., 2013)

Compared to direct plasma treatment of microorganisms on surfaces, the liquid environment provides an additional barrier preventing direct impact of electrons and ions in plasma with microorganisms in water. However, plasma induced processes such as UV-light and reactive species dissolved in water can penetrate and interact with the microorganism (Malik et al., 2001). The molecular mechanism of its antimicrobial effect with microorganisms in water is still not well understood; various constituents of plasma, i.e. chemical production and physical processes, can affect the biological, chemical and physical processes in microorganisms (Liao et al., 2017; López et al., 2019). Numerous efforts from previous studies have realized that the reactive chemicals formed in plasma can stimulate oxidative stress in cells, which leads to DNA damage, cell cycle arrest and apoptosis (Fang, 2011; Zhang et al., 2013; Vatansever et al., 2013; Dezest et al., 2017; Vaze et al., 2017; Liao et al., 2017;). However, this effect is dose dependant; low concentrations of reactive chemicals in plasma stimulate cell proliferation, mutagenesis and differentiation while high doses can drive apoptosis and necrosis (Kalghatgi et al., 2010; Barekzi and Laroussi, 2012; Ma et al., 2013). In addition, microorganisms are very diverse, with different structures and may have different responses to plasma. For example, both gram negative and gram positive bacteria have shown susceptibility to plasma but gram negative is more sensitive which was linked to cell wall chemical resistance and/or respiration mechanism; cell walls of gram negative bacteria have a single layer of peptidoglycan compared to multiple layers in gram positive bacteria (Lunov et al., 2014; Lunov et al., 2015). However, the effect increases in line with increasing treatment time and plasma density, increasing the dosage of chemical species generated in plasma can kill such bacteria, even with a thicker defensive layer (Maisch et al., 2012; Baldanov et al., 2015; Al-rawaf et al., 2018).

Compared to planktonic culture, defined as floating single cells in a culture medium, biofilms represent a serious challenge in water treatment, where cells are denser and more resistant to conventional anti-microbial agents due to the protection provided by its extracellular polymeric substances (EPS) (Sehar and Naz, 2016). Biofilms in water are monitored and mainly treated through chemical disinfection such as chlorine (Liu et al., 2016). Even in the presence of conventional disinfectants in water, biofilms persist and grow, which forces authorities to increase the level of conventional disinfectant agents to improve the disinfection results and prevent pathogenic microorganisms being released into water during the shedding period of the biofilm (Helmi et al., 2008; Henne et al., 2012). However, increasing the level of disinfection

affects the aesthetic quality and can lead to production of DBPs in the treated effluent, which requires additional management. In addition, such a method is not effective against biofilms harbouring microorganisms resistant to conventional disinfection agents. A number of studies have demonstrated effective treatment and inactivation of biofilms in water by plasma (Sun et al., 2018; Zhou et al., 2019). In comparison with planktonic samples, treatment of biofilms took longer, which was associated with its cell density and protective extracellular matrix (Soler-Arango et al., 2019).

2.3.1.3 Plasma reactors for water treatment

In recent years, research towards plasma reactors and their development for water treatment has increased significantly, focusing specifically in maximizing contact between plasma and the liquid solution while reducing treatment time as a cost-efficient treatment option. Continuous development has led to an expanding category of various reactors depending on discharge type, electrode configurations, i.e. pin-to-pin, pin-to-plate, plate-to-plate electrode configurations and coaxial geometry, or electrode designs, i.e. multiple pins, brush electrodes and coated electrodes, to generate strong electric field and high plasma density that improves treatment efficiency (Bruggeman and Leys, 2009; Vanraes, 2016).

Several reviews have emphasised the substantial influence of material, reactor design and operational parameters on the performance of the reactor. Malik provided an insight comparing treatment efficiency of different existing plasma reactors (Malik, 2010). This was followed by Stratton *et al*, identifying and characterizing design parameters that influence treatment efficiency of these reactors and thus may assist in new designs (Stratton et al., 2015). Initially, numerous electrode configurations have been developed and these were classified depending on the plasma-liquid phase distribution, i.e. remote, direct and indirect (Bruggeman and Leys, 2009). Recently, Vanraes extended this classification into six reactor types (Figure 2.5) (Vanraes, 2016):
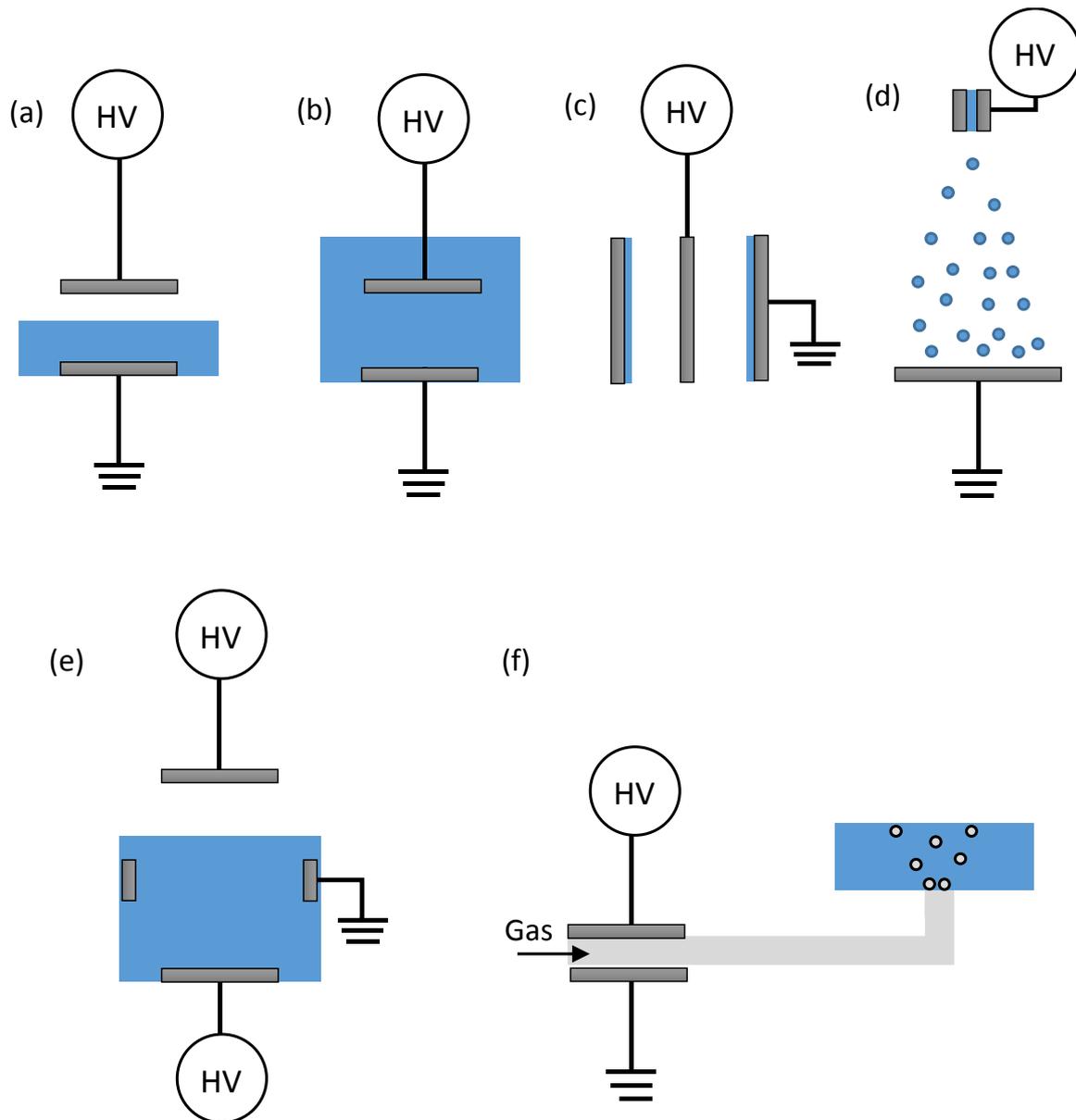
Figure 2.6: General designs of different types of plasma reactor: (a) Electrohydraulic discharge reactor, (b) Gas phase discharge reactor, (c) Coaxial reactor with falling water film, (d) spray discharge reactor, (e) hybrid reactor and (f) remote discharge reactor. Adapted from (Vanraes, 2016).

Electrohydraulic discharge and gas-phase discharge are the two most common reactor types used in initial studies. Since plasma is generated directly in the liquid, electrohydraulic discharge was considered suitable for scaling up due to a relatively high area of plasma-liquid contact and hence direct interaction of plasma with the contaminants. However, electrohydraulic discharge requires a strong electrical field for cavitation i.e. formation of vapour or bubbles in liquid during discharge (Starikovskiy et al., 2011). Treatment efficiency of electrohydraulic discharges is often affected by the electrode material and suffers from

discharge electrode corrosion that leads to particles being released during plasma treatment, reducing the lifetime of the system and contaminating the water being treated. Yet, some of the particles eroded from these metals, such as from titanium electrodes, were found to enhance pollutant degradation and vice versa (Parkansky et al., 2013). Coated electrodes, corrosion resistant metals or dielectric barriers have been employed to increase electrode lifetime, followed by low pulse energy to lower temperature loading and clean the electrode from products generated in solution (Potocký et al., 2009). Further improvement in energy efficiency and reduction of mass-transfer limitations that manifest in these reactors was achieved by combining methods that enhance plasma-liquid or erosion particle contact and may facilitate the onset of plasma generation to reduce the energy consumption in boiling or heating the liquid, i.e. from 1~2 MV/cm to 30 kV/cm. This includes several batch, semi-batch and bubble column reactors, where a certain volume of solution under treatment remains in the reactor until completion of treatment time, coupled with processes such as external bubbling of gas in liquid through an opening, ultrasonic cavitation, recirculation of water and rotating electrodes (Bruggeman and Leys, 2009; Vanraes, 2016). The mechanism that leads to the production of reactive species by these methods in liquid, specifically bubbling, is inconclusive and still not fully understood. However, studies have shown that such systems are useful in several applications other than water treatment such as synthesis, sterilisation and surface treatment (Samukawa et al., 2012; Adamovich et al., 2017).

Compared to electrohydraulic discharge, plasma discharge in the gas phase has shown greater energy efficiency since cavitation is not required (Stratton et al., 2015). However, the utilization of the reactive species generated in the gas phase and the plasma-liquid interface using these reactors relies on their diffusion coefficient from gas to solution. Spray discharge and novel reactors in the form of coaxial electrode configurations utilizing liquid films has received increasing attention due to their reported higher removal and energy efficiencies as compared to other designs in Figure 2.5 (Malik, 2010). Such reactors use liquid film and liquid spray, where flow rates have substantial influence on performance due to surface-to-volume ratio. The mass transfer of reactive species formed in plasma can be enhanced by utilizing the large surface area-to-volume ratio and proximity of plasma to the liquid surface found in such reactors. Spraying or using liquid films can further increase the plasma-liquid contact for mass transfer, in comparison to reactors where treatment was achieved over a water bulk in batch

configuration. This leads to shorter treatment times, lower energy demand and higher treatment, with maximum treatment of more than 90% of contaminants in water achieved (Sano et al., 2003; Kobayashi et al., 2010; Aziz et al., 2018). According to Stratton *et al,* gas discharges found in spray configuration achieve 150 times higher energy yield in comparison to electrohydraulic discharge, with no bubbling (Stratton et al., 2015). The effectiveness of liquid spraying and liquid films has been demonstrated in hybrid reactors, using both operations, i.e. gas phase and electrohydraulic discharge simultaneously (Kobayashi et al., 2010). Remote discharge reactors were originally used for ozone production and subsequently injected or bubbled through the liquid for treatment. New approaches utilize various feed gases to generate chemical reactive species other than ozone (Zhang et al., 2006; Tang et al., 2009). Compared to the reactors mentioned earlier, treatment efficiency is less pronounced. The difference was explained with the lack of utilization of short-lived species, generated in the plasma-liquid interface and in the liquid. Using a different approach, such reactors were used to produce PAW and added to water for treatment (Zhang et al., 2006; Kim et al., 2013).

Although the results and potential advantages offered by these reactors for PWT were promising, the demands for higher system throughput or treatment efficiency and versatile designs with low energy demand remain as challenges to the implementation of PWT. Table 2.16 summarize specific advantages and disadvantages of the aforementioned types of reactor.

Table 2.16: Advantages and disadvantaged of the plasma reactors used for water treatment.

Type of reactor	Description	Advantages	Disadvantages
Electrohydraulic discharge	Plasma generated directly in the liquid phase	- High area of plasma liquid contact	- High energy required for cavitation (formation of vapour or bubbles in liquid) - Suffers electrode corrosion affecting longevity of the system

Bubble discharge	Plasma generated directly in the liquid phase through externally applied bubbles	- No cavitation required - Enhanced efficiency by plasma formation compared to electrohydraulic discharge - Aid mixing the solution during treatment to increase plasma-liquid contact	- Particles clogging the small gas inlets. - Energy leaks and heats the water lowering treatment efficiency - Submerged electrode with no barrier or coating suffers corrosion
Gas phase discharge	Plasma generated in the gas phase or over a liquid film	- No cavitation required - Increase treatment efficiency for gas phase discharge over thin water films due to increase plasma-liquid contact - Induces degradation of volatile contaminants in the gas phase	- Relies on diffusion of plasma species in the gas phase into liquid - Requires stirring mechanism to enhance plasma-liquid contact
Spray discharge	Plasma generated in contact with spraying liquid	- High plasma liquid contact - Shorter treatment time - Lower energy demand due to no cavitation required	- Small nozzle orifice of spray-heads susceptible to blockage - Lack of control over mean droplet size - Broad droplet distribution
Hybrid reactors	Combination of electrohydraulic and gas phase discharge	- Combine the advantages of both gas phase and electrohydraulic discharge - High plasma-liquid contact	- Associated high energy consumption at high applied voltage (< 20 kV)
Remote discharge	Remote plasma generation, without direct contact with liquid under treatment	- Large production of ozone and PAW as source of treatment of contaminated water	- Lack of utilizing short-lived species, generated in the plasma-liquid interface and in liquid - Lower treatment efficiency

Using methylene blue as a model contaminant, selected results from studies using aforementioned reactors were compared and summarized in Table S2.1 in the appendix. Studies with no pre- or post-treatment and only relying on plasma for treatment were selected. Hybrid reactors could not be included due to comparable data not being available and limited numbers of studies but are expected to improve treatment efficiency combining the advantages of liquid and gas discharges. However, the main drawback is the associated high-energy consumption (greater than 20 kV applied voltage) compared to lower voltages used in other types of reactor in Table 2.17 for chemical degradation (Na et al., 2012).

In terms of performance, reactors operating liquid sprays and water films have shown the highest treatment efficiency which could be due to higher surface-area-to-volume ratio and a shorter distance for mass transfer of plasma species from gas into liquid compared to reactors operating in bulk liquid. Malik has estimated about 1,000 times improvement in energy efficiency for treatment using water film and 2,000 times improvement using water spray compared to electrohydraulic discharge (Malik, 2010). Thus, reactors operating water film or spray provide the advantage of high surface-area-to-volume ratio for efficient treatment.

In this study, the MPR was operated in the water film mode. Although the microfluidic device can be operated with water droplets as an analogous model for water spray reactors, the use of water film has been the focus of study due to easier flow control and reproducible film size distribution. Water droplets involve difficulty in control over droplet size due to the tendency of droplets to merge or break up at high shear stress, thus resulting in broad droplet size distribution and difficulty in reproducibility (Gu et al., 2011).

2.3.1.4 Continuous flow reactors

The reactors described above with different geometries have produced promising results, with the optimal design associated with a high surface area-to-volume ratio observed with spray or coaxial reactors. These initial studies were imperative in determining such key parameters related to efficient contaminant degradation and disinfection of water. Although they were not representative in developing reactors with low costs and high productivity of potable water; most of these reactors treat small volumes of water in static configurations either with or without recirculation (Vanraes, 2016; Cui et al., 2018). Compared to batch type reactors,

continuous flow reactors have the potential to provide large volumes of potable water at lower costs by reducing treatment time. Continuous flow processes involve a continuous movement of materials from one point to another; in terms of water treatment, high volumes of contaminated water can be introduced continuously into such a reactor and continuously discharge potable water.

Whilst flow reactors allow higher volumes and faster processing than batch type reactors, sufficient residence time to allow maximum interaction between plasma and contaminant in water is required to obtain potable water before it exits the system. In batch reactors, residence time is defined by how long the media resides in the reactor while flow rate determines the residence time of solution in a continuous flow reactor. A continuous flow reactor, operating without recirculation and treating water in a single pass configuration, is attractive in overcoming the issues of space, long residence times and high costs associated with batch treatment, to achieve high treatment efficiency and provide large volumes of potable water (Simon et al., 2006). Experimental studies evaluating the treatment efficiency and energy cost in continuous-flow reactors for chemical degradation (Gerrity et al., 2010; Dojčinović et al., 2016; Ceriani et al., 2018) and water disinfection (Singh et al., 2019) have shown promising results for improved energy efficiency in comparison to static configurations used currently (Gerrity et al., 2010; Johnson et al., 2016; Singh et al., 2019). Water films and spray were employed, taking advantage of their large surface-area-to-volume ratio that benefits fast processing in flow reactors, but difficulty in flow control caused broad size distribution of formed water droplets and film. Thus limited mass transfer of plasma species in the gas phase into liquid. Optimizing such operational parameters to maximize their potential and improve limitations with mass transfer and residence time is important in further understanding how the application of water treatment can be developed in continuous flow. This leaves a margin of progress in improving treatment efficiency of plasma in single pass configuration of continuous flow type reactors for water. This includes developing a robust and efficient continuous flow reactor that can treat water efficiently and be adapted to small and large-scale applications. Such scalable systems can provide flexibility for on demand potable water and replace or complement water treatment facilities.

Microreactors, defined as miniaturized reactors with characteristic dimensions in micrometres and sample volumes in nano-to microlitre, may have a key role as an optimizing tool and develop scalable flow systems for PWT. In particular, microreactors built upon microfluidic technology, which deals with the behaviour and manipulation of nano- or microlitre fluids allows exploitation of miniaturised dimensions to carry out multiple reactions in flow conditions. Their potential in industrial applications are expected to be analogous to bulk reactors and thus can provide guides on developing industrial design (Suryawanshi et al., 2018). Several studies have exploited such benefits of continuous flow microfluidics to develop various microfluidic platforms in areas such as synthesis (Lin et al., 2004; Ma et al., 2017; Jensen, 2017), particle separation (Karle et al., 2016; Hejazian et al., 2015; Shields et al., 2015), extractions (Wang and Luo, 2017; Tang et al., 2016; Tetala and Vijayalakshmi, 2016) and screenings assays (Du et al., 2016; Lifton, 2016). However, the full potential of microfluidics for PWT is yet to be realized.

2.4 Microfluidics

Microfluidics refers to devices and methods that allow control of the spatial and temporal behaviour of fluid with length scales less than a millimetre (Luo and Duan, 2012). The inherent characteristics of microfluidic systems have demonstrated their advantages in action in terms of high surface-area-to-volume ratios, increased speed of analysis/throughput, high sensitivity, portability and cost-effectiveness in regards to fabrication, reduced chemical reagents and waste effluent (Minteer, 2006; Luo and Duan, 2012). This results in powerful techniques to control and measure chemical reactions or physical/biological processes, which has influenced the creation of various miniaturised devices for biological and chemical analysis.

2.4.1 Microfluidic reactors for water treatment

Although limited and not reported as frequently as conventional bulk reactors, microfluidic reactors for water treatment have demonstrated promising results in overcoming various limitations found in bulk and batch type reactors. Initial studies developed catalytic microreactors that exploited the advantages of microfluidics to enhance catalytic efficiency for oxidation reactions of contaminants compared to conventional bulk catalytic reactors used in water treatment. The degradation of organic pollutants was achieved in seconds with these

microreactors (Dapeng and Jiuhui, 2009; Silva, 2015; Silva et al., 2016). An expanding area regarding photocatalytic water treatment in microfluidic research, utilizing catalysts and light to drive oxidative processes and degrade contaminants in water, has demonstrated high mass transfer efficiency between the liquid and catalyst surface, achieving more than 100 times reaction rate constants and reaction times in seconds compared to hours in corresponding bulk reactors (Wang et al., 2014; Azzouz et al., 2018). Water treatment in micromagnetofluidic devices, which employ magnetic nanoparticles to remove heavy metals in water, was considered to enhance mixing to improve heavy metal capture in highly metal laden water (Kefou et al., 2016). Other areas of water treatment such as microfluidic desalination using methods such as electrodialysis to provide potable water from salt water were developed, providing insight on ion transport and hence aiding the optimization of macro-scale desalination systems (Roelofs et al., 2015). New areas of hybrid systems in a microfluidic device for water treatment have been developed, combining electrocoagulation for the removal of contaminants and ion concentration polarization for desalination of water, while minimizing power consumption, contaminants and salt in water compared to bulk reactor systems (Choi et al., 2017).

These studies have highlighted the advantages of the microfluidic approach in water treatment by improving treatment efficiency and providing insights into the treatment process at a micro-scale that was difficult to study in bulk systems. Thus, by exploiting the advantages of miniaturisation, integration of non-thermal plasmas within microfluidic platforms can be utilised to enhance the oxidation process induced by plasma to remove contaminants in water. Compared to the aforementioned microreactors, the MPR does not require precursors such as catalysts for oxidation of contaminants and disinfection of water, thus keeping operational cost and maintenance low. This eliminates the need for catalyst separation and regeneration from treated effluent, which could be toxic when consumed or harmful if released unprocessed to the environment. On the other hand, electrocoagulation does not require chemical additives that are expensive to precipitate contaminants in water. However, blockage may occur in the microchannel due to electrocoagulation, especially water with high concentration of contaminants, and requires neutralization of the disposed waste (Moussa et al., 2017).

2.4.2 Microfluidic plasma reactor

In the past, miniaturisation of analytical equipment has inspired the integration of plasma technology into microreactors for applications such as spectrometry to generate non-thermal microplasmas, a plasma of dimensions less than a millimetre (Karanassios, 2004). The spatial confinement of microplasma in microreactors is a promising ionization source due to their unique characteristics such as high electron density, causing high rates of excitation and ionization, and low breakdown voltage (Schoenbach and Becker, 2016a). Thus, the last 20 years has seen growth in research of microplasmas with its integral role as one of the most powerful excitation and ionisation sources in developing miniaturised synthetic reactors, detectors, spectrometers and other technological applications in medicine and the environment (Olabanji and Bradley, 2011; Stauss et al., 2014; Ishii et al., 2015; Schoenbach and Becker, 2016b; Wengler et al., 2018).

Due to the low discharge voltage required to generate a microplasma, (about 1 kV), some studies have applied microplasmas for water treatment, where it is either generated directly on water or used to generate reactive chemicals to treat water. A microplasma jet is an example of a microplasma used for direct disinfection of water (Shen et al., 2016). Shimizu *et al* used a dielectric barrier discharge microplasma generated on the surface of water for degradation of a textile dye in water (Shimizu et al., 2013). Shirke *et al* used microplasma as a remote discharge to form ozone and added it to water (Shirke et al., 2014). Although the generation of microplasmas in microreactors is well established, microplasmas generated in a microfluidic reactor for continuous flow treatment has yet to be realized for the degradation of contaminants and disinfection of water.

The use of continuous flow microfluidic reactors with integrated plasma technology provides an opportunity for utilizing the inherent benefits of microfluidics in its application for PWT, overcoming limitations such as mass transfer in bulk reactors. Although combining microfluidics with relatively large-scale water treatment creates potential problems in terms of sample volume, this contrast can be bridged by placing multiple devices in parallel. On the other hand, the microreactor can be developed for a wide array of applications such as synthesis reactors, analytical applications and installation with in-line water supply systems that do not require high volume throughput. Microfluidics may provide some benefit for

prospective portable plasma reactor devices for water treatment on demand in the future, eliminating expensive consumables.

2.4.3 Fabrication of microfluidic plasma reactor

Various materials such as polydimethylsiloxane (PDMS) or glass can be used for the fabrication of an MPR (McCreedy, 2001; Ren et al., 2013). Plasma production in channels with a hydraulic diameter below 1 mm, i.e. microchannel, has been reported in PDMS and glass reactors (Olabanji and Bradley, 2011; Ishii et al., 2015; Wengler et al., 2018). In terms of plasma generation, high chemical and thermal stability of the reactor material is required to ensure that reaction is not affected by material transformation during plasma ignition. PDMS is attractive due to low production cost and ease of processing , yet poor thermal and chemical stability leads to deterioration or under-performance of the reactor. PDMS has a low thermal conductivity of 0.18 W m^{-1} K^{-1}, an order of magnitude lower than glass, which equates to poor thermal distribution as a consequence of varying internal or external temperature of the device and poor chemical stability, with the tendency to absorb molecules and solvents, interfering with analysis (Erickson et al., 2003; Toepke and Beebe, 2006). However, glass has favourable properties such as better thermal and chemical stability compared to PDMS but the process of fabricating glass-based microreactors compared to PDMS is expensive (Ren et al., 2013). With both liquid and gas introduced at the same time into the proposed MPR, a glass microreactor is ideal as it can withstand high-pressure driven experiments, up to 400 atm (Tiggelaar et al., 2007). Under high-pressure conditions, PDMS is susceptible to elastic deformations, which affect pressure distribution within the channels, and thus alters the flow regime over time (Gervais et al., 2006). Glass is not permeable, with relatively low adsorption compared to PDMS and thus its chemical inertness, biocompatibility and tolerance to high-pressure conditions allows the reaction to be contained and ensures longevity of the reactor (Eichholz et al., 1965). This makes glass the material of choice due to its thermal and chemical stability for prolonged water processing of samples spiked with chemical or biological agents. These initial investigations using glass reactors were based on a dielectric barrier discharge (DBD) mode of activation.

2.4.3.1 Dielectric barrier discharge

DBD, commonly known as the silent discharge, is based on the use of at least one electrical insulator i.e. dielectric barrier, between two planar or cylindrical electrodes separated by a small gap between 0.1 to 100 mm (Kogelschatz, 2003; Fridman, 2008). The dielectric layer could be of various materials such as glass, quartz, ceramic or a layer of water around one (single barrier) or both (double barrier) of the electrodes. DBD is ignited by a sinusoidal or pulsed AC power source, with an amplitude of 1-100 kV. The discharge mode is either glow or microdischarge. When the applied high voltage across the discharge gap between the electrodes is high enough, an electron avalanche forms from the cathode leading to fast streamer propagation towards the anode. These streamers, known as microdischarge, are randomly distributed across the discharge gap between the electrode and leads to breakdown in various working media i.e. liquid and gas phases. The dielectric constant and thickness of the dielectric barrier limits the transport of current and formation of spark or arc in the discharge gap. By increasing the electrical conductivity of the dielectric, it interferes with and limits the current flow in generating streamers in the discharge gap. For double barrier reactors, higher voltage was applied to enhance the local electric field compared to a single barrier. However, higher degradation efficiency was found using double barriers compared to a single barrier of similar dimensions, which was assumed to be caused by a higher energy density (Yamatake, 2007).

2.5 Summary

Applications of non-thermal plasma in various types of plasma reactors have been investigated and proven effective in treatment of contaminated water samples; water film and spray discharge were the most effective due to high surface-area-to-volume ratio. However, most plasma reactors investigated operated batch type systems in static configuration, which is not as effective, compared to continuous flow type reactors for treating large volumes of water. Batch type reactors in static configuration were limited in terms of mass transfer of plasma species formed in the gas phase into liquid, long treatment times and high cost. Miniaturization of non-PWT reactors for chemical processing have overcome similar limitations with corresponding bulk reactors. However, these reactors require additives or precursors for

enhanced water treatment. Integration of plasma technology with microreactors built upon microfluidic technology is attractive due to no precursor being required and the inherent advantages of microfluidics may help overcome the limitation of current bulk plasma reactors. Single pass plasma treatment of water in a continuous flow reactor is of current interest for their simple configuration, which can be achieved in a microfluidic reactor. So far, the application of MPR for the removal of contaminants and disinfection of water is yet to be developed.

Chapter 3 Methodology

This chapter explains the equipment used for the production of plasma in a microfluidic device and the experimental procedures conducted. The geometry and characteristics of the microfluidic reactor and plasma source are described. The applied analytical, chemical and microbiological assays are discussed.

3.1 Fabrication of the microfluidic device

The microfluidic device was fabricated on a glass substrate in the Lab-on-a-Chip Fabrication Facility at the University of Hull. Standard photolithography coupled with wet etching techniques (Scheuble et al., 2017) were used to produce the standard design of the MPR used in this study (Figure 3.1). The microfluidic devices were fabricated using Schott B270 glass blank wafers (Telic, California USA), 1 or 3 mm thick, as top plate and wafers pre-coated with low reflective chromium and photoresist , 1 mm thick as bottom plate and 1 mm or 3 mm as the top plate. The coated wafers were exposed to UV light from a UV exposure box (196-5251 RS components, UK) for 60 seconds through a patterned photo-mask (MicroLitho Ltd, Chelmsford, UK) with the desired channel design made using AutoCAD (Autodesk, USA) (Figure 3.1). The photoresist layer is degraded where it has been exposed to UV light and dissolved away by a developer (AZ351, Microchemicals GmbH, Germany in a 4:1 dilution), for one minute, exposing the desired pattern on the chromium layer (Figure 3.1.c). The chromium layer was etched using a chromium etchant (Fisher Scientific, UK). The exposed glass layer was wet-etched to the desired depth of 50 or 100 μm using a buffered HNO_3/HF solution (2% by vol HF and 5% by vol HNO_3, Fisher Scientific UK) (Figure 3.1.d). After wet etching, both the photoresist and chromium layer were stripped using acetone and followed by chrome etchant (Fisher Scientific UK), (Figure 3.1.e, f, g). The glass blank wafers were drilled with access holes (1/16" outer diameter (OD)) for the inlet and outlet using a CNC machine (Datron, Milton Keynes, UK) (Figure 3.1.h). Both drilled and etched wafers were cleaned and degreased with acetone, followed by isopropanol and submerged in piranha solution (3:1 by volume concentration H_2SO_4 : 30% H_2O_2) for 1 hour. The cleaned glass wafers were then washed with deionized water. The top plates with drilled holes were aligned with the etched wafer, thermally bonded together by applying slight pressure by hand and placed in a furnace (Northern Kilns UK) and

heated to 585°C for 10 hours in air, sealing the reactor permanently (Figure 3.1.i). After bonding, fluorinated ethylene propylene (FEP) tubing (1/16" OD x 0.030" inner diameter (ID)) was glued into the access holes using Araldite two part epoxy adhesive (Huntsman Advance Materials, UK).
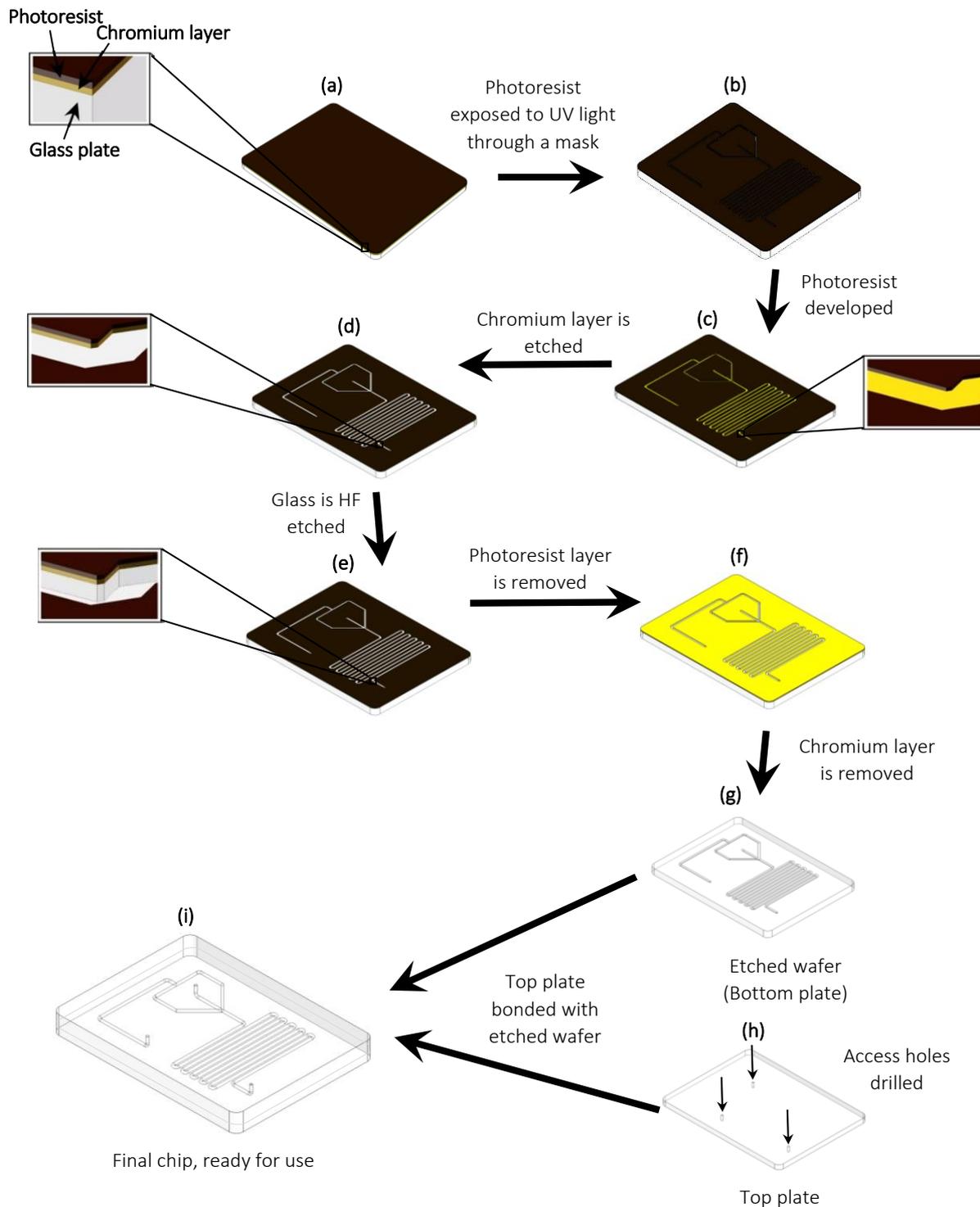
Figure 3.1: Schematic illustration of the photolithography and wet etching process employed in fabricating the microfluidic device used in this study. Adapted from (Scheuble et al., 2017).

3.2 Microfluidic device layout

The initial design of the glass microfluidic device used in this study is presented in Figure 3.2. Glass was used as substrate due to its dielectric properties (dielectric constant ε_r: 5 - 10 (10 kHz – 10 MHz)) which prevents arc formation and limits the charge and energy deposited in a single microdischarge (Kogelschatz et al., 1997). The design of the microfluidic device was adapted from (Cvetković et al., 2012). In order to maintain a continuous two-phase flow of liquid and gas, it was modified at the outlet so that the sample was collected directly after the serpentine channel. The device consisted of two separate in-plane inlets for liquid (1) and gas feeds (2), the T-junction where gas splits into two streams (3), the Y-junction where both liquid and gas meet (4), the serpentine channel after the Y-junction (5) before finally reaching the outlet for sample collection (6) (Figure 3.2 (a)). The cross-sectional geometry of the microchannel (mc) is considered as trapezoidal or semi-circular, (Width$_{mc}$ x Depth$_{mc}$ = 330 μm x 50 μm and 390 μm x 100 μm) (Figure 3.3).
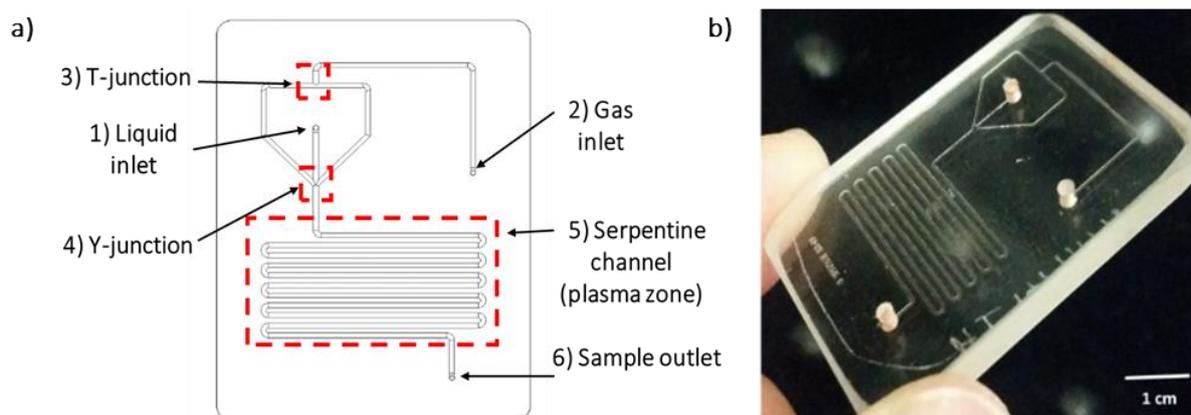
Figure 3.2: Sketch of the general design (a) and photograph (b) of the microfluidic device used in this study.
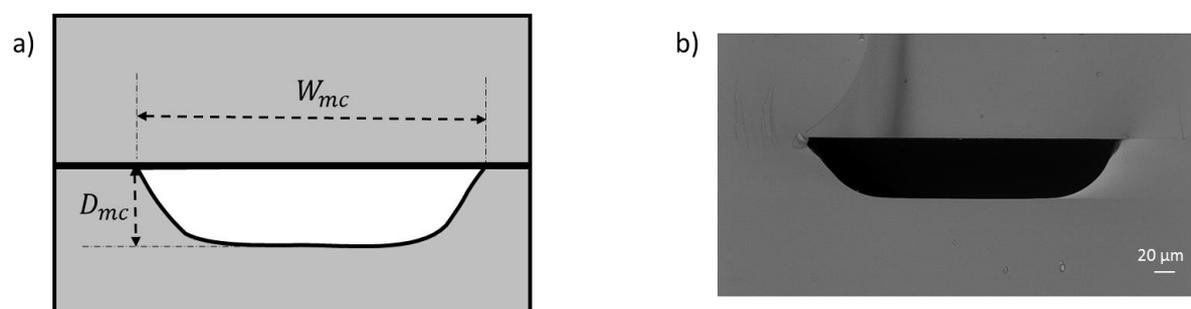
Figure 3.3: a) Schematic diagram of the geometry and dimensions of the microchannel's cross section: width (W$_{mc}$) and depth of the microchannel (D$_{mc}$). b) SEM image of the microchannel.

The plasma zone comprised of the serpentine channel after the Y-junction and before the outlet. The initial length of the serpentine channel (L_{ch}), as fabricated, was L_{ch} = 212 mm long. The channel length of 212 mm was adopted for initial studies on the effect of plasma treatment on the residence time of liquid in the reactor. Further modification of the reactor design with longer serpentine channels, L_{ch} = 395 and 595 mm, were fabricated and used for further trials on residence time. Figure 3.4 shows the schematic layout of the different versions of the microfluidic device. The later designs of the microfluidic devices with a longer serpentine channel had both the inlets and outlet positioned away from the serpentine channel with a larger distance between the side endpoints of the microchannel and the edge of the device. This was to facilitate the placement of the electrodes and to prevent electrical discharges around the outside of the devices.
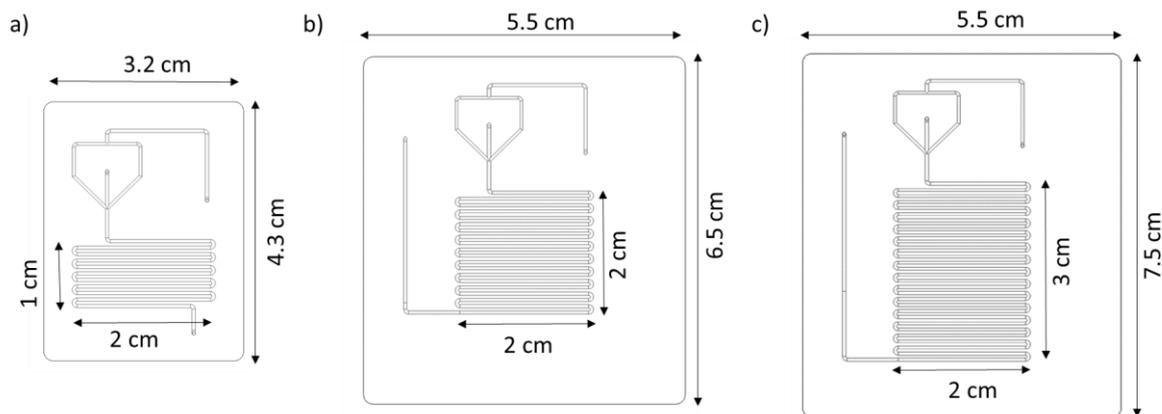
Figure 3.4: Different dimensions of the MPR used in this study: a) MPR1, b) MPR2 and c) MPR3.

3.2.1 Electrodes

Copper tape (RS Components Ltd., UK) was used as the high voltage and ground electrodes (el) in this study (Length$_{el}$ x Width$_{el}$ x Thickness$_{el}$ = 2 cm x 1 cm x 35 μm (MPR1), 2 cm x 2 cm x 35 μm (MPR2) and 2 cm x 3cm x 35 μm (MPR3)). The electrodes were aligned to the serpentine microchannel. Thus, plasma generation created between the conducting electrodes occurred in the gas space along the two-phase flow in the serpentine channel.

For visual observation of plasma generation in the microchannel between conductive electrodes placed in parallel to the serpentine channel during two-phase flow, indium tin oxide (ITO) coated glass (Length x Width x Thickness$_{glass}$ x Thickness$_{ITO}$ = 2 cm x 1 cm x 1.1 mm x 1850 Å) (ThePiHut, Haverhill Suffolk, England, UK) and conductive paint (Bare conductive Ltd., UK)

(Length x Width x Thickness$_{ITO}$ = 2 cm x 1 cm x ~35 μm) were used as high-voltage and ground electrodes, respectively. Conductive carbon adhesive tabs (Agar Scientific, Stansted Essex, England, UK) were used as electrical connection points on both electrodes. Kapton tape (RS Components Ltd., UK) was used for thermal and electrical insulation of the microfluidic reactor and the electrode. Photographs of plasma generated in the microchannel were taken using a Nikon D3200 DSLR with a 60 mm lens and 1:2.8 aperture (ISO:12800, Exposure time: 1/ 100 s) (Nikon Corp., Japan).

3.3 Experimental setup

The schematic diagram of the experimental set-up using the proposed microfluidic reactor is shown in Figure 3.5. The set-up consists of a flow control system, electric system and a sample collection zone. The liquid flow rate and gas flow were controlled using separate pressure sources to pump each fluid directly into the device: via syringe pump (Cronus Sigma 2000C, SMI-LabHut Ltd., UK) and a pressure regulator (WIKA Instruments Ltd., UK), respectively. Thus, reaching the optimum point for the flow regimes of gas-liquid two-phase flow could be achieved. The influence of various flow rates and gas pressures on flow regime is discussed in Chapter 4. Various carrier gases were supplied to the microfluidic device: Air was provided by an in-house compressor, argon (99.9995% specialty grade, BOC Ltd., UK) and oxygen (99.999% specialty grade BOC Ltd., UK).
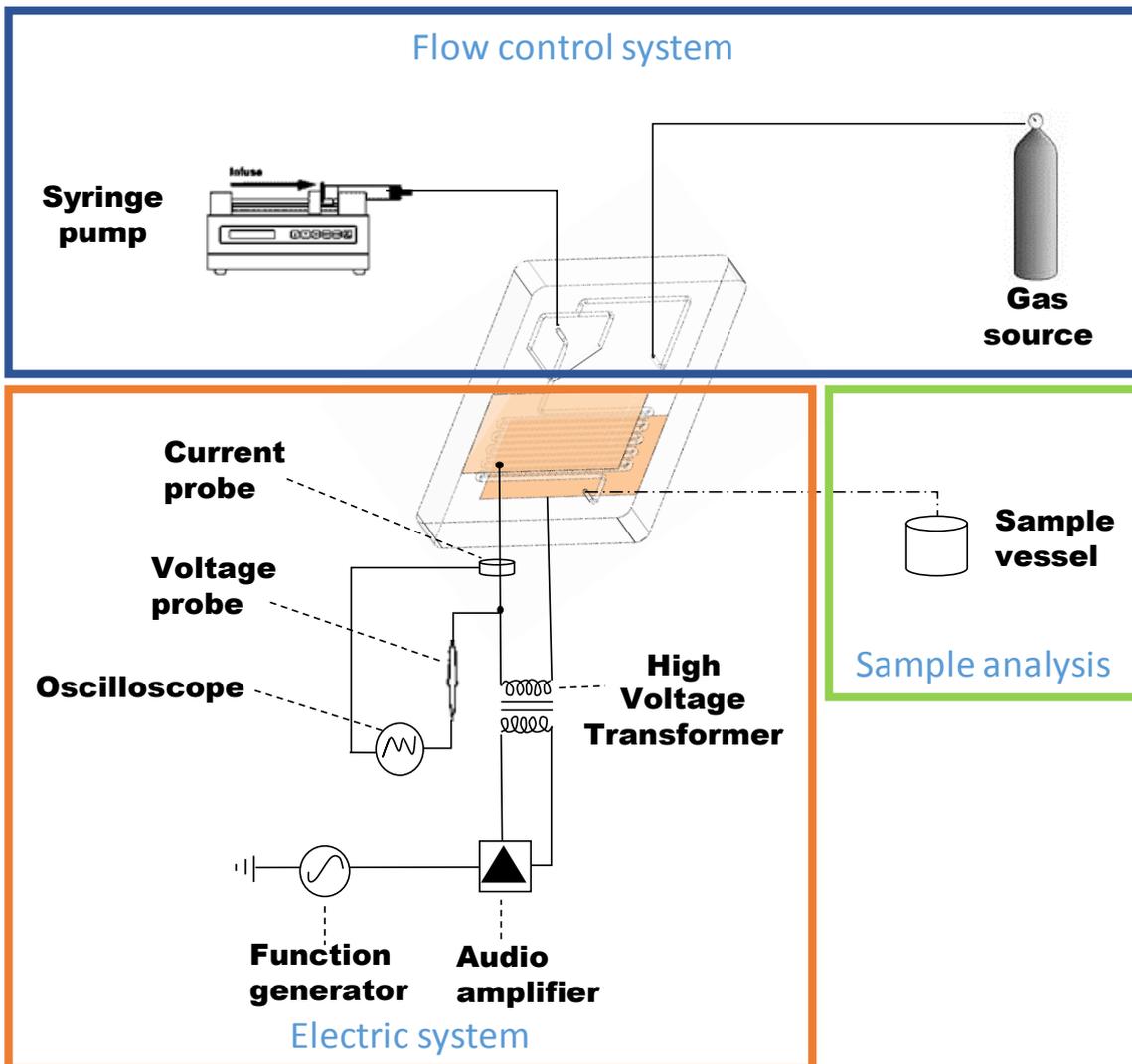
Figure 3.5: Schematic diagram of the experimental setup used for all the investigations carried out in this study.

High voltage (HV) applied to the electrodes was provided by a power supply which consisted of a signal generator (TTi TG1000), audio amplifier (ProSound 1600) and custom-built high voltage transformer (Amethyst Designs). The signal generator produced the desired sinusoidal signal and the audio amplifier amplified the output signal. The audio amplifier modulated the input voltage from the power supply to the primary side of the transformer and the transformer stepped up the voltage to levels suitable to break down the gas. Current and voltage measurements were made with a Pearson 4100 current monitor (1 V/A) and a Tektronix 1000:1 voltage probe, measured using a Tektronix DPO3014 digital oscilloscope.

3.4 Operating conditions

3.4.1 Gas pressure and liquid flow rate

An in-house regulated gas line was employed to control the gas flow rate by changing the pressure of the gas entering the inlet and the total feed liquid flow rate was controlled using the syringe pump. Although the gas and liquid sources were directly connected to the chip, a pressure drop from the connectors to the microchannel was expected. In addition, high gas pressure, greater than 1atm, accompanied with low liquid flow rate, less than 30 µL/min, led to backflow, with water flowing in the reverse direction. Prior to plasma generation, the microfluidic device was left to run for 3 to 5 minutes when liquid flow rate was changed to stabilize a steady pressure and generation of the two-phase flow. Table 3.1 shows the operated values used in this study to acquire a two-phase annular flow regime in the microchannels. Resulting flow regimes of the two-phase flow were observed in the serpentine region of the chip using food dye (Thermo Fisher Scientific, UK) in deionised water, mounted on an inverted light microscope (Zeiss Primovert). Liquid film thickness was obtained from the microscope images, with reference length scales used to calibrate the measurements of the liquid film.

Table 3.1: Operational parameters, i.e. liquid flow rate and gas pressure used with the MPR.

	Length (L_{ch}) of the serpentine channel (mm)	Liquid flow rates (µL/min)	Gas Pressure (atm)
MPR 1	212	35 - 100	$1 - 2$
MPR 2	395	35 - 100	3
MPR 3	595	35 - 100	6

3.4.2 Electrical measurements and calculations

The MPRs were powered using a HV power supply with a frequency of 17 kHz. The applied voltage(peak-to-peak) was varied using the audio amplifier, ranging from 0 to maximum of 13 kV HV source. A high voltage probe (Tektronix 1000:1 voltage probe) and current probe (Pearson 4100) connected to a Tektronix DPO3014 digital oscilloscope were used to measure and characterize the supplied power. The average power applied on the microfluidic device was calculated using 3.1 (Archambault-Caron et al., 2015):

$$P_t = \int_0^t \sqrt{V_t^2 \times I_t^2} \; dt \qquad\qquad \text{Equation 3.1}$$

where P_t is the deposited power over one period in Watts, t is the period in seconds, V is the applied voltage measured in Volts and I is the input current measured in Amperes.

3.4.3 Reactor temperature

During plasma generation in the microchannel, the temperature of the MPR was measured over time. The experimental temperature of the microfluidic device was measured with an infrared thermometer (Maplin Electronics, UK) and a thermal camera (Fluke 279 FC Thermal Imaging camera) at a distance of 20 cm above the reactor. The average temperature of the dielectric surface of the microfluidic reactor was evaluated by the measurement of the electrode temperature. Temperature readings assumed uniform heat transfer from the electrode to the dielectric surface; these readings did not take into account the cooling of the dielectric surface by heat conduction through the compressive case, incoming gas and liquid flow, bulk of dielectric material and subsequent convective transfer from electrode to surrounding air. Actual temperature measurements inside the microchannel were not possible.

Figure 3.6 shows the final assembly of the MPR used in this study. The original setup was modified to include a heatsink (2 x 2.5 cm, 3 x 6 cm) (RS Components Ltd., UK) attached on both sides of the microfluidic reactor, a thermal pad (1.5 X 2.5 cm, 2.5 x 2.5 cm, 3.5 x 2.5 cm) (Akasa Ltd., UK) to further improve electrode contact with the heatsink and a miniature cooling fan (ThePiHut, Haverhill Suffolk, England, UK) to promote air circulation. The microreactor device was fixed into a compressive case made of poly(methyl methacrylate) (PMMA) (4.5 x 5.5 x 1.5 cm) with windows to allow inlet tubing and electrical connections.
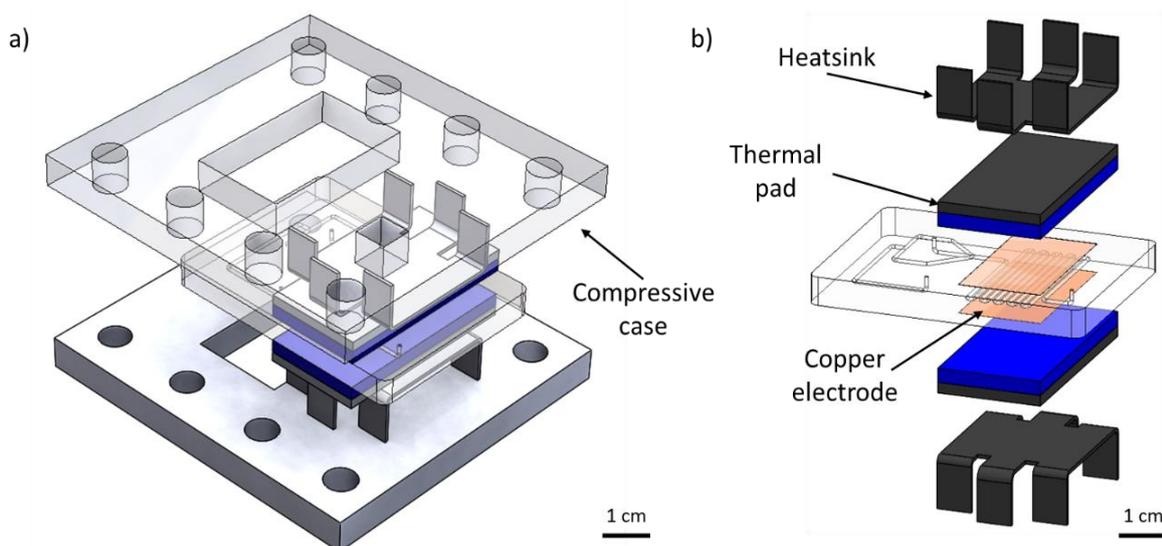
Figure 3.6: (a) Schematic diagram of the microfluidic plasma device. (b) Exploded view of the final assembly.

3.5 Analysis of MB and water samples

3.5.1 UV-Vis Spectrophotometry

Colorimetric analysis for MB solution (Sigma-Aldrich, UK) (5 mg/L), before and after plasma treatment, was performed using a Perkin Elmer Lambda 40 UV-Vis spectrophotometer, operating single beam optical systems, wavelength range of 200 – 900 nm, slit width of 2 nm and UV grade PMMA cell with a path length of 1 cm. Calibration of absorbance is based on chemical concentration according to Beer-Lambert's law (Swinehart, 1962) using Equation 3.2:

$$A = \mathcal{E}\, c\, l \qquad\qquad \text{Equation 3.2}$$

where A is absorbance, $\mathcal{E}$ is the molar extinction coefficient ($M^{-1}\,cm^{-1}$), c is the sample concentration (M) and l is the cell path length (cm). For the control experiments, colorimetric analysis was performed of 5 mg/L MB solution treated at various temperatures (30 – 100 °C) and pH values (3.0 – 10.0) without plasma treatment. MB solution was prepared at different pH values using 1 M hydrochloric acid (Thermo Fisher Scientific, UK) and 1 M sodium hydroxide (Thermo Fisher Scientific, UK) to adjust the pH of the deionized water before adding MB and measured using a pH and temperature meter (Jenway 4510 Conductivity Meter, UK). 10 mL of MB solution was continuously stirred on a hot plate magnetic stirrer (Stuart equipment, UK) with a mercury thermometer to monitor the temperature. The solution was left to cool to room temperature before analysis.

3.5.2 Liquid chromatography-Mass Spectroscopy (LC-MS)

Analysis of MB before and after plasma treatment was performed using an Agilent Technologies 6540 UHD Accurate-Mass Q-TOF LC/MS. Samples were injected into the LC through an injection valve with an injection loop of 20 μL. A 100 mm C18 column with 2.1 mm internal diameter and 2.5 μm particle size (ACE-HPLC, UK) was used and set at a column temperature of 40 °C. Gradient elution with mobile phase A (0.1% acetic acid in water) and mobile phase B (0.1% acetic acid in 100% acetonitrile) was used with a constant flow rate of 300 μL/min in total. The aforementioned mobile phases, with organic acid standard solutions, were prepared using HPLC grade reagents (Sigma-Aldrich, UK).

The mass spectrometer was operated in the positive ion mode in the mass range of 65 – 980 atomic mass units (m/z) at a rate of 1 scan per second. Samples were injected into an electron spray ionization (ESI) source at a flow rate of 20 μL/min, nebuliser pressure of 15 psig, gas flow and temperature of 5 L/min and 325°C, respectively. Nitrogen was used as the nebulising gas.

3.5.3 Ion Chromatography

Water quality standards of surface water differ due to different environmental conditions, intended human use and changes induced by treatment processes. Ion concentrations in various water samples, i.e. deionized water, soft and hard tap water samples, before and after plasma treatment were measured using high performance anion and cation exchange chromatography (Ion Chromatography Dionex Model ICS 5000, Thermo Fisher, UK). The instrumentation control, data acquisition and processing were executed by the software Chromeleon Data System version 7.2 (Thermo Scientific, Dionex). The electrical signals detected were integrated in μS (microSiemens).

Anions were analysed by the IC system, consisting of an isocratic pump, conductivity detector, an injection valve with an injection loop for 10 μL, 2 mm AG18 guard column, 2 mm analytical IonPac AS18 separation column, coupled with a 2 mm Anion Self-Regenerating ADRS 600 suppressor. All components were from Thermo Scientific, Dionex, UK. Chromatographic anion runs were carried out at 23°C under gradient elution using potassium hydroxide, 18 mM - 45 mM, as base eluent and flow rate of 250 μL/min. Cations were analysed using the same IC

system consisting of an isocratic pump, conductivity detector, an injection valve with an injection loop of 5 μL, 3 mm CG16 guard column, 3 mm analytical IonPac CS16 separation column, coupled with a 2 mm Cation Self-Regenerating CDRS 600 suppressor. Chromatographic cation runs were carried out at 60°C under isocratic elution using 39 mM methanesulphonic acid as the base eluent and flow rate of 360 μL/min. The eluents and organic acid standard solutions were prepared using HPLC grade reagents (Sigma-Aldrich, UK).

Prior to sample analyses, IC standards were measured and calibrated using Thermo Scientific Dionex Six Cation (II) standard 046070 and Seven Anion standard in deionized water 056933. These standard solutions were stored at 4°C until use. Table 3.2 shows the concentration of the ions in the standard solutions.

Table 3.2: Summary table of metal ions concentration in the standard solutions.

Cation Standard		Anion standard	
Chemical	Concentration (mg/L)	Chemical	Concentration (mg/L)
Water	(99.9%)	Hydrochloric acid	(pH 3.0 ± 0.3)
Sodium Fluoride	20	Lithium Chloride	50
Sodium Chloride	30	Sodium Chloride	200
Sodium Nitrite	100	Ammonium Chloride	250
Sodium Bromide	100	Potassium Chloride	500
Sodium Nitrate	100	Magnesium Chloride	250
Potassium Phosphate (monobasic	150	Calcium Chloride	500
Sodium Sulphate (dibasic)	150		

3.6 Microbiology

3.6.1 Microorganisms

E. coli (NCIMB 10244) and *P. aeruginosa* (ATCC 47085) were obtained from the National Collection of Industrial, Food and Marine Bacteria, UK and the American Type Culture Collection, US, respectively. Both were used as model microorganisms for plasma treatment using the MPR. Stocks were stored at -80°C in a freezing mix containing di-potassium hydrogen phosphate (12.6 g/L), potassium dihydrogen phosphate (3.6 g/L), tri-sodium citrate (0.9 g/L),

ammonium sulphate (1.8 g/L), glycerol (300 g/L), magnesium sulphate (1.8 g/L) and deionised water (1100 mL). All components used to prepare the freezing mix were from Thermo Fisher Scientific, UK. Frozen stocks were thawed and streaked on nutrient agar media (Oxoid, UK) under sterile conditions and incubated at 37°C for 24 hours. The inoculated agar plates were kept at 4°C and replaced every 4 weeks. All media such as nutrient broths, phosphate buffered saline (PBS) and agar plates were autoclaved at 120°C for 20 minutes.

3.6.2 Bacterial growth

The microbial culture was prepared for the cultivation of *E. coli* and *P. aeruginosa* as follows. A loop of the microbial culture from previously prepared agar streak plate was inoculated into 10 mL of sterilized 13 mg/L nutrient broth (Oxoid, UK). Broth cultures were left to grow at 185 rpm in a rotary shaker at 37°C for 15 hours. The nutrient broth contained Lab-Lemco beef extract, yeast extract, peptone and sodium chloride at concentrations of 1.0, 2.0, 5.0 and 5.0 g/L, respectively.

Antibiotic susceptibility of both bacteria was determined using antibiotic susceptibility discs (Mastring-S M26 for Gram-negative rods, Mast Group Ltd., UK). Table 3.3 shows the list of antibiotics in Mastring-S M26. 100 μL of the bacteria grown in nutrient broth ($OD_{600nm} = 1.0$), 10-fold dilution, was spread on nutrient agar plate. Antibiotic susceptibility discs were placed on the inoculated plates, left to grow at 37°C for 24 hours and inhibition zones were measured using callipers (Mauser, Switzerland). Bacteria strains were considered according to the inhibition zones produced. This method was used to confirm the presence of streptomycin resistant *E. coli* and ampicillin resistant *P. aeruginosa*.

Table 3.3: Summary table of antibiotics and concentration in Mastring-S M26.

M26	
Antibiotic	Concentration
Ampicillin	25 μg
Chloramphenicol	50 μg
Colistin Sulphate	100 μg
Kanamycin	30 μg
Nalidixic acid	30 μg
Nitrofurantoin	50 μg
Streptomycin	25 μg
Tetracycline	100 μg

3.6.3 Microbial culture in water

A PBS tablet (Oxoid, UK) was dissolved in 100 mL of deionised water, autoclaved at 120°C for 20 minutes, and filtered through a 0.22 μm membrane (Pall Acrodisc).This solution was used for washing and diluting the microbial culture. The resulting PBS contained sodium chloride (8.0 g/L), potassium chloride (0.2 g/L), di-sodium hydrogen phosphate (1.15 g/L) and potassium dihydrogen phosphate (0.2 g/L) with a pH of 7.3 ± 0.2 at 25°C). The resulting culture was centrifuged at 3000 rpm for 5 minutes. The resulting pellet was washed by suspending the pellet in filtered PBS solution, re-centrifuged at 3000 rpm for 5 minutes and re-suspended in filtered PBS. The microbial suspension was diluted in filtered PBS to obtain an optical density (OD$_{600nm}$) of 0.4 for *E. coli* and *P. aeruginosa* using a Jenway 6305 spectrophotemeter, which corresponds to ~10^8 CFU per mL.

3.6.4 Microbiological analysis

3.6.4.1 Microbial adhesion test

The microfluidic reactor was assessed for blockage and bacterial adherence to the microchannel walls. Bacteria suspended in PBS with a concentration of 10^8 CFU was left for 24 hours continuously infused into the microfluidic reactor using each liquid flow rates of 35, 40, 60 80, 90 and 100 μL/min and 1 atm gas pressure. Excess bacterial suspension in the microchannel was removed and the channel dried with filtered air driven by the syringe pump for 1 hour. 1% w/v fluorescein salt/PBS mixture (excitation wavelength of 485 nm and emission filter of 520 nm) (Sigma-Aldrich, UK) was pumped into the microfluidic reactor and excess fluid removed with pumped filtered air. The microchannel was visualised using epifluorescent microscopy (Nikon Eclipse E600 epifluorescence microscope, Tokyo, Japan) mounted with an F-View II black and white digital camera (Soft Imaging System Ltd., Helperby, UK, supplied by Olympus, Hertfordshire, UK). This system was operated using Cell-F image visualisation software (Olympus, UK) for image capture and analysis. The microchannel was focused using a 100X objective to image the fluorescence intensity of the microchannel. The presence of fluorescence at an increased intensity indicated the adherence of bacteria.

3.6.4.2 16S Sequencing

The 16S rRNA gene sequencing was used as a standard method to confirm the bacterial used in this study. For the DNA extraction, 500 µL of overnight microbial culture was transferred to a sterile Eppendorf tube, centrifuged at 5000 rpm for 5 minutes, the pellet was washed and re-suspended in 500 µL of molecular grade water (MGW). The sample was heated at 100°C for 5 minutes, centrifuged at 5000 rpm for 5 minutes and 100 µL of the supernatant transferred to a sterile Eppendorf tube. This contained the template DNA. 1 µL of the extracted DNA was mixed with 5 µL of Biomix (Bioline, UK), 3 µL of molecular grade water (MGW) and 1 µL of 16s primer mix, containing primers 27F (5′-AG AGT TTG ATC MTG GCT CAG-3′) and 518R (5′-ATT ACC GCG GCT GCT GG-3′) (Frank et al., 2008; Abbas et al., 2017) with a final concentration of 10 pmol. MGW was used as control with no DNA. 16s primer mix was used to amplify a hypervariable region of the 16S rRNA gene.

Polymerase Chain Reaction (PCR) was performed using a GTQ-Cycler 96 (Hain Scientific). The following PCR conditions were used: initial denaturation at 94°C for 2 mins, then five cycles of 94°C for 30 s and 40°C for 1 min and then 30 cycles of 94°C for 30 s, 50°C for 1 min and 72°C for 3 min. The PCR product was analysed by agarose gel electrophoresis to check the size and that the control was clear. Agarose (1.5 g) was dissolved in 100 mL of TBE (Tris/Borate/EDTA) buffer and cast into a gel tray with a well comb in place. 5 µL of the sample was run on the agarose gel with 2 µL of OrangeG loading dye per sample for visualisation alongside a 100bp Hyperladder (Bioline). The PCR product was cleaned using ExoSAP (Thermo) to remove excess primer and unincorporated dNTPs. The ExoSAP protocol consisted of mixing 5 µL of post PCR product with 2 µL of EXOSAPIT reagent, leaving it to incubate at 37°C for 15 minutes followed by 80°C for 15 minutes. Following the ExoSAP protocol, 3 µL of the clean PCR product was mixed with 6 µL of MWG and 1 µL of either forward or reverse 16S primer. The purified sequencing product was then ready for Sanger sequencing. Sanger DNA sequencing was performed using BigDye v3.1 terminator and run on an ABI 3730 48-well capillary DNA Analyser (Applied Biosystems, California, USA). These 16S sequences obtained by Sanger sequencing were compared to known sequences of 16S ribosomal RNA (bacteria and archaea) using the Basic Local Alignment Search Tool (BLAST) to obtain the highest % similarity (NCBI 2015, 2019).

3.6.4.3 Spread plate method

The concentration of viable cells was evaluated using a standard spread plate method. Agar plates were prepared using 28 grams of nutrient agar (Oxoid, UK) per litre of deinoized water. The agar solution was sterilized and cooled to 50°C before adding the desired antibiotic. Selective petri dishes were prepared with streptomycin (50 µg/mL) for *E. coli* and ampicillin (100 µg/mL) for *P. aeruginosa*. For mixed bacterial cultures, MacConkey agar (Oxoid, UK) was used for selective differentiation of both bacteria, i.e. *E. coli* colonies appeared as pink colour while *P. aeruginosa* colonies exhibited no colour. Serial dilutions of the bacterial suspension were prepared, with dilutions up to $1:10^8$. Diluted samples of 100 µL were spread onto the surface of the agar plate using a sterile spreader. The inoculated Petri dish was left to incubate at 37°C for 24 hours before colony counting. The numbers of colonies formed were counted to determine the concentration of bacteria in the undiluted sample as CFU/mL. The limit of detection for spread plating 100 µL of the diluted sample was 1 CFU for $1:10^8$ dilution and the limit of quantification from a countable range of $25 - 150$ CFU.

Minimum inhibitory concentrations (MIC) for *E. coli* and *P. aeruginosa* were determined by varying the concentration of streptomycin and ampicillin and assessing bacterial growth using CFU counts. *E. coli* and *P. aeruginosa* inoculum with 10^8 CFU/mL were spread on plates containing various concentrations of 50 to 500 µg/mL of streptomycin or ampicillin and left to grow at 37°C for 24 hours. MIC was defined as the minimum concentration to inhibit visible growth (Wiegand et al., 2008). In each experiment, CFU counts in the uninoculated PBS were measured prior to inoculation for plasma treatment for viable growth of bacteria. Samples were collected before infusion of the bacterial suspension into the microfluidic reactor and from the outlet to compare the CFU to account for possible bacterial adhesion to the tubing and microchannel walls. Before each experiment, the microfluidic reactor, syringe and PTFE tubing were sterilized with 2% v/v sodium dodecyl sulphate (Sigma-Aldrich, UK) followed by rinses of autoclaved deionised water and ethanol. The microfluidic reactor, syringe and tubing were wrapped in autoclave packaging and sterilised for 20 minutes at 120°C. Three repeats of CFU measurements in uninoculated PBS and inoculated PBS before and after plasma treatment were carried out and compared.

3.6.4.4 Live/Dead Assay

Live/Dead stains were diluted in dimethyl sulfoxide (Sigma-Aldrich, UK) according to the manufacturer's instructions and individually diluted in a 1:10 ratio in sterile distilled water. Diluted propidium iodide and SYTO 9 were mixed together in a 1:1 ratio and 10 μL was spread across the sample, which was left to air dry in the dark. Samples were stored in the dark at 4°C and analysed for potentially viable or damaged cells using epifluorescent microscopy as described in section 3.6.5.3. Under the microscope, viable cells appeared green while non-viable or damaged cells appeared red. The percentage bacterial coverage of live and dead bacteria was measured using separate selective UV filters for propidium iodide (excitation wavelength of 535 nm and emission filter of 617 nm) and SYTO 9 (excitation wavelength of 485 nm and emission filter of 498) across the same field of view. A minimum of 10 fields of view using each UV filter were taken per sample.

To examine cell viability before and after plasma treatment, samples were treated using a live/dead stain (LIVE/DEAD™ BacLight™ bacteria viability kit, Invitrogen, Scotland). 10 μL of collected bacterial samples, before and after plasma treatment, were loaded onto the surface of clean stainless steel coupons (L x W x H: 1.5 mm x 1.5 mm x 1 mm) (SS316 with 2B finish) and allowed to air dry in a microbiological Class II safety hood. Before bacterial samples were loaded on stainless steel coupons, surfaces were initially cleaned with 50% nitric acid, followed by sterile deionised water, ethanol and finally rinsed with sterile deionised water for 15 minutes each, blown with compressed air and left to dry in a microbiological Class II safety hood. Populations of live and/or dead bacteria without plasma treatment were investigated as controls to validate that viable bacteria were SYTO9 positive (green) and nonviable bacteria were propidium iodide positive (red). Control for dead bacterial cells was prepared by centrifuging, at 3000 rpm, 5 mL of the microbial culture (OD600: 0.4 for both *E. coli* and *P. aeruginosa*), washing the pellet with PBS, re-centrifuged, resuspended in 5 mL of 70% ethanol and left for 1 hour. For live bacterial controls, microbial cultures were centrifuged and suspended in 5 mL of PBS. For mixed cultures, equal volumes of live and dead microbial cultures were combined and vortexed in sterilised Eppendorf tubes.

3.6.4.5 Scanning Electron Microscope for microbial samples

Stainless steel coupons loaded with bacterial samples as described in section 3.6.5.3 and unloaded coupons as a control were immersed in 4% glutaraldehyde (Sigma-Aldrich, UK) overnight at 4°C to fix the bacterial cells. 10 mL of autoclaved and filtered dionised water was used to clean the surface of the coupons at a 45° angle. Sample coupons were left to dry for 1 hour in a microbiological Class II safety hood followed by sequential immersion in ethanol (Sigma-Aldrich)/water mixture (30%, 50%, 70%, 90% and 100%) for 10 minutes for each concentration and left to dry in the Class II fume hood for 1 hour. Prior to SEM analysis, samples were stored at room temperature in a desiccator with silica gel. Samples were attached to aluminium pin stubs with adhesive carbon tabs before sputter coating with gold/palladium coating (Model: SC7640, Polaron, Au target, coating time: 30 seconds, 5 mA current. 800 V). The SEM was carried out using a Supra 40VP with SmartSEM software (Carl Zeiss Ltd. UK) and images were taken using an acceleration voltage of 2kV and a working distance of approximately 6 mm.

3.7 Statistical analysis

The standard error of the means are shown on graphs and tables using error bars, and lower/upper limits, respectively. p values were determined at the 95% confidence level using two-way ANOVA. IBM SPSS Statistic (Version 24) was used to perform statistical calculations. Post hoc analysis with Tukey's test was performed for all data. The level of statistical significance was set at $p < 0.05$ for all tests. (IBM SPSS Stat., Ver. 24)

Chapter 4 Device characterisation of the microfluidic plasma reactor

This chapter investigates the internal flow regimes, behaviour of the plasma discharge, and the effect of non-thermal plasma on the ion concentrations of water using the MPR.

4.1 Introduction

Non-thermal plasma is known to produce long- and short-lived chemical species in the plasma-liquid interface and in water at ambient conditions (Gorbanev et al., 2016). Interaction of non-thermal plasma and liquid has led to several studies addressing a variety of applications and prospective remediation such as surface modification (Inagaki, 2014; Desmet et al., 2009), analytical chemistry (Karanassios, 2004; Yuan et al., 2011), synthesis (Yanling et al., 2014; Peng et al., 2018a), material processing (Taylor and Pirzada, 1994), food processing (Thirumdas et al., 2015) and environmental remediation (Mizuno, 2007; Liao et al., 2017; Surowsky et al., 2015). However, despite the advantages of non-thermal plasma, implementation outside of the laboratory and into real life applications or industry, specifically using direct treatment of water with non-thermal plasma treatment, has yet to occur.

So far, non-thermal plasma in water industries was generated in remote discharge reactors to produce ozone, which is subsequently transported to water under treatment. However, several studies have demonstrated the superiority of direct plasma treatment compared to ozone and emphasize the advantage of direct plasma-liquid interaction to utilize plasma processes and highly reactive chemicals formed in plasma and the plasma-liquid interphase such as UV radiation and the hydroxyl radical. Yamatake *et al* compared bubble discharge, i.e. plasma generated in gas bubbles formed in water, with remote discharge for ozone production and found decomposition of acetic acid in bubble discharge but no decomposition using the remote discharge reactor (Atsushi Yamatake et al., 2006a). This difference was explained with the production of oxygen radicals, excited gas atoms and hydroxyl radicals through plasma-liquid interaction and none in remote discharge due to short lifetimes before they can reach the water under treatment. Dobrynin *et al* compared remote discharge and gas discharge i.e. plasma generated above liquid, for treatment of *Bacillus* spores and found a higher rate of inactivation through direct treatment using gas discharge than remote discharge (Dobrynin et al., 2010). In addition to utilizing reactive chemicals in plasma with short lifetime, inactivation

of the *Bacillus* spores was further assisted by the UV radiation in gas discharge but not in remote discharge. Other than reactive chemicals with short lifetimes and plasma processes, long-lived reactive species transferred from the gas phase into water or through recombination processes and rapid conversion of short-lived chemicals, can further enhance the treatment efficiency of contaminants in water (Jiang et al., 2014; Foster, 2017; Gorbanev et al., 2016).

Due to the short lifetime of some of the reactive chemicals generated in liquid or the plasma-liquid interface such as the hydroxyl radical with a lifetime of 2.7 microseconds (Attri et al., 2015), studies have focused on investigating the contribution of longer-lived chemicals for water treatment and the quality of water, specifically long-lived reactive oxygen species (ROS) and reactive nitrogen species (RNS). Some studies used remote discharge to produce plasma-activated water (PAW) and added it to the water for treatment; PAW has been commonly investigated for the disinfection of water but its application in chemical degradation is yet to be investigated (Gorbanev et al., 2016; Chauvin et al., 2017; Back et al., 2018; Judée et al., 2018; Zhou et al., 2018; Pai et al., 2018). Zhang et al. reported effective disinfection of *Staphylococcus aureus* by ROS in PAW using 2% oxygen in argon carrier gas (Zhang et al., 2013). Taylor et al. attributed long-lived ROS and RNS generated in PAW using air as the carrier gas with the inactivation of *E. coli.* Zhou *et al* identified peroxynitrite, generated from reaction of nitrite and hydrogen peroxide, in PAW using air as the carrier gas as a critical chemical for the inactivation of *E. coli*. Chauvin *et al* demonstrated effective inactivation of *Colletotrichum gloeosporioides* using PAW, where a higher activation rate was observed with PAW generated using air than oxygen as the carrier gas (Wu et al., 2018). Using oxygen as the carrier gas, ROS (hydrogen peroxide and ozone) were detected while RNS (nitrate and nitrite) and ROS were both detected using air, which was attributed to the inactivation of *C. gloeosporioides*; the mechanism involving RNS for the inactivation was not explained. Interestingly, some studies have shown future agricultural application of long-lived chemicals in PAW other than in the biomedical field. In a review by Thirumdas *et al,* direct plasma interaction with water or indirect interaction using PAW can be applied as an irrigation liquid for seed germination (Thirumdas et al., 2017). Judee *et al* used PAW as an irrigation liquid for plant growth and found increased growth of coral lentils, though thresholds of the RNS and ROS level in PAW for growth may differ when applied with different families of seeds (Judée et al., 2018). Wang *et al* used PAW

for food sterilization, inactivating *Staphylococcus aureus* inoculated on strawberries and found no changes in the physical properties of the PAW treated strawberries (Ma et al., 2015).

These initial studies have demonstrated the benefits of the long-lived chemicals as prospective fertilizers, food sterilizers and as residual antimicrobial agents in water for prevention of subsequent contamination after treatment (Thirumdas et al., 2018; Kaushik et al., 2018). In addition, chemical quality of PAW can last for days; Buendia et al. observed the plasma effect on pH and nitrate lasting for at least 14 days; nitrate levels increased during and after treatment, which was assumed to be from the conversion of nitrite to nitrate (Buendia et al., 2018). However, these long-lived species could pose a risk to the environment and individuals who consume such water on a regular basis. One of the major cause of eutrophication is an excess of nutrients in water, most commonly inorganic nitrogen and phosphorous (Yang et al., 2008). Formation of ammonium, nitrites and nitrates in plasma-activated water are implicated as an additional source of nutrient pollution when released in to aquatic environments (González et al., 2008; Lunau et al., 2013). Inorganic ions such as nitrates are known to be a health hazard due to their metabolic reduction to nitrite causing a condition called methemoglobinemia, a blood disorder where a low level of oxygen is present in blood that can result in cyanosis (Fewtrell, 2004). Thus, the overall quality of plasma treated water in the future may require legal compliance with specific standards and guidelines for certain applications. For example, with drinking water, ion concentration such as nitrates over the UK regulated standard level, 50 mg/L, impairs the potability of plasma treated water (DWI, 2010). However, stricter regulation of setting nitrate levels between 1.5 and 4 mg/L has been proposed to meet good ecological status in surface freshwater and groundwater used for abstraction of potable water (HC, 2018).

Several studies have shown that levels of these ions present in water after plasma treatment depends on various factors such as carrier gas, power consumption, plasma density, type of plasma reactor and treatment or residence time of liquid in plasma. Liu *et al* reported a decrease of RNS (nitrite and nitrate ions) in water when the air gap increases; the concentration of nitrite was lower than nitrate due to reaction with ozone or with nitrate (Liu et al., 2016). Judee at al. observed similar trends of increasing concentration of nitrate, nitrite, ammonia, ammonium ions and hydrogen peroxide in tap water as treatment time increases;

bicarbonate concentration decreases as treatment time increases, which was attributed to conversion into gaseous carbon dioxide but yet to be validated (Judée et al., 2018). Bafoil *et al* compared nitrate ion in tap and deionised water after plasma treatment and found higher nitrate concentration in tap water compared to deionised water (Bafoil et al., 2018). Pai *et al* observed direct correlation between nitrite generation and power, with higher concentration of nitrite was generated using higher power input (Pai et al., 2018). Peng *et al* compared direct plasma treatment of water using spray discharge and gas phase discharge and found two times higher fixation rate of nitrite, nitrate and ammonium using the spray discharge (Peng et al., 2018b). The observed result was attributed to the short distance between plasma and the spray liquid and thus allow faster dissociation of nitrogen to react with hydrogen or hydroxyl radical to form nitrate and nitrite. By using oxygen, less production of RNS in water benefits the process, specifically with plasma reactors in static configurations operating in the range of hours for treatment, but due to cost, air was widely used in most studies. Although the added benefit of long-lived species in water can further enhance the efficiency of PWT, production of high nitrogen containing effluent after treatment will require additional removal process through chemical reduction or further diluting the solution. However, such applications increase operational cost and would not be effective when applied in large scale where more concentrated solutions are produced.

In the present work, the effect of plasma generated in a MPR on water composition in terms of ion levels was investigated. To the best of our knowledge, ion measurements in plasma treated water using a microfluidic device has not yet been reported previously. The aim of this chapter is to investigate the internal flow regimes, behaviour of the plasma discharge and evaluate the presence and concentration of ion species in plasma treated water using a MPR. We focus on the relationship between ion concentration and residence time of liquid in plasma.

4.2 Experimental set-up

The experimental reactor set-up is as described in Chapter 3.3. A non-thermal plasma generated by a DBD set-up using a microfluidic reactor and air carrier gas at atmospheric pressure was evaluated. The MPR was powered using a HV power supply with a frequency of 17 kHz and applied voltage of 10 kV. Gas-liquid two-phase flow in the microchannel was

established, in a microfluidic reactor with 100 μm channel depth, gas flow and liquid flow rate controlled at 1 atm and 35 to 150 μL/min, respectively. Water from three different sources was used in this investigation: Milli-Q water,soft tap water sourced from Manchester Metropolitan University, and hard tap water sourced from the University of Hull. Tap water samples were allowed to run to waste for 5 minutes to remove stagnant water from the distribution system and then collected and filled to the brim of a high-density polyethylene 1 L bottle. The water samples were filtered through a 0.22 μm syringe filter (Pall Acrodisc) and processed within 48 hours of collection.

The initial temperature of the water samples was room temperature, approximately 22°C. Samples were directly injected (10 μL for anion and 5 μL for cation) into the ion chromatograph within 30 minutes of plasma treatment. Ion chromatography (IC) was used as a reference method for determination of ions in the water samples before and after plasma treatment. A description of the equipment has been presented in Chapter 3.5.3. Four dilutions (dilution factor of 10^1, 10^2, 10^3 and 10^4) of the standard solution (Thermo Scientific Dionex Six Cation (II) standard 046070 and Seven Anion standard in deionized water 056933) were used to plot the calibration curve of the peak area against concentration. The standard chromatograms for both anions and cations detected using IC can be seen in Figure S4.2 in the appendix. Both cations and anions of interest were separated completely within a total run time of less than 15 minutes. The retention times of the anions and cations with their relative standard deviation obtained using a known standard solution are presented (Table S4.1 in the appendix).

4.3 Results and Discussion

4.3.1 Flow characterisation

Multiphase flows are created when two or more immiscible constituents, such as liquid and gas, are simultaneously injected and come into contact in closed microchannels. The immiscible phases can form different flow regimes, which depend on acting forces such as surface tension, viscosity, inertia and gravity (Taitel and Dukler, 1976; Coleman and Garimella, 1999). Microscopic images were acquired showing the bottom view of the microfluidic device, with various flow regimes observed depending on the flow rates of gas and liquid (Figure 4.1). Liquid was injected into the microfluidic devices at flow rates between 30 and 150 μL/minute

and gas flow pressures at 1 and 2 atm in 100 and 50 μm deep channels respectively. In microfluidic devices, small variations in the flow rate conditions can lead to flow regime transitions, i.e. from stratified to annular flow and annular to plug flow patterns (Taitel and Dukler, 1976).
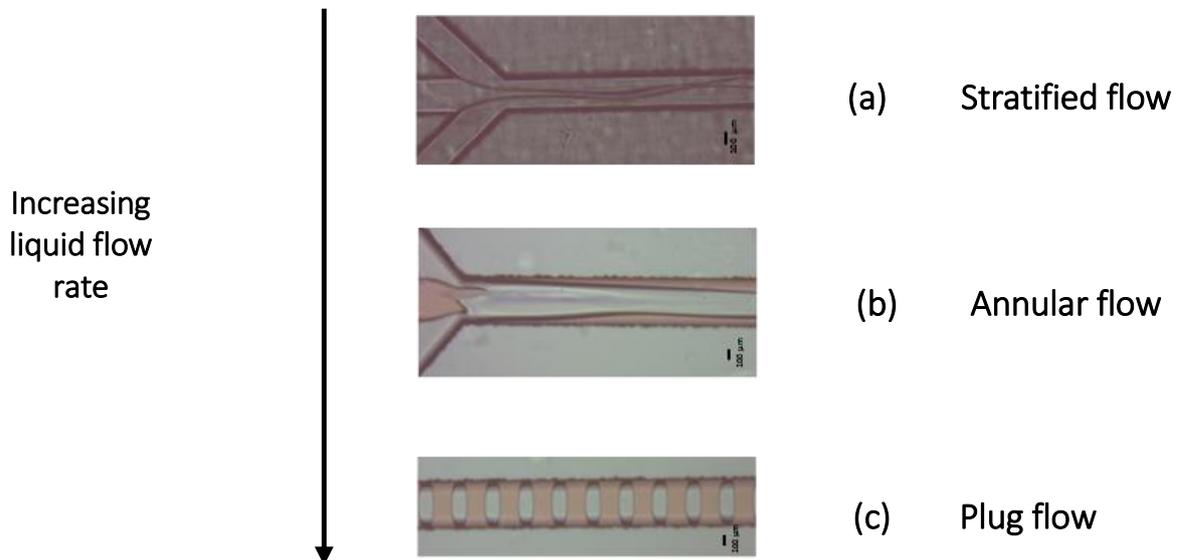
Figure 4.1: Optical microscope images of various dual phase flow regimes using 1 atm gas pressure and various liquid flow rates of less than 35 μL/min for (a) stratified flow, 35-100 μL/min for (b) annular flow and greater than 100 μL/min for (c) plug flow and 1 atm gas flow pressure of compressed air in a 100 μm microchannel depth.

In the system, annular and plug flow were the two major flow regimes observed depending on the applied flow conditions. Annular flow was sustained at liquid flow rates between 35 - 100 μL/minute (Figure 4.2) while plug flow was observed at flow rates greater than 100 μL/minute in 100 μm deep channels. Liquid flow rates below 35 μL/minute led to the eventual failure (leaking) of the syringe containing the liquid. This was because the liquid flow rate was insufficient to prevent gas from passing back through the liquid inlet channels and into the syringe.

	100 μm channel depth (1 bar gas pressure)	50 μm channel depth (2 bar gas pressure)
>100 μl/minute		
100 μl/minute		
75 μl/minute		
50 μl/minute		
35 μl/minute		
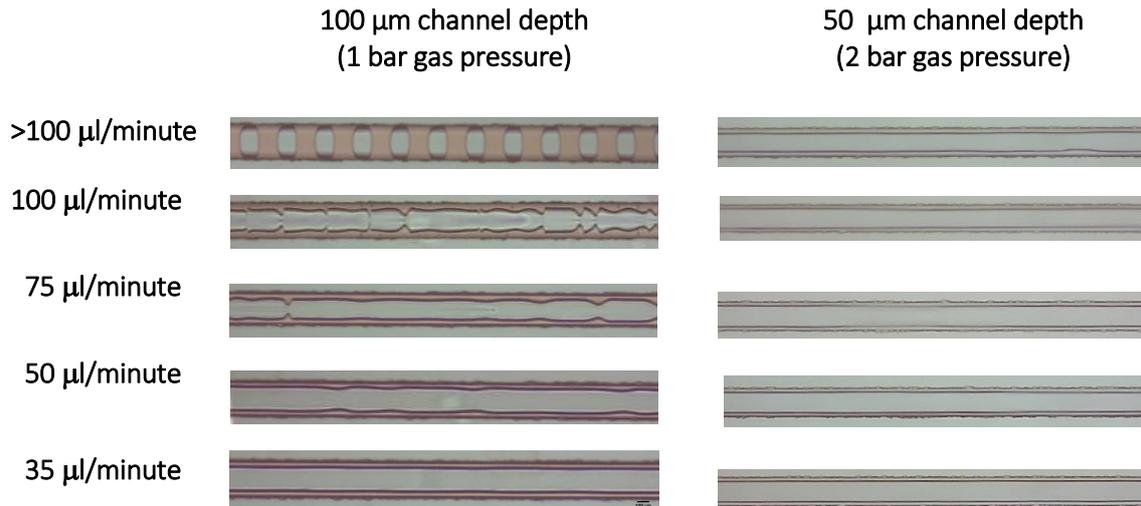
Figure 4.2: Optical microscope images of the annular flow regime observed using various liquid flow rates, 100 and 50 μm channel depth using 1 and 2 atm gas pressure of compressed air, respectively.

The generation of stratified flow was transient and not generated under any of the flow conditions employed due to the attraction between the glass microchannel wall and the liquid column at both low and high flow rates, resulting in annular flow or plug flow. Huh *et al* used a vacuum pump attached to the outlet to achieve stratified flow in a straight channel configuration (Huh et al., 2002) while Shahriari *et al* further increased the hydrophobicity of the channel walls through deposition of fluorosilane (Shahriari et al., 2016). However, such strategies were not studied with the current set-up since a vacuum pumping system may provide enough drawing capacity to attain stratified flow but the U-bends of the serpentine channel impede the gas flow and leads to low pressure areas. This result to flow regime transition caused by water attracted to the walls (Rosaguti et al., 2004; Maharudrayya et al., 2006). This includes plasma reacting and leading to surface modification of the fluorosilane film with etching reactions (Williams et al., 2003). Prevention of transition to plug flow is important, as this leads to an effective reduction in the plasma-liquid interfacial area, which influences the degradation of contaminants in liquid treated by the device (Gobert et al., 2017). Annular flow was then employed to test the plasma discharge within the microfluidic devices. With annular flow, the liquid is expelled from the centre of the microchannel and flows as a thin film along the channel wall while gas flows continuously in the middle, providing a continuous gas core for discharge. Liquid flow rates were set to 35 - 100 μL/minute as minimum and maximum to avoid flow regime transition, or gas entering the sample syringe.

4.3.2 Film thickness and Residence time

Flow rates between 35 - 100 µL/min of liquid and 4-8 mL/min of gas flow at 1-2 atm gas pressure were further investigated. These conditions produced a thin film of liquid on the walls of the microchannel, enabling control of two key parameters for plasma water treatment: liquid film thickness and residence time. Both parameters are critical in the control of mass transfer of the plasma species into the bulk of the liquid and the plasma-liquid interaction in the MPR.

In general, the microfluidic device operated with liquid films in the order of micrometres and residence times of seconds, compared to batch type plasma reactors reported in literature with residence times in the order of several minutes or hours and film thicknesses of several millimetres (Dojčinović et al., 2011; Vanraes, 2016; Jones and Raston, 2017; Aziz et al., 2018; Krupež et al., 2018). The mean residence time of the solution in two-phase annular flow along the plasma discharge zone was calculated as the ratio of the inner volume of the reactor to the volumetric flow rate (Fogler, 1999), ranging from 3 - 9 seconds and 1 - 5 seconds in 100 µm and 50 µm channel depths, respectively. Thin film characteristics were adjusted by varying the liquid flow rate, with the average film thickness found to increase as a function of liquid flow rate. Thin liquid films were achieved at low flow rates of less than 50 µL/min, with an estimated liquid film thickness, ranging from 60 to 100 µm and 40 to 60 µm in 100 µm and 50 µm channel depths, respectively. The stability of the liquid film observed in the microchannels was reduced at higher flow rates. Film thicknesses varied over time using flow rates greater than 35 µL/min in 100 µm deep channels. Less surface deformation of the liquid film was observed in the 50 µm channel depth compared to 100 µm using similar liquid flow rates but with higher gas flow pressure (Figure 4.2). It is possible that surface deformation may have an effect on plasma stability, which is likely to be detrimental to effective treatment, but it is also likely to lead to greater mixing which should enhance treatment (Bruggeman et al., 2007).

Residence time and the liquid film thickness are important parameters with significant effects on maximizing plasma-liquid interfacial area and mass transfer of plasma induced species into the bulk of the liquid (Malik, 2010; Foster et al., 2018). Highly reactive species have inherently short lifetimes, i.e. approximately microseconds for solvated electrons, hence they do not have

much time to migrate into the liquid being treated and react as desired with the contaminants in the sample (Foster et al., 2018). Therefore, it is advantageous to have as thin a layer of water as possible to maximise the effectiveness of the plasma treatment process.

4.3.3 Electrical characterisation

With the MPR, the gas space and liquid film are effectively isolated from the circuit. An illustration of the main capacitive components, i.e. the dielectric barrier and gas (Figure 4.3).
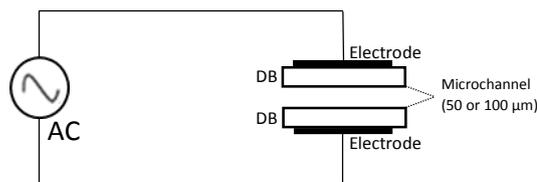
Figure 4.3: Schematic (a) representation and electrical equivalent circuit of the microfluidic chip.

Characteristic current-voltage (I-V) sinusoidal waveforms of a DBD generated in the microfluidic device using flowing air and deionized water is shown in Figures 4.4 and 4.5. The current waveform, with numerous narrow peaks was observed with the microfluidic device operating DBD, where discharge is generated within a gas filled cavity in the form of filamentary streamers. In this case, each narrow peak represents plasma filaments passing across the channel of the MPR. As the applied voltage was increased, the number of plasma filaments observed increased in number and amplitude (Figure 4.4). The use of a dielectric barrier along the discharge path prevents the filamentary discharge transforming to an arc or spark resulting from an increase applied voltage and this allows the discharge to be sustained at low input power (Brandenburg, 2017).

Applied voltage (p-p)	Frequency : 17 kHz
1 kV	
3 kV	
5 kV	
7 kV	
9 kV	
10 kV	

Time (Seconds)
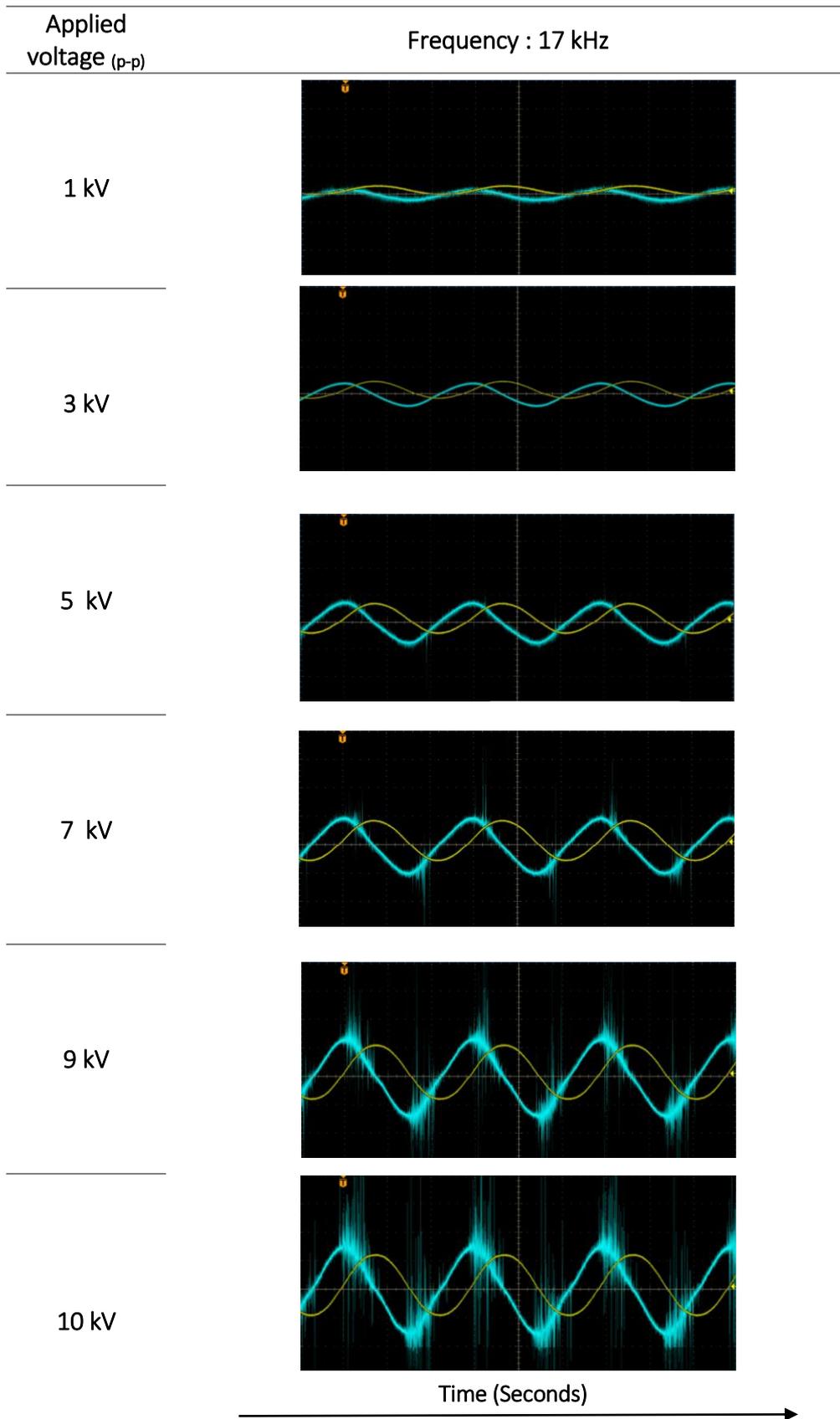
Figure 4.4: Applied voltage and discharge current at an inlet air pressure of 1 atm, 100 µL /min liquid flow rate, 2 mm barrier thickness and a channel depth of 100 µm. Current traces are shown in green while voltage traces in yellow.
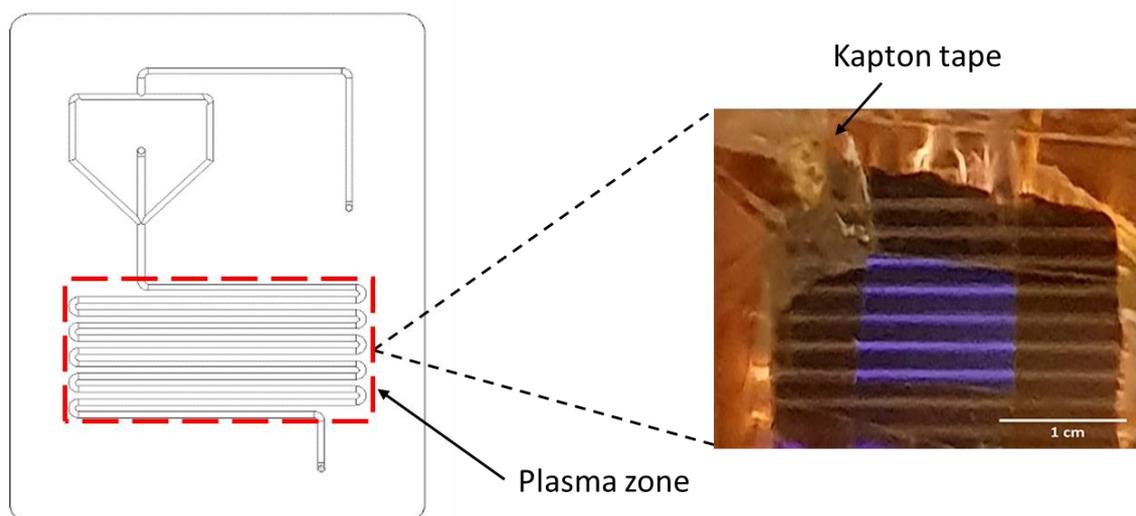
Figure 4.5: Photograph of chip during plasma generation using an ITO electrode (indium tin oxide) top view (Frequency: 17 kHz, Applied voltage (peak-to-peak): 12-13 kV) (Gas flow pressure: 1 atm, liquid flow rate (35 µL/min).

The electrode voltage from the AC power supply was controlled at a peak-to-peak applied voltage of approximately 10 kV and the frequency was set to 17 kHz. In general, for the applied voltage used, the average power consumption was found to be 13.0 ± 0.7 W (Brandenburg, 2017). The rate of plasma generation was predicted to be constant based on a consistent applied AC voltage to the plasma reactor at various liquid flow rates (Figure S4.1 in the appendix). It was assumed that the plasma generation in the microfluidic devices was confined to the gas column within the microchannel and transfer of the reactive species formed in the gas phase was dependent on the gas-liquid interface and residence time of liquid in plasma.

Figure 4.2 shows the gas space decreasing as a function of increasing liquid flow rate. At higher flow rates, film thickness and surface deformation increased which may leave less space for plasma generation and affect the gas volume for excitation and ionization (Jones and Raston, 2017). As of yet, the effect of plasma on the stability of the annular flow regime in our device is unknown. However, it is assumed that the plasma discharge does not have any significant effect on the flow regime inside the devices, with heat removal by external substrates, i.e. heatsink and thermal pad, decrease remote heating of the reactor and thus prevent thermal spots that may cause evaporation of water in the microchannel. Under a given power input supplied to the device, the rate of generated plasma species was assumed to reach a pseudo-steady state.

Numerous studies have found treatment efficiency by plasma discharges to be influenced by the liquid to gas volume ratio (Fogler, 1999). So far, limited studies were performed with a similar reactor configuration and examined plasma generation in a dual phase annular flow regime. Wengler *et al* reported the application of plasma for organic synthesis (Wengler et al., 2018). They used a microfluidic device equipped with transparent indium tin oxide as both ground and high-voltage electrodes for controlled oxidation of alkyl C-H bonds of cyclohexane in synthesising polyamide fibres. In this work, copper was chosen as both ground and high voltage electrode.

Previous studies have shown the significance of the type of electrode used for plasma generation. Parkansky *et al* found particles eroded from titanium electrodes during plasma generation promote degradation of contaminant in water (Parkansky et al., 2013). However, over time, erosion of the electrode affects the performance and duration of the electrode and overall, the lifetime of the plasma system (Lukeš et al., 2006; Parkansky et al., 2012). Gnapowski *et al* shown that plasma generation over time led to corrosion products formed over the surface of electrode, which reduced the amount of plasma generated (Gnapowski et al., 2019). With the microfluidic reactor, unwanted erosion and etching of the electrode was avoided due to both electrode isolated from liquid and plasma. However, the performance of the DBD microfluidic reactor can be influenced by the electrical property of the electrode material such as ionization energy for electron emission and electrical resistivity as well as other parameters such as thickness and geometric area. Wang *et al* compared various electrode materials in their DBD reactor, with results showing higher NO removal efficiency using tungsten than copper and stainless steel (Wang et al., 2012). This was further explained by secondary electron emission coefficient, i.e. proportional to the square root of the metallic density, which is higher in tungsten compared to copper and stainless steel, resulting in higher rate of ionisation and excitation of the carrier gas to form reactive chemicals. In this current work, our electrodes are not made of tungsten or transparent materials i.e. ITO (indium tin oxide) but of copper tape, which is cheaper and more accessible. Copper tape was chosen, with low electrical resistance of 0.003 Ω/sq. while surface resistance of standard ITO glass varies from 4 to 12 Ω/sq. which limits its conducting ability for plasma generation.

4.3.4 Temperature

During plasma generation in the microchannel, the temperature of the MPR was measured over time. The initial temperature of the dielectric material of the microfluidic reactor was at room temperature, between 20 and 24 °C. Initiating plasma generation results in an increase in temperature on both the electrode and the dielectric surface over time. Overall, the rising temperature during initiation of plasma reduced the lifetime of the microfluidic reactor when installed and left running for prolonged periods of time (less than30 minutes). The continuous high input power and voltage drop over the electrodes due to poor load balancing at the power supply causes the reactor temperature rise to more than 85°C in under 30 minutes resulting in thermal fracture which is identified as low stress breakage due to large temperature gradients on the dielectric surface. The rise of temperature gradients is due to thermal spots formed at the electrical wire and both the copper electrode, causing an uneven thermal distribution on the dielectric surface. Figure 4.6 shows an example of a single wavy crack caused by thermal fracture on the microfluidic reactor and a thermal image of the reactor in operation. As shown, the liquid temperature out of the outlet does not exceed the electrode temperature, between 30-35 °C. Since the microdischarges formed in the microchannel are small, short-lived and distributed along the serpentine channel, the microdischarges were regarded to provide minimum contribution to large-scale heat transfer and generation (Jidenko et al., 2010; Tirumala et al., 2014). Heat transfer to liquid and gas occurs solely through conduction and convection from the dielectric surface.

The amount of heat applied to the dielectric surface defines the ability of the microfluidic reactor to effectively run for long periods. As shown in Figure 4.7, the temperature was higher for the reactor with thinner dielectric barrier, which is due to less area for heat transfer and conducts heat at a much slower rate. Thus, the final model incorporated a heatsink, which transfers the heat generated away from the reactor surface. The reduction in dielectric surface temperature lead to increased longevity of the reactor, running up to 8 hours while plasma was ignited with surface temperature less than 50°C, applied voltage of 10 $kV_{(p-p)}$ and

frequency of 17 kHz. The liquid temperature downstream of the DBD was measured at less than 5 °C difference with room temperature.

a)

b)
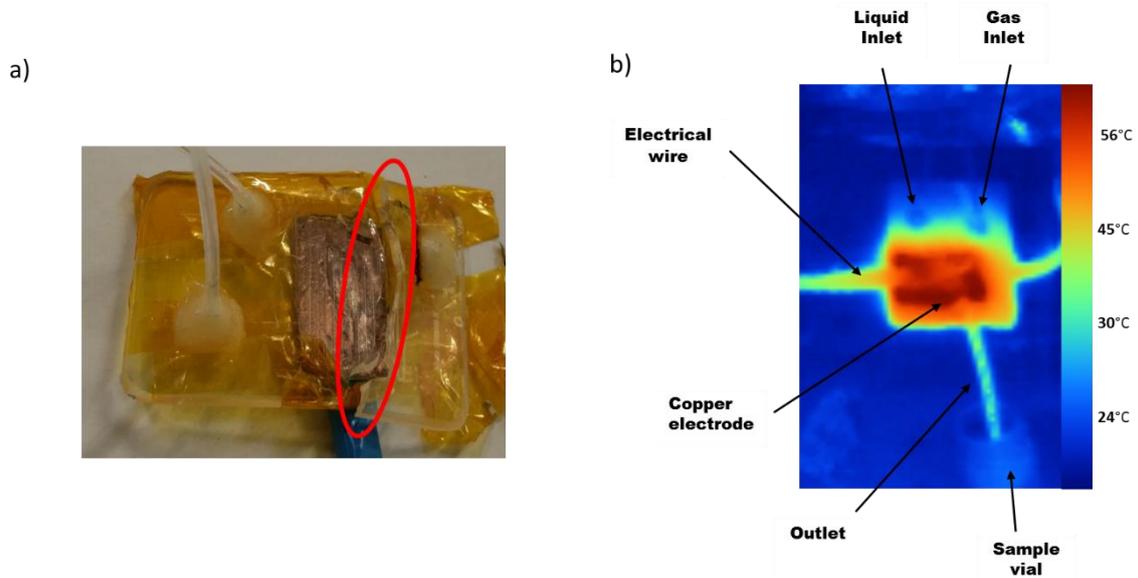
Figure 4.6: a) Image of a thermal fracture (red circle) of the MPR. b) Thermal image of the MPR during plasma ignition.
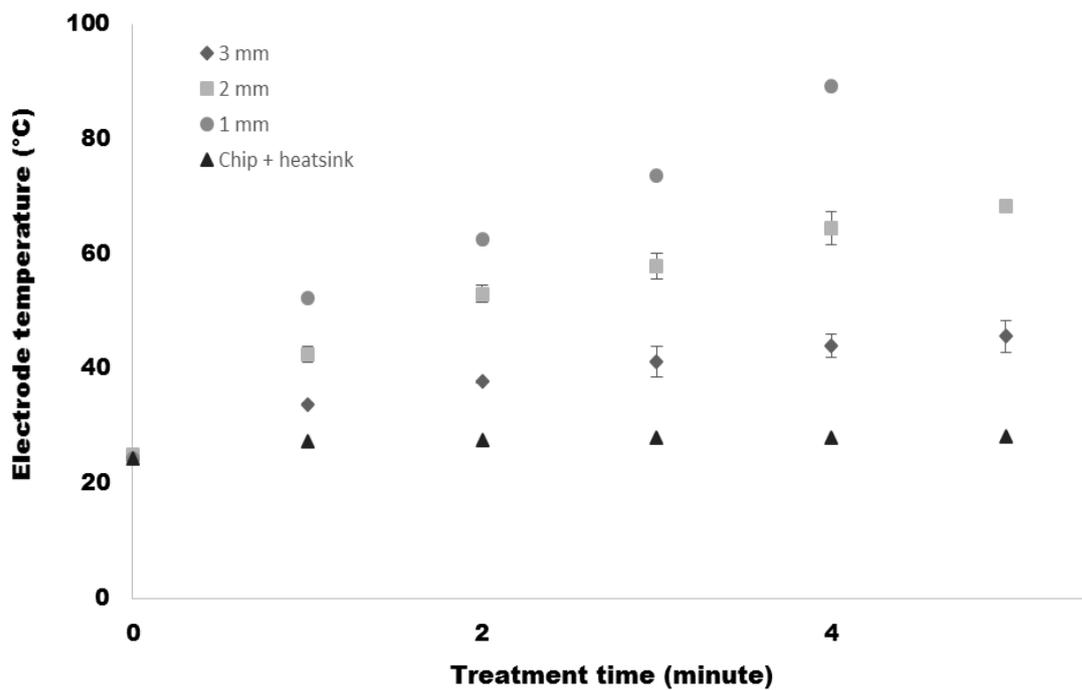
Figure 4.7: (a) Variation of electrode temperature over time: applied voltage 10 kV$_{(p-p)}$ and frequency 17 kHz. Error bars represent standard errors n = 3. Statistical significance, $\rho > 0.05$.

4.3.5 Chemical effects yielded in water by plasma treatment using a microfluidic plasma reactor

In this section, the formation of ROS and RNS, as detected by IC, was evaluated. Ion chromatograms of anions and cations, with corresponding retention times, using a standard sample with anions and cations of interest are shown in Figure S4.2 and Table S4.1 in the appendix. The composition ratio of the ion species, dependant on the water sample and residence time in the plasma discharge zone, was investigated.

4.3.5.1 Effect of plasma treatment using a microfluidic reactor on anion levels in water

Measurements of the initial concentration of anions in the three different water samples were performed and compared after plasma treatment. Overall, no significant change or formation was observed in hard and soft water samples for fluoride, chloride, bromide, phosphate and sulphate in any of the samples ($p < 0.05$). No formation of these anions was detected in Milli-Q water after plasma treatment (Figure S4.3 in the appendix).

Concentration of both nitrate and nitrite was observed to increase with increasing residence time, from around 3 to 9 seconds (Figure 4.8). The formation and change in concentration of nitrogen species in Milli-Q water and the tap water samples is due to the presence of nitrogen in air as the carrier gas for plasma generation.

a)

b)
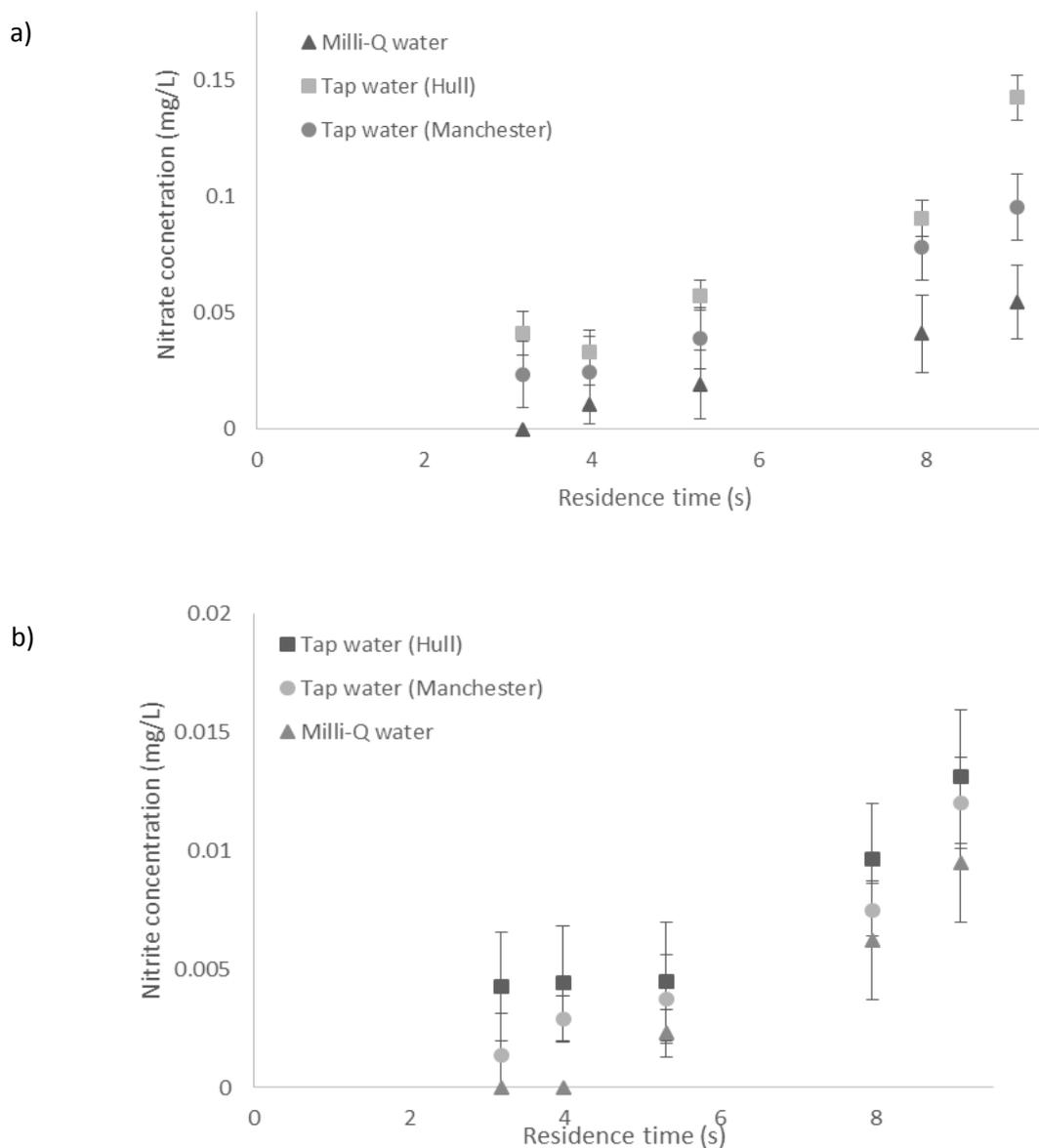
Figure 4.8 : a) Nitrate concentration and b) nitrite concentration in water samples collected after plasma treatment for various residence times using the MPR. Error bars represent standard errors n = 3. Statistical significance, $\rho > 0.05$.

Nitrite and nitrate at zero concentration at lower residence time could be explained by the low detection limits of the IC system. A maximum of 0.013 mg/L of nitrite and 0.143 mg/L of nitrate after 9 seconds of plasma treatment was measured in the water samples. These observed outcomes of nitrate and nitrite concentrations are lower than maximum outcomes in PAW generated in other types of electric discharge and plasma reactors (Chauvin et al., 2017; Judée et al., 2018; Thirumdas et al., 2018; Kaushik et al., 2018; Zhou et al., 2018). Even with the tap water samples, concentrations are considerably lower than the maximum standard levels

recommended in potable water, which are 50 mg/L for nitrate and 0.50 mg/L for nitrite in the UK (DWI, 2010). This is probably explained by the substantial low residence time of the water sample in the plasma discharge zone of between 3 and 9 seconds using a continuous-flow microfluidic system, compared to residence time in the range of hours with reactors in static configuration. However, these guidelines not only relate to the water quality but as well the treatment process and so far, plasma treatment is yet to be considered in meeting quality guidelines for potable water. Compared to static configuration, the microfluidic system demonstrate that lower level of ions can be attained in continuous flow configuration and lower residence time of liquid under treatment in plasma.

The mechanism involved in generating nitrate and nitrite in water is the result of mass transfer or dissolution of reactive nitrogen species, formed in air plasma by gas-phase reactions of dissociated nitrogen and oxygen, into water (Adamovich et al., 2017; Judée et al., 2018). Studies have shown that NO, N_2^+ and N are generated by plasma using air or nitrogen as the carrier gas. In contact with liquid, RNS react with water molecules and subsequently generate H^+ ions in water, as shown in Equations 4.1 and 4.2, reducing the pH of the media (Judée et al., 2018). HNO_2 and HNO_3 reach equilibrium with their hydrolysed H^+, NO_2^- and NO_3^- ions.

$$NO_2 + NO_2 + H_2O \rightarrow NO_2^- + NO_3^- + 2H^+ \qquad \text{Equation 4.1}$$
$$NO + NO_2 + H_2O \rightarrow 2NO_2^- + 2H^+ \qquad \text{Equation 4.2}$$
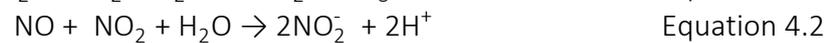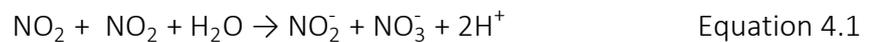
The results show that the overall concentration of nitrite in all three water samples after plasma treatment is lower by comparison to nitrate. This is due to the subsequent transformation of nitrite to nitrate ions by reacting with nitrate and ROS such as ozone, as shown in Equations 4.3 and 4.4, or disproportionation of nitrite to nitrate under acidic conditions (pH<3.5), as shown in Equation 4.5. This leads to a higher ratio of nitrate to nitrite concentration over the treatment time due to increasing competition leading to decomposition of nitrite to nitrate.

$$O_3 + NO_2^- \rightarrow NO_3^- + O_2 \qquad \text{Equation 4.3}$$
$$NO_3 + NO_2^- \rightarrow NO_2 + NO_3^- \qquad \text{Equation 4.4}$$
$$3NO_2^- + 3H^+ + H_2O \rightarrow 2NO + NO_3^- + 2H_3O^+ \qquad \text{Equation 4.5}$$
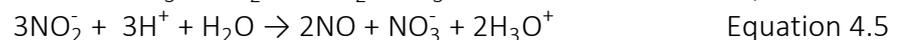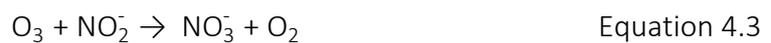
The starting pH for all three samples were relatively similar and significantly differed in conductivity (Table 4.1).

Table 4.1: Parameters of the water samples before plasma treatment.

Sample	pH	Conductivity (µS/cm)	Temperature (°C)
Milli-Q water	7.26	0.2	21.2
Soft water (Manchester)	7.36	109.4	21.2
Hard water (Hull)	7.95	747	21.2

After plasma treatment, no significant difference in pH was observed between before and after plasma treatment of the soft and hard water, maximum pH difference of 0.46 and 0.28 for soft and hard water, respectively. Thus, Equation 4.3 and 4.4 may have been the dominant reactions in the microfluidic reactor during plasma ignition in driving transformation of nitrite to nitrate. Other chemical species such as hydrogen peroxide were not measured by the IC, which may have contributed on the pH difference. Compared to drastic decrease in pH of buffer and saline samples after plasma treatment, Schmidt *et al* associated the buffering components in tap water, such as carbonate, impede pH change in tap water, especially with hard water (Schmidt et al., 2019). At 35 µL/min liquid flow rate, pH change from 7.26 to 5.5 was observed with Milli-Q water, which to an extent was contributed to exposure to air at prolonged period (1.5 hour) when collecting the minimum volume of 2 mL to measure pH. The control experiment of collecting MIlli-Q water for 1.5 hour, with no plasma treatment, showed pH decrease from 7.26 to 5.93, which is due to formation of carbonic acid and dissociates into carbonate or bicarbonate in water (Riché et al., 2006). Carbonate ions in Milli-Q water without plasma treatment were detected using the IC (Figure S4.3 in the appendix).

Regardless of water conductivity, increasing production of nitrates and nitrite ions as residence time increases was detected in all three water samples. However, the effect of water conductivity on formation of ions in plasma treated water is yet to be understood. Initially, high conductivity of water was expected to affect the propagation of streamers leading to less plasma density and thus, low rate production of chemical species in plasma treated water. Hamdan *et al* found decreasing plasma volume with increasing liquid conductivity using bubble discharge (Hamdan et al., 2017). Using spark discharge over water surface, Midi *et al* concluded that water conductivity has a significant effect on the electric field which affects the electric potential distribution (Midi et al., 2013). Akishev *et al* reported decrease in strength of the electric field in liquid with high conductivity. Kornev *et al* found no significant change in composition of nitrate and nitrite with increasing conductivity using spark and corona

discharge, but concentration of nitrogen containing ions decreased with increasing conductivity when dielectric barrier discharge was used (Kornev et al., 2013). This was further explained with the reduction of the density and energy of the microdischarge. However, no significant reduction in nitrate and nitrite concentrations in water after plasma treatment was observed, specifically with the hard water sample, when using the MPR. This could be due to the high surface-area-to-volume-ratio and power density of the plasma generated in the microchannel compared to plasma generated in bigger gas space (Ohtsu and Fujita, 2004), which may compensate the effect of conductivity and thus enhance conduction, leading to production of chemical species. Thus, similar linear behaviour was observed with all three water samples with different conductivity.

4.3.5.2 Effect of plasma treatment using microfluidic reactor on cation levels in water

After plasma treatment, no significant change in concentration of sodium, potassium, magnesium and calcium was observed ($p < 0.05$). However, an increasing concentration of ammonium ions was observed with all three water samples as residence time in plasma increases. Figure 4.10 shows ammonium concentration increasing with residence time, with a maximum of 0.0061 mg/L of ammonium measured in hard water at around 9 seconds of residence time in the plasma discharge zone.
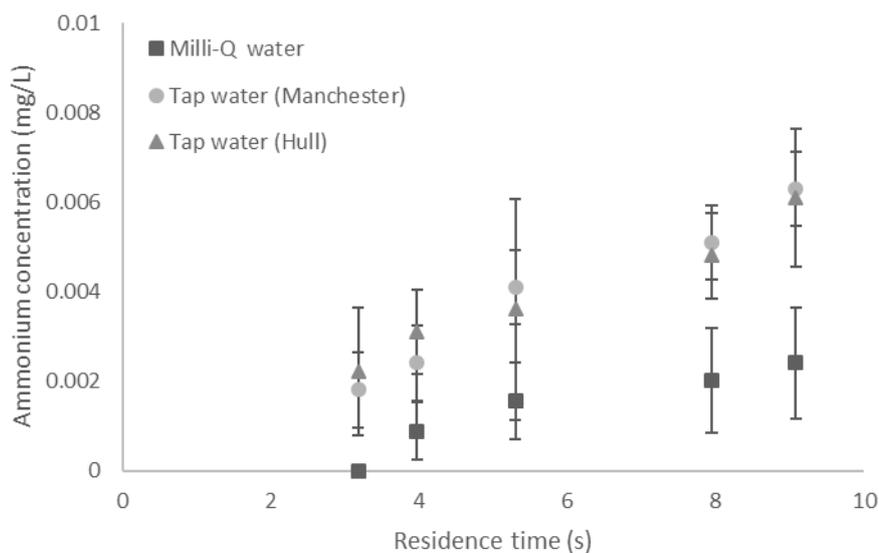
Figure 4.9: Ammonium concentration in water samples collected after plasma treatment in various residence times using a MPR. Error bars represent standard errors n = 3. Statistical significance, $p > 0.05$. (n=3).

The formation of ammonium ions in plasma treated water is described in a two-step mechanism via the dissociation of water molecules to form hydrogen gas in the gas phase, followed by reaction of hydrogen with excited nitrogen in the plasma phase to form ammonia (Judée et al., 2018). Ammonia undergoes an acid-base reaction in water, as shown in Equations 4.6 to 4.10.

$$H_2O^* + H_2O \rightarrow \ ^*H + \ ^*OH + \ H_2O \qquad \text{Equation 4.6}$$
$$H_2O^* + \ ^*H \rightarrow \ H_2 + \ ^*OH \qquad \text{Equation 4.7}$$
$$^*OH + H_2O^* \rightarrow \ ^*H + \ H_2O_2 \qquad \text{Equation 4.8}$$
$$N_2^* + 3\ H_2 \rightarrow \ 2\ NH_3 \qquad \text{Equation 4.9}$$
$$NH_3 + 3\ H^+ \leftrightharpoons \ 2\ NH_4^+ \qquad \text{Equation 4.10}$$

An increase in ammonium production due to the pH and conductivity of the water samples was considered. However, similar linear behaviour of ammonium production was obtained with all three water samples with similar pH but different conductivity. The independence of the steady production of ammonium, including the nitrogen-containing species on the initial concentration of ammonium measured in Milli-Q and tap water samples has led to the assumption that increased plasma-interaction with increasing residence time caused an increase in the formation of ions where conductivity has a negligible effect. This could be due to the inherent advantage of microfluidics with high surface-area-to-volume ratio and dimensions in μm leading to higher power density (Ohtsu and Fujita, 2004) and thus results to production of nitrogen species in water,

4.4 Summary

Characterisation of the process parameters and the generation of ions in the water samples by dielectric barrier discharge using an MPR was investigated. The main findings were:

- Gas-liquid annular flow was employed due to limitation of experimental equipment and flow regime transition using low or high gas pressure and liquid flow rates.
- Film thickness varied over residence time by changing the liquid flow rate, which affects the plasma liquid interfacial area and mass transfer of species formed in the gas phase during plasma ignition the plasma-liquid interface and in liquid.
- Preliminary results with the MPR operating DBD confirm increasing number of plasma filaments as applied voltage increase.

- Longevity of the MPR was improved by using heatsink as passive exchanger of heat generated in the electrodes during plasma ignition.

- Using air as the carrier gas for plasma generation, concentration of nitrogen-containing ions, i.e. nitrate, nitrite and ammonium, increase with increasing residence time.

- No significant difference was observed with pH after plasma treatment of soft and hard water samples. This was contributed to low levels of ions formed in water after plasma treatment due to short residence time in the range of seconds and buffer components such as carbonate.

- Effect of conductivity on concentration of ions detected in water after plasma treatment using the MPR was negligible. This could be due to the high surface-area-to-volume ratio in microfluidic system and higher plasma density in smaller gas space, which compensate the effect of conductivity.

The obtained concentration of the nitrogen-containing ions is substantially lower than the recommended standard ion levels in potable water. Compared to plasma reactors in static configurations, operating in the range of hours, low level of ions was attained in a continuous flow configuration with treatment time in the range of seconds. The MPR has the potential to form high quality of water, free of chemical or biological contaminants, without introducing high levels of ionic species in water treated by non-thermal plasma using air as carrier gas.

Chapter 5 Chemical degradation of methylene blue using a microfluidic plasma reactor

This chapter investigates the process parameters such as residence time of the sample solution in the discharge zone, type of gas applied, dielectric thickness, channel depth and length that influence the degradation of methylene blue (MB) using the MPR. The results in this chapter has been published.

5.1 Introduction

The exposure of consumers to contaminants in supplied water presents risks to the human health and aquatic environment. Industrial wastewaters predominantly possess organic and inorganic chemicals such as textile dyes with small amounts (less than 1 mg/L) can contaminate tonnes of water and many of these industries discharges are highly coloured (Kant, 2012; Khan and Malik, 2014; Holkar et al., 2016). According to the World Bank, an estimated 20% of global water pollution comes from textile processing and most of the effluent from textile industries is discharged untreated to receiving water sources (Kant, 2012). The discharge of wastewater without effective treatment can be mixed to freshwater and surface water sources that can ultimately enter potable water. Thus, water quality must be verified since textile dyes at low concentrations, i.e. less than 1 mg/L, in water are highly visible, affecting the aesthetic quality and safety of potable water (Kant, 2012). In humans, dyes are known to be toxic, which causes skin irritation, dermatitis, dysfunction of organs such as kidneys and liver, harm intestinal bacteria and carcinogenic degradation products. In addition, studies have reported its impact on photosynthetic activity in aquatic plants when discharged and accumulates in aquatic sources due to limiting the light to penetrate through water (Gita et al., 2017).

Azo dyes represent the most abundant class of synthetic dye found in contaminated water, with complex structures such as aromatic ring, which are not easily degradable either naturally or by conventional water treatment methods (Shu and Chang, 2005). Established technologies such as combined physico-chemical or biological methods are often incapable of reducing dye concentration to desired and/or legislated values of colour in treated water i.e. less than 15 TCU (True Colour Unit) to colourless (Robinson et al., 2001; WHO, 2004; Adegoke and Bello, 2015). For example, adsorption such as activated carbon are commonly used in removing dye

in contaminated water. However, the high capital cost, deterioration over time as number of cycle increases and difficulty in regeneration of adsorbent materials are some of the present day challenge in such conventional method (De Gisi et al., 2016). In addition, accumulation of concentrated and toxic compounds, since they are simply transferred rather than treated, presents essential post-treatment of incineration that consumes extensive amounts of energy (Gupta et al., 2012; Yagub et al., 2014; Nawaz and Ahsan, 2014). Degradation products of such organic azo dyes includes aromatic amines, which are known as mutagenic and even carcinogenic (Chung, 2016). If the complete mineralisation of organic contaminants, transformation of contaminants into harmless products such as carbon dioxide and water, is achieved, no highly toxic or concentrated by-products would be present in the processed water, which can be produced by conventional water treatment methods (Lin and Green, 1987; Ippolito et al., 2011).

Considering the relevance of mineralizing of such contaminants, plasma-based water treatment has shown a promising solution of driving advance oxidation processes in solution for water disinfection and treatment. Several laboratory-scale plasma reactors have been developed for organic contaminant degradation as described in Chapter 2.4.3, which have adopted various types of plasma discharge, in water or at the water-gas interface. However, these have proven difficult to implement at the macro-scale (Foster, 2017). Plasma-based water treatment approaches have often been based on batch type reactors, which can achieve high levels of contaminant degradation, but at the cost of long residence times (Malik, 2010). Ideally, any processing system for water treatment should be continuous flow, which would require a large plasma-liquid interfacial area for plasma species to be generated and diffuse into the liquid, allowing for treatment of varying quantities of effluent within a short space of time to meet supply and demand. Innovative continuous flow plasma reactors such as falling water film reactors and reactors with radial flow have been applied to increase plasma- liquid interfacial area to improve treatment efficiency (Dojčinović et al., 2016; Wang et al., 2017b). In these systems thin films of water flow along the inner walls of a vertical cylindrical electrode and come into contact with plasma. These reactors performed favourably in terms of high degradation capability, with high mass transfer of plasma species into the thin film of solution along the discharge. However, fluid control and even film distribution were difficult to achieve

which can affect pollutant degradation efficiency. In addition, these systems are susceptible to electrode erosion processes.

Recently, by exploiting the advantages of miniaturisation, effective dielectric barrier discharge (DBD) systems within microfluidic platforms operated at atmospheric pressure have been presented and utilised for plasma characterisation and synthesis reactions (Olabanji and Bradley, 2011; Yamanishi et al., 2013; Schelcher et al., 2014; Ishii et al., 2015; Tatoulian et al., 2017), but these systems have yet to be applied to plasma based water treatment. Plasma microfluidic devices have also been employed recently for plasma synthesis in dual phase plasma–liquid systems, in particular for gold nanoparticle synthesis (Li and Lin, 2018), for synthesis reactions (Zhang et al., 2018), and for controlled oxidative processes (Wengler et al., 2018), with all three studies indicating the potential of dual phase plasma–liquid microfluidic systems for studies in plasma water treatment. Microfluidics refers to devices and methods that allow the control of the spatial and temporal behaviour of fluids within dimensions less than a millimetre (Luo and Duan, 2012). The high surface-area-to-volume ratios inherent to microfluidic systems used in a range of different applications present significant enhancement of the observed reaction rate compared to traditional, macroscale bulk reactors. Utilising a microfluidic approach can benefit PWT by maximising the plasma–liquid interfacial area, enhancing mass transfer and reducing transfer distance of reactive species in plasma to liquid in continuous flow. Although each device may only process a small volume at a time, larger volumes can be processed by operating multiple devices in parallel (Iles, 2009).

For these reasons, this work focuses on evaluating a continuous flowing system using a MPR for water treatment based on the degradation of MB as a model azo dye contaminant. MB can be found in wastewater that causes undesirable environmental impact on receiving waters, and subsequently on human health (Cragan, 1999; Soni et al., 2012; Giwa et al., 2013). The MPR utilizes a DBD at atmospheric pressure, with the plasma generated in the gas stream of a continuous gas–liquid two-phase flow. The effect of residence time of the solution in the discharge zone, type of gas applied, barrier thickness and channel depth and length were evaluated.

5.2 Experimental set-up

The experimental set-up described in chapter 3.3 was used for this investigation. Both gas and liquid were introduced into separate inlets of the MPR. Gas pressure was regulated to 1 or 2 atm gauge in channel depth of 100 and 50 μm, respectively. Operating conditions of MPR1, MPR2 and MPR3 reactors with 50 μm channel depth were described in Chapter 3.4.1. The gas volume flow rate was approximately measured by attaching a Hamilton gas-tight syringe to the outlet, while desired flow regimes were generated within the microchannel of the device. The gas volume collected from the outlet was measured as a function of time for device inlet pressures of 1 and 2 atm. This gave 4 and 8 mL/min measured in devices with 50 and 100 μm channel depth, respectively. Liquid flow rate was controlled within the range of 35 to 100 μL/min. Resulting flow regimes were observed in the serpentine regions of the chip using an inverted light microscope (Zeiss Primovert). For this experiment, a fixed applied voltage of 10 kV_{p-p} and a frequency of 17 kHz with air, argon and oxygen as the gas source were used. Barrier thicknesses of the microfluidic devices were modified by using different thickness top plates (1 − 3 mm) to achieve the desired top plate total thickness of 2 and 4 mm whilst maintaining a bottom plate thickness of 1mm.

Analytical grade MB (Sigma Aldrich), with a concentration of 5 mg/L in deionised water (18.2 MΩ/cm at room temperature) and kept at pH 7.4 ± 0.5 by 0.1 M phosphate buffer, was used as a model sample for evaluation of the MPR. The concentration of MB was monitored, before and after plasma treatment, using a UV-vis spectrophotometer (Perkin Elmer Lambda 40) described in Chapter 3.5.1. The percentage of MB degradation due to plasma treatment was calculated using Equation 5.1;

$$Degradation\ (\%) = \left(1 - \frac{[MB]}{[MB_0]}\right) \times 100 \qquad \text{Equation 5.1}$$

where $[MB]_0$ is the initial concentration of the MB solution and $[MB]$ is the final concentration after plasma treatment. The by-products formed with plasma treated MB solution were identified by means of a mass spectrometer coupled with ESI-MS described in Chapter 3.5.2.

5.3 Results and discussion

5.3.1 Effect of liquid flow rate

The residence time of the liquid in the plasma zone was controlled by changing the flow rate of the liquid entering the MPR. To investigate the effect of residence time on the degradation efficiency of MB by non-thermal plasma generated in the MPR, flow rates ranging from 35 to 100 µL/min were used in a 100 µm channel depth using air as the working gas for the initial study. Figure 5.1 shows the efficiency of degradation of MB with respect to liquid flow rate (Fig. 5.1a) and decolourization of the MB solution (Fig. 5.1b). Lower flow rates, which correspond to increasing residence time of the liquid in the plasma zone resulted in increased degradation efficiency of MB due to a longer plasma-liquid interaction. This increases the number of reactions and collisions between the MB in liquid and the reactive species formed in plasma leading to MB degradation.
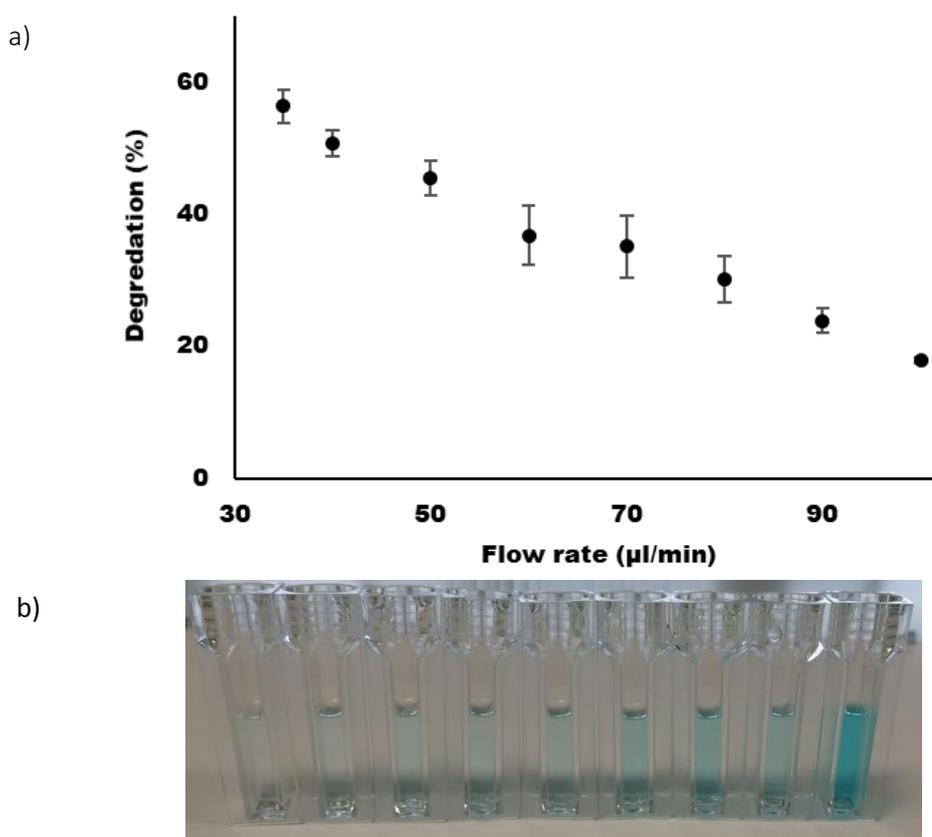
Figure 5.1: Degradation efficiency of MB in air non-thermal plasma at 1 atm of gas pressure as a function of liquid flow rate of liquid in the plasma zone using 100 µm channel depth. Error bars represent standard errors. (n=3, R^2= 0.9851, p < 0.05) (b) Colour variation of plasma treated MB solution at various flow rates. From left to right: 35, 40, 50, 60, 70, 80, 90, 100 µL/minute and untreated.

5.3.2 Effect of channel depth

The effect of changing the channel depth was investigated, with Figure 5.2 showing the effect of reducing the channel depth of the microfluidic device on the degradation of MB, using air as the working gas. The use of a shallower channel depth, 50 μm compared to 100 μm, reduced the residence time of the liquid in the microchannel. Despite the shorter residence time, the results show significant improvement in MB degradation, with a maximum of 97% achieved, using a shallower channel depth and a liquid flow rate of 35 μL/min compared to 100 μm channel depth. The maximum residence time calculated in the 50 μm deep channel device was 5 seconds.
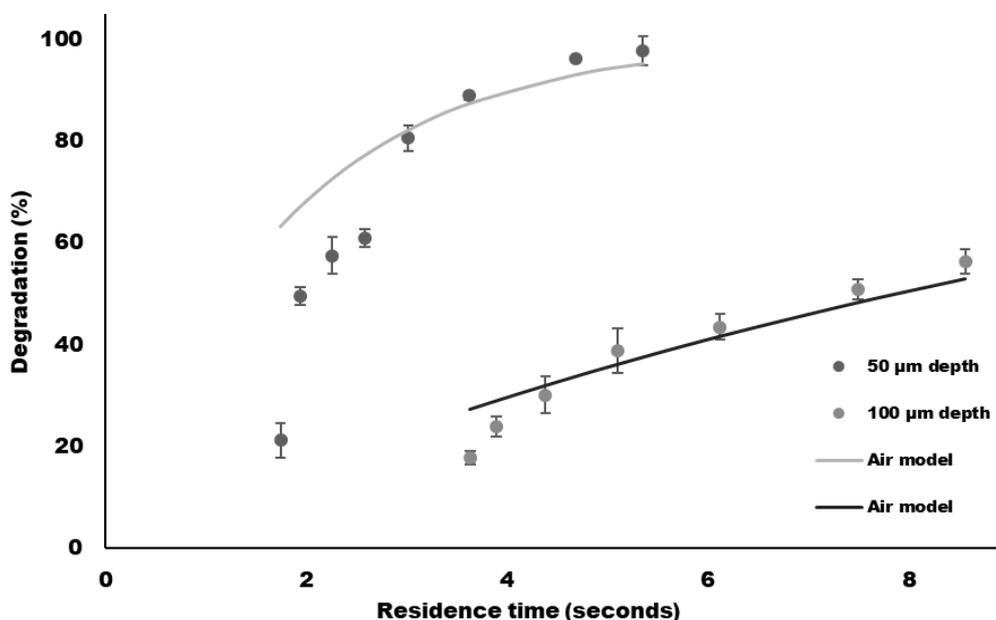
Figure 5.2: Degradation efficiency at different channel depths of 50 and 100 μm, air as feed gas at 4 and 8 mL/min respectively, applied voltage at 10 kV and frequency of 17 kHz. 100 μm (k = 0.088 s^{-1}, R^2 = 0.9952) and 50 μm channel depth (k = 0.573 s^{-1}, R^2 = 0.8938). Error bars represent standard errors n = 3. Statistical significance, $p < 0.05$.

The discharge gap distance, i.e. the channel depth of the microfluidic device, is important in terms of breakdown voltage. With a small gap distance, lower breakdown voltage and higher discharge current is expected (Yoon et al., 2018). Hence, decreasing the discharge gap from 100 μm to 50 μm, increases the power density in the discharge zone when using the same applied voltage (Ohtsu and Fujita, 2004). As a result, a more reactive environment is expected and consequently the collision probability is increased between the reactive species in the plasma and the liquid in the channels. In addition, using a shallower channel reduced the liquid

film thickness compared to the deeper channels, which would have improved the utilisation of short-lived radicals for MB degradation in solution. Finally, the increase in pressure from 1 to 2 atm led to an overall increase in the density of gas in the discharge regions, and potentially an increase in the concentration of active plasma species.

5.3.3 Effect of barrier thickness

The effect of thickness of the glass dielectric layer of the MPR was investigated, with Figure 5.3 shows MB degradation for different barrier thicknesses. The results show that decreasing the barrier thickness improved MB degradation. As the barrier increases in thickness, the capacitance due to the barrier decreases, resulting in a greater voltage drop across the barrier, and less voltage applied across the gas gap. This results in a reduction of power applied to the plasma region, reducing the electron density and chance of collisions in the gas space, leading to a lower concentration of ions and excited atoms formed in the plasma (Li et al., 2008; Tao et al., 2008; Liu et al., 2012; Yang et al., 2013).

In the literature, only cases of pseudo-first order plasma based degradation of MB at similar concentrations to this work were reported (Q. Wang et al., 2013; Yin et al., 2014; Thagard et al., 2016). The experimental results obtained here indicated that the degradation rate of MB in 100 µm channel depth fitted the pseudo-first order kinetic model. However, the data obtained using the 50 µm channel depth (Figure 5.3 a) has a lower R^2 value compared to the 100 µm channel depth (Figure 5.3 b) on the calculated model. For both experiments, starting concentrations (5 mg/L) used were equal, therefore other effects such as enhancement of mass transfer of plasma species from the gas phase into the liquid phase are predicted to be occurring in the 50 µm channel depth, which results in the observed higher degradation of MB.
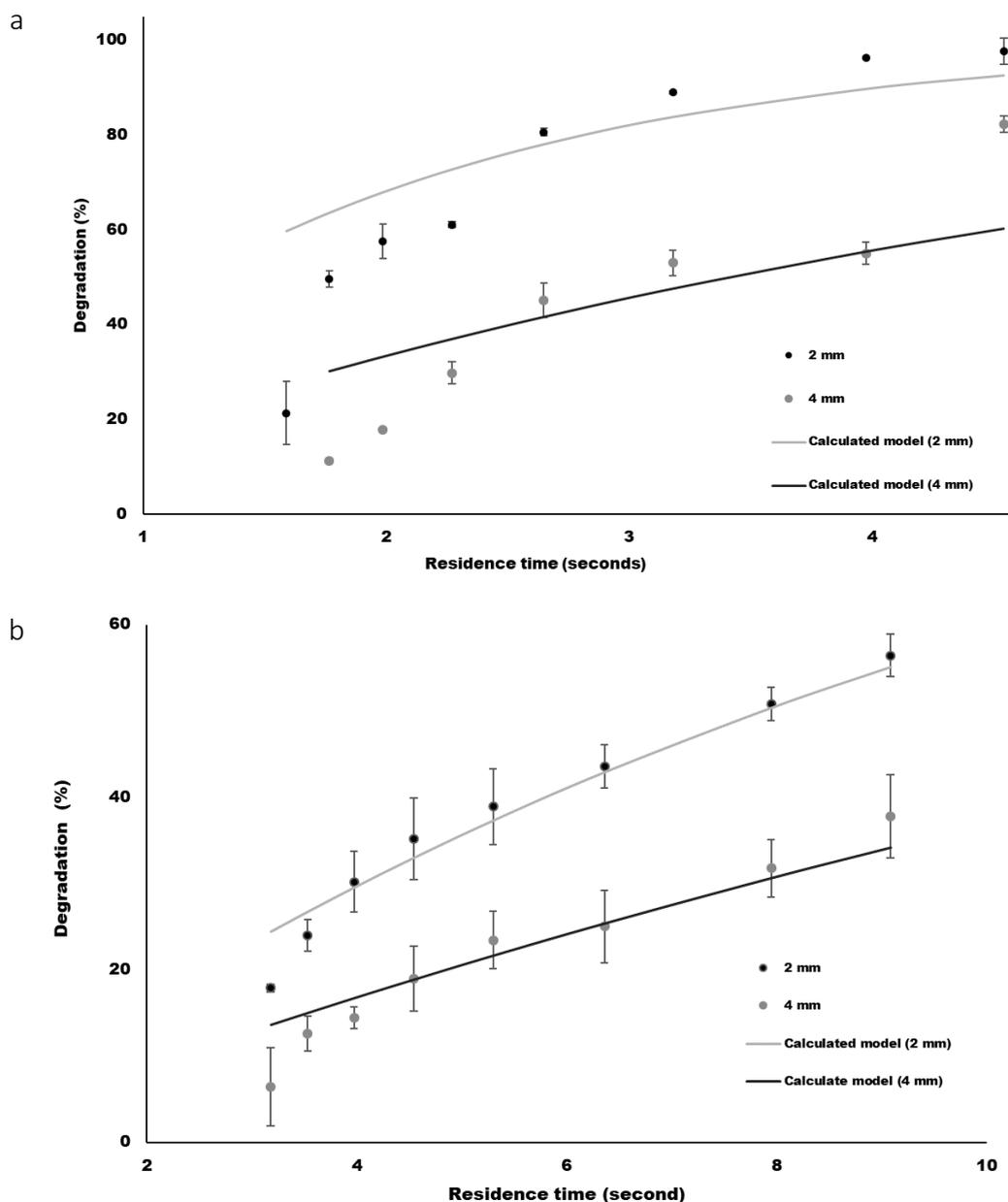
Figure 5.3: Effect of barrier thickness on MB degradation in constant plasma discharge with an applied voltage of 10 kV, frequency of 17 kHz, gas flow pressure of 1-2 atm and channel depth of 50 μm (a) and 100 μm (b). Total barrier thicknesses of 2 ± 0.1 (•) and 4 ± 0.1 (•) mm were used in this study. 50 μm channel depth (2 mm: k = 0.573 s^{-1}, R^2 = 0.8938, 4 mm: k = 0.203, R^2 = 0.9393) and 100 μm (2 mm: k = 0.088 s^{-1}, R^2 = 0.9952, 4 mm: k = 0.046, R^2 = 0.9577). Error bars represent standard errors n = 3. Statistical significance, $p < 0.05$.

5.3.4 Effect of gas pressure

The gas flow rate of the carrier gas in the plasma zone was controlled by changing the gas pressure of the carrier gas entering the MPR1 with channel depth of 50 μm. Changing the gas flow pressure from 2 to 3 atm has not shown any significant difference in the degradation of

MB (Figure 5.4). By increasing the gas pressure, the water film flows as a smooth film along the microchannel wall and results in thin films, as shown in Chapter 4.3.1. The similarity of the observed trends of MB degradation for both 2 and 3 atm used in 50 μm channel depth suggests that the results are affected negligibly by increasing the gas flow pressure. The results showed no statistical difference ($p > 0.05$) between the degradation of MB using 2 and 3 atm gas pressure. Although, increasing the gas pressure does reduce the residence time of the gas phase and increase the density of gas in the plasma zone, effective degradation of MB was compensated for by the higher residence time of the liquid and more efficient mass transfer of plasma species from the gas phase to the thin water films.
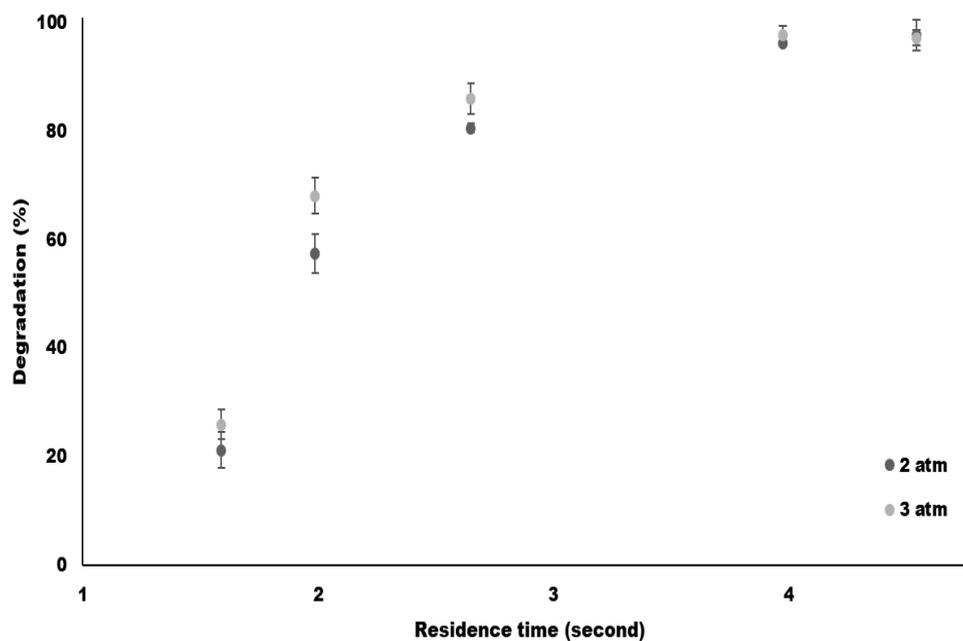
Figure 5.4: Effect of gas flow on MB degradation in constant plasma discharge using air as carrier gas with an applied voltage of 10 kV, frequency of 17 kHz and channel depth of 50 μm. Total barrier thicknesses of 2 mm was used in this study. Error bars represent standard errors n = 3. Statistical significance, ρ > 0.05.

5.3.5 Effect of channel length

In section 5.3.1, higher residence time lead to higher degradation of MB. Thus, amendments were made to the design of the MPR to include longer lengths of serpentine channel to enable higher residence times. The length of the serpentine channel was 395 for MPR2 and 595 mm for MPR3. Higher gas flow pressure was used to achieve annular flow for the new designs i.e. 4 and 6 atm for MPR2 and MPR3, respectively.

Compared to MPR1 where the film thickness was uniform at full length of the serpentine channel described in Chapter 4.3.1, various thickness of the water film was observed along sections of the serpentine channel of MPR2 and MPR3 (Figure 5.5). This was due to waves (b) and liquid ring flow (c), characterised by a liquid bridge separating two consecutive gas slugs, formed towards the outlet of the reactor. This could be due to decreasing gas-liquid relative velocity as both gas and liquid pass more channel bends in MPR2 and MPR3 compared to MPR1 where formation of liquid bridge was suppressed by high velocity gas streams along its shorter channel (Taitel and Dukler, 1976). As mentioned in Chapter 4.3.2, formation of surface deformation along the water film such as waves and liquid ring flow observed in MPR2 and MPR3 may affect plasma stability for water treatment but their occurrence likely improves mixing for enhanced mass transfer during treatment (Bruggeman et al., 2007).
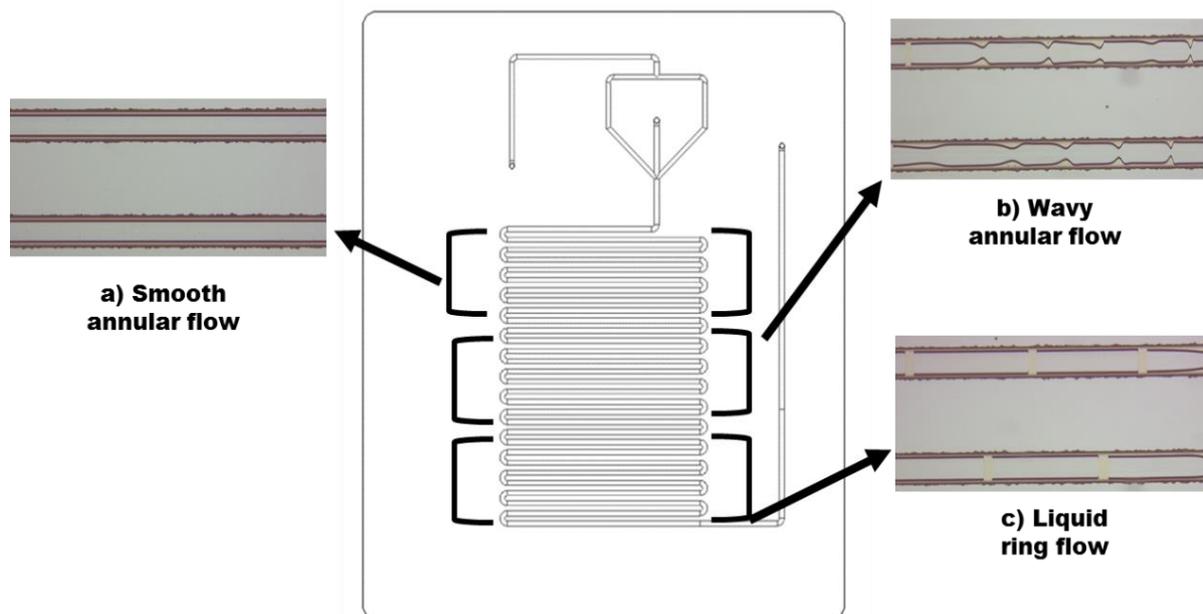
Figure 5.5: Images of the flow patterns taken from each section of the MPR3 with operating with 6 atm gas flow pressure and 60 µL/min.

MB degradation increases as the residence time in each microfluidic reactor increases (Figure 5.6). There was no significant difference in MB degradation between MPR1, MPR2 and MPR3. Results show that MPR3 took the longest residence time to achieve the maximum MB degradation of 95% in 13 seconds compared to 96% in 8 seconds for MPR2 and 97% in 5 seconds for MPR1.
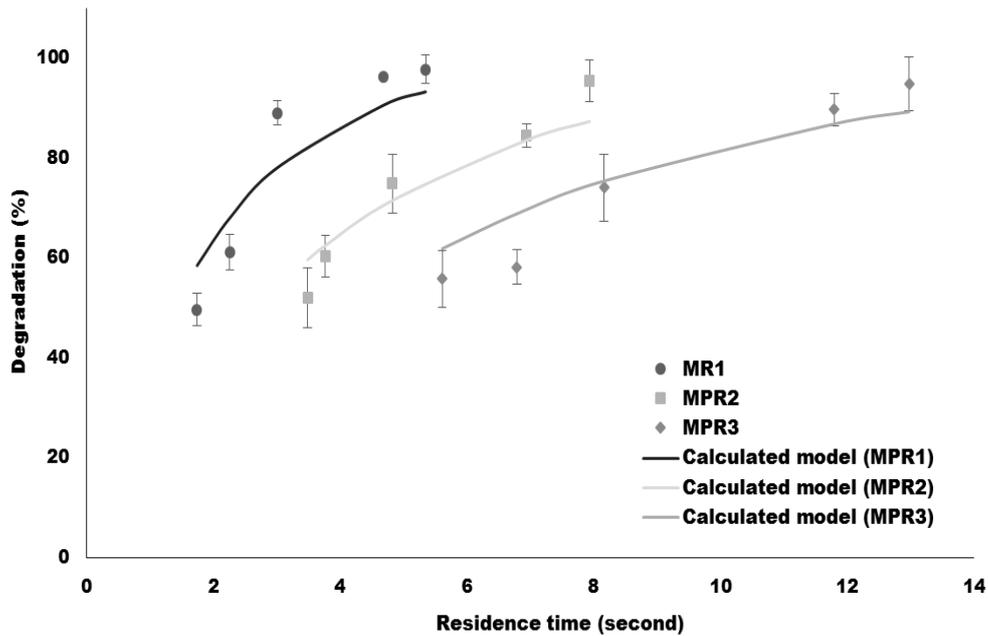
Figure 5.6: Effect of channel length on MB degradation in constant plasma discharge using air as carrier gas with an applied voltage of 10 kV, frequency of 17 kHz and channel depth of 50 μm. Total barrier thicknesses of 2 mm was used in this study. MPR1 (k = 0.573 s^{-1}, R^2 = 0.8938,), MPR2 (k = 0.259 s^{-1}, R^2 = 0.9648) and MPR3 (k = 0.171 s^{-1}, R^2 = 0.8385). Error bars represent standard errors n = 3. Statistical significance, $p < 0.05$.

Increasing surface area of electrode was used to occupy the length of the serpentine channel for each reactor as described in Chapter 3.2.1. The resistivity of the electrode decreases with its surface area (Meaden, 2013). As a result, more current can be delivered for the same voltage applied to all three reactors to generate plasma along the area of the serpentine channel. However, the effects are small with no significant difference in MB degradation between the three reactors. This could be due to an increasing area of parasitic capacitance for longer channels, which is associated with the capacitance between the parallel channels. This includes power loss from poor load balancing at the power supply that causes the reactor temperature to rise, described in Chapter 4.3.4. Surface deformation of the water film along sections of the serpentine channel of MPR2 and MPR3 may reduce the oxidation process by leaving less space for plasma generation, affecting the gas volume for ionization and reducing the mass transfer of plasma species from the gas phase to the liquid phase (Malik, 2010; Thagard et al., 2016; Vanraes, 2016). Thus, compared to MPR1, longer residence time was required to achieve more than 95% MB degradation.

5.3.6 Effect of working gas

MPR1 was operated using air, argon and oxygen as the working gases. MB degradation was more evident when oxygen was used as the working gas (Figure 5.7). By increasing the residence time of the MB solution in the plasma discharge zone, exposure of the MB solution to plasma increased and higher MB degradation was achieved. Kinetic behaviour of the degradation process was obtained by fitting the data to a pseudo-first order kinetic model using Equation 5.6 derived from Equations 5.2 to 5.5, based on the relationship between the degradation efficiency (η), rate constant (k) and estimated residence time (t) (Yin et al., 2014; Thagard et al., 2016).

$$\frac{d[Mb]}{dt} = -k\,[Mb] \qquad \text{Equation 5.2}$$

$$\int_{[Mb]_o}^{[Mb]} \frac{d[Mb]}{[Mb]} = -\int_0^t kdt \qquad \text{Equation 5.3}$$

$$[Mb] = [Mb]_o\,e^{-kt} \qquad \text{Equation 5.4}$$

$$\frac{[Mb]}{[Mb]_o} = e^{-kt} \qquad \text{Equation 5.5}$$

$$\eta = 1 - e^{-kt} \qquad \text{Equation 5.6}$$

The rate constant obtained by the best fit of Equation 5.6 to the data in Fig. 5.7 is 0.088 s^{-1}, 0.11 s^{-1} and 0.13 s^{-1} for air, argon and oxygen respectively. This model was used to postulate the order of the reaction kinetics which shows that using the microfluidic device allowed high degradation efficacy to be achieved, with residence times in the order of seconds rather than minutes or hours that have been reported in numerous studies using plasma reactors (Dojčinović et al., 2011; Jones and Raston, 2017; Aziz et al., 2018; Krupež et al., 2018; Attri et al., 2018). However, the rate of change of degradation with respect to residence time decreases with increasing residence time, due to the first order kinetics of the degradation process. In addition to residence time, degradation can be enhanced depending on the working gas (Figure 5.7).
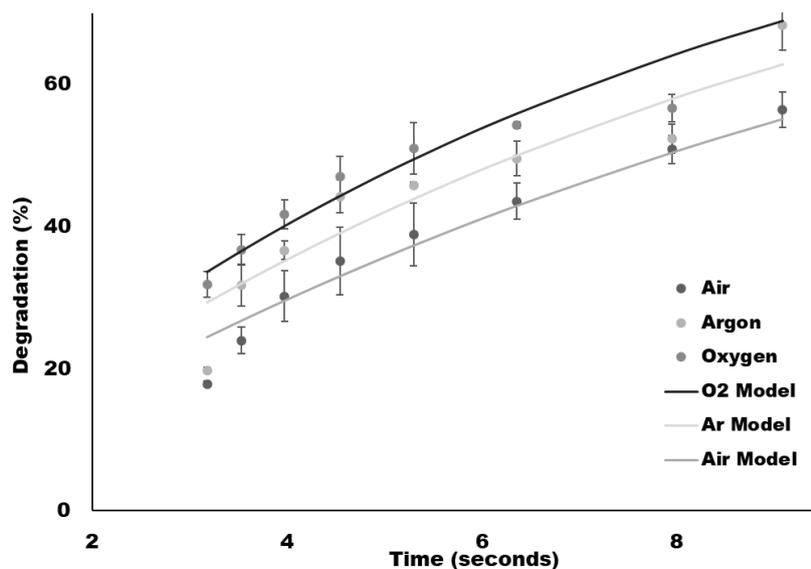
Figure 5.7: Degradation efficiencies with different working gases at 1 atm of gas pressure, applied voltage at 10 kV and frequency of 17 kHz. Air (k = 0.088 s^{-1}, R^2 = 0.9952), argon (k = 0.11 s^{-1}, R^2 = 0.9927) and oxygen (k = 0.13 s^{-1}, R^2 = 0.9898). Channel depth of 100 µm. Error bars represent standard error, n = 3. Statistical significance, $p < 0.05$.

High-energy electrons (e*) generated in the plasma produce reactive free radicals by reactions at the plasma-liquid interface, generating the species shown in Equation 5.8 (Locke and Shih, 2011; Samukawa et al., 2012; Ruma et al., 2014):

$$H_2O \; + \; e^* \quad \rightarrow \quad \cdot OH \; + \; H \cdot \; + \; e^- \qquad \text{Equation 5.7}$$

However, nitrogen containing species generated in plasma indicated in Chapter 4.3 are known to scavenge reactive species such as ozone and hydroxyl radicals (Equations 5.9 and 5.10) (Nikitenko et al., 2004; Son et al., 2011):

$$O_3 \; + \; NO_2^- \quad \rightarrow \quad O_2 \; + \; NO_3^- \qquad \text{Equation 5.8}$$
$$OH^\cdot \; + \; NO_2^- \quad \rightarrow \quad OH^- \; + \; NO_2^\cdot \qquad \text{Equation 5.9}$$
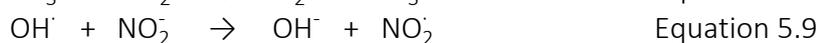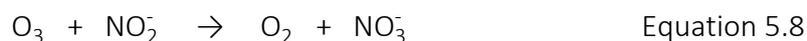
The greater degradation of MB observed with argon and oxygen as the working gases compared to air can be attributed to the absence of scavenging nitrogen species (Feng et al., 2016; Kovačević et al., 2017). The use of argon mainly relies on electron impact ionization of water molecules to produce hydroxyl radicals and hydrogen peroxide (Hamdan et al., 2017). With plasma discharges conducted in pure oxygen, greater amounts of reactive oxygen species were produced, in addition to hydroxyl radicals. (Bruggeman et al., 2016; Sano et al., 2002).

5.3.7 Degradation of MB

To give a qualitative indication of the types of degradation products produced by plasmas in different working gases, mass spectra were obtained for untreated and plasma treated MB samples that were processed through the MPR. Untreated MB showed a prominent peak at 284 m/z consistent with its molecular structure (Figure 5.8). After plasma treatment, differences in relative intensity of the 284 m/z peak and a number of fragments of MB were observed for each working gas used. Several studies have reported routes of MB degradation and intermediates after plasma treatment, which were consistent to the peaks obtained in this study (Wang et al., 2017a; Shirafuji et al., 2017; Bansode et al., 2017). The spectra obtained using oxygen as the working gas produced the greatest number of degradation products, compared to air and nitrogen. Although concentrations cannot be determined from these measurements and so it is not possible to determine the extent of mineralisation, it is clear that a significant number of degradation fragments are present in the samples following plasma treatment.
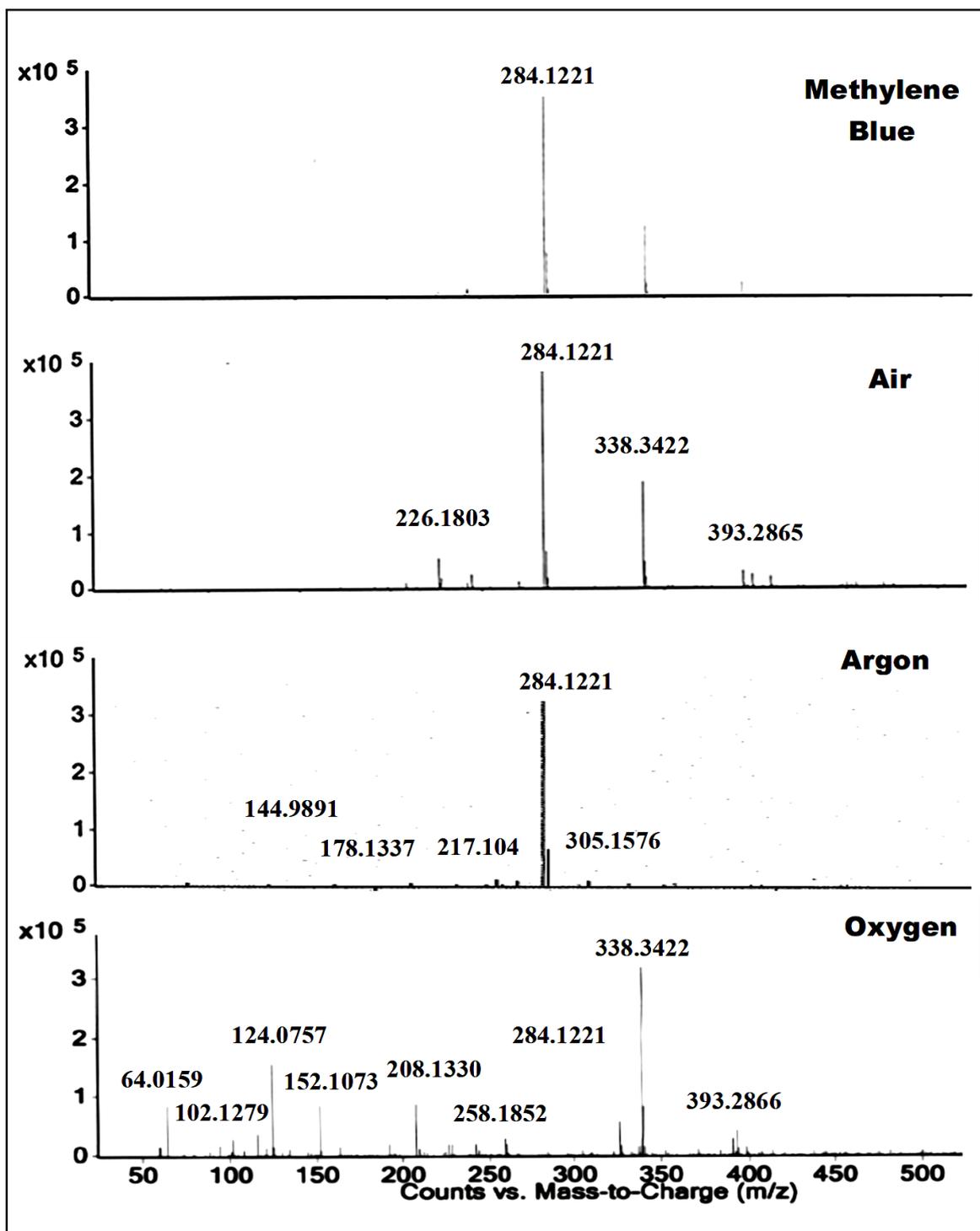
Figure 5.8: Comparison of mass spectra of plasma treated and untreated MB. Various ions as detected by the MS. Molecular ion (MB⁺) = m/z 284.1221. Results taken with the different working gases at 1 atm inlet pressure, applied voltage at 10 kV, frequency of 17 kHz, liquid flow rate of 35 μL/min and channel depth of 100 μm.

MB is a relatively large molecule that requires many steps for its complete mineralisation to CO_2, H_2O and inorganic salts. MB is a water-soluble salt that dissociates in water and produces a chloride anion and MB cation. The LC-MS spectra shows a decrease in intensity of the peak corresponding to the MB cation (284 m/z), with several peaks were observed, which may have been caused by bombardment of plasma species such as electrons or products such as hydroxyl radicals from hydrogen peroxide (Figure 5.8). Such processes lead to hydroxylation of the MB cation and intermediates to form polyhydroxyl compounds such as peak 338, 305 and 144 m/z (Figure 5.9). These products continuously react with the reactive species formed in plasma and ultimately produce light ions with smaller m/z values, less than 200 m/z. In some studies, demethylation of MB caused by high-energy electrons generated in plasma were proposed as another option of MB degradation (Huang et al., 2010; Benetoli et al., 2012; Wang et al., 2017a; Bansode et al., 2017). In this mechanism, the $N-CH_3$ bond is regarded as the weakest bond that can easily be attacked and lead to a successive demethylation pathway resulting in demethylated products of MB such as peak 244, 226, 228, 261 and 240 m/z (Figure 5.9) (Yin et al., 2014). Based on the production of the degradation products corresponding to the prominent peaks identified on the LC-MS spectra, a mechanism of MB degradation was proposed (Figure 5.10). Successive hydroxylation of these products through the addition of hydroxyl groups results to the production of opened ring products of MB and leads to mineralization products (Oliveira et al., 2007; Benetoli et al., 2012).
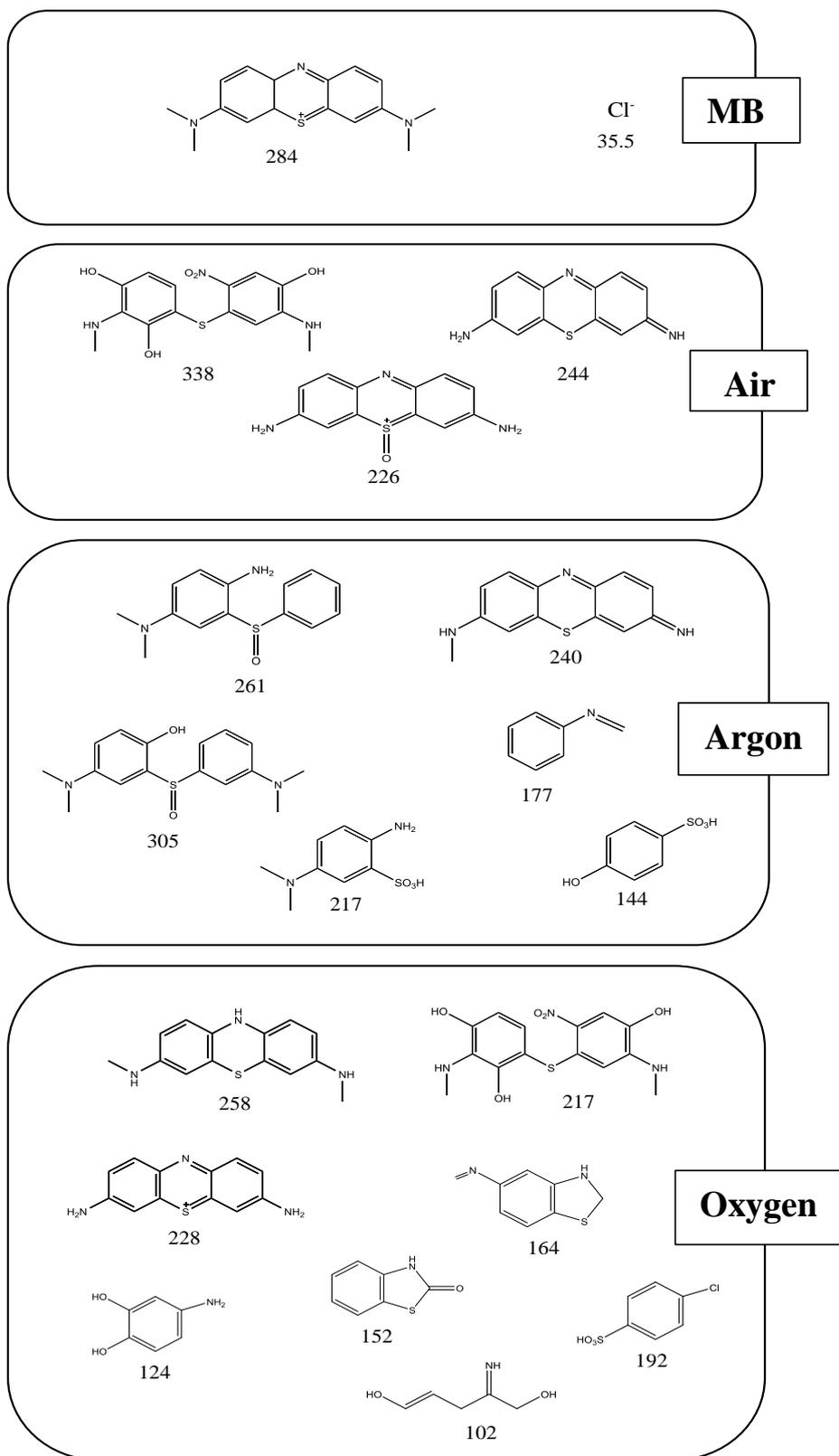
Figure 5.9: intermediates that correspond to prominent peaks identified by the LC-MS for the different working gases.

Figure 5.10: Possible pathways of MB degradation based on the degradation products related to the peaks in the mass spectra obtained.

5.4 Summary

The influence of the process parameters employed for the degradation of methylene blue using atmospheric pressure plasma generated in a microfluidic device was investigated. The degradation rates of the MB solution varied as a function of liquid flow rate, working gas, channel depth and barrier thickness. The main findings are:

- Degradation was enhanced by using: lower liquid flow rates, thinner dielectric barriers and shallow channel depths.
- With air as the carrier gas, a degradation of 97% was achieved at a liquid flow rate of 35 μL/min, a barrier thickness of 2 mm and channel depth of 50 μm.
- Increasing the gas flow pressure showed no significant difference in MB degradation.
- Increasing the length of the serpentine region showed no significant difference in MB degradation.
- Oxygen was found to be the most effective working gas. Higher number of fragments were detected using oxygen as the working gas.

Since many water sources contain not only chemical but also microbiological contaminants, it is important to investigate the anti-microbial activity of plasma generated in a microfluidic reactor. The aim of this chapter is to optimise the process parameters to achieve the highest degradation of MB in air plasma and apply to other contaminants in water.

Chapter 6 Microbial inactivation using a microfluidic plasma reactor

This chapter investigated the use of atmospheric-pressure plasma generated in a microfluidic plasma reactor for microbial inactivation of E. coli and P. aeruginosa, representative of Gram negative bacteria found in contaminated water.

6.1 Introduction

The greatest risk imposed by pathogenic microbes in water is related to the consumption of potable water contaminated with pathogenic microorganisms that pass untreated through the chemical and physical water treatment processes. Even though some of these microorganisms may not pose a problem to healthy individuals, pathogenic and opportunistic microorganisms can cause infections in immunocompromised individuals. Healthcare associated infections (HCAIs), defined as infections acquired as a consequence of healthcare intervention, are the most common incident that compromises patient safety globally (Allegranzi et al., 2011). In England, the prevalence of HCAIs in 2011 was 6.4%, with around 300,000 patients acquiring HCAIs annually costing the NHS £1 billion (Andrew et al., 2018). The implications caused by HCAIs are exacerbated with intensive care unit (ICU) patients, due to risks associated with invasive devices. Data included in a report by the WHO showed that hospital-wide prevalence of HCAIs varied from 3.5% to 12% and 5.7% to 19.1% in developed and developing countries, respectively (WHO, 2011). However, the proportion of patients acquiring at least one HCAI in ICU was significantly higher, with approximately 30% in developed countries and 4.4% to 88.9% in developing countries.

The body has several mechanisms to counteract extracellular invasion and production of toxic substances by pathogenic microorganisms in tissue but immunocompromised patients are more susceptible to acquiring HCAIs and developing life-threatening complications such as sepsis, meningitis and endocarditis, due to an impaired immune system (Monegro and Regunath, 2018). Waterborne HCAIs, caused by opportunistic waterborne microorganisms such as *P. aeruginosa*, are one of the most prevalent causes of mortality and morbidity incidences in settings such as healthcare (Ferranti et al., 2014). According to the report from the European Surveillance System, 8.3% of patients admitted in the ICU for more than 2 days acquired at least one HCAI, with *P. aeruginosa* as the most frequently isolated microorganism

(ECDC, 2017). Neonates in these settings are at higher risk of HCAIs, with several deaths of neonates in NICUs reported and directly linked to contaminated water systems (Wise, 2012; Walker et al., 2014). Kadambari et al. reported 93% of outbreaks was attributed to *Pseudomonas* infections in neonatal units, with 18% associated deaths, based on the Neonatal Infection Surveillance Network between 2005 and 2011 in the UK (Kadambari et al., 2014). HCAIs caused by *Pseudomonas* spp. increased by 26.6% between 2013 and 2017 in the UK; *P. aeruginosa* was the most frequently isolated bacteria, with approximately 82% of incidences caused by this bacteria reported (PHE, 2018). At several outbreaks of HCAIS in the UK that caused morbidity and mortality in NICUs, pathogen intrusion into hospital water distribution systems was verified as the source of infection (Mora-Rodríguez et al., 2015; Wise, 2012; Kinsey et al., 2017; J Walker and Moore, 2015). A systematic review by Jefferies et al. highlighted water and surfaces in contact with contaminated water were the main sources of outbreaks of *P. aeruginosa* infections in NICUs, both in developed and developing countries (Jefferies et al., 2012). In addition to HCAIs caused by *P. aeruginosa*, other microbes such as *E. coli* were increasingly detected in outbreaks of waterborne HCAIs. Bou-Antoun et al. reported a sustained annual increase of HCAIs caused by *E. coli* in the UK, with a 6% increase between 2012 and 2014 and the incidence recorded in neonates less than 1 year old was higher compared to older patients between 1 and 64 years of age (Bou-Antoun et al., 2016).

In recent times, dramatic reductions of HCAI outbreaks caused by some microorganisms under surveillance in the NHS in England were recorded; methicillin-resistant *Staphylococcus aureus* (MRSA) and *Clostridium difficile* incidence reduced by around 25% and 17% between 2012 and 2017, respectively (Andrew et al., 2018). However, their report included a 1.5% and 17% increase of *E. coli* and methicillin-susceptible *S. aureus* (MSSA) HCAI incidence over the same period, respectively; more than 5,500 patients were killed by *E. coli* infections in 2015, which cost the NHS £2.3 billion by 2018. Concerns of multi-drug resistant bacteria in waterborne HCAIs outbreaks were emphasised in these studies due to the reduction of therapeutic effectiveness of antimicrobial agents such as antibiotics in treating infected patients. According to the O'Neill commission in 2016, approximately 700,000 patients die annually due to infections caused by antibiotic resistant microorganisms, with an estimated 10 million deaths by 2050 and a cumulative global cost of $100 trillion as the emergence and spread of antibiotic resistant microorganisms continues to grow (O'Neill, 2018). Thus, before such pathogens reach

patients, especially immunocompromised individuals, efforts have focused on controlling the misuse of antibiotics, implementing safe practices of better hygiene and improved sources of safe water.

In the UK, national guidance for safe water has been put into place, implementing routine water quality monitoring in augmented care units with specified interventions in the event of high microbial counts in treated water such as microbial counts of more than 0 and more than 10 CFU/ 100 mL of *E. coli* and *P. aeruginosa*, respectively (DoH, 2013; DoH, 2016). Interventions to improve water quality in such events include the application of conventional methods such as boiling of water, replacement of filters, pipework with high deposits of scales or biofilms being replaced, and disinfection(Bichai et al., 2008). Chlorination is an established effective conventional method of disinfection, reducing the number of bacteria in contaminated water, but it can be challenging to maintain adequate levels throughout the water distribution system (residual levels of less than or equal to 0.5 mg/L) to prevent recolonization of treated water and biofilm formation Li and Mitch, 2018). This includes problems of emerging concern such as toxic by-products in events of hyperchlorination, inefficient disinfection of some pathogens of clinical concern such as *P. aeruginosa,* an increase in antibiotic resistance of planktonic organisms, with studies reporting protection of waterborne pathogens by biofilms and other organisms such as amoeba (Bridier et al., 2011; Mao et al., 2018; Hou et al., 2019). While maintenance of pipework is required to prevent against leakage that can allow external contaminants into treated water and preserve the physical integrity of the distribution system by preventing the growth of deposits, it constitutes a significant management challenge for both an operational and public health point of view, including financial liability (Pollard, 2016). Several studies have focused on finding alternative methods of disinfection, with higher efficacy than chlorine, such as antibiofilm surface modifications and coatings to prevent biofilm deposition leading to water contamination and biocorrosion in distribution systems (Sadekuzzaman et al., 2015; Kregiel et al., 2019). Installation of point-of-use filters (0.2 μm filtration units) at the exit of water outlets have been reported as effective in terms of dealing with contaminated tap water without the drawbacks of chemical based disinfection to subdue HCAI outbreaks and supply an immediate source of microbe free water in the event of a HCAI outbreak (Loveday et al., 2014; Falkinham III et al., 2015). In a 2-year study, Trautmann et al. reported a significant reduction of *P. aeruginosa* infections in a surgical ICU; from 3.9

incidences per month before point-of-use filter installation to 0.8 incidences per month after point-of-use filter installation (Cervia et al., 2008). Yet, point-of-use filtrations were costly in terms of hospital wide application and replacement being incapable of eradicating and only blocking the discharge of microorganisms to the treated effluent and the environment from the filter outlet. Radical strategies involving water free patient care such as the removal of sinks and the covering of water dispersal sources such as toilets, wash basins and sink drains where spray of water droplets could occur demonstrated a significant reduction of HCAIs (Mathers et al., 2018; Shaw et al., 2018; Livingston et al., 2018). Hopman *et al.* reported a reduction in the rate of patient colonization with Gram-negative bacteria, particularly patients with longer admissions in the ICU from a 2.5 to 3.6 fold reduction (Hopman et al., 2017). However, in such studies, they relied on bottled water and disposable materials. Water free patient care relying on bottled water is ineffective as a long-term strategy, increasing the costs of patient care and problems with storage space for large patient population. In addition, some studies traced ICU outbreaks of HCAIs caused by *P. aeruginosa* to bottled water and thus, regular testing is required to ensure bottled water is sterile (Eckmanns et al., 2008; Naze et al., 2010).

Other than the presence of antibiotic resistant bacteria in treated water, antibiotic resistance genes and antibiotics are only partially removed by conventional water treatment methods and enter treated water supplies (Rizzo et al., 2013). So far, there is poor understanding of such contaminants in water supplies, in terms of health impact and levels that lead to resistance in bacteria, with no maximum limit of antibiotics established by the EU and other international organizations (Rizzo et al., 2013). Previous studies of residual antibiotics, up to 1 ng/L, in drinking water have reported no harmful effects to human health but the implications of potential toxicity from long-term exposure, bioaccumulation and effect during developmental periods have yet to be further investigated (Simazaki et al., 2015; Wang et al., 2016; Jin et al., 2016; Li et al., 2017; Wang et al., 2017). Nonetheless, some studies reported that antibiotics and antibiotic resistance genes in ng/L to µg/L in aquatic environments could cause the acquisition of antibiotic resistance in bacteria (Sandegren, 2014; Danner et al., 2019), with the antimicrobial effect of antibiotic lost in treating biofilms (Cairns et al., 2018).

Microbial biofilms can be formed from attached single cells and multicellular aggregates on surfaces (Kragh et al., 2016). To effectively prevent the development of biofilms, which can

lead to recontamination of treated water, several studies have focused on interfering in the attachment process during water distribution and improving treatment efficiency for 100% disinfection. A recent report by the European Commission highlighted improving the efficacy of water treatment, upgrading water treatment facilities with more advanced treatment technologies for the purpose of preventing waterborne microorganism that may develop to biofilms in distribution systems, reducing antibiotic resistance and providing potable water (Isabella et al., 2018). Specifically, advanced oxidation processes using non-thermal plasma has gained significant interest as an effective advanced treatment technology for the chemical-free treatment of water (Foster, 2017). Microbial inactivation was attributed to be a consequence of the combined effect of the plasma process and generated reactive species. Compared to direct plasma-microorganism interaction in studies such as surface treatment, the presence of liquid acted as an additional barrier that impeded the direct interaction of plasma with the microorganisms in water. However, plasma generated in water has been attributed to plasma-induced changes in treated water. Plasma-liquid interaction leads to plasma processes such as UV light and the formation of several reactive species such as hydrogen peroxide, ozone and hydroxyl radicals, which are considered to be the main reactive species that promote the bacterial inactivation process (Foster, 2017).

Several reactors using non-thermal plasma have demonstrated effective inactivation of various strains of bacteria such as *Pseudomonas aeruginosa*, *Bacillus subtillus*, *Escherichia coli*, *Listeria monocytogenes*, *Acidithiobacillus ferrooxidans*, *Legionella gratiana*, *Staphylococcus aureus* and *Staphylococcus epidermis* (Mai-Prochnow et al., 2014; Tian et al., 2015; Johnson et al., 2016; Zhang et al., 2017; Shaw et al., 2018; Pai et al., 2018; Kondeti et al., 2018). In a recent review by Liao *et al.,* the antimicrobial efficacy of non-thermal plasma can be affected by several factors including environmental elements such as pH and process parameters of reactors such as input power, treatment time and gas type (Liao et al., 2017). So far, studies have focused on improving reactor design parameters that can enhance performance in both batch and continuous flow configurations, as well as energy efficiency and mass transfer of plasma species from gas into liquid for treatment (Malik, 2010). Higher treatment efficiencies using water films and spray discharge in plasma reactors was established for degradation of some organic and inorganic contaminants yet limited studies have been reported in terms of their antimicrobial application in a continuous flow system (Malik, 2010; Vanraes, 2016). Production

of plasma-activated water using water film or spray discharge containing high concentrations of long-lived species with antimicrobial properties such as hydrogen peroxide was reported as a tool for disinfection (Scholtz et al., 2015). Burlica et al. reported inactivation of *E. coli* grown on agar by plasma-activated water, generated by spray discharge and sprayed onto the sample (Burlica et al., 2010). Compared to water film or spray discharge, several studies have demonstrated inactivation of bacteria in water using other types of discharges. Liu et al. used electrohydraulic discharge, where plasma is generated in water inoculated with *S. aureus*. Kim et al. used remote discharge to generate plasma-activated water and injected into water inoculated with *E. coli* (Kim et al., 2013). Rashmei *et al.* demonstrated effective disinfection of *E. coli* and *Enterococcus faecalis* in water using gas discharge where plasma is generated on the surface of the liquid (Rashmei et al., 2016).

This work focused on evaluating the antimicrobial efficiency of non-thermal plasma generated in a microfluidic plasma reactor. With microscale devices, the high surface-area-to-volume ratio inherent to microfluidics allows high plasma-microorganism interaction and mass transfer of plasma species into water for disinfection while operating in a continuous gas-liquid flow system. The optimised operating parameters from Chapter 5 were evaluated against opportunistic pathogens *E. coli* and *P. aeruginosa,* which are commonly isolated from waterborne HCAIs, focusing on microbial death and maximum antimicrobial efficiency.

6.2 Experimental set-up

The same experimental set-up described in Chapter 3.3 was used in this chapter. Antibiotic resistant strains of *E. coli* (NCIMB 10244, UK) and *P. aeruginosa* (ATCC 47085, US) were investigated in these assays. Cells were diluted in 10 mL sterile PBS (phosphate buffered saline) solution, prepared using sterile membrane filtered water (MilliporeElix, USA), to an optical density (OD) of 0.4 at 600 nm using a UV-vis spectrophotometer (Jenway 6305, UK), calibrated against sterile PBS. The sterile PBS used contains sodium chloride (8.0 g/L), potassium chloride (0.2 g/L), di-sodium hydrogen phosphate (1.15 g/L) and potassium dihydrogen phosphate (0.2 g/L) at a pH of 7.3 ± 0.2 at 25°C. Cell counts were determined in CFU/mL using serial dilutions and the spread plate method, before and after plasma treatment, as described in Chapter 3.6. Cell counts of 5.4 x 10^8 and 7.0 x 10^8 CFU/mL were determined for *E. coli* and *P. aeruginosa*, respectively. For mixed bacterial cultures, MacConkey agar (Oxoid, UK) was used for selective

differentiation of both bacteria, i.e. *E. coli* colonies appeared pink in colour while *P. aeruginosa* colonies showed no colour. Cell counts of 3.0 x 10^5 and 5.0 x 10^5 CFU/mL for *E. coli* and *P. aeruginosa*, respectively, were determined in mixed bacterial culture.

Both air and the inoculated liquid sample were introduced into separate inlets of the microfluidic plasma reactor. Gas flow pressure was regulated to 2 bar in a channel depth of 50 μm while using air as the carrier gas. Bacterial colonies from planktonic and mixed culture samples were counted before entering the inlet and after exiting the outlet. The collection of samples was carried out after 3 to 5 minutes without plasma to stabilize the liquid flow and 5 minutes after initiating plasma generation in the reactor. The experiments were repeated at least three times using independently grown cultures. To test for adhesion and blockage over time, samples were left to continuously flow for 24 hours using a 35 μL/min - 100 μL/min liquid flow rate. Fluorescence test was performed to check areas showing fluorescence, which was used to indicate bacterial adhesion on the channel walls. Morphological changes were observed using SEM and viability of plasma treated bacteria were observed using LIVE/DEAD assay. Both method were described in Chapter 3.

Treatment of planktonic and mixed culture samples of *E. coli* and *P. aeruginosa* by AP-DBD generated in MPR1 with serpentine channel length of 212 mm and channel depth of 100 and 50 μm were studied. A fixed applied voltage of 10 kV_{p-p} and a frequency of 17 kHz with air as the gas source were used.

6.3 Results and discussion

6.3.1 Microbial adhesion

For every treatment, a control experiment with the inoculated sample flowing into the reactor treated only by the flow of the air as carrier gas but without plasma ignition was carried out. Bacteria tend to adhere to surfaces, forming microcolonies and developing biofilms (Tuson and Weibel, 2013). In continuous flowing systems, fluid flow can enhance transfer of substrates such as nutrients in the bulk liquid to the adhered bacterial colonies or biofilms (Taherzadeh et al., 2012). This allows the development of colonies and established biofilms on the surface of the channel, which may significantly affect the number of bacteria leaving the reactor via

the outlet and cause blockages in the microchannel over time. No adhesion of large bacterial aggregates was observed on the channel walls but a cloudy appearance was observed in the fluorinated ethylene propylene (FEP) tubing using *E. coli* inoculated water. Similar results were observed with *P. aeruginosa* (Figure 6.1).

a) b) c) d)
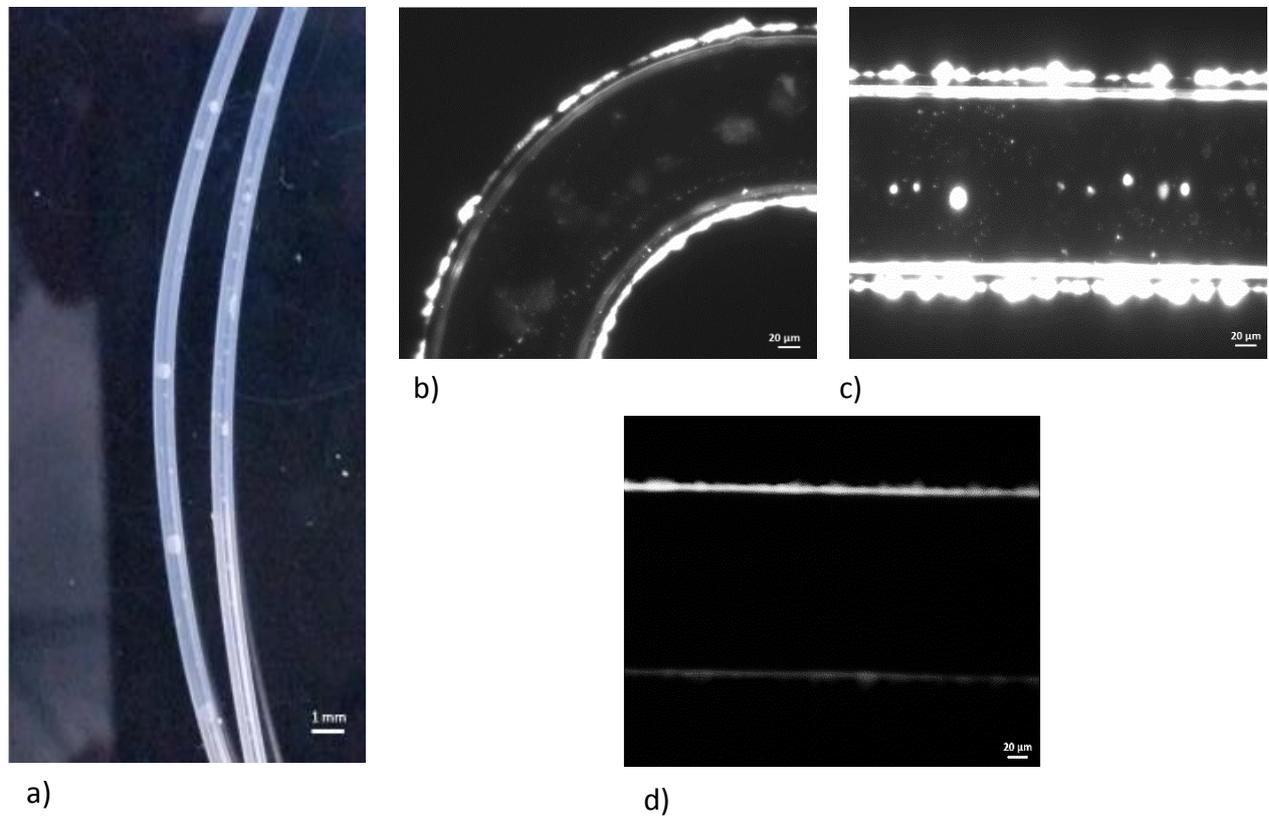
Figure 6.1: Image of the FEP tubing (a) and epifluorescence microscopy images of the microchannel (b and c) after 24 hours continuous flow of inoculated liquid and d) after plasma ignition. Liquid flow rate of 100 µL/min and 2 atm gas pressure were used.

No blockages and no significant reduction in bacterial counts over time was observed for both *E. coli* and *P. aeruginosa* ($p > 0.05$) as the solution containing these bacteria flowed through the reactor (Figure 6.2). This could be due to the enhanced fluid velocity and pressure from both air and liquid in the microchannel with small channel diameter, i.e. µm, compared to wide channel, i.e. mm, exerting shear forces on the attaching cells, inhibiting cell attachment and thus resulting in detachment of these cells (Rijnaarts et al., 1993; Donlan, 2002; Taherzadeh et al., 2012). No further observation of fluorescing bacteria on channel walls was made in areas where plasma was formed (Figure 6.1 (d)). This could be due to multiple processes and reactive species formed during plasma ignition where antimicrobial activity occurs upon bombardment with bacteria attached on surface of the channel walls and in water (Burts et al., 2009; Scholtz et al., 2015).
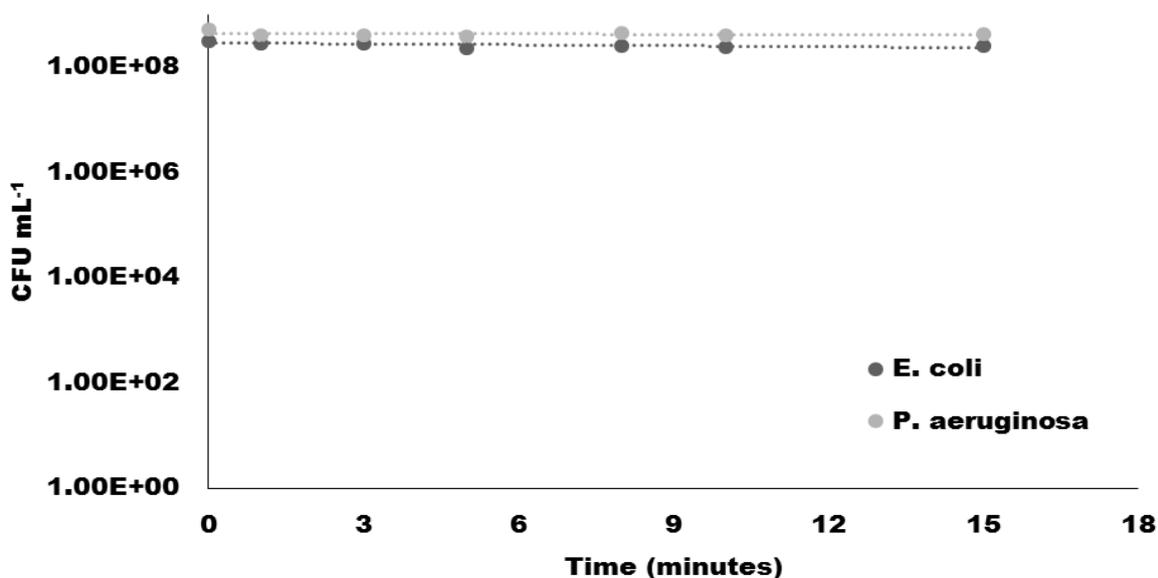
Figure 6.2: Measurement of E. coli and P. aeruginosa before entering the inlet (defined at 0 minute) and after exiting the outlet where samples was collected at various times, 100 µL/min liquid flow rate and 2 atm gas pressure. Error bars represent standard errors n = 3. Statistical significance, $\rho < 0.05$.

6.3.2 Plasma treatment of bacteria in monoculture samples

Planktonic and mixed bacterial samples were treated at various residence times by non-thermal plasma generated in the microchannel. The residence time of the inoculated liquid in the plasma zone was regulated through changing the liquid flow rate entering the microfluidic plasma reactor. Before plasma treatment, 16S, Sanger sequencing was used to determine and confirm the identity of obtained bacterial samples (Figure S6.3 in the appendix).

The surviving CFU/mL of the *E. coli* and *P. aeruginosa* over residence time showed that the reduction of *E. coli* and *P. aeruginosa* increased with increasing residence time. There was significant difference ($\rho < 0.05$) between untreated and plasma treated bacterial samples (Figure 6.3 and 6.4). Both bacterial strains were 100% inactivated where no colonies were observed, using 35 µL/min liquid flow rate with residence time of 5.3 seconds in the plasma zone. However, compared to *P. aeruginosa*, *E. coli* was inactivated more rapidly; no colonies were observed at lower residence time of 4.6 seconds after 24 hours of incubation. A statistically significant difference ($\rho < 0.05$) was observed between the plasma treated *E. coli* and *P. aeruginosa* as monoculture samples. This result indicated that *P. aeruginosa* may

require a higher residence time for further interaction between the bacteria and reactive species formed in the gas and liquid phase during plasma ignition or increased plasma density for a higher rate of inactivation.

Though both *E. coli* and *P. aeruginosa* are classified as Gram-negative bacteria, the composition of their extracellular polymeric substance (EPS), which acts as protection from external forces and maintain biofilm architecture, differs. In *E. coli*, the composition of its EPS include various polysaccharides, proteins, membrane lipid and β-1,6-N-acetyl-D-glucosamine as polysaccharide adhesin for biofilm formation (Goller et al., 2006) while the EPS matrix of *P. aeruginosa* includes galactose- and mannose-rich Psl polysaccharide, protein, extracellular DNA, nucleic acid and other molecules (Ma et al., 2009). The use of plasma to treat *E. coli* and *P. aeruginosa* may be limited by its ability to penetrate the EPS matrix; the outer membrane of *P. aeruginosa* is 10 to 100 fold less permeable than *E. coli* and thus may lead to slow transport of reactive species formed in the gas and liquid phase during plasma ignition into the bacteria (Breidenstein et al., 2011; Gellatly and Hancock, 2013). However, a recent study on *E. coli* has found that during plasma treatment, the heat shock protein 33 (Hsp33) is activated to prevent protein aggregation, increasing the survival rate of bacteria that over-express the Hsp33 encoding gene (Krewing et al., 2019). The Hsp33 gene is present in *P. aeruginosa* but similar studies have not yet been reported (Groitl et al., 2017). Little is yet known in regards to waterborne bacteria developing resistance to plasma, similar to antibiotics. Yet, a recent study with *P. aeruginosa* has shown that plasma interferes with cell-to-cell communication in bacteria via quorum sensing, defined as the ability to regulate gene expression in response to changes in cell density. This limits the regulation of gene expression in bacteria, and thus results in reduction of virulence (Flynn et al., 2016). Different types of protein damage occur as a result, which eventually leads to membrane permeation, membrane depolarization and bacterial inactivation (Yost and Joshi, 2015).

After 72 hours of incubation, emerging colonies of *E. coli* and *P. aeruginosa* were observed on agar plates with samples treated at residence times of between 1 and 3 seconds. The number of new colonies was low, less than 100 CFU/mL. No new colonies were detected in agar plates with samples treated with residence time greater than 4 seconds.
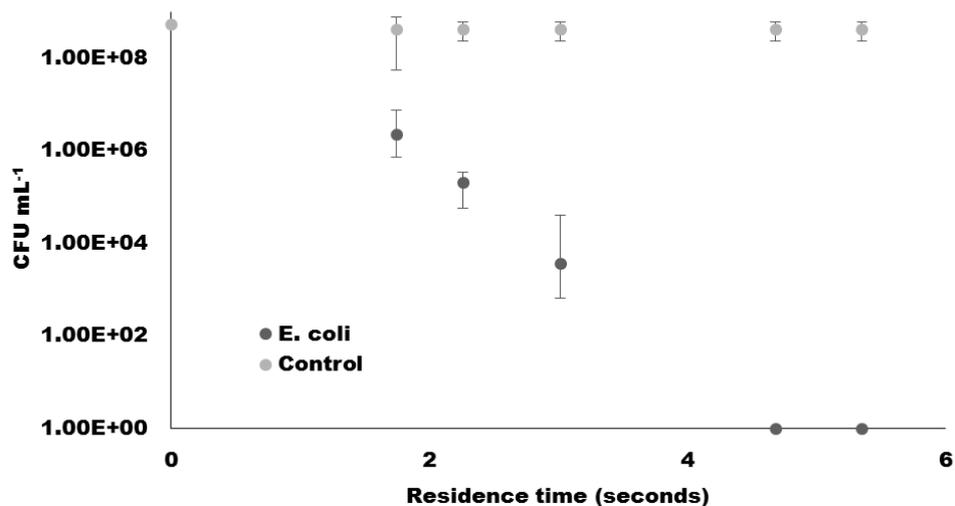
Figure 6.3: Surviving CFU/mL of monoculture E. coli in water after plasma treatment at various residence times. CFU/mL at 0 seconds indicates the starting CFU of E. coli in water introduced into the inlet while the subsequent results refer to samples collected from the outlet. Error bars represent standard errors n = 3. Statistical significance, $p < 0.05$.
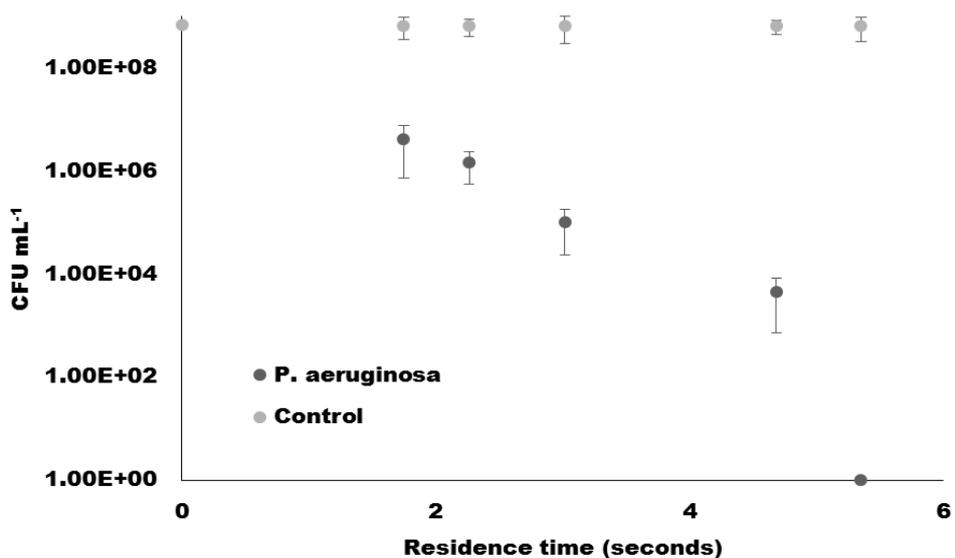
Figure 6.4: Surviving population of monoculture P. aeruginosa in water before and after plasma treatment at various residence times. With the control data, CFU/mL at 0 seconds indicates the starting population of P. aeruginosa in water introduced into the inlet while the subsequent results refer to samples collected from the outlet. Error bars represent standard errors n = 3. Statistical significance, $p < 0.05$.

The microfluidic plasma reactor was able to achieve bacterial inactivation in the range of seconds of treatment, which showed it was sufficient to induce inactivation of bacteria in the water. The differences in residence time of liquid in plasma between the microfluidic reactor and plasma reactors reported in literature, demonstrate great influence of mass transfer on

disinfection by non-thermal plasma in shorter periods, i.e. from minutes and hours to seconds of treatment. Malik et al. reported that the surface-area-to-volume ratio of water under treatment affected mass transfer, indicating that high treatment efficiency observed using water spray or film was due to their large surface-area-to-volume ratio (Malik, 2010). Compared to conventional reactors, with liquid depths of cm or mm, reducing channel size down to those found in microfluidic devices in the order of microns increases surface-area-to-volume ratio as the scale of the water film is reduced to micrometres. Thus, greater mass transfer and penetration of reactive chemicals from gas into liquid was obtained as compared to bulk reactors in static configuration with smaller surface-area-to-volume ratios where plasma interacts at the interface of the bulk liquid.

Using air as the carrier gas for non-thermal plasma generation, complete inactivation of bacteria was achieved. Different carrier gases such as oxygen, nitrogen and argon have been used for plasma-based disinfection of water (Mai-Prochnow et al., 2014; Tian et al., 2015; Johnson et al., 2016; Zhang et al., 2017; Shaw et al., 2018; Pai et al., 2018; Kondeti et al., 2018). However, air is more attractive as an abundant and cheap source for plasma generation for cost effective plasma based water disinfection. As the main components of air are oxygen and nitrogen, a combination of ROS and RNS can be formed. Short-lived species (NO, OH and superoxide) and long-lived species described in Chapter 4 (nitrates, nitrites, ammonium) induce anti-microbial effect but the full mechanism of the direct oxidative effect induced by each individually or the synergy of these chemicals has yet to be understood. For example, hydrogen peroxide is a known effective disinfectant. In addition, when reacted with other chemicals generated in plasma such as nitrate, peroxynitrite forms, as shown in equation 6.1 and 6.2, which has been suggested to induce an anti-microbial effect (Zhou et al., 2018). Peroxynitrite toxicity in microorganisms has been suggested to induce an oxidative stress response through oxidation and nitration of critical cell components. For example, the oxidation of the mitochondrial membrane leads to release of pro-apoptotic factors and peroxynitrite-induced hyperactivation of the nuclear enzyme poly (ADP-ribose) polymerase causing reduction of ATP and NAD^+, ultimately leading to apoptosis, necrosis or dysfunction (Szabó et al., 2007; Islam et al., 2017).

$$NO_2^- + H_2O_2 + H^+ \rightarrow O=NOOH + H_2O \qquad \text{Equation 6.1}$$
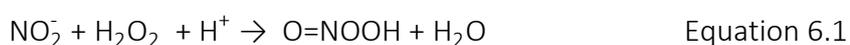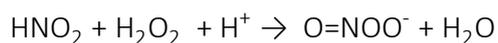
$$HNO_2 + H_2O_2 + H^+ \rightarrow O=NOO^- + H_2O \qquad \text{Equation 6.2}$$

6.3.3 Plasma treatment of mixed culture samples

Both *E. coli* and *P. aeruginosa* in water was used to investigate the efficiency of the microfluidic plasma reactor in treating mixed microbial bacterial cultures in water. Upon using the MacConkey agar, no reduction in CFU/mL was observed in the mixed culture sample with *E. coli* and *P. aeruginosa* initial total concentration of 7.40×10^5 CFU/mL and 5.40×10^5 CFU/mL for each bacteria) (Figure 6.5).
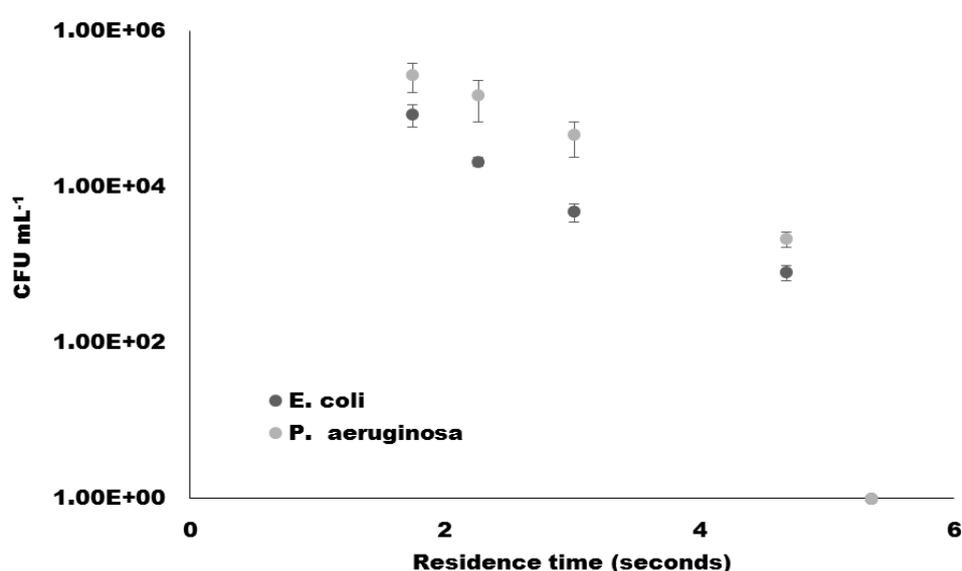
Figure 6.5: Surviving populations of E. coli and P. aeruginosa after plasma treatment at various residence times. Error bars represent standard errors n = 3. Statistical significance, $p < 0.05$.

The result showed a significant reduction in CFU/mL of both bacteria as residence time increased; no colonies of either bacteria were observed after a residence time of 5 seconds. The results of plasma treated mixed culture samples showed no statistical difference ($p > 0.05$) between the amount of surviving *E.coli* and *P. aeruginosa*; there was a significant difference ($p < 0.05$) in CFU/mL of the mixed culture sample before and after plasma treatment at all residence times tested. However, compared to the monoculture *E. coli* from the previous section, several colonies of *E. coli* were observed on agar plates with samples treated with 4 seconds of residence time, whereas no colonies were observed in the monoculture counterpart. After 72 hours of incubation, emerging colonies of *E. coli* and *P. aeruginosa* were observed on agar plates with less than 4 seconds of residence time but no significant increase

in colonies observed for both colonies, less than 500 CFU/mL for both *E. coli* and *P. aeruginosa*. No new colonies were detected with a residence time of more than 4 seconds.

Several papers have indicated that there was inactivation of bacteria after plasma treatment, yet few had further examined possible regrowth of colonies after more than 24 hours incubation (Yingguang et al., 2011; Sanaei and Ayan, 2015; Ercan et al., 2018). In this study, a higher residence time showed no regrowth of bacteria after an incubation period of 72 hours, which could be due to a higher degree of plasma and water interaction inducing oxidative stress, which killed the bacterial samples in water. However, regrowth of small colonies was detected on agar plates, with samples treated with shorter residence times, after 72 hours incubation and the counts remained the same after a further 24 hours incubation. This may be indicative of small colony variant (SCV) bacteria, an aberrant form of bacteria generated in response to environmental stress, characterized with a slow growth rate, reduced metabolic activity and increased resistance to antibiotics, which are able to recover over time when provided with essential factors such as nutrients (Proctor, 2006). Several studies indicated SCV bacteria to be less virulent due to less efficient colonization but infections facilitated by SCV bacteria were over 100 fold resistant to treatment than normal strains (Proctor, 2006). Initial studies of *P. aeruginosa*, *E. coli* and *S. aureus* SCV strains reported their ability to remain within the host cells and cause recurrent or chronic infections despite the use of antibiotics (Melter and Radojevič, 2010; Xia et al., 2017; Pestrak et al., 2018). In this study, treated samples were left on agar for further incubation, which has the essential factors such as nutrients that may have led to the bacterial regrowth observed (Kriegeskorte et al., 2014). Similar to SCV bacteria, viable but nonculturable (VBNC) bacteria, which refers to live bacteria in a state of low metabolic activity, which cannot be cultured, remains a concern for potential risks upon exposure. The current method of spread plating fails to detect bacteria treated by non-thermal plasma that have entered the VBNC state. Although there are conflicting viewpoints in terms of virulence of VBNC bacteria, some studies have found resuscitation of VBNC bacteria in favourable conditions such as nutrient availability and temperature-induced resuscitation (Ramamurthy et al., 2014). This potentially allows bacteria to cause infections prior to or after it enters the body. However, this may not be reflective in terms of non-thermal plasma inducing SCV or VBNC states in bacteria during and after treatment. This is due to stronger antimicrobial effect than conventional disinfectants, with effects such as acidification and

presence of long-lived species as residual disinfectant against regrowth of bacterial colonies in plasma treated water. As observed in plates with samples treated at a longer residence time, no colonies were detected after 72 hours of incubation compared to samples treated with shorter residence times, which were assumed to be SCV or resuscitated VBNC *E. coli* and *P. aeruginosa*. Virulence and resistance of regrown bacteria in SCV or VBNC states detected in plasma treated water has yet to be reported. This generates concern and further research is required in terms of survival and virulence of surviving strains.

6.3.4 Scanning Electron Microscope (SEM)

SEM analysis was employed to visualise the effect of non-thermal plasma treatment on bacteria in water using a microfluidic plasma reactor. Images of untreated *E. coli* and *P. aeruginosa* confirmed the presence of healthy cells with the cell membrane appearing smooth and intact (Figure 6.6). After plasma treatment, both bacterial species showed distinct signs of damage such as irregular shape, dimples on the surface, craters, holes and burst cell membranes. This may have led to its content being released and resulting in its inactivation.
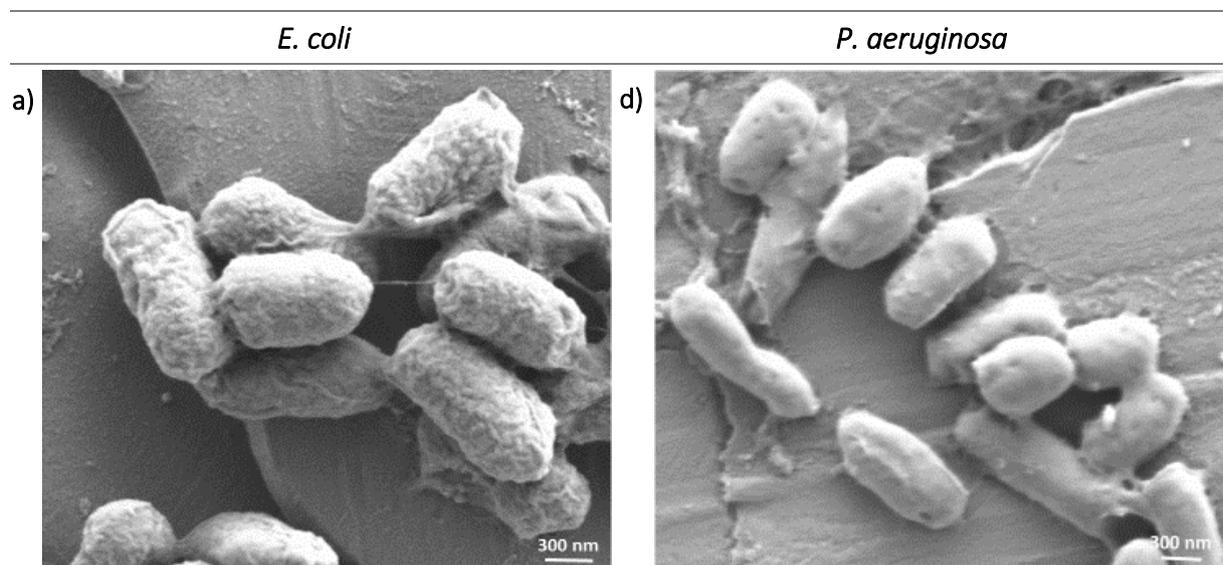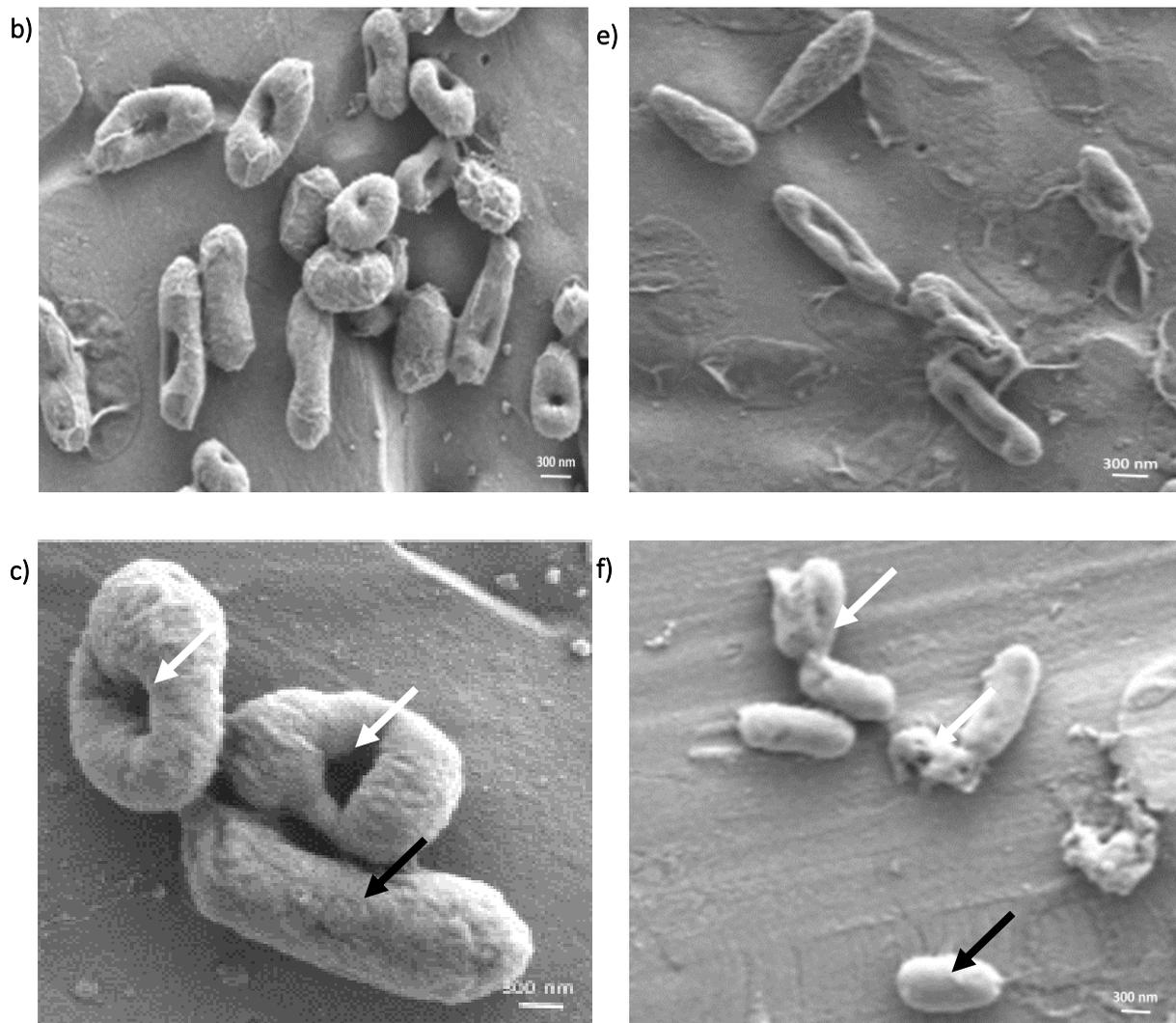
E. coli	*P. aeruginosa*

Figure 6.6: SEM images *of E. coli* (a, b, c) and *P. aeruginosa* (d, e, f) before and after plasma treatment. Untreated *E. coli* (a) and *P. aeruginosa* (d). Plasma treated *E. coli* (b, c) and *P. aeruginosa* (e, f). Images a and d correspond to control samples, images b and e to samples treated with a 5 seconds residence time and images c and f to samples treated with a 3 second residence time. Black arrows indicate intact cells while white arrows indicate dimples or damaged cells.

The appearance of such distinct damage on cells after plasma treatment has been previously reported for *E. coli* and *P. aeruginosa*; plasma treatment results in ruptured cell membrane and leakage of contents, affecting their metabolic functions and ability to replicate and grow, which leads to the death of the bacteria (Ziuzina et al., 2015; Sun et al., 2018). A series of chemical and physical reaction processes induced simultaneously by plasma processes such as UV light, high-voltage electric fields, and reactive species generated in plasma can lead to inactivation of cells (Montie et al., 2000; Mounir Laroussi et al., 2002). According to Laroussi et al., OH radicals compromise cellular viability through oxidation of proteins and

polyunsaturated fatty acids in the bacterial cytoplasmic membrane i.e. lipid peroxidation, reducing its permeability, barrier function, and transport of ions and molecules in and out of cells (Laroussi and Leipold, 2004). Thus, prolonged exposure to plasma causes rupture of cell membranes, leakage of intracellular components and exposure of genetic material to the surrounding environment. Mendis et al., theoretically predicted that such morphological change is caused by electrostatic disruption of the cell membrane, specifically electrostatic stress caused by charge collection on the outer membrane exceeding the tensile strength of the cell membrane (Mendis et al., 2000). In addition, such electrostatic disruption is more pronounced in Gram-negative bacteria with irregular structure, rough surface and thin membranes compared to Gram-positive cells with a smoother surface and thicker peptidoglycan layer Mai-Prochnow et al., 2016). Some papers displayed SEM images comparing Gram-negative and Gram-positive bacteria where similar irregularity of the cell membrane was observed with inactivated Gram-negative bacteria while inactivated Gram-positive bacteria show intact cell membrane with associated changes in configuration, i.e. from long to short chains after plasma treatment (Laroussi et al., 2002; Lee et al., 2019;). This was further explained by differences in strength due to the thickness of the cell wall.

In the SEM images, dead cells were identified with burst membranes but cells with intact membranes were also observed (Figure 6.6 (c, f)), which were assumed to be live, VBNC or SCV bacteria recovered. However, some studies reported that plasma was not specific with damaging the cell membrane only, detecting reactive species such as hydrogen peroxide within the cells after plasma treatment. These reactive species can exert intercellular damage and lead to oxidation of lipid, proteins, carbohydrates and nucleic acid (Joshi et al., 2011; Dobrynin et al., 2011; Yost and Joshi, 2015). Yost et al., found that long exposure of *E. coli* to plasma of 5 to 10 minutes led to oxidative stress of the DNA through oxidation of DNA bases, causing DNA fragmentation (Yost and Joshi, 2015). At the same time, they found OxyR and SoxR, regulator proteins that detect oxidative stress and regulate antioxidant genes, activated in *E.coli* in the presence of hydrogen peroxide after plasma treatment. However, an imbalance due to increasing accumulation of reactive species treatment over cellular detoxifying capacity of the cell during prolonged plasma led to oxidation of the regulator proteins and oxidative stress-induced cell death.

6.3.5 Live/Dead Assay

A Live/Dead assay was conducted on cells treated with plasma since SEM was limited in determining viability of treated cells, specifically the cells with intact membranes (Figure 6.6). Plasma treated *E. coli* and *P. aeruginosa* were double stained with SYTO9/propidium iodide (PI) and observed by epifluorescence microscopy. SYTO9 permeates the intact cell membrane of living cell and stains the cell green while PI cannot permeate through the cell membrane of living cells and stains dead cells with disrupted cell membranes red. Representative live and dead cell controls for the Live/Dead assay were tested (Figure S6.4 in the appendix). Results from the Live/Dead staining indicated dead *E. coli* and *P. aeruginosa* after plasma treatment; control *E. coli* and *P. aeruginosa* showed green fluorescence while plasma treated *E. coli* and *P. aeruginosa* showed red fluorescence (Figure 6.7). This showed that plasma affected the permeability of the cell membrane, which allowed PI to enter the cell, emitting red fluorescence upon binding to the DNA. Thus, dead *E. coli* and *P. aeruginosa* were identified in plasma treated water. Likewise, no green fluorescence was detected in samples treated in 5 seconds residence time after 72 hours incubation. However, this method is limited in providing indication of red fluorescing bacteria in VBNC or SCV state, which under favourable conditions such as nutrient availability can potentially re-grow. In some samples treated with longer residence times, a small fraction of green fluorescence was detected indicating live cells (Figure 6.7 (c, f)). This may correspond to some of the bacteria detected in the SEM images with intact membrane after plasma treatment. However, as previously mentioned, plasma treatment was not specific in causing damage to the cell membrane for inactivation. Thus, such bacteria with intact cell membranes but with compromised function allows permeation of SYTO9 (Schmidt-Emrich et al., 2015).
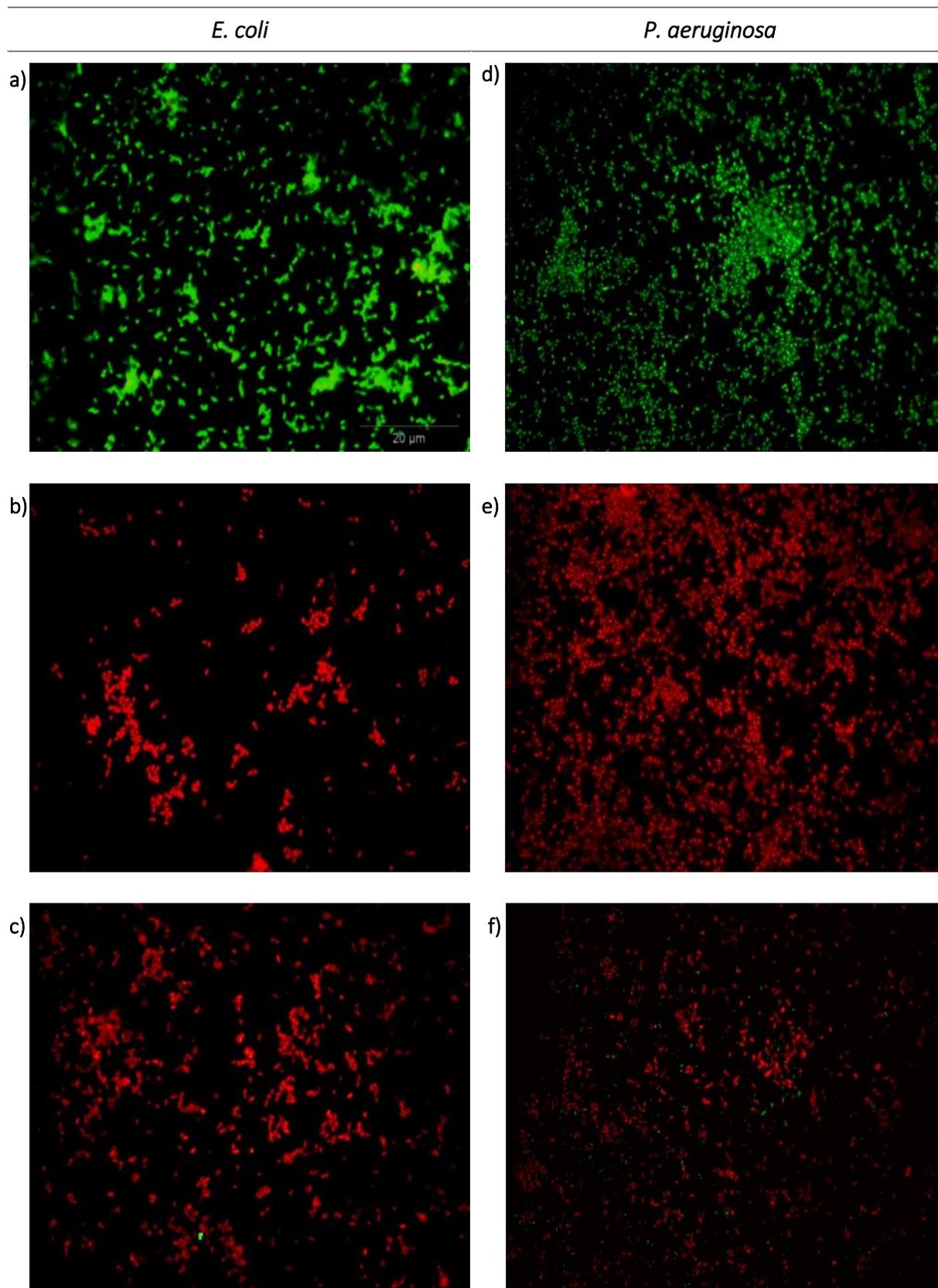
Figure 6.7: *E. coli* (a, b, c) and *P. aeruginosa* (d, e, f) viability according to Live/Dead assay results before and after plasma treatment. Images a and d correspond to control samples,

images b and e to samples treated with a 1 second residence time and images c and f to samples treated with a 5 second residence time.

6.4 Summary

Antimicrobial efficacy of a microfluidic plasma reactor was investigated. The main findings were:

- Both *E. coli* and *P. aeruginosa* showed the same trend, with decreasing bacterial viability as residence time in plasma increases.
- Using air as the carrier gas, effective disinfection of water was achieved. Full inactivation of both bacteria (10^8 CFU/mL maximum number of each bacteria treated) as monoculture and mixed culture was achieved after 5 seconds of residence time in the plasma region of the plasma microfluidic reactor.
- Mixed bacterial culture samples may induce protection to plasma compared to the monoculture samples.
- Compared to *E. coli, P. aeruginosa* is less susceptible to plasma, probably due to a thicker EPS matrix that offers an extra barrier.
- The ability of plasma to penetrate the bacteria was confirmed with SEM and Live/Dead assay. SEM analysis reveals changes in cell morphology, with ruptured cell membrane, while Live/Dead assays revealed dead and non-culturable cells after plasma treatment. Results may correspond to live, dead VBNC or SCV cells.

This work demonstrated that non-thermal plasma has the potential to replace chemicals and disinfectants for water treatment methods. The microfluidic plasma reactor allows the control of fluid flow dynamics, and utilizes its inherent advantages such as large surface-area-to-volume ratio to facilitate improved mass transfer and plasma penetration of water, leading to cell damage and reducing the viable bacterial counts by 8 orders of magnitude in seconds.

Chapter 7 Conclusion and further work

The primary aim of this work was to develop and characterise a microfluidic reactor that allows for the evaluation of the effect of several operating parameters on the treatment efficiency of chemical and biological contaminants in water using atmospheric pressure non-thermal plasma. Further optimisation of these parameters was carried out to achieve maximum treatment efficiency of these contaminants using air as carrier gas.

Initial characterisation of the microfluidic reactor and influence of non-thermal plasma using air as carrier gas in water resulted in the following findings:

- Plasma was generated in the microfluidic reactor using a two-phase gas-liquid annular flow regime. Both film thickness and residence time of the liquid film formed on the walls of the microchannel was regulated by changing the liquid flow rate.
- As the applied voltage increases, the number of discharges formed in the microchannel increase, in conjunction with reactor temperature. Reactor temperature and longevity was improved by installing a heatsink.
- Using air as the carrier gas, concentration of nitrogen containing ions, such as nitrate, nitrite and ammonium, increase with increasing residence time in range of seconds.

Treatment of a chemical contaminant in the form of MB solution was investigated.

- A longer residence time of the liquid film in the plasma achieved by decreasing the liquid flow rate increases the treatment efficiency of MB; this is due to increasing reactions and collisions between plasma generated species and MB in water. Increasing the gas flow rate showed no signifacant difference in MB degradation.
- The degradation efficiency of MB using the MPR has a maximum of 97% using air as the carrier gas, liquid flow rate of 35 µL/min, a barrier thickness of 2 mm and channel depth of 50 µm.
- Oxygen was found to be the most effective working gas. Higher number of fragments were detected using oxygen as the working gas.

To enhance the influence of residence time on the treatment of MB solution, MPR with longer serpentine channel was used.

- Increasing the length of the serpentine channel showed no significant difference in MB degradation; this is due to power loss from power loading and increasing area of parasitic capacitance.

The influence of process parameters on the anti-microbial effect of non-thermal plasma against *E. coli* and *P. aeruginosa* using a MPR was investigated.

- Using air as the carrier gas, effective disinfection of water was achieved. 100% disinfection of both bacteria (10^8 CFU/mL maximum number of each bacteria treated) as monoculture and mixed culture was achieved after 5 seconds of residence time in the plasma region of the plasma microfluidic reactor.
- Non-thermal plasma induces rupture of the cell membrane with a Live/Dead assay revealing dead bacteria after plasma treatment.

To conclude, maximum treatment efficiency of an organic contaminant, in the form of MB, and biological contaminant, in the form of *E. coli* and *P. aeruginosa* was achieved in air plasma using the MPR. Low levels of ionic species were generated in the plasma treated water. Miniaturized plasma-based reactors have a promising future for application to water treatment and other applications such as chemical synthesis. Multiple MPR devices can be operated in an array to produce an effective continuous flow system for the removal of persistent organic molecules and biological contaminants from water resources. Such a system can be highly portable and operate without the need for reagents or consumables, to provide high quality drinking water or process water for critical applications, for example, in neonatal care in hospitals.

7.1 Future work

In situ measurement of plasma properties would be advantageous in identifying and quantifying the reactive species formed during plasma generation in the MPR, including reactive species formed in water after plasma treatment. This would help further understand the mechanism involved in the degradation or inactivation of chemical and biological contaminants in water. In addition, optimizing the microfluidic reactor to achieve complete treatment of contaminants.

Further investigation in treating hazardous contaminants such as pesticides and mixed contaminants in water, simulating industrial effluents with contaminants that pass through untreated by conventional methods is important for comparison of efficiency with conventional water treatment methods. Identification of the intermediates and separation fo by-products formed during and after treatement is important to allow assessment of toxicity,

Reactor design is another area for further investigation. This includes reducing parasitic capacitance by either reducing the length of the channel or shaping the electrode similar to the shape of the channel. Further development in reducing power loading on the electrodes which affects the reactor temperature is important to improve longevity and energy consumption of such reactors; this includes pulsed power generator and investigating different electrode material and fabrication material such as quartz with higher temperature resistance than glass.

Numerous studies have reported effective treatment of a wide array of contaminants in water compared to conventional treatment and AOP methods. However, plasma technology is yet to be applied for direct treatment of water in industrial scale. A compact plasma system in the form of MPR has been developed so far for laboratory scale experiments and short treatment times, i.e. in seconds. Scaled up versions or multiple arrays of MPRs that can treat high throughput volume as a continuous system are still to be developed.

Appendix

Table S2.1: List of experimental works on the treatment of methylene blue solution with various types of discharge and reactors. Publications including pre- or post-treatment of water solution have been omitted.

Reactor	Type of Plasma/Electrode	Gas/Voltage/Energy	Performance	Reference
Electro-hydraulic	- Pulsed plasma arc, titanium	- 48 mJ pulses for 5 minutes	- 42% degradation after 5 minutes treatment and 14 days of aging, increased to 44% after 3 months	(Parkansky et al., 2013)
	- Pulse discharge, stainless steel	- Air, 80-100 V per 0-2 µs, 80 W	- 94.5% degradation after 30 minutes of treatment	(Jin et al., 2014)
	- Pulsed plasma arc, stainless steel	- 32 - 80 V, 40 – 217 mJ	- 30 to 80% MB degradation achieved after 3 minutes of treatment with multi-electrode reaching 100% removal	(Meirovich et al., 2016)
	- Pulsed plasma discharge, Tungsten/iron/aluminium	- 800 V	- More than 80% MB removal after 2 min of treatment with higher treatment efficiency using tungsten	(Son et al., 2015)
	- Pulsed arc, carbon/low carbon steel/ iron	- 2.6 – 192 mJ	- Higher removal efficiency observed using iron electrodes compared to carbon, achieving 99.8% removal after 4 min treatment	(Parkansky et al., 2012)
Bubble	- DBD multiple bubble jet, tungsten/copper	- Argon/oxygen/dry air, 6 - 8 kV, 10 W for oxygen, air/ 40 W for argon	- 100% degradation after 20 minutes treatment using oxygen bubble jet and high flow rate, 4.0 SLM	(Nishiyama et al., 2013)
	- Streamer/micro-arcs, Kanthal A-1 (Fe 71.02%, Al- 5.8%, Cr- 22%, Mn-0.4%, Si-0.7% C-0.08%)	- Argon, 1.7 kV, 16.5 W	- MB concentration decreases over time following an exponential decay; maximum of ~ 20 minutes to 100 % degradation with initial concentration of 100 mg/L.	(Anghel et al., 2015)
	- Pulsed streamer, Tungsten/stainless steel	- Air, 30 kV, 1.3 W	- 95.7% decomposition after 10 min treatment at 1.13 W power while 93.6% attained after 20 min treatment at 0.42 W.	(Abdelaziz et al., 2018)
	- Electrohydraulic discharge with bubbles, Copper/ stainless steel	- Oxygen/Argon, 17 kV, 19 W	- Slower degradation using argon compared to oxygen, maximum absorption decreased by 58% for argon while 98% for oxygen after 15 minutes of plasma treatment	(Magureanu et al., 2007)
	- AC glow discharge, stainless steel	- Air, 2-15 kV, 6 W	- Total degradation reached after 40 minutes of treatment. 50% degradation after 8 minutes of treatment	(Nikiforov, 2009)
Gas phase	- DBD, silver paste/stainless steel	- Air, 14-18 kV, 0.68 – 2.1 W	- < 97% degradation after 25 minutes of treatment	(Reddy et al., 2013)
	- Streamer discharge, tungsten	- Air, 23 kV, 66 W	- 100 % degradation after 8 min treatment time in 150 mg/L alkalinity, 95.6% degradation after 10 minutes of treatment in 300 mg/L alkalinity	(Singh et al., 2016)
	- DBD, tungsten	- Nitrogen, 2.57 kV, 59.2 W	- Initial decomposition of MB at lower temperature of solution treated but decreases at higher temperature, i.e. 47 °C.	(Benetoli et al., 2011)
	- Pulsed corona, copper	- Air	- Complete decomposition of MB after 10 minutes of plasma exposure.	(Magureanu et al., 2013)
	- DBD, silver paste/stainless steel	- Air/oxygen, 12 kV, 0.5 W	- 90% degradation after 45 min treatment using oxygen as carrier gas compared to air with 56% degradation after 80 min.	(Magureanu et al., 2008)
	- Microwave atmospheric pressure plasma	- Argon, 150 W	- MB solution become colourless after 30 minutes of plasma treatment	(García et al., 2017)
Spray	- DBD, copper/stainless steel	- Air/argon, 6-12 kV ~0.8 W/cm^2	- 100% degradation which decreases with increasing voltage	(Shibata and Nishiyama, 2012)
	- Corona discharge, copper/ stainless steel	- Air, 20 kV, 4 W	- 95.7% degradation after 3 hours of treatment with air	(Liu et al., 2015)
Remote	- Pulsed DBD plasma jet, copper	- Air, 15 kV,16 W	- Initial increase in treatment efficiency followed by a slower decomposition over time for a time period of 130 minutes	(Foster et al., 2013)
	- DBD, copper tape, aluminium rod	- Air, 40 W	- 95% of MB degradation after 30 minutes of ozone treatment	(Czapka et al., 2017)
	- DBD	- Oxygen, 10 kV, 0.6 W	- More than 90% MB degradation after 5 min of treatment. Higher degradation observed at higher pH value, > 7.	(Zhao et al., 2014)
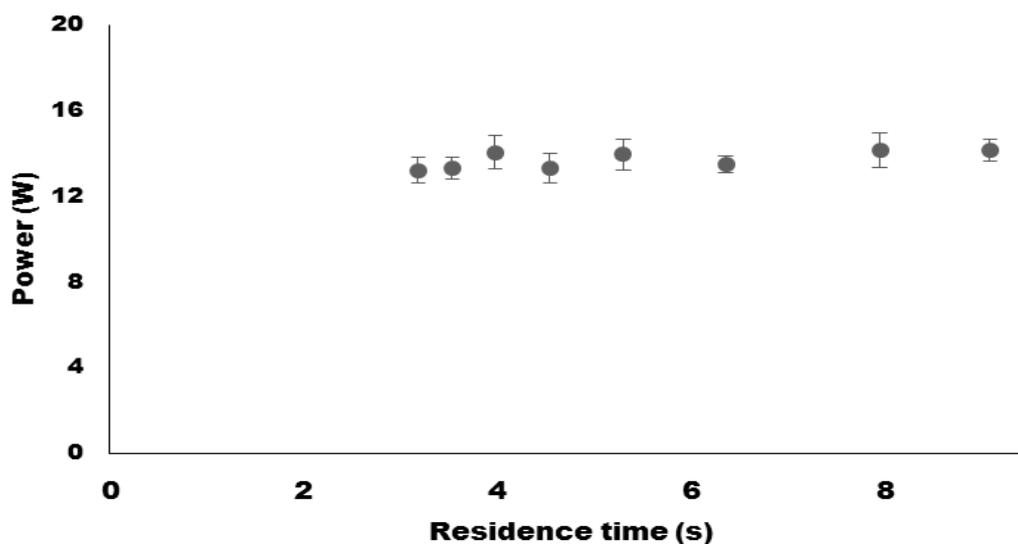
Figure S4.1: Calculated power versus residence time, with frequency of 17 kHz and 17 kV$_{p-p}$ applied voltage.

Table S4.1: Retention time for standard ions at optimized ion chromatographic conditions in untreated and plasma treated water samples (n=5).

	Retention time (min)	Standard deviation (min)	Standard deviation %
Fluoride (F$^-$)	3.70	0.005	0.13
Chloride (Cl$^-$)	5.57	0.004	0.08
Nitrite (NO$_2^-$)	6.75	0.005	0.07
Sulphate (SO$_4^{2-}$)	8.7	0.026	0.29
Bromide (Br$^-$)	9.21	0.025	0.27
Nitrate (NO$_3^-$)	10.55	0.044	0.42
Phosphate (PO$_4^{3-}$)	13.16	0.081	0.62
Sodium (Na$^+$)	5.72	0.011	0.19
Ammonium (NH$_4^+$)	6.64	0.007	0.10
Potassium (K$^+$)	8.31	0.068	0.82
Magnesium (Mg^{2+})	10.23	0.22	2.08
Calcium (Ca^{2+})	12.62	0.21	1.70
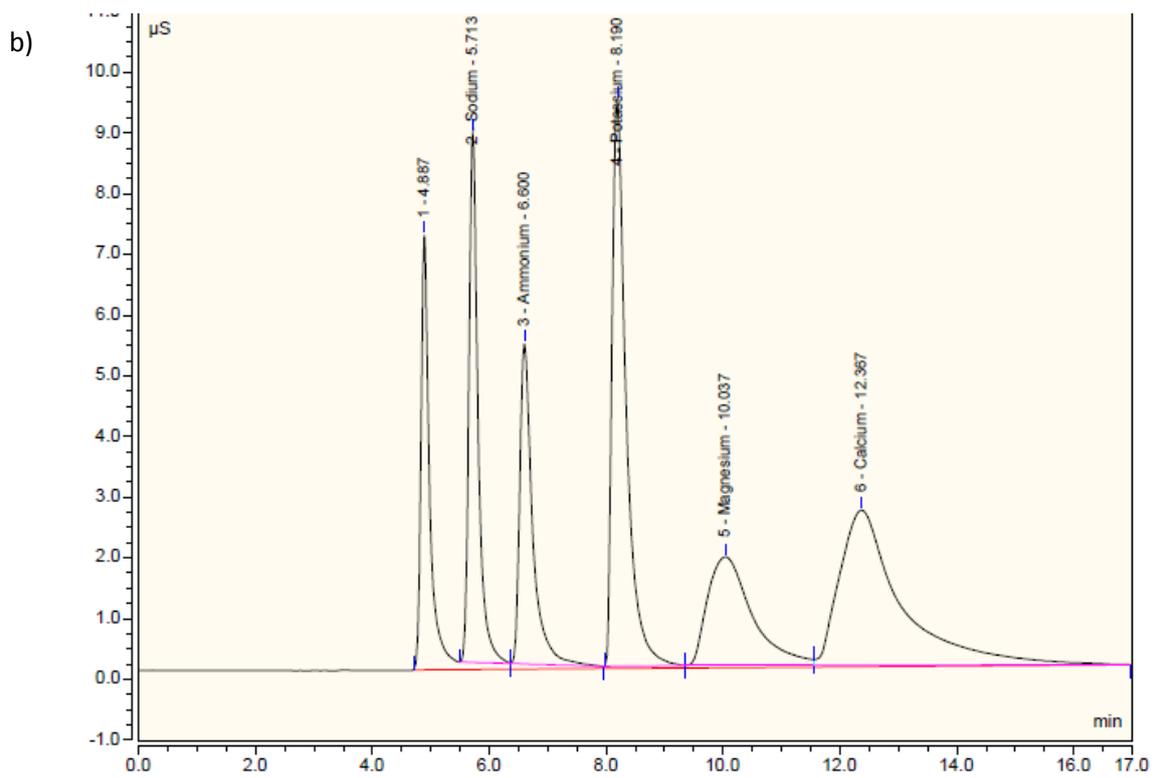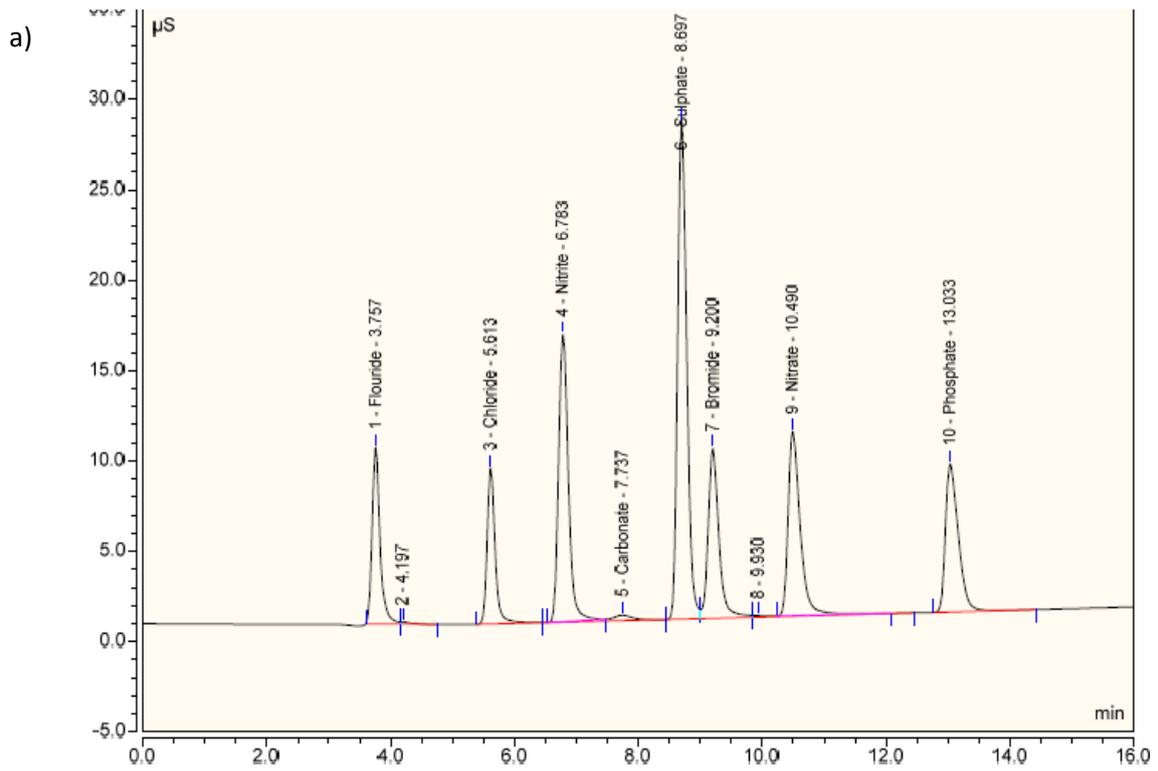
Figure S4.2: Ion chromatograms for (a) anions and (b) cations measured in standard samples using the IC
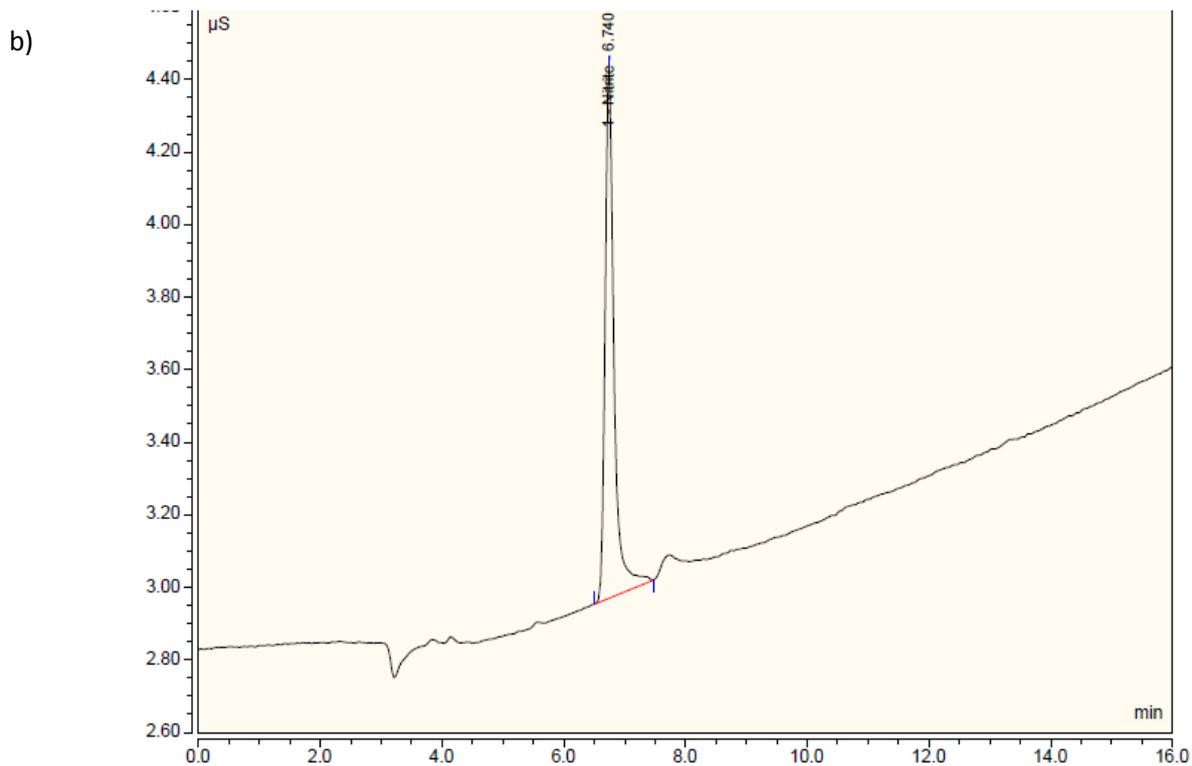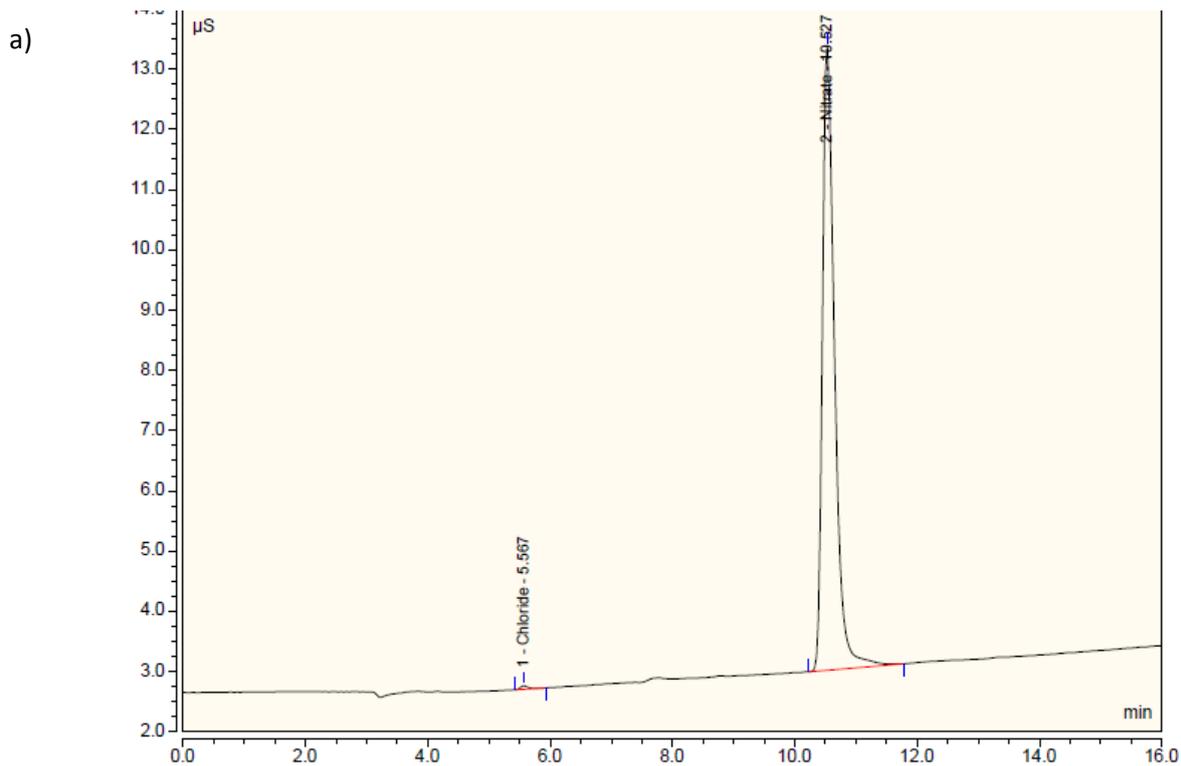
Figure S4.3: Ion chromatograms showing (a) nitrate and (b) nitrite in Milli-Q water after plasma treatment.
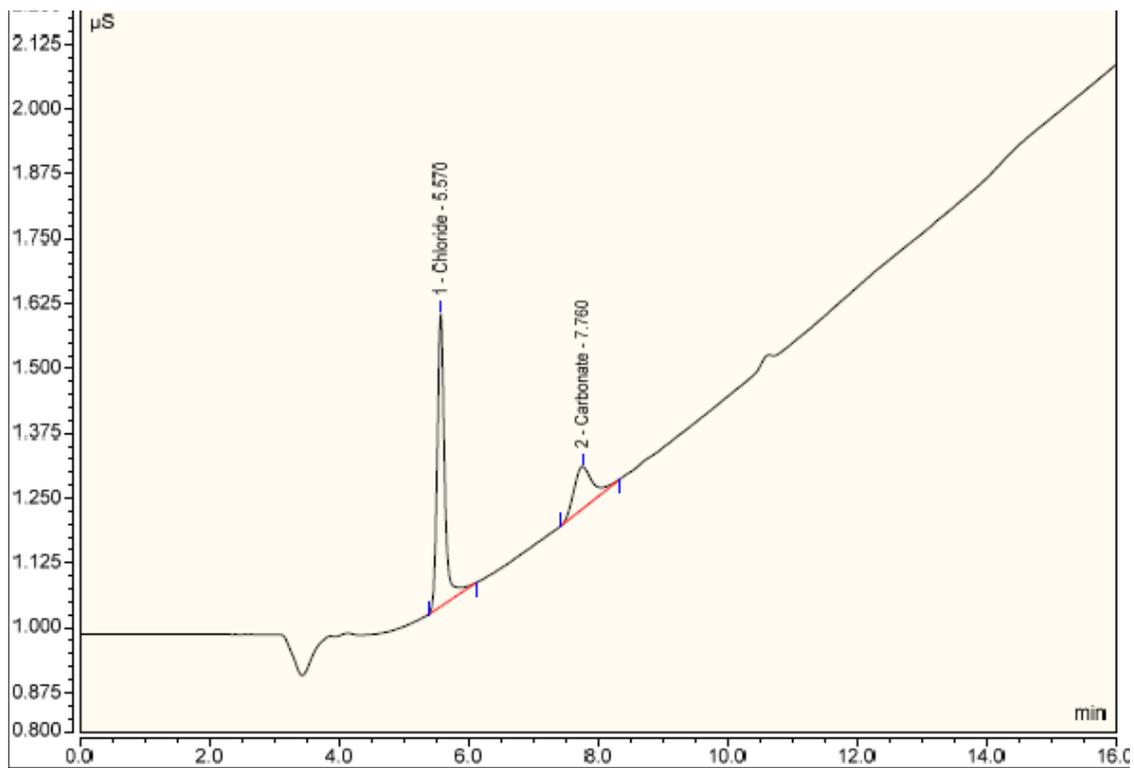
Figure S4.4: Ion chromatogram detecting carbonate in Milli-Q water without plasma treatment using the ion chromatography.
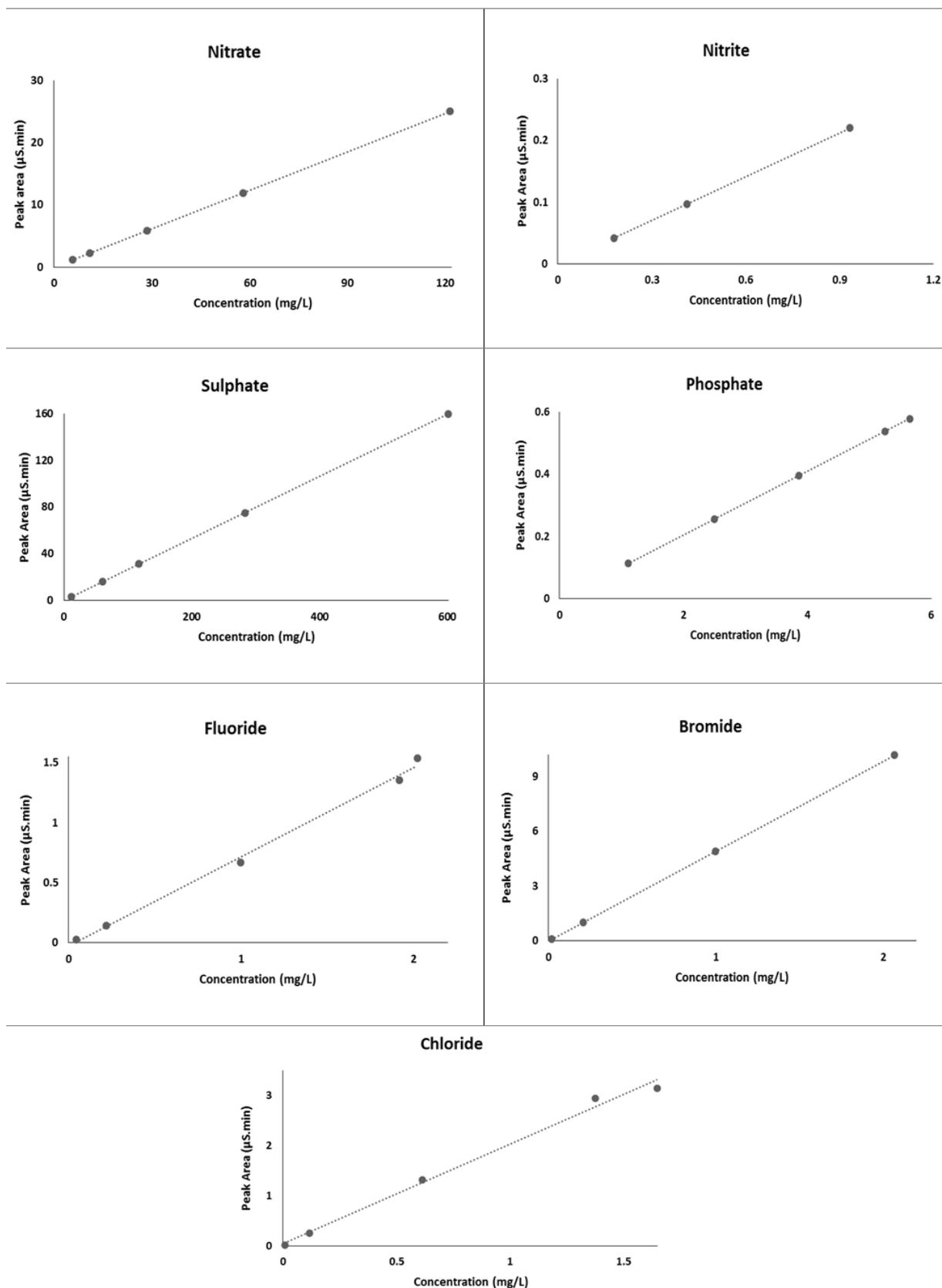
Figure S4.5: Standard calibration curve of anions in water using ion chromatography. Nitrate (R^2 = 1), nitrite (R^2 = 1), sulphate (R^2 = 1), phosphate (R^2 = 1), fluoride (R^2 = 0.9954), bromide (R^2 = 1) and chloride (R^2 = 0.9924). Error bars represent standard errors (n = 3).
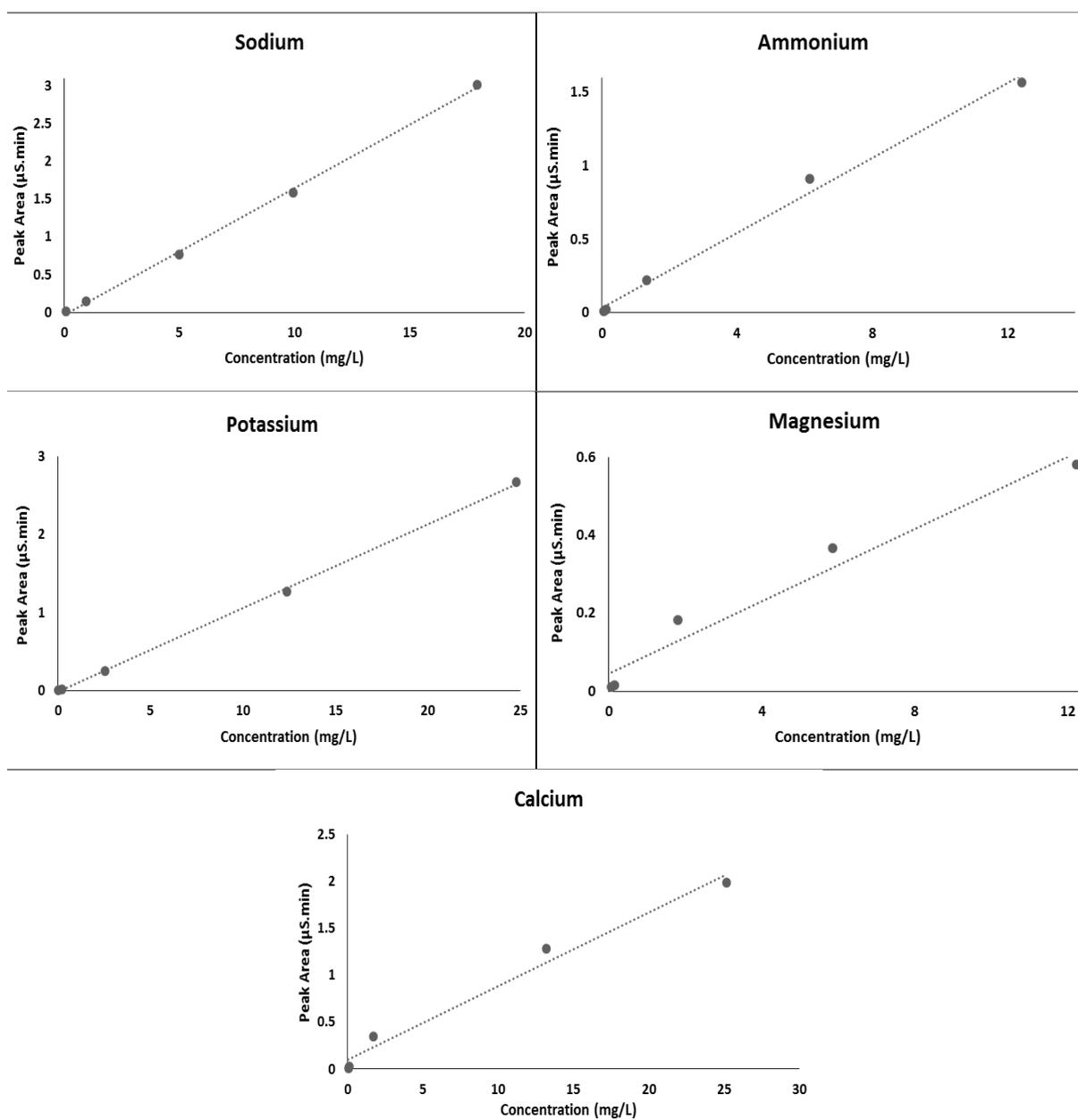
Figure S4.6: Standard calibration curve of anions in water using ion chromatography. Sodium (R^2 = 0.9989), ammonium (R^2 = 0.9929), potassium (R^2 = 0.9995), magnesium (R^2 = 0.9617) and calcium (R^2 = 0.9808). Error bars represent standard errors (n = 3).
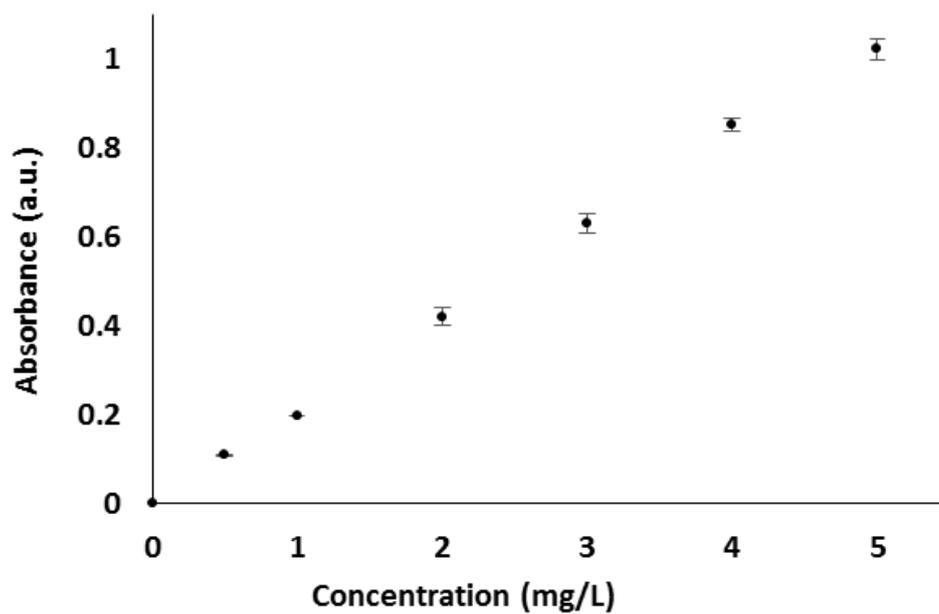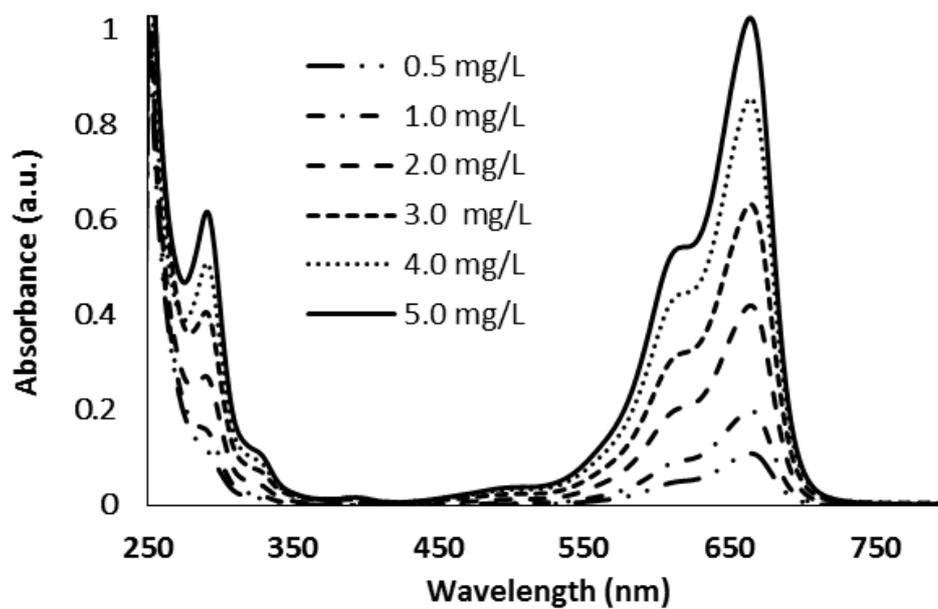
Figure S5.1: a) Calibration curve of methylene blue, stock concentration of 5 mg/L. b) UV-vis spectra of methylene blue at various concentration. Error bars represent standard errors n = 3. (R^2 = 0.999)
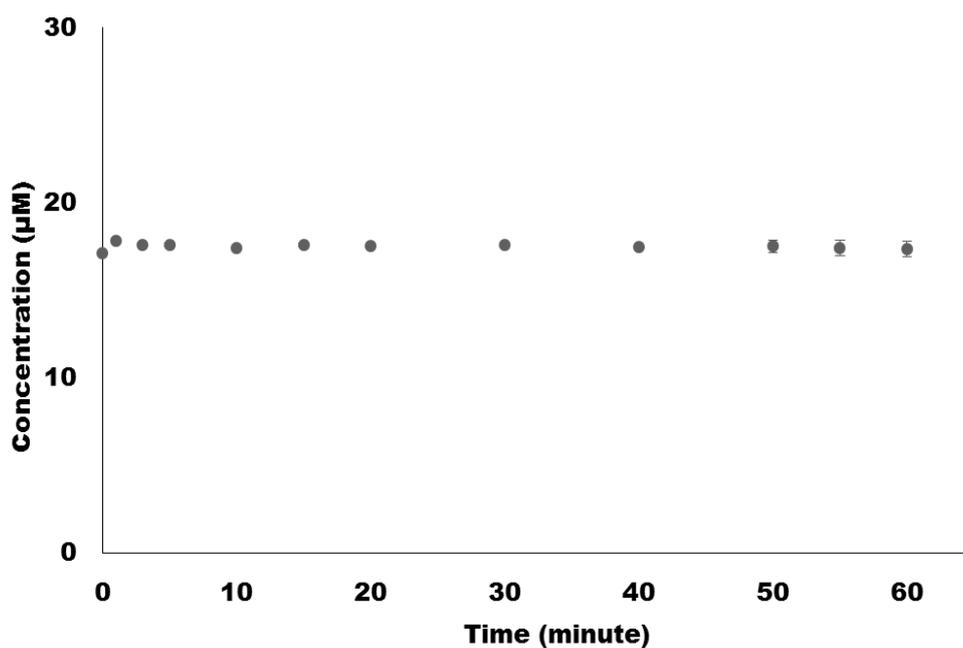
Figure S5.2: Degradation of MB versus time in the absence of plasma under UV light.
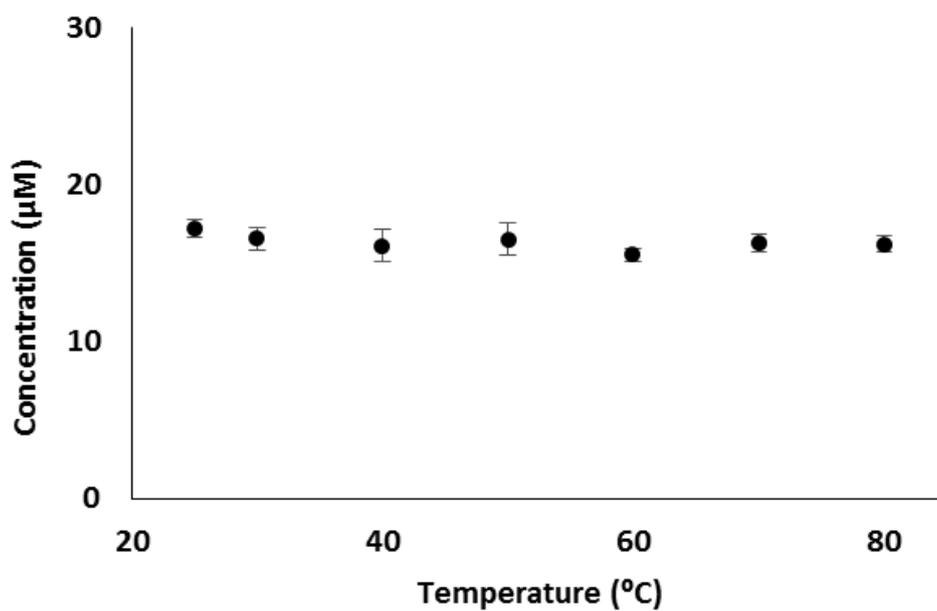
Figure S5.3: Degradation of MB versus temperature in absence of plasma.
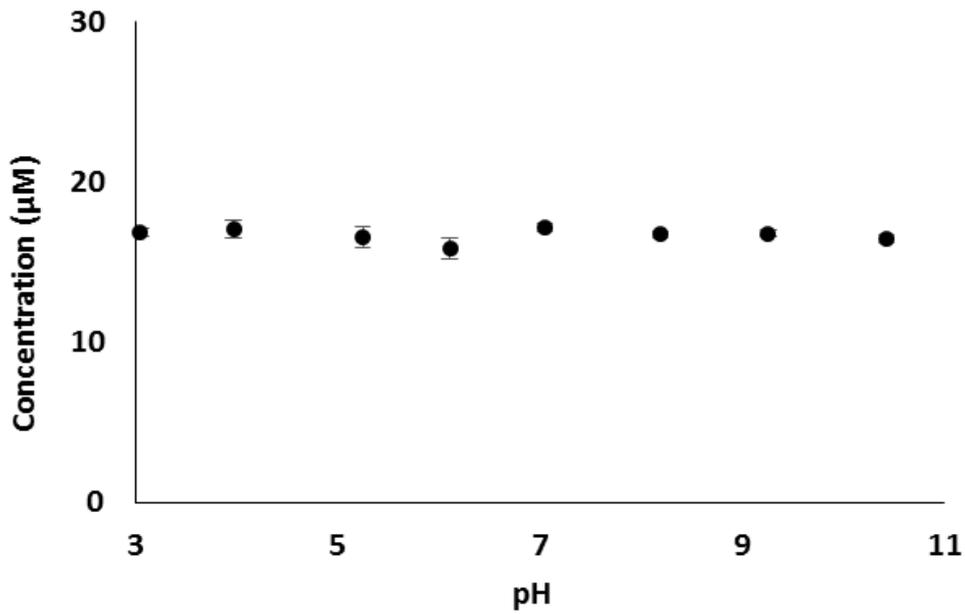
Figure S5.4: Degradation of MB versus pH in absence of plasma.
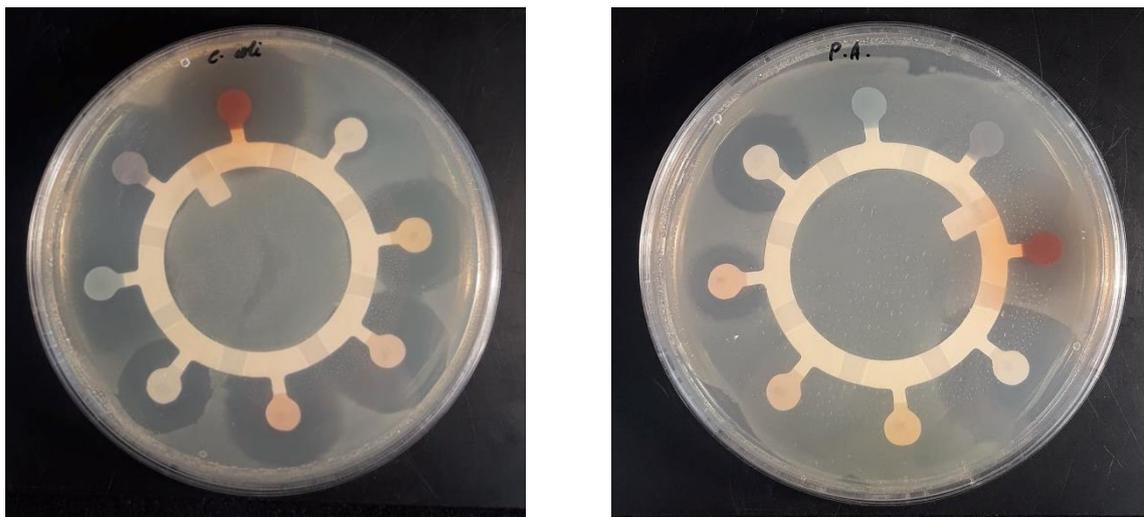
a)   b)

Figure S6.1: Susceptibility of *E. coli* (a) and *P. aeruginosa* (b) with different antibiotics (Ampicillin (•), Chloramphenicol (•), Colistin Sulphate ( ), Kanamycin (•), Nalidixic acid (•), Nitrofurantoin (•), Streptomycin ( ), Tetracycline (•)). With *E. coli*, inhibition zones were observed with all antibiotics except streptomycin while with *P. aeruginosa*, inhibition zones were observed with streptomycin, colistin sulphate and kanamycin.

Figure S6.2: Agarose gel electrophoresis of 16S rRNA PCR products from *E. coli* (A) and *P. aeruginosa* (B), lane X: marker, 100 bp DNA ladder and lane C: negative control.

E. coli

```
Query   12   GCCTAGC-CATGCAAGTCGAACGGTAACAGGAAGCAGCTTGCTGCTTCGCTGACGAGTGG   70
             |||||  |  |||||||||||||||||||||||||||||||||||| ||||||||||||||
Sbjct   19   GCCTAACACATGCAAGTCGAACGGTAACAGGAAGCAGCTTGCTGCTTTGCTGACGAGTGG   78

Query   71   CGGACGGGTGAGTAATGTCTGGGAAACTGCCTGATGGAGGGGGATAACTACTGGAAACGG   130
             ||||||||||||||||||||||||||||||| ||||||||||||||||||||||||||||
Sbjct   79   CGGACGGGTGAGTAATGTCTGGGAAACTGCCNGATGGAGGGGGATAACTACTGGAAACGG   138

Query   131  TAGCTAATACCGCATAACGTCGCAAGACCAAAGAGGGGGACCTTCGGGCCTCTTGCCATC   190
             ||||||||||||||||||||||||||||||||||||||||||||| ||||||||||||||
Sbjct   139  TAGCTAATACCGCATAACGTCGCAAGACCAAAGAGGGGGACCTTAGGGCCTCTTGCCATC   198

Query   191  GGATGTGCCCAGATGGGATTAGCTAGTAGGTGGGGTAACGGCTCACCTAGGCGACGATCC   250
             ||||||||||||||||||||||||||||||||||||||||||||||||||||||||||||
Sbjct   199  GGATGTGCCCAGATGGGATTAGCTAGTAGGTGGGGTAACGGCTCACCTAGGCGACGATCC   258

Query   251  CTAGCTGGTCTGAGAGGATGACCAGCCACACTGGAACTGAGACACGGTCCAGACTCCTAC   310
             ||||||||||||||||||||||||||||||||||||||||||||||||||||||||||||
Sbjct   259  CTAGCTGGTCTGAGAGGATGACCAGCCACACTGGAACTGAGACACGGTCCAGACTCCTAC   318

Query   311  GGGAGGCAGCAGTGGGGAATATTGCACAATGGGCGCAAGCCTGATGCAGCCATGCCGCGT   370
             ||||||||||||||||||||||||||||||||||||||||||||||||||||||||||||
Sbjct   319  GGGAGGCAGCAGTGGGGAATATTGCACAATGGGCGCAAGCCTGATGCAGCCATGCCGCGT   378

Query   371  GTATGAAGAAGGCCTTCGGGTTGTAAAGTACTTTCAGCGGGGAGGAAGGGAGTAAAGTTA   430
             ||||||||||||||||||||||||||||||||||||||||||||||||||||||||||||
Sbjct   379  GTATGAAGAAGGCCTTCGGGTTGTAAAGTACTTTCAGCGGGGAGGAAGGGAGTAAAGTTA   438

Query   431  ATACCTTTGCTCATTGACGTTACCCGCAGAAGAAGCACCGGCTAACTCCGTGCCAGCAGC   490
             ||||||||||||||||||||||||||||||||||||||||||||||||||||||||||||
Sbjct   439  ATACCTTTGCTCATTGACGTTACCCGCAGAAGAAGCACCGGCTAACTCCGTGCCAGCAGC   498

Query   491  CGCGGGTAATAC   502
             |||||  ||||||
Sbjct   499  CGCGG-TAATAC   509
```

P. aeruginosa

```
Query  8     CGGGGCTAATTCTGTTGGTAACGTCAA-NCAGCAAGGTATTAACTTACTGCCCTTCCTCC  66
             ||| ||| ||||||||||||||||||||  ||||||||||||||||||||||||||||||||
Sbjct  491   CGGTGCTTATTCTGTTGGTAACGTCAAAACAGCAAGGTATTAACTTACTGCCCTTCCTCC  432

Query  67    CAACTTAAAGTGCTTTACAATCCGAAGACCTTCTTCACACACGCGGCATGGCTGGATCAG  126
             ||||||||||||||||||||||||||||||||||||||||||||||||||||||||||||
Sbjct  431   CAACTTAAAGTGCTTTACAATCCGAAGACCTTCTTCACACACGCGGCATGGCTGGATCAG  372

Query  127   GCTTTCGCCCATTGTCCAATATTCCCCACTGCTGCCTCCCGTAGGAGTCTGGACCGTGTC  186
             ||||||||||||||||||||||||||||||||||||||||||||||||||||||||||||
Sbjct  371   GCTTTCGCCCATTGTCCAATATTCCCCACTGCTGCCTCCCGTAGGAGTCTGGACCGTGTC  312

Query  187   TCAGTTCCAGTGTGACTGATCATCCTCTCAGACCAGTTACGGATCGTCGCCTTGGTAGGC  246
             ||||||||||||||||||||||||||||||||||||||||||||||||||||||||||||
Sbjct  311   TCAGTTCCAGTGTGACTGATCATCCTCTCAGACCAGTTACGGATCGTCGCCTTGGTAGGC  252

Query  247   CTTTACCCCACCAACTAGCTAATCCGACCTAGGCTCATCTGATAGCGTGAGGTCCGAAGA  306
             ||||||||||||||||||||||||||||||||||||||||||||||||||||||||||||
Sbjct  251   CTTTACCCCACCAACTAGCTAATCCGACCTAGGCTCATCTGATAGCGTGAGGTCCGAAGA  192

Query  307   TCCCCCACTTTCTCCCTCAGGACGTATGCGGTATTAGCGCCCGTTTCCGGACGTTATCCC  366
             ||||||||||||||||||||||||||||||||||||||||||||||||||||||||||||
Sbjct  191   TCCCCCACTTTCTCCCTCAGGACGTATGCGGTATTAGCGCCCGTTTCCGGACGTTATCCC  132

Query  367   CCACTACCAGGCAGATTCCTAGGCATTACTCACCCGTCCGCCGCTGAATCCAGGAGCAAG  426
             ||||||||||||||||||||||||||||||||||||||||||||||||||||||||||||
Sbjct  131   CCACTACCAGGCAGATTCCTAGGCATTACTCACCCGTCCGCCGCTGAATCCAGGAGCAAG  72

Query  427   CTCCCTTCATCCGCTCGACTTGCATGTGTTAGGCCTGCCGCCAGCGTTCAATCTGAGCCA  486
             ||||||||||||||||||||||||||||||||||||||||||||||||||||||||||||
Sbjct  71    CTCCCTTCATCCGCTCGACTTGCATGTGTTAGGCCTGCCGCCAGCGTTCAATCTGAGCCA  12

Query  487   TGATTAAA   494
             |||| |||
Sbjct  11    TGATCAAA   4
```

Figure S6.3: Nucleotide sequences obtained from *E. coli* and *P. aeruginosa* sample (Sbjct (i.e. subject)) compared to sequence database (Query) found in BLAST.
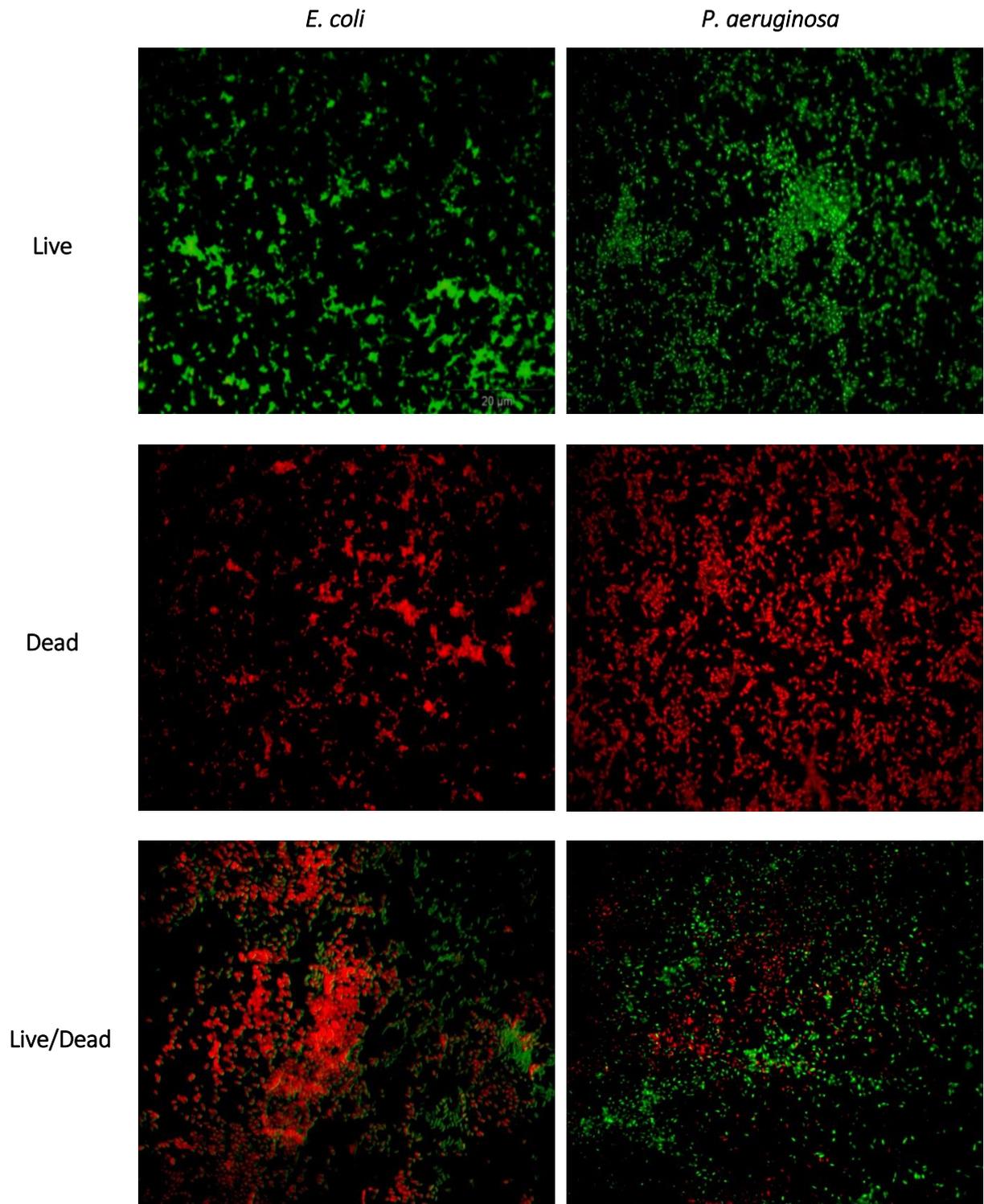
Figure S6.4: Live/Dead cell viability assay of control *E. coli* and *P. aeruginosa*.

References

Abbas, M., Emonet, S., Köhler, T., Renzi, G., Van Delden, C., Schrenzel, J. and Hirschel, B. (2017) 'Ecthyma gangrenosum: Escherichia coli or Pseudomonas aeruginosa?' *Frontiers in microbiology*, 8 p. 953.

Abdel-Shafy, H. I. and Mansour, M. S. (2016) 'A review on polycyclic aromatic hydrocarbons: source, environmental impact, effect on human health and remediation.' *Egyptian Journal of Petroleum*, 25(1) pp. 107-123.

Abdelaziz, A. A., Ishijima, T. and Tizaoui, C. (2018) 'Development and characterization of a wire-plate air bubbling plasma for wastewater treatment using nanosecond pulsed high voltage.' *Journal of Applied Physics*, 124(5) p. 053302.

Adamovich, I., Baalrud, S. D., Bogaerts, A., Bruggeman, P., Cappelli, M., Colombo, V., Czarnetzki, U., Ebert, U., Eden, J.G., Favia, P. and Graves, D.B., (2017) 'The 2017 Plasma Roadmap: Low temperature plasma science and technology.' *Journal of Physics D: Applied Physics*, 50(32) p. 323001.

Adegoke, K. A. and Bello, O. S. (2015) 'Dye sequestration using agricultural wastes as adsorbents.' *Water Resources and Industry*, 12 pp. 8-24.

Ainger, C., Butler, D., Caffor, I., Crawford-Brown, D., Helm, D. and Stephenson, T. (2009) 'A low carbon water industry in 2050.' *Environment Agency*.

Allegranzi, B., Nejad, S. B., Combescure, C., Graafmans, W., Attar, H., Donaldson, L. and Pittet, D. (2011) 'Burden of endemic health-care-associated infection in developing countries: systematic review and meta-analysis.' *The Lancet*, 377(9761) pp. 228-241.

Al-rawaf, A. F., Fuliful, F. K., Khalaf, M. K. and Oudah, H. K. (2018) 'Studying the non-thermal plasma jet characteristics and application on bacterial decontamination.' *Journal of Theoretical and Applied Physics,* 12(1) pp. 45-51.

An, G., Sun, Y., Zhu, T. and Yan, X. (2011) 'Degradation of phenol in mists by a non-thermal plasma reactor.' *Chemosphere*, 84(9) pp. 1296-1300.

Andrew, M., Carl, B. and Alex, B. (2018)' Raising standards of infection prevention and control in the NHS.' House of Commons.

Anghel, S., Zaharie-Butucel, D. and Vlad, I. (2015) 'Single electrode Ar bubbled plasma source for methylene blue degradation and concurrent synthesis of carbon based nanoparticles.' *Journal of Electrostatics*, 75 pp. 63-71.

Anpilov, A., Barkhudarov, E., Bark, Y. B., Zadiraka, Y. V., Christofi, M., Kozlov, Y. N., Kossyi, I., Kop'ev, V. A., Silakov, V.P., Taktakishvili, M.I. and Temchin, S.M., (2001) 'Electric discharge in water as a source of UV radiation, ozone and hydrogen peroxide.' *Journal of Physics D: Applied Physics*, 34(6) p. 993.

Archambault-Caron, M., Gagnon, H., Nisol, B., Piyakis, K. and Wertheimer, M. R. (2015) 'Precise energy and temperature measurements in dielectric barrier discharges at atmospheric pressure.' *Plasma Sources Science and Technology*, 24(4) p. 045004.

Attri, P., Tochikubo, F., Park, J. H., Choi, E. H., Koga, K. and Shiratani, M. (2018) 'Impact of Gamma rays and DBD plasma treatments on wastewater treatment.' *Scientific reports*, 8(1) p. 2926.

Attri, P., Kim, Y. H., Park, D. H., Park, J. H., Hong, Y. J., Uhm, H. S., Kim, K.-N., Fridman, A., and Choi, E.H., (2015) 'Generation mechanism of hydroxyl radical species and its lifetime prediction during the plasma-initiated ultraviolet (UV) photolysis.' *Scientific reports*, 5 p. 9332.

Aziz, K. H. H., Mahyar, A., Miessner, H., Mueller, S., Kalass, D., Moeller, D., Khorshid, I. and Rashid, M. A. M. (2018) 'Application of a planar falling film reactor for decomposition and mineralization of methylene blue in the aqueous media via ozonation, Fenton, photocatalysis and non-thermal plasma: A comparative study.' *Process Safety and Environmental Protection*, 113 pp. 319-329.

Azzouz, I., Habba, Y. G., Capochichi-Gnambodoe, M., Marty, F., Vial, J., Leprince-Wang, Y. and Bourouina, T. (2018) 'Zinc oxide nano-enabled microfluidic reactor for water purification and its applicability to volatile organic compounds.' *Microsystems & Nanoengineerin*g, 4 p. 17093.

Back, J., Stadlmayr, W., Jabornig, S., Winkler, F., Winkler, K. and Rupprich, M. (2018) 'Removal of Arsenic from Water with Non-Thermal Plasma (NTP), *Coagulation and Membrane Filtration*.' Water, 10(10) p. 1385.

Bafoil, M., Jemmat, A., Martinez, Y., Merbahi, N., Eichwald, O., Dunand, C. and Yousfi, M. (2018) 'Effects of low temperature plasmas and plasma activated waters on Arabidopsis thaliana germination and growth.' *PloS one*, 13(4) p. e0195512.

Bagheri, M. and Mirbagheri, S. A. (2018) 'Critical review of fouling mitigation strategies in membrane bioreactors treating water and wastewater.' *Bioresource technology*, 258 pp. 318-334.

Bai, N., Sun, P., Zhou, H., Wu, H., Wang, R., Liu, F., Zhu, W., Lopez, J. L., Zhang, J. and Fang, J., (2011) 'Inactivation of Staphylococcus aureus in water by a cold, He/O2 atmospheric pressure plasma microjet.' *Plasma Processes and Polymers*, 8(5) pp. 424-431.

Baldanov, B., Semenov, A., Ranzhurov, T. V., Nikolaev, E. and Gomboeva, S. (2015) 'Action of plasma jets of a low-current spark discharge on microorganisms (Escherichia coli).' *Technical Physics*, 60(11) pp. 1729-1731.

Baloul, Y., Rabat, H., Hong, D., Chuon, S. and Aubry, O. (2016) 'Preliminary Study of a Non-thermal Plasma for the Degradation of the Paracetamol Residue in Water.' *International Journal of Plasma Environmental Science & Technology*, 10 pp. 102-107.

Banaschik, R., Burchhardt, G., Zocher, K., Hammerschmidt, S., Kolb, J. F. and Weltmann, K. D. (2016) 'Comparison of pulsed corona plasma and pulsed electric fields for the decontamination of water containing Legionella pneumophila as model organism.' *Bioelectrochemistry*, 112 pp. 83-90.

Bansode, A. S., More, S. E., Siddiqui, E. A., Satpute, S., Ahmad, A., Bhoraskar, S. V. and Mathe, V. L. (2017) 'Effective degradation of organic water pollutants by atmospheric non-thermal plasma torch and analysis of degradation process.' *Chemosphere*, 167 pp. 396-405.

Barekzi, N. and Laroussi, M. (2012) 'Dose-dependent killing of leukemia cells by low-temperature plasma.' *Journal of Physics D: Applied Physics*, 45(42) p. 422002.

Bayen, S. (2012) 'Occurrence, bioavailability and toxic effects of trace metals and organic contaminants in mangrove ecosystems: a review.' *Environment international*, 48 pp. 84-101.

Benetoli, L. O. d. B., Cadorin, B. M., Postiglione, C. d. S., Souza, I. G. d. and Debacher, N. A. (2011) 'Effect of temperature on methylene blue decolorization in aqueous medium in electrical discharge plasma reactor.' *Journal of the Brazilian Chemical Society*, 22(9) pp. 1669-1678.

Benson, R., Conerly, O. D., Sander, W., Batt, A. L., Boone, J. S., Furlong, E. T., Glassmeyer, S. T., Kolpin, D. W., Mash, H.E., Schenck, K.M. and Simmons, J.E., (2017) 'Human health screening and public health significance of contaminants of emerging concern detected in public water supplies.' *Science of The Total Environment*, 579 pp. 1643-1648.

Bichai, F., Payment, P. and Barbeau, B. (2008) 'Protection of waterborne pathogens by higher organisms in drinking water: a review.' *Canadian journal of microbiology*, 54(7) pp. 509-524.

Bitton, G. (2014) Microbiology of drinking water production and distribution. John Wiley & Sons Inc.

Bou-Antoun, S., Davies, J., Guy, R., Johnson, A. P., Sheridan, E. A. and Hope, R. J. (2016) 'Descriptive epidemiology of Escherichia coli bacteraemia in England, April 2012 to March 2014.' *Eurosurveillance*, 21(35).

Bourke, P., Ziuzina, D., Han, L., Cullen, P. and Gilmore, B. (2017) 'Microbiological interactions with cold plasma.' *Journal of applied microbiology*, 123(2) pp. 308-324.

Bradu, C., Magureanu, M. and Parvulescu, V. (2017) 'Degradation of the chlorophenoxyacetic herbicide 2, 4-D by plasma-ozonation system.' *Journal of hazardous materials*, 336 pp. 52-56.

Brandenburg, R. (2017) 'Dielectric barrier discharges: progress on plasma sources and on the understanding of regimes and single filaments.' *Plasma Sources Science and Technology*, 26(5) p. 053001.

Breidenstein, E. B., de la Fuente-Núñez, C. and Hancock, R. E. (2011) 'Pseudomonas aeruginosa: all roads lead to resistance.' *Trends in microbiology*, 19(8) pp. 419-426.

Bridier, A., Briandet, R., Thomas, V. and Dubois-Brissonnet, F. (2011) 'Resistance of bacterial biofilms to disinfectants: a review.' *Biofouling*, 27(9) pp. 1017-1032.

Bruggeman, P. and Leys, C. (2009) 'Non-thermal plasmas in and in contact with liquids.' Journal of Physics D: Applied Physics, 42(5) p. 053001.

Bruggeman, P., Locke, B. and Lu, X. (2013) 'Assessment of potential applications of plasma with liquid water.' Low Temperature Plasma Technology Methods and Applications, pp. 367-400.

Bruggeman, P., Graham, L., Degroote, J., Vierendeels, J. and Leys, C. (2007) 'Water surface deformation in strong electrical fields and its influence on electrical breakdown in a metal pin–water electrode system.' Journal of Physics D: Applied Physics, 40(16) p. 4779.

Bruggeman, P., Schram, D., González, M. Á., Rego, R., Kong, M. G. and Leys, C. (2009) 'Characterization of a direct dc-excited discharge in water by optical emission spectroscopy.' Plasma Sources Science and Technology, 18(2) p. 025017.

Bruggeman, P., Kushner, M. J., Locke, B. R., Gardeniers, J. G., Graham, W., Graves, D. B., Hofman-Caris, R., Maric, D., Reid, J.P., Ceriani, E. and Rivas, D.F., (2016) 'Plasma–liquid interactions: a review and roadmap.' Plasma sources science and technology, 25(5) p. 053002.

Buendia, J. A., Perez-Lopez, E. and Venkattraman, A. (2018) 'System-level model and experiments for irrigation water alkalinity reduction and enrichment using an atmospheric pressure dielectric barrier discharge.' Water research, 144 pp. 728-739.

Burkhardt-Holm, P. (2011) 'Linking water quality to human health and environment: the fate of micropollutants.' *Institute of Water Policy*, National University of Singapore: Singapore.

Burlica, R., Grim, R., Shih, K. Y., Balkwill, D. and Locke, B. (2010) 'Bacteria inactivation using low power pulsed gliding arc discharges with water spray.' *Plasma Processes and Polymers*, 7(8) pp. 640-649.

Burts, M. L., Alexeff, I., Meek, E. T. and McCullers, J. A. (2009) 'Use of atmospheric non-thermal plasma as a disinfectant for objects contaminated with methicillin-resistant Staphylococcus aureus.' *American journal of infection control*, 37(9) pp. 729-733.

Cairns, J., Ruokolainen, L., Hultman, J., Tamminen, M., Virta, M. and Hiltunen, T. (2018) 'Ecology determines how low antibiotic concentration impacts community composition and horizontal transfer of resistance genes.' *Communications biology*, 1(1) p. 35.

Ceriani, E., Marotta, E., Schiorlin, M., Ren, X., Ceretta, C., Gobbo, R., Tampieri, F. and Paradisi, C. (2018) 'A versatile prototype plasma reactor for water treatment supporting different discharge regimes.' *Journal of Physics D: Applied Physics*, 51(27) p. 274001.

Cervia, J. S., Ortolano, G. A. and Canonica, F. P. (2008) 'Hospital tap water: A reservoir of risk for health care-associated infection.' *Infectious Diseases in Clinical Practice*, 16(6) pp. 349-353.

Cha, S. and Park, Y.-S. (2014) 'Plasma in dentistry.' *Clinical plasma medicine*, 2(1) pp. 4-10.

Chauvin, J., Judée, F., Yousfi, M., Vicendo, P. and Merbahi, N. (2017) 'Analysis of reactive oxygen and nitrogen species generated in three liquid media by low temperature helium plasma jet.' *Scientific reports*, 7(1) p. 4562.

Cheng, H. H., Chen, S.S., Yoshizuka, K. and Chen, Y. C. (2012) 'Degradation of phenolic compounds in water by non-thermal plasma treatment.' *Journal of water chemistry and technology*, 34(4) pp. 179-189.

Choi, S., Kim, B. and Han, J. (2017) 'Integrated pretreatment and desalination by electrocoagulation (EC)–ion concentration polarization (ICP) hybrid.' *Lab on a Chip*, 17(12) pp. 2076-2084.

Choudhury, B., Portugal, S., Mastanaiah, N., Johnson, J. A. and Roy, S. (2018) 'Inactivation of Pseudomonas aeruginosa and Methicillin-resistant Staphylococcus aureus in an open water

system with ozone generated by a compact, atmospheric DBD plasma reactor.' *Scientific Reports*, 8(1) p. 17573.

Chu, P. K. and Lu, X. (2013) Low temperature plasma technology: methods and applications. CRC Press.

Chung, K. T. (2016) 'Azo dyes and human health: a review.' *Journal of Environmental Science and Health*, Part C, 34(4) pp. 233-261.

Chung, W. C. and Chang, M. B. (2016) 'Review of catalysis and plasma performance on dry reforming of CH4 and possible synergistic effects.' *Renewable and Sustainable Energy Reviews*, 62 pp. 13-31.

Cizmas, L., Sharma, V. K., Gray, C. M. and McDonald, T. J. (2015) 'Pharmaceuticals and personal care products in waters: occurrence, toxicity, and risk.' *Environmental Chemistry Letters*, 13(4) pp. 381-394.

Coleman, J. W. and Garimella, S. (1999) 'Characterization of two-phase flow patterns in small diameter round and rectangular tubes.' *International Journal of Heat and Mass Transfer*, 42(15) pp. 2869-2881.

Conrads, H. and Schmidt, M. (2000) 'Plasma generation and plasma sources.' *Plasma Sources Science and Technology*, 9(4) p. 441.

Council, C. C. and Council, A. C. (2006) 'Drinking Water Chlorination: A Review of Disinfection Practices and Issues.' *Water Conditioning and Purification International*, p. 68.

Cragan, J. D. (1999) 'Teratogen update: methylene blue.' *Teratology*, 60(1) p. 42.

Cristina, M. L., Spagnolo, A. M., Orlando, P. and Perdelli, F. (2013) 'The role of the environment in the spread of emerging pathogens in at-risk hospital wards.' *Reviews in Medical Microbiology*, 24(4) pp. 104-112.

Cui, Y., Cheng, J., Chen, Q. and Yin, Z., (2018) 'The Types of Plasma Reactors in Wastewater Treatment.' *IOP Conference Series: Earth and Environmental Science*, 208 (1) p. 012002).

Cvetković, B. Z., Lade, O., Marra, L., Arima, V., Rinaldi, R. and Dittrich, P. S. (2012) 'Nitrogen supported solvent evaporation using continuous-flow microfluidics.' *Rsc Advances*, 2(29) pp. 11117-11122.

Czapka, T., Mirkowska, A. and Palewicz, M. (2017) 'Decolorization of methylene blue in aqueous medium using dielectric barrier discharge plasma reactor.' *Power*, 2 p. 7.

Da Silva, B., Habibi, M., Ognier, S., Schelcher, G., Mostafavi-Amjad, J., Khalesifard, H., Tatoulian, M. and Bonn, D. (2016) 'Silver nanocluster catalytic microreactors for water purification.' *The European Physical Journal Special Topics*, 225(4) pp. 707-714.

Da Silva, B. T. (2015) 'Development of catalytic microreactors by plasma processes: application to wastewater treatment.' *Education For Chemical Engineers*, 8(4) pp. e119-e123.

Danner, M. C., Robertson, A., Behrends, V. and Reiss, J. (2019) 'Antibiotic pollution in surface fresh waters: occurrence and effects.' *Science of the Total Environment*.

Danny, S., Elliot, S. and Gaynor, J. (2018) Almost one in two people in UK worry their water is contaminated, survey finds. [Online] [Accessed 21 June 2019] https://www.djsresearch.co.uk/UtilitiesMarketResearchInsightsAndFindings/article/Almost-one-in-two-people-in-UK-worry-their-water-is-contaminated-survey-finds-04195v

Dapeng, L. and Jiuhui, Q. (2009) 'The progress of catalytic technologies in water purification: A review.' *Journal of Environmental Sciences*, 21(6) pp. 713-719.

de Brito Benetoli, L. O., Cadorin, B. M., Baldissarelli, V. Z., Geremias, R., de Souza, I. G. and Debacher, N. A. (2012) 'Pyrite-enhanced methylene blue degradation in non-thermal plasma water treatment reactor.' *Journal of hazardous materials*, 237 pp. 55-62.

De Gisi, S., Lofrano, G., Grassi, M. and Notarnicola, M. (2016) 'Characteristics and adsorption capacities of low-cost sorbents for wastewater treatment: a review.' *Sustainable Materials and Technologies*, 9 pp. 10-40.

Decker, B. K. and Palmore, T. N. (2013) 'The role of water in healthcare-associated infections.' *Current opinion in infectious diseases*, 26(4) p. 345.

Deng, Y. and Zhao, R. (2015) 'Advanced oxidation processes (AOPs) in wastewater treatment.' *Current Pollution Reports*, 1(3) pp. 167-176.

Desmet, T., Morent, R., De Geyter, N., Leys, C., Schacht, E. and Dubruel, P. (2009) 'Nonthermal plasma technology as a versatile strategy for polymeric biomaterials surface modification: a review.' *Biomacromolecules*, 10(9) pp. 2351-2378.

Dezest, M., Bulteau, A.-L., Quinton, D., Chavatte, L., Le Béchec, M., Cambus, J. P., Arbault, S., Nègre-Salvayre, A., Clement, F. and Cousty, S., (2017) 'Oxidative modification and electrochemical inactivation of Escherichia coli upon cold atmospheric pressure plasma exposure.' *PloS one*, 12(3) p. e0173618.

Dobrin, D., Bradu, C., Magureanu, M., Mandache, N. and Parvulescu, V. (2013) 'Degradation of diclofenac in water using a pulsed corona discharge.' Chemical engineering journal, 234 pp. 389-396.

Dobrynin, D., Fridman, G., Mukhin, Y. V., Wynosky-Dolfi, M. A., Rieger, J., Rest, R. F., Gutsol, A. F. and Fridman, A. (2010) 'Cold plasma inactivation of Bacillus cereus and Bacillus anthracis (anthrax) spores.' *IEEE Transactions on Plasma Science*, 38(8) pp. 1878-1884.

Dobrynin, D., Friedman, G., Fridman, A. and Starikovskiy, A. (2011) 'Inactivation of bacteria using dc corona discharge: role of ions and humidity.' *New journal of physics*, 13(10) p. 103033.

DoH (2013) Health Technical Memorandum 07-04: Water management and water efficiency – best practice advice for the healthcare sector. UK: (Department of Health Report).

DoH (2013) Health Technical Memorandum 07-04: Water management and water efficiency – best practice advice for the healthcare sector. UK: (DOH Report).

DOH. (2016) Health Technical Memorandum 04-01: Safe water in healthcare premises.

Dojčinović, B. P., Roglić, G. M., Obradović, B. M., Kuraica, M. M., Kostić, M. M., Nešić, J. and Manojlović, D. D. (2011) 'Decolorization of reactive textile dyes using water falling film dielectric barrier discharge.' *Journal of hazardous materials*, 192(2) pp. 763-771.

Dojčinović, B. P., Obradović, B. M., Kuraica, M. M., Pergal, M. V., Dolić, S. D., Inđić, D. R., Tosti, T. B. and Manojlović, D. D. (2016) 'Application of non-thermal plasma reactor for degradation and detoxification of high concentrations of dye Reactive Black 5 in water.' *J. Serb. Chem. Soc.*, 81(7) pp. 829-845.

Dolezalova, E. and Lukes, P. (2015) 'Membrane damage and active but nonculturable state in liquid cultures of Escherichia coli treated with an atmospheric pressure plasma jet.' *Bioelectrochemistry*, 103 pp. 7-14.

Donko, Z. (2013) Electrical discharges in gases. [Online] [Accessed 23 April 2019] http://plasma.szfki.kfki.hu/~zoli/research_en.cgi

Donlan, R. M. (2002) 'Biofilms: microbial life on surfaces.' *Emerging infectious diseases*, 8(9) p. 881.

Dore, M. H. (2015) 'Waterborne Disease Outbreaks and the Multi-barrier Approach to Protecting Drinking Water.' *Global Drinking Water Management and Conservation*, pp. 13-31.

Du, G., Fang, Q. and den Toonder, J. M. (2016) 'Microfluidics for cell-based high throughput screening platforms—A review.' *Analytica chimica acta*, 903 pp. 36-50.

DWI (2015) 'Drinking water quality in England The position after 25 years of regulation.' The Stationery Office Limited.

DWI (2009) 'Drinking Water Safety: Guidance to health and water professionals.' The Stationery Office Limited.

DWI (2010) 'What are the drinking water standards.' The Stationery Office Limited.

DWI (2017) 'Report of the Drinking Water Inspectorate's Investigation into the Cryptosporidium Contamination of Franklaw Treatment Works in August 2015.' The Stationery Office Limited.

DWI (2018) 'The Water Supply (Water Quality) (Amendment) Regulations 2018.' The Stationery Office Limited.

ECDC. (2017) 'Healthcare-associated infections acquired in intensive care units.' ECDC. Annual epidemiological report for 2015.

Eckmanns, T., Oppert, M., Martin, M., Amorosa, R., Zuschneid, I., Frei, U., Rüden, H. and Weist, K. (2008) 'An outbreak of hospital-acquired Pseudomonas aeruginosa infection caused by contaminated bottled water in intensive care units.' *Clinical Microbiology and Infection*, 14(5) pp. 454-458.

Eichholz, G., Nagel, A. E. and Hughes, R. (1965) 'Adsorption of Ions Dilute Aqueous Solutions on Glass and Plastic Surfaces.' *Analytical Chemistry*, 37(7) pp. 863-868.

Elliott, S. M., Erickson, M. L., Krall, A. L. and Adams, B. A. (2018) 'Concentrations of pharmaceuticals and other micropollutants in groundwater downgradient from large on-site wastewater discharges.' *PloS one*, 13(11) p. e0206004.

Ercan, U.K., İbiş, F., Dikyol, C., Horzum, N., Karaman, O., Yıldırım, Ç., Çukur, E. and Demirci, E.A., (2018) 'Prevention of bacterial colonization on non-thermal atmospheric plasma treated surgical sutures for control and prevention of surgical site infections.' *PloS one*, 13(9), p.e0202703.

Erickson, D., Sinton, D. and Li, D. (2003) 'Joule heating and heat transfer in poly (dimethylsiloxane) microfluidic systems.' *Lab on a Chip*, 3(3) pp. 141-149.

EU (2008) 'European Union. Water framework directive 2008/105/EC.' European parliament and of the council.

EurEau. (2019) 'Treating micropollutants at waste water treatment plants Experiences and developments from European countries'.

Falkinham III, J. O., Hilborn, E. D., Arduino, M. J., Pruden, A. and Edwards, M. A. (2015) 'Epidemiology and ecology of opportunistic premise plumbing pathogens: Legionella pneumophila, Mycobacterium avium, and Pseudomonas aeruginosa.' *Environmental health perspectives*, 123(8) pp. 749-758.

Fang, F. C. (2011) 'Antimicrobial actions of reactive oxygen species.' *MBio*, 2(5).

Fawell, J. and Nieuwenhuijsen, M. J. (2003) 'Contaminants in drinking waterEnvironmental pollution and health.' *British medical bulletin*, 68(1) pp. 199-208.

Ferranti, G., Marchesi, I., Favale, M., Borella, P. and Bargellini, A. (2014) 'Aetiology, source and prevention of waterborne healthcare-associated infections: a review.' *Journal of medical microbiology*, 63(10) pp. 1247-1259.

Feng, X., Yan, B., Yang, Q., Jin, Y. and Cheng, Y. (2016) 'Gas–liquid dielectric barrier discharge falling film reactor for the decoloration of dyeing water.' *Journal of Chemical Technology & Biotechnology*, 91(2) pp. 431-438.

Fewtrell, L. (2004) 'Drinking-water nitrate, methemoglobinemia, and global burden of disease: a discussion.' *Environmental health perspectives*, 112(14) pp. 1371-1374.

Flynn, P.B., Busetti, A., Wielogorska, E., Chevallier, O.P., Elliott, C.T., Laverty, G., Gorman, S.P., Graham, W.G. and Gilmore, B.F., (2016) 'Non-thermal plasma exposure rapidly attenuates bacterial AHL-dependent quorum sensing and virulence.' *Scientific reports*, 6, p.26320.

Fogler, H. S. (1999) 'Elements of chemical reaction engineering.' Upper Saddle River, N.J. :Prentice Hall PTR.

Foster, J. E. (2017) 'Plasma-based water purification: Challenges and prospects for the future.' *Physics of Plasmas*, 24(5) p. 055501.

Foster, J. E., Adamovsky, G., Gucker, S. N. and Blankson, I. M. (2013) 'A comparative study of the time-resolved decomposition of methylene blue dye under the action of a nanosecond repetitively pulsed DBD plasma jet using liquid chromatography and spectrophotometry.' *IEEE Transactions on Plasma Science*, 41(3) pp. 503-512.

Foster, J. E., Mujovic, S., Groele, J. and Blankson, I. M. (2018) 'Towards high throughput plasma based water purifiers: design considerations and the pathway towards practical application.' *Journal of Physics D: Applied Physics*, 51(29) p. 293001.

Frank, J. A., Reich, C. I., Sharma, S., Weisbaum, J. S., Wilson, B. A. and Olsen, G. J. (2008) 'Critical evaluation of two primers commonly used for amplification of bacterial 16S rRNA genes.' *Applied Environment Microbiology*, 74(8) pp. 2461-2470.

Fridman, A. (2008) Plasma chemistry. Cambridge university press.

Fridman, G., Friedman, G., Gutsol, A., Shekhter, A., Vasilets, V. and Fridman, A. (2008), 'Applied plasma medicine.' *Plasma Processes* and Polymers, 5(6) 503.

Fux, C., Wilson, S. and Stoodley, P. (2004) 'Detachment characteristics and oxacillin resistance of Staphyloccocus aureus biofilm emboli in an in vitro catheter infection model.' *Journal of bacteriology*, 186(14) pp. 4486-4491

García, M. C., Mora, M., Esquivel, D., Foster, J. E., Rodero, A., Jiménez-Sanchidrián, C. and Romero-Salguero, F. J. (2017) 'Microwave atmospheric pressure plasma jets for wastewater treatment: Degradation of methylene blue as a model dye.' *Chemosphere*, 180 pp. 239-246.

Gellatly, S. L. and Hancock, R. E. (2013) 'Pseudomonas aeruginosa: new insights into pathogenesis and host defenses.' *Pathogens and disease*, 67(3) pp. 159-173.

Gerrity, D., Stanford, B. D., Trenholm, R. A. and Snyder, S. A. (2010) 'An evaluation of a pilot-scale nonthermal plasma advanced oxidation process for trace organic compound degradation.' *Water research*, 44(2) pp. 493-504.

Gervais, T., El-Ali, J., Günther, A. and Jensen, K. F. (2006) 'Flow-induced deformation of shallow microfluidic channels.' *Lab on a Chip*, 6(4) pp. 500-507.

Gita, S., Hussan, A. and Choudhury, T. (2017) 'Impact of textile dyes waste on aquatic environments and its treatment.' *Environ. Ecol.*, 35(3C) pp. 2349-2353.

Giwa, A., Bello, I. and Olajire, A. (2013) 'Removal of basic dye from aqueous solution by adsorption on melon husk in binary and ternary systems.' *Chemical and Process Engineering Research*, 13 pp. 51-68.

Gleick, P. and Schneider, S. (1996) 'Encyclopedia of climate and weather.' *Water Resources*, 2 pp. 817-823.

Gnapowski, S., Kalinowska-Ozgowicz, E., Śniadkowski, M. and Pietraszek, A. (2019) 'Investigation of the Condition of the Gold Electrodes Surface in a Plasma Reactor.' *Materials*, 12(13) p. 2137.

Gobert, S. R., Kuhn, S., Braeken, L. and Thomassen, L. C. (2017) 'Characterization of milli-and microflow reactors: mixing efficiency and residence time distribution.' *Organic Process Research & Development*, 21(4) pp. 531-542.

Gogoi, A., Mazumder, P., Tyagi, V. K., Chaminda, G. T., An, A. K. and Kumar, M. (2018) 'Occurrence and fate of emerging contaminants in water environment: A review.' *Groundwater for Sustainable Development*, 6 pp. 169-180.

Goller, C., Wang, X., Itoh, Y. and Romeo, T. (2006) 'The cation-responsive protein NhaR of Escherichia coli activates pgaABCD transcription, required for production of the biofilm adhesin poly-β-1, 6-N-acetyl-d-glucosamine.' *Journal of bacteriology*, 188(23) pp. 8022-8032.

Gomez, E., Rani, D. A., Cheeseman, C., Deegan, D., Wise, M. and Boccaccini, A. (2009) 'Thermal plasma technology for the treatment of wastes: a critical review.' *Journal of hazardous materials*, 161(2-3) pp. 614-626.

González, F. U. T., Herrera-Silveira, J. A. and Aguirre-Macedo, M. L. (2008) 'Water quality variability and eutrophic trends in karstic tropical coastal lagoons of the Yucatán Peninsula.' *Estuarine, Coastal and Shelf Science*, 76(2) pp. 418-430.

Gorbanev, Y., O'Connell, D. and Chechik, V. (2016) 'Non-Thermal Plasma in Contact with Water: The Origin of Species.' *Chemistry–A European Journal*, 22(10) pp. 3496-3505.

Grabowski, L., Van Veldhuizen, E., Pemen, A. and Rutgers, W. (2006) 'Corona above water reactor for systematic study of aqueous phenol degradation.' *Plasma Chemistry and Plasma Processing*, 26(1) pp. 3-17.

Gray, J. (2008) 'Water contamination events in UK drinking-water supply systems.' *Journal of water and health*, 6(S1) pp. 21-26.

Groitl, B., Dahl, J. U., Schroeder, J. W. and Jakob, U. (2017) 'Pseudomonas aeruginosa defense systems against microbicidal oxidants.' *Molecular microbiology*, 106(3) pp. 335-350.

Gu, H., Duits, M. H. and Mugele, F. (2011) 'Droplets formation and merging in two-phase flow microfluidics.' *International journal of molecular sciences*, 12(4) pp. 2572-2597.

Gunatilake, S. (2015) 'Methods of removing heavy metals from industrial wastewater.' *Methods*, 1(1) p. 14.

Gupta, V. K., Ali, I., Saleh, T. A., Nayak, A. and Agarwal, S. (2012) 'Chemical treatment technologies for waste-water recycling—an overview.' *Rsc Advances*, 2(16) pp. 6380-6388.

Hall, C. W. and Mah, T.-F. (2017) 'Molecular mechanisms of biofilm-based antibiotic resistance and tolerance in pathogenic bacteria.' *FEMS microbiology reviews*, 41(3) pp. 276-301.

Hamdan, A., Čerņevičs, K. and Cha, M. S. (2017) 'The effect of electrical conductivity on nanosecond discharges in distilled water and in methanol with argon bubbles.' *Journal of Physics D: Applied Physics*, 50(18) p. 185207.

Hartmann, J., van der Aa, M., Wuijts, S., de Roda Husman, A. M. and van der Hoek, J. P. (2018) 'Risk governance of potential emerging risks to drinking water quality: Analysing current practices.' *Environmental Science & Policy*, 84 pp. 97-104.

Hayashi, N., Akiyoshi, Y., Kobayashi, Y., Kanda, K., Ohshima, K. and Goto, M. (2013) 'Inactivation characteristics of Bacillus thuringiensis spore in liquid using atmospheric torch plasma using oxygen.' *Vacuum*, 88 pp. 173-176.

Heberlein, J. (1992) 'Generation of thermal and pseudo-thermal plasmas.' *Pure and applied chemistry*, 64(5) pp. 629-636.

Hejazian, M., Li, W. and Nguyen, N. T. (2015) 'Lab on a chip for continuous-flow magnetic cell separation.' *Lab on a Chip*, 15(4) pp. 959-970.

Helmi, K., Skraber, S., Gantzer, C., Willame, R., Hoffmann, L. and Cauchie, H.-M. (2008) 'Interactions of Cryptosporidium parvum, Giardia lamblia, vaccinal poliovirus type 1, and

bacteriophages ΦX174 and MS2 with a drinking water biofilm and a wastewater biofilm.' *Applied Environment Microbiology*, 74(7) pp. 2079-2088.

Henne, K., Kahlisch, L., Brettar, I. and Höfle, M. G. (2012) 'Analysis of structure and composition of bacterial core communities in mature drinking water biofilms and bulk water of a citywide network in Germany.' *Applied Environment Microbiology*, 78(10) pp. 3530-3538.

Herzberg, M. and Elimelech, M. (2007) 'Biofouling of reverse osmosis membranes: role of biofilm-enhanced osmotic pressure.' *Journal of Membrane Science*, 295(1) pp. 11-20.

Hoeben, W., Van Veldhuizen, E., Rutgers, W. and Kroesen, G. (1999) 'Gas phase corona discharges for oxidation of phenol in an aqueous solution.' *Journal of physics D: Applied physics*, 32(24) p. L133.

Hofman-Caris, R. and Hofman, J. (2017) 'Limitations of Conventional Drinking Water Technologies in Pollutant Removal.' *Applications of Advanced Oxidation Processes (AOPs) in Drinking Water Treatment* (pp. 21-51).

Holkar, C. R., Jadhav, A. J., Pinjari, D. V., Mahamuni, N. M. and Pandit, A. B. (2016) 'A critical review on textile wastewater treatments: possible approaches.' *Journal of environmental management*, 182 pp. 351-366.

Hopkins, S., Shaw, K. and Simpson, L. (2011) 'English national point prevalence survey on healthcare-associated infections and antimicrobial use.' London (United Kingdom): Health Protection Agency.

Hopman, J., Tostmann, A., Wertheim, H., Bos, M., Kolwijck, E., Akkermans, R., Sturm, P., Voss, A., et al. (2017) 'Reduced rate of intensive care unit acquired gram-negative bacilli after removal of sinks and introduction of 'water-free'patient care.' *Antimicrobial Resistance & Infection Control*, 6(1) p. 59.

Hou, A.-m., Yang, D., Miao, J., Shi, D.-y., Yin, J., Yang, Z.-w., Shen, Z.-q., Wang, H.-r., et al. (2019) 'Chlorine injury enhances antibiotic resistance in Pseudomonas aeruginosa through over expression of drug efflux pumps.' *Water research*, 156 pp. 366-371.

HPSC. (2015) Guidelines for the prevention and control of infection from water systems in healthcare facilities. HSE Health Protection Surveillance Centre (HPSC).

Huang, F., Chen, L., Wang, H. and Yan, Z. (2010) 'Analysis of the degradation mechanism of methylene blue by atmospheric pressure dielectric barrier discharge plasma.' *Chemical Engineering Journal*, 162(1) pp. 250-256.

Huh, D., Tung, Y.-C., Wei, H.-H., Grotberg, J. B., Skerlos, S. J., Kurabayashi, K. and Takayama, S. (2002) 'Use of air-liquid two-phase flow in hydrophobic microfluidic channels for disposable flow cytometers.' *Biomedical Microdevices*, 4(2) pp. 141-149.

Hutchins, C. F., Moore, G., Thompson, K.-A., Webb, J. and Walker, J. T. (2017) 'Contamination of hospital tap water: the survival and persistence of Pseudomonas aeruginosa on conventional and 'antimicrobial'outlet fittings.' *Journal of Hospital Infection*, 97(2), pp.156-161.

Hutton, G., Rodriguez, U., Napitupulu, L., Thang, P. and Kov, P. (2008) 'Economic impacts of sanitation in Southeast Asia.' *Jakarta: World Bank*.

Iles, A. (2009) Microsystems for the enablement of nanotechnologies. Vol. 5.

Inagaki, N. (2014) Plasma surface modification and plasma polymerization. CRC Press.

Ippolito, J., Barbarick, K. and Elliott, H. (2011) 'Drinking water treatment residuals: a review of recent uses.' *Journal of Environmental Quality*, 40(1) pp. 1-12.

Isabella, S., Navarro, C. A., Robert, L., Dimitar, M. and Teresa, L. (2018) State of the Art on the Contribution of Water to Antimicrobial Resistance.

Isbary, G., Zimmermann, J., Shimizu, T., Li, Y. F., Morfill, G., Thomas, H., Steffes, B., Heinlin, J., Karrer, S. and Stolz, W., (2013) 'Non-thermal plasma—More than five years of clinical experience.' *Clinical Plasma Medicine*, 1(1) pp. 19-23.

Ishii, C., Stauss, S., Kuribara, K., Urabe, K., Sasaki, T. and Terashima, K. (2015) 'Atmospheric pressure synthesis of diamondoids by plasmas generated inside a microfluidic reactor.' *Diamond and Related Materials*, 59 pp. 40-46.

Islam, B. U., Habib, S., Ali, S. A. and Ali, A. (2017) 'Role of peroxynitrite-induced activation of poly (ADP-ribose) polymerase (PARP) in circulatory shock and related pathological conditions.' *Cardiovascular toxicology*, 17(4) pp. 373-383.

Jackson, P. J., Dillon, G. R., Irving, T. E. and Stanfield, G. (2001) Manual on treatment for small water supply systems. DWI 70/2/137: Drinking Water Inspectorate (DWI).

Jefferies, J. M. C., Cooper, T., Yam, T. and Clarke, S. C. (2012) 'Pseudomonas aeruginosa outbreaks in the neonatal intensive care unit—a systematic review of risk factors and environmental sources.' *Journal of medical microbiology*, 61(8) pp. 1052-1061.

Jensen, K. F. (2017) 'Flow chemistry—microreaction technology comes of age.' *AIChE Journal*, 63(3) pp. 858-869.

Jiang, B., Zheng, J., Liu, Q. and Wu, M. (2012) 'Degradation of azo dye using non-thermal plasma advanced oxidation process in a circulatory airtight reactor system.' *Chemical Engineering Journal,* 204 pp. 32-39.

Jiang, B., Zheng, J., Qiu, S., Wu, M., Zhang, Q., Yan, Z. and Xue, Q. (2014) 'Review on electrical discharge plasma technology for wastewater remediation.' *Chemical Engineering Journal*, 236 pp. 348-368.

Jidenko, N., Bourgeois, E. and Borra, J. (2010) 'Temperature profiles in filamentary dielectric barrier discharges at atmospheric pressure.' *Journal of physics D: applied physics*, 43(29) p. 295203.

Jin, L., Jiang, L., Han, Q., Xue, J., Ye, H., Cao, G., Lin, K. and Cui, C. (2016) 'Distribution characteristics and health risk assessment of thirteen sulfonamides antibiotics in a drinking water source in East China.' *Huan jing ke xue= Huanjing kexue*, 37(7) pp. 2515-2521.

Jin, Y., Wu, Y., Cao, J. and Wu, Y. (2014) 'Optimizing decolorization of methylene blue and methyl orange dye by pulsed discharged plasma in water using response surface methodology.' *Journal of the Taiwan Institute of Chemical Engineers*, 45(2) pp. 589-595.

Johnson, D. C., Bzdek, J. P., Fahrenbruck, C. R., Chandler, J. C., Bisha, B., Goodridge, L. D. and Hybertson, B. M. (2016) 'An innovative non-thermal plasma reactor to eliminate microorganisms in water.' *Desalination and Water Treatment*, 57(18) pp. 8097-8108.

Jones, D. B. and Raston, C. L. (2017) 'Improving oxidation efficiency through plasma coupled thin film processing.' *Rsc Advances*, 7(74) pp. 47111-47115.

Jones, O. A., Green, P. G., Voulvoulis, N. and Lester, J. N. (2007) 'Questioning the excessive use of advanced treatment to remove organic micropollutants from wastewater.' *Environmental science & technology*, 41(14) pp. 5085-5089.

Joshi, S. G., Cooper, M., Yost, A., Paff, M., Ercan, U. K., Fridman, G., Friedman, G., Fridman, A., et al. (2011) 'Nonthermal dielectric-barrier discharge plasma-induced inactivation involves oxidative DNA damage and membrane lipid peroxidation in Escherichia coli.' *Antimicrobial agents and chemotherapy*, 55(3) pp. 1053-1062.

Judée, F., Simon, S., Bailly, C. and Dufour, T. (2018) 'Plasma-activation of tap water using DBD for agronomy applications: Identification and quantification of long lifetime chemical species and production/consumption mechanisms.' *Water research*, 133 pp. 47-59.

Kadambari, S., Botgros, A., Clarke, P., Vergnano, S., Anthony, M., Chang, J., Collinson, A., Embleton, N., et al. (2014) 'Characterizing the burden of invasive Pseudomonas infection on neonatal units in the UK between 2005 and 2011.' *Journal of Hospital Infection*, 88(2) pp. 109-112.

Kalghatgi, S., Friedman, G., Fridman, A. and Clyne, A. M. (2010) 'Endothelial cell proliferation is enhanced by low dose non-thermal plasma through fibroblast growth factor-2 release.' *Annals of biomedical engineering*, 38(3) pp. 748-757.

Kamba, P. F., Kaggwa, B., Munanura, E. I., Okurut, T. and Kitutu, F. E. (2017) 'Why regulatory indifference towards pharmaceutical pollution of the environment could be a missed opportunity in public health protection. a holistic view.' *Pan African Medical Journal*, 27(1).

Kanazawa, S., Kawano, H., Watanabe, S., Furuki, T., Akamine, S., Ichiki, R., Ohkubo, T., Kocik, M., and Mizeraczyk, J., (2011) 'Observation of OH radicals produced by pulsed discharges on the surface of a liquid.' *Plasma Sources Science and Technology*, 20(3) p. 034010.

Kant, R. (2012) 'Textile dyeing industry an environmental hazard.' *Natural science*, 4(1) pp. 22-26.

Karanassios, V. (2004) 'Microplasmas for chemical analysis: analytical tools or research toys?' *Spectrochimica Acta Part B: Atomic Spectroscopy*, 59(7) pp. 909-928.

Karle, M., Vashist, S. K., Zengerle, R. and von Stetten, F. (2016) 'Microfluidic solutions enabling continuous processing and monitoring of biological samples: A review.' *Analytica chimica acta*, 929 pp. 1-22.

Kaushik, N. K., Ghimire, B., Li, Y., Adhikari, M., Veerana, M., Kaushik, N., Jha, N., Adhikari, B., Lee, S.J., Masur, K. and Von Woedtke, T., (2018) 'Biological and medical applications of plasma-activated media, water and solutions.' *Biological chemistry*, 400(1) pp. 39-62.

Kefou, N., Karvelas, E., Karamanos, K., Karakasidis, T. and Sarris, I. E. (2016) 'Water purification in micromagnetofluidic devices: mixing in MHD micromixers.' *Procedia engineering*, 162 pp. 593-600.

Khan, S. and Malik, A. (2014) 'Environmental and health effects of textile industry wastewater.' *Environmental deterioration and human health: Springer*, pp. 55-71.

Kim, H. S., Cho, Y. I., Hwang, I. H., Lee, D. H., Cho, D. J., Rabinovich, A. and Fridman, A. (2013) 'Use of plasma gliding arc discharges on the inactivation of E. Coli in water.' *Separation and Purification Technology*, 120 pp. 423-428.

Kim, H. S., Wright, K. C., Hwang, I. W., Lee, D. H., Rabinovich, A., Fridman, A. and Cho, Y. (2013) 'Concentration of hydrogen peroxide generated by gliding arc discharge and inactivation of E. coli in water.' *International Communications in Heat and Mass Transfer*, 42 pp. 5-10.

Kinsey, C. B., Koirala, S., Solomon, B., Rosenberg, J., Robinson, B. F., Neri, A., Halpin, A. L., Arduino, M. J., Moulton-Meissner, H., Noble-Wang, J. and Chea, N., (2017) 'Pseudomonas aeruginosa outbreak in a neonatal intensive care unit attributed to hospital tap water.' *Infection control & hospital epidemiology*, 38(7) pp. 801-808.

Kobayashi, T., Sugai, T., Handa, T., Minamitani, Y. and Nose, T. (2010) 'The effect of spraying of water droplets and location of water droplets on the water treatment by pulsed discharge in air.' *IEEE Transactions on Plasma Science*, 38(10) pp. 2675-2680.

Kogelschatz, U. (2003) 'Dielectric-barrier discharges: their history, discharge physics, and industrial applications.' *Plasma chemistry and plasma processing*, 23(1) pp. 1-46.

Kogelschatz, U., Eliasson, B. and Egli, W. (1997) 'Dielectric-barrier discharges. Principle and applications.' *Le Journal de Physique IV*, 7(C4) pp. C4-47-C44-66.

Kondeti, V. S. K., Phan, C. Q., Wende, K., Jablonowski, H., Gangal, U., Granick, J. L., Hunter, R. C. and Bruggeman, P. J. (2018) 'Long-lived and short-lived reactive species produced by a cold atmospheric pressure plasma jet for the inactivation of Pseudomonas aeruginosa and Staphylococcus aureus.' *Free Radical Biology and Medicine*, 124 pp. 275-287.

Kornev, I., Osokin, G., Galanov, A., Yavorovskiy, N. and Preis, S. (2013) 'Formation of nitrite- and nitrate-ions in aqueous solutions treated with pulsed electric discharges.' *Ozone: Science & Engineering*, 35(1) pp. 22-30.

Korobeynikov, S. and Melekhov, A. (2016) Streamers and partial discharges in water. Vol. 754: IOP Publishing.

Kovačević, V. V., Dojčinović, B. P., Jović, M., Roglić, G. M., Obradović, B. M. and Kuraica, M. M. (2017) 'Measurement of reactive species generated by dielectric barrier discharge in direct contact with water in different atmospheres.' *Journal of Physics D: Applied Physics*, 50(15) p. 155205.

Kragh, K. N., Hutchison, J. B., Melaugh, G., Rodesney, C., Roberts, A. E., Irie, Y., Jensen, P. Ø., Diggle, S. P., et al. (2016) 'Role of multicellular aggregates in biofilm formation.' *MBio*, 7(2) pp. e00237-00216.

Kregiel, D., Rygala, A., Kolesinska, B., Nowacka, M., Herc, A. S. and Kowalewska, A. (2019) 'Antimicrobial and Antibiofilm N-acetyl-L-cysteine Grafted Siloxane Polymers with Potential for Use in Water Systems.' *International journal of molecular sciences*, 20(8) p. 2011.

Krewing, M., Stepanek, J. J., Cremers, C., Lackmann, J.-W., Schubert, B., Müller, A., Awakowicz, P., Leichert, L. I., et al. (2019) 'The molecular chaperone Hsp33 is activated by atmospheric-pressure plasma protecting proteins from aggregation.' *Journal of the Royal Society Interface*, 16(155) p. 20180966.

Kriegeskorte, A., Grubmüller, S., Huber, C., Kahl, B.C., von Eiff, C., Proctor, R.A., Peters, G., Eisenreich, W. and Becker, K., (2014) 'Staphylococcus aureus small colony variants show common metabolic features in central metabolism irrespective of the underlying auxotrophism.' *Frontiers in cellular and infection microbiology*, 4, p.141.

Krugly, E., Martuzevicius, D., Tichonovas, M., Jankunaite, D., Rumskaite, I., Sedlina, J., Racys, V. and Baltrusaitis, J. (2015) 'Decomposition of 2-naphthol in water using a non-thermal plasma reactor.' *Chemical Engineering Journal*, 260 pp. 188-198.

Krupež, J., Kovačević, V. V., Jović, M., Roglić, G. M., Natić, M. M., Kuraica, M. M., Obradović, B. M. and Dojčinović, B. P. (2018) 'Degradation of nicotine in water solutions using a water falling film DBD plasma reactor: direct and indirect treatment.' *Journal of Physics D: Applied Physics*, 51(17) p. 174003.

Krzeminski, P., Tomei, M. C., Karaolia, P., Langenhoff, A., Almeida, C. M. R., Felis, E., Gritten, F., Andersen, H. R., Fernandes, T., Manaia, C.M. and Rizzo, L., (2018) 'Performance of secondary wastewater treatment methods for the removal of contaminants of emerging concern implicated in crop uptake and antibiotic resistance spread: A review.' *Science of the Total Environment*, *648*, pp.1052-1081.

Lange, H., Sioda, M., Huczko, A., Zhu, Y., Kroto, H. and Walton, D. (2003) 'Nanocarbon production by arc discharge in water.' *Carbon*, 41(8) pp. 1617-1623.

Laroussi, M. and Leipold, F. (2004) 'Evaluation of the roles of reactive species, heat, and UV radiation in the inactivation of bacterial cells by air plasmas at atmospheric pressure.' *International Journal of Mass Spectrometry*, 233(1-3) pp. 81-86.

Laroussi, M., Richardson, J. P. and Dobbs, F. C. (2002) 'Effects of nonequilibrium atmospheric pressure plasmas on the heterotrophic pathways of bacteria and on their cell morphology.' *Applied Physics Letters*, 81(4) pp. 772-774.

Lee, M.-J., Kwon, J.-S., Jiang, H. B., Choi, E. H., Park, G. and Kim, K.-M. (2019) 'The antibacterial effect of non-thermal atmospheric pressure plasma treatment of titanium surfaces according to the bacterial wall structure.' *Scientific reports*, 9(1) p. 1938.

Leggett, H. C., Cornwallis, C. K. and West, S. A. (2012) 'Mechanisms of pathogenesis, infective dose and virulence in human parasites.' *PLoS pathogens*, 8(2) p. e1002512.

Li, D. E. and Lin, C. H. (2018) 'Microfluidic chip for droplet-based AuNP synthesis with dielectric barrier discharge plasma and on-chip mercury ion detection.' *Rsc Advances*, 8(29) pp. 16139-16145.

Li, H., Zhu, X. and Ni, J. (2011) 'Comparison of electrochemical method with ozonation, chlorination and monochloramination in drinking water disinfection.' *Electrochimica Acta*, 56(27) pp. 9789-9796.

Li, M., Li, C., Zhan, H., Xu, J. and Wang, X. (2008) 'Effect of surface charge trapping on dielectric barrier discharge.' *Applied Physics Letters*, 92(3) p. 031503.

Li, N., Ho, K. W., Ying, G.-G. and Deng, W.-J. (2017) 'Veterinary antibiotics in food, drinking water, and the urine of preschool children in Hong Kong.' *Environment international*, 108 pp. 246-252.

Liao, X., Liu, D., Xiang, Q., Ahn, J., Chen, S., Ye, X. and Ding, T. (2017) 'Inactivation mechanisms of non-thermal plasma on microbes: a review.' *Food Control*, 75 pp. 83-91.

Li, X. F. and Mitch, W. A. (2018) 'Drinking water disinfection byproducts (DBPs) and human health effects: multidisciplinary challenges and opportunities.' *ACS Publications*, 1681-1689.

Liang, Y., Wu, Y., Sun, K., Chen, Q., Shen, F., Zhang, J., Yao, M., Zhu, T., and Fang, J., (2012) 'Rapid inactivation of biological species in the air using atmospheric pressure nonthermal plasma.' *Environmental science & technology*, 46(6) pp. 3360-3368.

Liao, X., Liu, D., Xiang, Q., Ahn, J., Chen, S., Ye, X. and Ding, T. (2017) 'Inactivation mechanisms of non-thermal plasma on microbes: a review.' *Food Control*, 75 pp. 83-91.

Lifton, V. A. (2016) 'Microfluidics: an enabling screening technology for enhanced oil recovery (EOR).' *Lab on a Chip,* 16(10) pp. 1777-1796.

Lin, S. D. and Green, C. D. (1987) 'Wastes from water treatment plants: Literature review, results of an Illinois survey, and effects of alum sludge application to cropland.' *Illinois State Water Survey*.

Lin, X. Z., Terepka, A. D. and Yang, H. (2004) 'Synthesis of silver nanoparticles in a continuous flow tubular microreactor.' *Nano letters*, 4(11) pp. 2227-2232.

Lindsay, A., Anderson, C., Slikboer, E., Shannon, S. and Graves, D. (2015) 'Momentum, heat, and neutral mass transport in convective atmospheric pressure plasma-liquid systems and implications for aqueous targets.' *Journal of Physics D: Applied Physics*, 48(42) p. 424007.

Liu, D., Liu, Z., Chen, C., Yang, A., Li, D., Rong, M., Chen, H. and Kong, M. (2016) 'Aqueous reactive species induced by a surface air discharge: Heterogeneous mass transfer and liquid chemistry pathways.' *Scientific reports*, 6 p. 23737.

Liu, S., Gunawan, C., Barraud, N., Rice, S. A., Harry, E. J. and Amal, R. (2016) 'Understanding, monitoring, and controlling biofilm growth in drinking water distribution systems.' *Environmental science & technology*, 50(17) pp. 8954-8976.

Liu, X., Zhang, H., Qin, D., Yang, Y., Kang, Y., Zou, F. and Wu, Z. (2015) 'Radical-Initiated Decoloration of Methylene Blue in a Gas–Liquid Multiphase System Via DC Corona Plasma.' *Plasma Chemistry and Plasma Processing*, 35(2) pp. 321-337.

Liu, Z., Wang, W., Zhang, S., Yang, D., Jia, L. and Dai, L. (2012) 'Optical study of a diffuse bipolar nanosecond pulsed dielectric barrier discharge with different dielectric thicknesses in air.' *The European Physical Journal D*, 66(12) p. 319.

Livingston, S. H., Cadnum, J. L., Gestrich, S., Jencson, A. L. and Donskey, C. J. (2018) 'A novel sink drain cover prevents dispersal of microorganisms from contaminated sink drains.' *Infection Control & Hospital Epidemiology*, 39(10) pp. 1254-1256.

Locke, B., Sato, M., Sunka, P., Hoffmann, M. and Chang, J. S. (2006) 'Electrohydraulic discharge and nonthermal plasma for water treatment.' *Industrial & engineering chemistry research*, 45(3) pp. 882-905.

Locke, B. R. and Shih, K. Y. (2011) 'Review of the methods to form hydrogen peroxide in electrical discharge plasma with liquid water.' *Plasma Sources Science and Technology*, 20(3) p. 034006.

Logar, I., Brouwer, R., Maurer, M. and Ort, C. (2014) 'Cost-benefit analysis of the Swiss national policy on reducing micropollutants in treated wastewater.' *Environmental science & technology*, 48(21) pp. 12500-12508.

Lood, R., Ertürk, G. and Mattiasson, B. (2017) 'Revisiting antibiotic resistance spreading in wastewater treatment plants–bacteriophages as a much neglected potential transmission vehicle.' *Frontiers in microbiology*, 8 p. 2298.

Loveday, H., Wilson, J., Kerr, K., Pitchers, R., Walker, J. and Browne, J. (2014) 'Association between healthcare water systems and Pseudomonas aeruginosa infections: a rapid systematic review.' *Journal of Hospital Infection*, 86(1) pp. 7-15.

Lu, P., Boehm, D., Bourke, P. and Cullen, P. J. (2017) 'Achieving reactive species specificity within plasma-activated water through selective generation using air spark and glow discharges.' *Plasma Processes and Polymers*, 14(8) p. 1600207.

Lukes, P., Clupek, M. and Babicky, V. (2011) 'Discharge filamentary patterns produced by pulsed corona discharge at the interface between a water surface and air.' *IEEE Transactions on Plasma Science*, 39(11) pp. 2644-2645.

Lukes, P., Locke, B. R. and Brisset, J. L. (2012) 'Aqueous-phase chemistry of electrical discharge plasma in water and in gas-liquid environments.' *Plasma chemistry and catalysis in gases and liquids*, 1 pp. 243-308.

Lukes, P., Dolezalova, E., Sisrova, I. and Clupek, M. (2014) 'Aqueous-phase chemistry and bactericidal effects from an air discharge plasma in contact with water: evidence for the formation of peroxynitrite through a pseudo-second-order post-discharge reaction of H2O2 and HNO2.' *Plasma Sources Science and Technology*, 23(1) p. 015019.

Lukes, P., Clupek, M., Babicky, V., Janda, V. and Sunka, P. (2005) 'Generation of ozone by pulsed corona discharge over water surface in hybrid gas–liquid electrical discharge reactor.' *Journal of Physics D: Applied Physics*, 38(3) p. 409.

Lukeš, P., Člupek, M., Babický, V., Šunka, P., Skalný, J., Štefečka, M., Novák, J. and Málková, Z. (2006) 'Erosion of needle electrodes in pulsed corona discharge in water.' *Czechoslovak Journal of Physics*, 56(2) pp. B916-B924.

Lunau, M., Voss, M., Erickson, M., Dziallas, C., Casciotti, K. and Ducklow, H. (2013) 'Excess nitrate loads to coastal waters reduces nitrate removal efficiency: mechanism and implications for coastal eutrophication.' *Environmental microbiology*, 15(5) pp. 1492-1504.

Lunov, O., Zablotskii, V., Churpita, O., Chánová, E., Syková, E., Dejneka, A. and Kubinová, Š. (2014) 'Cell death induced by ozone and various non-thermal plasmas: therapeutic perspectives and limitations.' *Scientific reports*, 4 p. 7129.

Lunov, O., Churpita, O., Zablotskii, V., Deyneka, I., Meshkovskii, I., Jäger, A., Syková, E., Kubinová, Š., and Dejneka, A., (2015) 'Non-thermal plasma mills bacteria: Scanning electron microscopy observations.' *Applied Physics Letters*, 106(5) p. 053703.

Luo, D. and Duan, Y. (2012) 'Microplasmas for analytical applications of lab-on-a-chip.' *TrAC Trends in Analytical Chemistry*, 39 pp. 254-266.

López, M., Calvo, T., Prieto, M., Múgica-Vidal, R., Muro-Fraguas, I., Alba-Elías, F. and Alvarez-Ordóñez, A. (2019) 'A review on non-thermal atmospheric plasma for food preservation: mode of action, determinants of effectiveness, and applications.' *Frontiers in microbiology*, 10.

Ma, J., Lee, S. M. Y., Yi, C. and Li, C. W. (2017) 'Controllable synthesis of functional nanoparticles by microfluidic platforms for biomedical applications–a review.' *Lab on a Chip*, 17(2) pp. 209-226.

Ma, L., Conover, M., Lu, H., Parsek, M. R., Bayles, K. and Wozniak, D. J. (2009) 'Assembly and development of the Pseudomonas aeruginosa biofilm matrix.' *PLoS pathogens*, 5(3) p. e1000354.

Ma, R., Wang, G., Tian, Y., Wang, K., Zhang, J. and Fang, J. (2015) 'Non-thermal plasma-activated water inactivation of food-borne pathogen on fresh produce.' *Journal of hazardous materials*, 300 pp. 643-651.

Ma, R., Feng, H., Liang, Y., Zhang, Q., Tian, Y., Su, B., Zhang, J. and Fang, J. (2013) 'An atmospheric-pressure cold plasma leads to apoptosis in Saccharomyces cerevisiae by accumulating intracellular reactive oxygen species and calcium.' *Journal of Physics D: Applied Physics*, 46(28) p. 285401.

Magureanu, M., Mandache, N. B. and Parvulescu, V. I. (2007) 'Degradation of organic dyes in water by electrical discharges.' *Plasma Chemistry and Plasma Processing*, 27(5) pp. 589-598.

Magureanu, M., Piroi, D., Mandache, N. B. and Parvulescu, V. (2008) 'Decomposition of methylene blue in water using a dielectric barrier discharge: optimization of the operating parameters.' *Journal of applied physics*, 104(10) p. 103306.

Magureanu, M., Bradu, C., Piroi, D., Mandache, N. B. and Parvulescu, V. (2013) 'Pulsed corona discharge for degradation of methylene blue in water.' P*lasma Chemistry and Plasma Processing*, 33(1) pp. 51-64.

Magureanu, M., Piroi, D., Mandache, N. B., David, V., Medvedovici, A. and Parvulescu, V. I. (2010) 'Degradation of pharmaceutical compound pentoxifylline in water by non-thermal plasma treatment.' W*ater Research*, 44(11) pp. 3445-3453.

Magureanu, M., Piroi, D., Mandache, N., David, V., Medvedovici, A., Bradu, C. and Parvulescu, V. (2011) 'Degradation of antibiotics in water by non-thermal plasma treatment.' *Water research*, 45(11) pp. 3407-3416.

Mahamuni, N. N. and Adewuyi, Y. G. (2010) 'Advanced oxidation processes (AOPs) involving ultrasound for waste water treatment: a review with emphasis on cost estimation.' *Ultrasonics sonochemistry*, 17(6) pp. 990-1003.

Maharudrayya, S., Jayanti, S. and Deshpande, A. (2006) 'Pressure drop and flow distribution in multiple parallel-channel configurations used in proton-exchange membrane fuel cell stacks.' *Journal of power sources*, 157(1) pp. 358-367.

Mai-Prochnow, A., Clauson, M., Hong, J. and Murphy, A.B., (2016) 'Gram positive and Gram negative bacteria differ in their sensitivity to cold plasma.' *Scientific reports*, 6, p.38610.

Mai-Prochnow, A., Murphy, A. B., McLean, K. M., Kong, M. G. and Ostrikov, K. K. (2014) 'Atmospheric pressure plasmas: infection control and bacterial responses.' *International journal of antimicrobial agents*, 43(6) pp. 508-517.

Maisch, T., Shimizu, T., Li, Y. F., Heinlin, J., Karrer, S., Morfill, G. and Zimmermann, J. L. (2012) 'Decolonisation of MRSA, S. aureus and E. coli by cold-atmospheric plasma using a porcine skin model in vitro.' *PloS one*, 7(4) p. e34610.

Malik, M. A. (2010) 'Water purification by plasmas: Which reactors are most energy efficient?' *Plasma Chemistry and Plasma Processing*, 30(1) pp. 21-31.

Malik, M. A., Ghaffar, A. and Malik, S. A. (2001) 'Water purification by electrical discharges.' *Plasma Sources Science and Technology*, 10(1) p. 82.

Mao, G., Song, Y., Bartlam, M. G., Gao, G. and Wang, Y. (2018) 'Long-term effects of residual chlorine on Pseudomonas aeruginosa in simulated drinking water fed with low AOC medium.' *Frontiers in microbiology*, 9 p. 879.

Margot, J., Rossi, L., Barry, D. A. and Holliger, C. (2015) 'A review of the fate of micropollutants in wastewater treatment plants.' *Wiley Interdisciplinary Reviews: Water*, 2(5) pp. 457-487.

Marotta, E., Schiorlin, M., Ren, X., Rea, M. and Paradisi, C. (2011) 'Advanced oxidation process for degradation of aqueous phenol in a dielectric barrier discharge reactor.' *Plasma Processes and Polymers*, 8(9) pp. 867-875.

Mathers, A. J., Vegesana, K., German Mesner, I., Barry, K. E., Pannone, A., Baumann, J., Crook, D. W., Stoesser, N., et al. (2018) 'Intensive care unit wastewater interventions to prevent transmission of multispecies Klebsiella pneumoniae carbapenemase–producing organisms.' *Clinical Infectious Diseases*, 67(2) pp. 171-178.

McCreedy, T. (2001) 'Rapid prototyping of glass and PDMS microstructures for micro total analytical systems and micro chemical reactors by microfabrication in the general laboratory.' *Analytica chimica acta*, 427(1) pp. 39-43.

Meaden, G. T. (2013) Electrical resistance of metals. Springer.

Meirovich, A., Parkansky, N., Boxman, R. L., Berkh, O., Barkay, Z. and Rosenberg, Y. (2016) 'Treatment of Methylene Blue water solution by submerged pulse arc in multi-electrode reactor.' *Journal of Water Process Engineering*, 13 pp. 53-60.

Mendis, D., Rosenberg, M. and Azam, F. (2000) 'A note on the possible electrostatic disruption of bacteria.' *IEEE Transactions on plasma science*, 28(4) pp. 1304-1306.

Melter, O. and Radojevič, B., (2010) 'Small colony variants of Staphylococcus aureus.' *Folia microbiologica*, 55(6), pp.548-558.

Metz, F. and Ingold, K. (2014) 'Sustainable wastewater management: is it possible to regulate micropollution in the future by learning from the past? A policy analysis.' *Sustainability*, 6(4) pp. 1992-2012.

Midi, N. S., Ohyama, R. I. and Yamaguchi, S. (2013) 'Underwater current distribution induced by spark discharge on a water surface.' *Journal of Electrostatics*, 71(4) pp. 823-828.

Miklos, D. B., Remy, C., Jekel, M., Linden, K. G., Drewes, J. E. and Hübner, U. (2018) 'Evaluation of advanced oxidation processes for water and wastewater treatment–A critical review.' *Water Research*, 139, pp.118-131.

Minear, R. A. (2017) 'Disinfection By-Products in Water Treatment The Chemistry of Their Formation and Control.' Routledge.

Minteer, S. D. (2006) 'Microfluidic techniques: reviews and protocols.' *Springer Science & Business Media*, 321.

Misra, N., Tiwari, B., Raghavarao, K. and Cullen, P. (2011) 'Nonthermal plasma inactivation of food-borne pathogens.' *Food Engineering Reviews*, 3(3-4) pp. 159-170.

Mizuno, A. (2007) 'Industrial applications of atmospheric non-thermal plasma in environmental remediation.' *Plasma Physics and Controlled Fusion*, 49(5A) p. A1.

Monegro, A. F. and Regunath, H. (2018) 'Hospital acquired infections.' StatPearls Publishing.

Montie, T. C., Kelly-Wintenberg, K. and Roth, J. R. (2000) 'An overview of research using the one atmosphere uniform glow discharge plasma (OAUGDP) for sterilization of surfaces and materials.' *IEEE Transactions on plasma science*, 28(1) pp. 41-50.

Mora-Rodríguez, J., Delgado-Galván, X., Ortiz-Medel, J., Ramos, H. M., Fuertes-Miquel, V. S. and López-Jiménez, P. A. (2015) 'Pathogen intrusion flows in water distribution systems: According to orifice equations.' *Journal of Water Supply: Research and Technology-Aqua*, 64(8) pp. 857-869.

Moreau, M., Orange, N. and Feuilloley, M. (2008) 'Non-thermal plasma technologies: new tools for bio-decontamination.' *Biotechnology advances*, 26(6) pp. 610-617.

Moussa, D. T., El-Naas, M. H., Nasser, M. and Al-Marri, M. J. (2017) 'A comprehensive review of electrocoagulation for water treatment: Potentials and challenges.' *Journal of environmental management*, 186 pp. 24-41.

Na, L., Jie, L., Yan, W. and Sato, M. (2012) 'Treatment of dye wastewater by using a hybrid gas/liquid pulsed discharge plasma reactor.' *Plasma Science and Technology*, 14(2) p. 162.

NCBI (National Center for Biotechnology Information), 2015. Basic local alignment search tool (BLAST). [Software]. [Accessed 07 July 2019]

Nawaz, M. S. and Ahsan, M. (2014) 'Comparison of physico-chemical, advanced oxidation and biological techniques for the textile wastewater treatment.' *Alexandria Engineering Journal*, 53(3) pp. 717-722.

Naze, F., Jouen, E., Randriamahazo, R., Simac, C., Laurent, P., Blériot, A., Chiroleu, F., Gagnevin, L., et al. (2010) 'Pseudomonas aeruginosa outbreak linked to mineral water bottles in a neonatal intensive care unit: fast typing by use of high-resolution melting analysis of a variable-number tandem-repeat locus.' *Journal of clinical microbiology*, 48(9) pp. 3146-3152.

Nguyen, T., Roddick, F. A. and Fan, L. (2012) 'Biofouling of water treatment membranes: a review of the underlying causes, monitoring techniques and control measures.' *Membranes*, 2(4) pp. 804-840.

Nikiforov, A., Deng, X., Xiong, Q., Cvelbar, U., DeGeyter, N., Morent, R. and Leys, C. (2016) 'Non-thermal plasma technology for the development of antimicrobial surfaces: a review.' *Journal of Physics D: Applied Physics*, 49(20) p. 204002.

Nikiforov, A. Y. (2009) 'An application of AC glow discharge stabilized by fast air flow for water treatment.' *IEEE Transactions on Plasma Science*, 37(6) pp. 872-876.

Nikitenko, S., Venault, L. and Moisy, P. (2004) 'Scavenging of OH radicals produced from H2O sonolysis with nitrate ions.' *Ultrasonics Sonochemistry*, 11(3-4) pp. 139-142.

Nishiyama, H., Nagai, R., Niinuma, K. and Takana, H. (2013) 'Characterization of DBD multiple bubble jets for methylene blue decolorization.' *Journal of Fluid Science and Technology*, 8(1) pp. 65-74.

Oehrlein, G. S. and Hamaguchi, S. (2018) 'Foundations of low-temperature plasma enhanced materials synthesis and etching.' *Plasma Sources Science and Technology*, 27(2) p. 023001.

Ognier, S., Iya-Sou, D., Fourmond, C. and Cavadias, S. (2009) 'Analysis of mechanisms at the plasma–liquid interface in a gas–liquid discharge reactor used for treatment of polluted water.' *Plasma Chemistry and Plasma Processing*, 29(4) pp. 261-273.

Ohtsu, Y. and Fujita, H. (2004) 'Influences of gap distance on plasma characteristics in narrow gap capacitively coupled radio-frequency discharge.' *Japanese journal of applied physics*, 43(2R) p. 795.

Olabanji, O. T. and Bradley, J. W. (2011) 'The development and analysis of plasma microfluidic devices.' *Surface and Coatings Technology*, 205 pp. S516-S519.

Oliveira, L., Gonçalves, M., Guerreiro, M., Ramalho, T., Fabris, J., Pereira, M. and Sapag, K. (2007) 'A new catalyst material based on niobia/iron oxide composite on the oxidation of organic contaminants in water via heterogeneous Fenton mechanisms.' *Applied Catalysis A: General*, 316(1) pp. 117-124.

Oller, I., Malato, S. and Sánchez-Pérez, J. (2011) 'Combination of advanced oxidation processes and biological treatments for wastewater decontamination—a review.' *Science of the total environment*, 409(20) pp. 4141-4166.

O'Neill, J. (2018) 'Tackling drug-resistant infections globally: Final report and recommendations. 2016.' HM Government and Welcome Trust: UK.

Oturan, M. A. and Aaron, J. J. (2014) 'Advanced oxidation processes in water/wastewater treatment: principles and applications. A review.' *Critical Reviews in Environmental Science and Technology*, 44(23) pp. 2577-2641.

Pai, K., Timmons, C., Roehm, K. D., Ngo, A., Narayanan, S. S., Ramachandran, A., Jacob, J. D., Ma, L. M., and Madihally, S.V., (2018) 'Investigation of the roles of plasma species generated by surface dielectric barrier discharge.' *Scientific reports*, 8(1) p. 16674.

Parkansky, N., Vegerhof, A., Alterkop, B. A., Berkh, O. and Boxman, R. L. (2012) 'Submerged arc breakdown of methylene blue in aqueous solutions.' *Plasma Chemistry and Plasma Processing*, 32(5) pp. 933-947.

Parkansky, N., Simon, E. F., Alterkop, B. A., Boxman, R. L. and Berkh, O. (2013) 'Decomposition of dissolved methylene blue in water using a submerged arc between titanium electrodes.' *Plasma Chemistry and Plasma Processing*, 33(5) pp. 907-919.

HC. (2018) UK Progress on Reducing Nitrate Pollution. House of Commons.

Peng, P., Chen, P., Schiappacasse, C., Zhou, N., Anderson, E., Chen, D., Liu, J., Cheng, Y., Hatzenbeller, R., Addy, M. and Zhang, Y., (2018a) 'A review on the non-thermal plasma-assisted ammonia synthesis technologies.' *Journal of Cleaner Production*, 177 pp. 597-609.

Peng, P., Chen, P., Addy, M., Cheng, Y., Zhang, Y., Anderson, E., Zhou, N., Schiappacasse, C., Hatzenbeller, R., Fan, L. and Liu, S., (2018b) 'In situ plasma-assisted atmospheric nitrogen fixation using water and spray-type jet plasma.' *Chemical communications*, 54(23) pp. 2886-2889.

Percival, S. L., Suleman, L., Vuotto, C. and Donelli, G. (2015) 'Healthcare-associated infections, medical devices and biofilms: risk, tolerance and control.' *Journal of medical microbiology*, 64(4) pp. 323-334.

Pestrak, M.J., Chaney, S.B., Eggleston, H.C., Dellos-Nolan, S., Dixit, S., Mathew-Steiner, S.S., Roy, S., Parsek, M.R., Sen, C.K. and Wozniak, D.J., (2018) 'Pseudomonas aeruginosa rugose small-colony variants evade host clearance, are hyper-inflammatory, and persist in multiple host environments.' *PLoS pathogens*, 14(2), p.e1006842.

PHE (2016) Voluntary surveillance of bacteraemia caused by Pseudomonas spp. and Stenotrophomonas spp. in England: 2008-2015. 32, UK.

PHE. (2018) Laboratory surveillance of Pseudomonas and Stenotrophomonas spp bacteraemia in England, Wales and Northern Ireland: 2017.

Plowman, R., Graves, N., Griffin, M., Roberts, J., Swan, A., Cookson, B. and Taylor, L. (2001) 'The rate and cost of hospital-acquired infections occurring in patients admitted to selected specialties of a district general hospital in England and the national burden imposed.' *Journal of hospital infection*, 47(3) pp. 198-209.

Pollard, S. (2016) Risk management for water and wastewater utilities. Iwa publishing.

Potocký, Š., Saito, N. and Takai, O. (2009) 'Needle electrode erosion in water plasma discharge.' *Thin Solid Films*, 518(3) pp. 918-923.

Proctor, R.A., Von Eiff, C., Kahl, B.C., Becker, K., McNamara, P., Herrmann, M. and Peters, G., (2006) 'Small colony variants: a pathogenic form of bacteria that facilitates persistent and recurrent infections.' *Nature Reviews Microbiology*, 4(4), pp.295-305.

Purevdorj, D., Igura, N., Ariyada, O. and Hayakawa, I. (2003) 'Effect of feed gas composition of gas discharge plasmas on Bacillus pumilus spore mortality.' *Letters in applied microbiology*, 37(1) pp. 31-34.

Rajasulochana, P. and Preethy, V. (2016) 'Comparison on efficiency of various techniques in treatment of waste and sewage water–A comprehensive review.' *Resource-Efficient Technologies*, 2(4) pp. 175-184.

Ramamurthy, T., Ghosh, A., Pazhani, G.P. and Shinoda, S., (2014) 'Current perspectives on viable but non-culturable (VBNC) pathogenic bacteria.' *Frontiers in public health*, 2, p.103.

Rashmei, Z., Bornasi, H. and Ghoranneviss, M. (2016) 'Evaluation of treatment and disinfection of water using cold atmospheric plasma.' *Journal of water and health*, 14(4) pp. 609-616.

Ratola, N., Cincinelli, A., Alves, A. and Katsoyiannis, A. (2012) 'Occurrence of organic microcontaminants in the wastewater treatment process. A mini review.' *Journal of Hazardous Materials*, 239 pp. 1-18.

Reddy, P. M. K., Sk, M. and Ch, S. (2014) 'Mineralization of aqueous organic pollutants using a catalytic plasma reactor.' *Indian Journal of Chemistry: A*, 53(4-5).

Reddy, P. M. K., Raju, B. R., Karuppiah, J., Reddy, E. L. and Subrahmanyam, C. (2013) 'Degradation and mineralization of methylene blue by dielectric barrier discharge non-thermal plasma reactor.' *Chemical Engineering Journal*, 217 pp. 41-47.

Ren, K., Zhou, J. and Wu, H. (2013) 'Materials for microfluidic chip fabrication.' *Accounts of chemical research*, 46(11) pp. 2396-2406.

Richardson, S. D. (2009) 'Water analysis: emerging contaminants and current issues.' *Analytical chemistry*, 81(12) pp. 4645-4677.

Richmonds, C., Witzke, M., Bartling, B., Lee, S. W., Wainright, J., Liu, C. C. and Sankaran, R. M. (2011) 'Electron-transfer reactions at the plasma–liquid interface.' *Journal of the American Chemical Society*, 133(44) pp. 17582-17585.

Riché, E., Carrié, A., Andin, N. and Mabic, S. (2006) 'High-purity water and pH.' *American Laboratory*, 38(13) p. 22.

Rijnaarts, H. H., Norde, W., Bouwer, E. J., Lyklema, J. and Zehnder, A. J. (1993) 'Bacterial adhesion under static and dynamic conditions.' *Appl. Environ. Microbiol.*, 59(10) pp. 3255-3265.

Rizzo, L., Manaia, C., Merlin, C., Schwartz, T., Dagot, C., Ploy, M., Michael, I. and Fatta-Kassinos, D. (2013) 'Urban wastewater treatment plants as hotspots for antibiotic resistant bacteria and genes spread into the environment: a review.' *Science of the total environment*, 447 pp. 345-360.

Robertson, J. and Oda, A. (1983) 'Combined application of ozone and chlorine or chloramine to reduce production of chlorinated organics in drinking water disinfection.', pp. 79-93.

Robinson, T., McMullan, G., Marchant, R. and Nigam, P. (2001) 'Remediation of dyes in textile effluent: a critical review on current treatment technologies with a proposed alternative.' *Bioresource technology*, 77(3) pp. 247-255.

Roelofs, S. H., van den Berg, A. and Odijk, M. (2015) 'Microfluidic desalination techniques and their potential applications.' *Lab on a Chip*, 15(17) pp. 3428-3438.

Romat, H., Zastawny, H., Chang, J. and Karpel Leitner, N. (2004) 'Pulsed arc discharges for water treatment and disinfection.' *Taylor & Francis*, 178, pp. 325-330.

Rosaguti, N., Fletcher, D. and Haynes, B. (2004) 'Laminar flow in a periodic serpentine channel.' *Proc. 15th Australasian Fluid Mechanics Conference*.

Ruma, Hosseini, S., Yoshihara, K., Akiyama, M., Sakugawa, T., Lukeš, P. and Akiyama, H. (2014) 'Properties of water surface discharge at different pulse repetition rates.' *Journal of Applied Physics*, 116(12) p. 123304.

Rumbach, P., Bartels, D. M., Sankaran, R. M. and Go, D. B. (2015a) 'The solvation of electrons by an atmospheric-pressure plasma.' *Nature communications*, 6 p. 7248.

Rumbach, P., Bartels, D. M., Sankaran, R. M. and Go, D. B. (2015b) 'The effect of air on solvated electron chemistry at a plasma/liquid interface.' *Journal of Physics D: Applied Physics*, 48(42) p. 424001.

Sadekuzzaman, M., Yang, S., Mizan, M. and Ha, S. (2015) 'Current and recent advanced strategies for combating biofilms.' *Comprehensive Reviews in Food Science and Food Safety*, 14(4) pp. 491-509.

Sala-Comorera, L., Blanch, A. R., Vilaró, C., Galofré, B. and García-Aljaro, C. (2016) 'Pseudomonas-related populations associated with reverse osmosis in drinking water treatment.' *Journal of environmental management*, 182 pp. 335-341.

Samukawa, S., Hori, M., Rauf, S., Tachibana, K., Bruggeman, P., Kroesen, G., Whitehead, J. C., Murphy, A. B., Gutsol, A.F., Starikovskaia, S. and Kortshagen, U., (2012) 'The 2012 plasma roadmap.' *Journal of Physics D: Applied Physics*, 45(25) p. 253001.

Sanaei, N. and Ayan, H., (2015) 'Bactericidal efficacy of dielectric barrier discharge plasma on methicillin-resistant Staphylococcus aureus and Escherichia coli in planktonic phase and colonies in vitro.' *Plasma Medicine*, 5(1).

Sanchez-Vizuete, P., Orgaz, B., Aymerich, S., Le Coq, D. and Briandet, R. (2015) 'Pathogens protection against the action of disinfectants in multispecies biofilms.' *Frontiers in microbiology*, 6 p. 705.

Sandegren, L. (2014) 'Selection of antibiotic resistance at very low antibiotic concentrations.' *Upsala journal of medical sciences*, 119(2) pp. 103-107.

Sano, N., Yamamoto, D., Kanki, T. and Toyoda, A. (2003) 'Decomposition of phenol in water by a cylindrical wetted-wall reactor using direct contact of gas corona discharge.' *Industrial & engineering chemistry research*, 42(22) pp. 5423-5428.

Sano, N., Kawashima, T., Fujikawa, J., Fujimoto, T., Kitai, T., Kanki, T. and Toyoda, A. (2002) 'Decomposition of organic compounds in water by direct contact of gas corona discharge: influence of discharge conditions.' *Industrial & engineering chemistry research*, 41(24) pp. 5906-5911.

Sarangapani, C., Misra, N., Milosavljevic, V., Bourke, P., O'Regan, F. and Cullen, P. (2016) 'Pesticide degradation in water using atmospheric air cold plasma.' *Journal of Water Process Engineering*, 9 pp. 225-232.

Sato, M. (2000) 'Pulsed discharge processing of organic contaminants in water.' *A monthly publication of The Japan Society of Applied Physics*, 69(3) pp. 301-304.

Sato, T., Kambe, M. and Nishiyama, H. (2005) 'Analysis of a methanol decomposition process by a nonthermal plasma flow.' *JSME International Journal Series B Fluids and Thermal Engineering*, 48(3) pp. 432-439.

Schelcher, G., Guyon, C., Ognier, S., Cavadias, S., Martinez, E., Taniga, V., Malaquin, L., Tabeling, P., and Tatoulian, M., (2014) 'Cyclic olefin copolymer plasma millireactors.' *Lab on a Chip*, 14(16) pp. 3037-3042.

Scheuble, N., Iles, A., Wootton, R. C., Windhab, E. J., Fischer, P. and Elvira, K. S. (2017) 'Microfluidic Technique for the Simultaneous Quantification of Emulsion Instabilities and Lipid Digestion Kinetics.' *Analytical chemistry*, 89(17) pp. 9116-9123.

Schmidt, M., Hahn, V., Altrock, B., Gerling, T., Gerber, I. C., Weltmann, K. D. and von Woedtke, T. (2019) 'Plasma-Activation of Larger Liquid Volumes by an Inductively-Limited Discharge for Antimicrobial Purposes.' *Applied Sciences*, 9(10) p. 2150.

Schmidt, T. C. (2018) 'Recent trends in water analysis triggering future monitoring of organic micropollutants.' *Analytical and bioanalytical chemistry*, 410(17) pp. 3933-3941.

Schoenbach, K. H. and Becker, K. (2016a) '20 years of microplasma research: a status report.' *The European Physical Journal D*, 70(2) pp. 1-22.

Schoenbach, K. H. and Becker, K. (2016b) '20 years of microplasma research: a status report.' *The European Physical Journal D*, 70(2) p. 29.

Scholtz, V., Pazlarova, J., Souskova, H., Khun, J. and Julak, J. (2015) 'Nonthermal plasma—a tool for decontamination and disinfection.' *Biotechnology advances*, 33(6) pp. 1108-1119.

Schwering, M., Song, J., Louie, M., Turner, R. J. and Ceri, H. (2013) 'Multi-species biofilms defined from drinking water microorganisms provide increased protection against chlorine disinfection.' *Biofouling*, 29(8) pp. 917-928.

Sehar, S. and Naz, I. (2016) 'Role of the biofilms in wastewater treatment.' *Microbial biofilms-importance and applications*, pp. 121-144.

Shah, A. D. and Mitch, W. A. (2011) 'Halonitroalkanes, halonitriles, haloamides, and N-nitrosamines: a critical review of nitrogenous disinfection byproduct formation pathways.' *Environmental Science & Technology*, 46(1) pp. 119-131.

Shahriari, A., Kim, M. M., Zamani, S., Phillip, N., Nasouri, B. and Hidrovo, C. H. (2016) 'Flow regime mapping of high inertial gas–liquid droplet microflows in flow-focusing geometries.' *Microfluidics and Nanofluidics*, 20(1) p. 20.

Shaw, E., Gavaldà, L., Càmara, J., Gasull, R., Gallego, S., Tubau, F., Granada, R., Ciercoles, P., et al. (2018) 'Control of endemic multidrug-resistant Gram-negative bacteria after removal of sinks and implementing a new water-safe policy in an intensive care unit.' *Journal of Hospital Infection*, 98(3) pp. 275-281.

Shaw, P., Kumar, N., Kwak, H. S., Park, J. H., Uhm, H. S., Bogaerts, A., Choi, E. H. and Attri, P. (2018) 'Bacterial inactivation by plasma treated water enhanced by reactive nitrogen species.' *Scientific reports*, 8(1) p. 11268.

Shaw, P., Kumar, N., Kwak, H. S., Park, J. H., Uhm, H. S., Bogaerts, A., Choi, E. H. and Attri, P. (2018) 'Bacterial inactivation by plasma treated water enhanced by reactive nitrogen species.' *Scientific reports*, 8(1) p. 11268.

Shen, J., Tian, Y., Li, Y., Ma, R., Zhang, Q., Zhang, J. and Fang, J. (2016) 'Bactericidal Effects against S. aureus and Physicochemical Properties of Plasma Activated Water stored at different temperatures.' *Scientific reports*, 6 p. 28505.

Shibata, T. and Nishiyama, H. (2012) 'Decomposition of methylene blue in water using mist flow plasma reactor.' 6.

Shields IV, C. W., Reyes, C. D. and López, G. P. (2015) 'Microfluidic cell sorting: a review of the advances in the separation of cells from debulking to rare cell isolation.' *Lab on a Chip*, 15(5) pp. 1230-1249.

Shimizu, K., Masamura, N. and Blajan, M. (2013) Water purification by using microplasma treatment. Vol. 441: IOP Publishing.

Shirafuji, T., Ishida, Y., Nomura, A., Hayashi, Y. and Goto, M. (2017) 'Reaction mechanisms of methylene-blue degradation in three-dimensionally integrated micro-solution plasma.' *Japanese Journal of Applied Physics*, 56(6S2) p. 06HF02.

Shirke, A., Li, S., Ebeling, D., Carter, M. T. and Stetter, J. R. (2014) 'Integrated ozone microreactor technology for water treatment.' *ECS Transactions*, 58(35) pp. 11-20.

Shu, H. Y. and Chang, M. C. (2005) 'Decolorization effects of six azo dyes by O3, UV/O3 and UV/H2O2 processes.' *Dyes and Pigments*, 65(1) pp. 25-31.

Simazaki, D., Kubota, R., Suzuki, T., Akiba, M., Nishimura, T. and Kunikane, S. (2015) 'Occurrence of selected pharmaceuticals at drinking water purification plants in Japan and implications for human health.' *Water Research*, 76 pp. 187-200.

Simoes, L. C. and Simões, M. (2013) 'Biofilms in drinking water: problems and solutions.' *Rsc Advances*, 3(8) pp. 2520-2533.

Simon, A., Krawtschenko, O., Reiffert, S.-M., Exner, M., Trautmann, M. and Engelhart, S. (2008) 'Outbreaks of Pseudomonas aeruginosa in pediatric patients–clinical aspects, risk factors and management.' *Journal of Pediatric Infectious Diseases*, 3(4) pp. 249-269.

Simon, J., Wiese, J. and Steinmetz, H. (2006) 'A comparison of continuous flow and sequencing batch reactor plants concerning integrated operation of sewer systems and wastewater treatment plants.' *Water science and technology*, 54(11-12) pp. 241-248.

Singh, R. K., Philip, L. and Ramanujam, S. (2017) 'Removal of 2, 4-dichlorophenoxyacetic acid in aqueous solution by pulsed corona discharge treatment: effect of different water constituents, degradation pathway and toxicity assay.' *Chemosphere*, 184 pp. 207-214.

Singh, R. K., Philip, L. and Ramanujam, S. (2019) 'Continuous flow pulse corona discharge reactor for the tertiary treatment of drinking water: Insights on disinfection and emerging contaminants removal.' *Chemical Engineering Journal*, 355 pp. 269-278.

Singh, R. K., Babu, V., Philip, L. and Ramanujam, S. (2016) 'Applicability of pulsed power technique for the degradation of methylene blue.' *Journal of Water Process Engineering*, 11 pp. 118-129.

Soler-Arango, J., Figoli, C., Muraca, G., Bosch, A. and Brelles-Mariño, G. (2019) 'The Pseudomonas aeruginosa biofilm matrix and cells are drastically impacted by gas discharge plasma treatment: A comprehensive model explaining plasma-mediated biofilm eradication.' *PloS one*, 14(6) p. e0216817.

Son, G., Lee, H., Gu, J. E. and Lee, S. (2015) 'Decoloration of methylene blue hydrate by submerged plasma irradiation process.' *Desalination and Water Treatment*, 54(4-5) pp. 1445-1451.

Son, H. S., Ahammad, A., Rahman, M., Noh, K.-M. and Lee, J. J. (2011) 'Effect of Nitrite and Nitrate as the Source of OH Radical in the O 3/UV Process with or without Benzene.' *Bulletin of the Korean Chemical Society*, 32(spc8) pp. 3039-3044.

Soni, M., Sharma, A. K., Srivastava, J. K. and Yadav, J. S. (2012) 'Adsorptive removal of methylene blue dye from an aqueous solution using water hyacinth root powder as a low cost adsorbent.' *International Journal of Chemical Sciences and Applications*, 3(3) pp. 338-345.

Sousa, J. C., Ribeiro, A. R., Barbosa, M. O., Pereira, M. F. R. and Silva, A. M. (2018) 'A review on environmental monitoring of water organic pollutants identified by EU guidelines.' *Journal of hazardous materials*, 344 pp. 146-162.

Starikovskiy, A., Yang, Y., Cho, Y. I. and Fridman, A. (2011) 'Non-equilibrium plasma in liquid water: dynamics of generation and quenching.' *Plasma Sources Science and Technology*, 20(2) p. 024003.

Stauss, S., Ishii, C., Pai, D. Z., Urabe, K. and Terashima, K. (2014) 'Diamondoid synthesis in atmospheric pressure adamantane–argon–methane–hydrogen mixtures using a continuous flow plasma microreactor.' *Plasma Sources Science and Technology*, 23(3) p. 035016.

Steed, K. A. and Falkinham, J. O. (2006) 'Effect of growth in biofilms on chlorine susceptibility of Mycobacterium avium and Mycobacterium intracellulare.' Appl. Environ. Microbiol., 72(6) pp. 4007-4011.

Stiefel, P., Schmidt-Emrich, S., Maniura-Weber, K. and Ren, Q., (2015) 'Critical aspects of using bacterial cell viability assays with the fluorophores SYTO9 and propidium iodide.' *BMC microbiology*, 15(1), p.36.

Stone, P. W. (2009) 'Economic burden of healthcare-associated infections: an American perspective.' *Expert review of pharmacoeconomics & outcomes research*, 9(5) pp. 417-422.

Stratton, G. R., Bellona, C. L., Dai, F., Holsen, T. M. and Thagard, S. M. (2015) 'Plasma-based water treatment: Conception and application of a new general principle for reactor design.' *Chemical Engineering Journal*, 273 pp. 543-550.

Stuart, M., Lapworth, D., Crane, E. and Hart, A. (2012) 'Review of risk from potential emerging contaminants in UK groundwater.' *Science of the Total Environment*, 416 pp. 1-21.

Sun, G. R., He, J. B. and Pittman Jr, C. U. (2000) 'Destruction of halogenated hydrocarbons with solvated electrons in the presence of water.' *Chemosphere*, 41(6) pp. 907-916.

Sun, P., Wu, H., Bai, N., Zhou, H., Wang, R., Feng, H., Zhu, W., Zhang, J., and Fang, J., (2012) 'Inactivation of Bacillus subtilis Spores in Water by a Direct-Current, Cold Atmospheric-Pressure Air Plasma Microjet.' *Plasma Processes and Polymers*, 9(2) pp. 157-164.

Sun, P. P., Araud, E. M., Huang, C., Shen, Y., Monroy, G. L., Zhong, S., Tong, Z., Boppart, S. A., Eden, J.G. and Nguyen, T.H., (2018) 'Disintegration of simulated drinking water biofilms with arrays of microchannel plasma jets.' *npj Biofilms and Microbiomes*, 4(1) p. 24.

Sun, Y., Zhang, Z. and Wang, S. (2018) 'Study on the bactericidal mechanism of atmospheric-pressure low-temperature plasma against Escherichia coli and its application in fresh-cut cucumbers.' *Molecules*, 23(4) p. 975.

Sunka, P., Babický, V., Clupek, M., Lukes, P., Simek, M., Schmidt, J. and Cernak, M. (1999) 'Generation of chemically active species by electrical discharges in water.' *Plasma Sources Science and Technology*, 8(2) p. 258.

Surowsky, B., Schlüter, O. and Knorr, D. (2015) 'Interactions of non-thermal atmospheric pressure plasma with solid and liquid food systems: a review.' *Food Engineering Reviews*, 7(2) pp. 82-108.

Suryawanshi, P. L., Gumfekar, S. P., Bhanvase, B. A., Sonawane, S. H. and Pimplapure, M. S. (2018) 'A review on microreactors: Reactor fabrication, design, and cutting-edge applications.' *Chemical Engineering Science*, 189 pp. 431-448.

Swinehart, D. (1962) 'The beer-lambert law.' *Journal of chemical education*, 39(7) p. 333.

Szabó, C., Ischiropoulos, H. and Radi, R. (2007) 'Peroxynitrite: biochemistry, pathophysiology and development of therapeutics.' *Nature reviews Drug discovery*, 6(8) p. 662.

Tachibana, K., Takekata, Y., Mizumoto, Y., Motomura, H. and Jinno, M. (2011) 'Analysis of a pulsed discharge within single bubbles in water under synchronized conditions.' *Plasma Sources Science and Technology*, 20(3) p. 034005.

Taitel, Y. and Dukler, A. (1976) 'A model for predicting flow regime transitions in horizontal and near horizontal gas-liquid flow.' *AIChE Journal*, 22(1) pp. 47-55.

Taherzadeh, D., Picioreanu, C. and Horn, H. (2012) 'Mass transfer enhancement in moving biofilm structures.' *Biophysical journal*, 102(7) pp. 1483-1492.

Tampieri, F., Durighello, A., Biondo, O., Gąsior, M., Knyś, A., Marotta, E. and Paradisi, C. (2019) 'Kinetics and products of air plasma induced oxidation in water of imidacloprid and

thiamethoxam treated individually and in mixture.' *Plasma Chemistry and Plasma Processing*, 39(3) pp. 545-559.

Tang, M., Wang, G., Kong, S. K. and Ho, H. P. (2016) 'A review of biomedical centrifugal microfluidic platforms.' *Micromachines*, 7(2) p. 26.

Tang, Q., Lin, S., Jiang, W. and Lim, T. (2009) 'Gas phase dielectric barrier discharge induced reactive species degradation of 2, 4-dinitrophenol.' *Chemical Engineering Journal*, 153(1-3) pp. 94-100.

Tao, S., Kaihua, L., Cheng, Z., Ping, Y., Shichang, Z. and Ruzheng, P. (2008) 'Experimental study on repetitive unipolar nanosecond-pulse dielectric barrier discharge in air at atmospheric pressure.' *Journal of Physics D: Applied Physics*, 41(21) p. 215203.

Tarabová, B., Lukeš, P., Janda, M., Hensel, K., Šikurová, L. and Machala, Z. (2018) 'Specificity of detection methods of nitrites and ozone in aqueous solutions activated by air plasma.' *Plasma Processes and Polymers*, 15(6) p. 1800030.

Tatoulian, M., Ognier, S. and Zhang, M. (2017) Diphasic gas/liquid plasma reactor. Google Patents.

Taylor, P. R. and Pirzada, S. A. (1994) 'Thermal plasma processing of materials: a review.' *Advanced Performance Materials*, 1(1) pp. 35-50.

Tetala, K. K. and Vijayalakshmi, M. (2016) 'A review on recent developments for biomolecule separation at analytical scale using microfluidic devices.' *Analytica chimica acta*, 906 pp. 7-21.

Thagard, S. M., Stratton, G. R., Dai, F., Bellona, C. L., Holsen, T. M., Bohl, D. G., Paek, E. and Dickenson, E. R. (2016) 'Plasma-based water treatment: development of a general mechanistic model to estimate the treatability of different types of contaminants.' *Journal of Physics D: Applied Physics*, 50(1) p. 014003.

Thirumdas, R., Sarangapani, C. and Annapure, U. S. (2015) 'Cold plasma: a novel non-thermal technology for food processing.' *Food biophysics*, 10(1) pp. 1-11.

Thirumdas, R., Kothakota, A., Kiran, K. C. S. S., Pandiselvam, R. and Prakash, V. U. B. (2017) 'Exploitation of Cold Plasma Technology in Agriculture.' *Advances in Research*, 12(4) pp. 1-7.

Thirumdas, R., Kothakota, A., Annapure, U., Siliveru, K., Blundell, R., Gatt, R. and Valdramidis, V. P. (2018) 'Plasma activated water (PAW): chemistry, physico-chemical properties, applications in food and agriculture.' *Trends in Food Science & Technology*, 77 pp. 21-31.

Tian, Y., Ma, R., Zhang, Q., Feng, H., Liang, Y., Zhang, J. and Fang, J. (2015) 'Assessment of the physicochemical properties and biological effects of water activated by non-thermal plasma above and beneath the water surface.' Plasma Processes and Polymers, 12(5) pp. 439-449.

Tiggelaar, R. M., Benito-López, F., Hermes, D. C., Rathgen, H., Egberink, R. J., Mugele, F. G., Reinhoudt, D. N., van den Berg, A., Verboom, W. and Gardeniers, H.J., (2007) 'Fabrication, mechanical testing and application of high-pressure glass microreactor chips.' *Chemical Engineering Journal*, 131(1-3) pp. 163-170.

Tirumala, R., Benard, N., Moreau, E., Fenot, M., Lalizel, G. and Dorignac, E. (2014) 'Temperature characterization of dielectric barrier discharge actuators: influence of electrical and geometric parameters.' *Journal of Physics D: Applied Physics*, 47(25) p. 255203.

Toepke, M. W. and Beebe, D. J. (2006) 'PDMS absorption of small molecules and consequences in microfluidic applications.' *Lab on a Chip*, 6(12) pp. 1484-1486.

Tuson, H. H. and Weibel, D. B. (2013) 'Bacteria–surface interactions.' *Soft matter*, 9(17) pp. 4368-4380.

Vanraes, P. (2016) Electrical discharge as water treatment technology for micropollutant decomposition. Ghent University.

Vanraes, P., Nikiforov, A. Y. and Leys, C. (2016) 'Electrical discharge in water treatment technology for micropollutant decomposition.' *Plasma Science and Technology—Progress in Physical States and Chemical Reactions*, pp. 429-478.

Vatansever, F., de Melo, W. C., Avci, P., Vecchio, D., Sadasivam, M., Gupta, A., Chandran, R., Karimi, M., Parizotto, N.A., Yin, R. and Tegos, G.P., (2013) 'Antimicrobial strategies centered around reactive oxygen species–bactericidal antibiotics, photodynamic therapy, and beyond.' *FEMS microbiology reviews*, 37(6) pp. 955-989.

Vaze, N. D., Park, S., Brooks, A. D., Fridman, A. and Joshi, S. G. (2017) 'Involvement of multiple stressors induced by non-thermal plasma-charged aerosols during inactivation of airborne bacteria.' *PloS one*, 12(2) p. e0171434.

Verlicchi, P., Barcelò, D., Pavlovic, D. M., Papa, M., Petrovic, M., Voulvolis, N. and Zambello, E. (2017) 'The impact and risks of micropollutants in the environment.' Innovative Wastewater Treatment & Resource Recovery Technologies: Impacts on Energy, Economy and Environment.

Virkutyte, J., Varma, R. S. and Jegatheesan, V. (2010) Treatment of micropollutants in water and wastewater. IWA Publishing.

Walker, J., Jhutty, A., Parks, S., Willis, C., Copley, V., Turton, J., Hoffman, P. and Bennett, A. (2014) 'Investigation of healthcare-acquired infections associated with Pseudomonas aeruginosa biofilms in taps in neonatal units in Northern Ireland.' *Journal of Hospital Infection*, 86(1) pp. 16-23.

Walker, J. and Moore, G. (2015) 'Pseudomonas aeruginosa in hospital water systems: biofilms, guidelines, and practicalities.' *Journal of Hospital Infection*, 89(4) pp. 324-327.

Wang, B., Dong, B., Xu, M., Chi, C. and Wang, C. (2017a) 'Degradation of methylene blue using double-chamber dielectric barrier discharge reactor under different carrier gases.' *Chemical Engineering Science*, 168 pp. 90-100.

Wang, B., Xu, M., Chi, C., Wang, C. and Meng, D. (2017b) 'Degradation of methyl orange using dielectric barrier discharge water falling film reactor.' *Journal of Advanced Oxidation Technologies*, 20(2).

Wang, H., Wang, N., Qian, J., Hu, L., Huang, P., Su, M., Yu, X., Fu, C., et al. (2017) 'Urinary antibiotics of pregnant women in Eastern China and cumulative health risk assessment.' *Environmental science & technology*, 51(6) pp. 3518-3525.

Wang, H., Wang, N., Wang, B., Zhao, Q., Fang, H., Fu, C., Tang, C., Jiang, F., Zhou, Y., Chen, Y. and Jiang, Q., (2016) 'Antibiotics in drinking water in Shanghai and their contribution to antibiotic exposure of school children.' *Environmental science & technology*, 50(5) pp. 2692-2699.

Wang, K. and Luo, G. (2017) 'Microflow extraction: A review of recent development.' *Chemical Engineering Science*, 169 pp. 18-33.

Wang, R., Kalchayanand, N., Schmidt, J. W. and Harhay, D. M. (2013) 'Mixed biofilm formation by Shiga toxin–producing Escherichia coli and Salmonella enterica serovar Typhimurium enhanced bacterial resistance to sanitization due to extracellular polymeric substances.' *Journal of food protection*, 76(9) pp. 1513-1522.

Wang, N., Zhang, X., Wang, Y., Yu, W. and Chan, H. L. (2014) 'Microfluidic reactors for photocatalytic water purification.' *Lab on a Chip*, 14(6) pp. 1074-1082.

Wang, Q., Tian, S. and Ning, P. (2013) 'Degradation mechanism of methylene blue in a heterogeneous Fenton-like reaction catalyzed by ferrocene.' *Industrial & Engineering Chemistry Research*, 53(2) pp. 643-649.

Wang, T., Sun, B. M., Xiao, H. P., Zeng, J. Y., Duan, E. P., Xin, J. and Li, C. (2012) 'Effect of reactor structure in DBD for nonthermal plasma processing of NO in N 2 at ambient temperature.' *Plasma Chemistry and Plasma Processing*, 32(6) pp. 1189-1201.

Watts, Associates, C. and Watts, C. (2007) 'Desk based review of current knowledge on pharmaceuticals in drinking water and estimation of potential levels.' Foundation for Water Research.

Wee, S. Y. and Aris, A. Z. (2017) 'Endocrine disrupting compounds in drinking water supply system and human health risk implication.' *Environment international*, 106 pp. 207-233.

Wengler, J., Ognier, S., Zhang, M., Levernier, E., Guyon, C., Ollivier, C., Fensterbank, L. and Tatoulian, M. (2018) 'Microfluidic chips for plasma flow chemistry: application to controlled oxidative processes.' *Reaction Chemistry & Engineering*, 3(6) pp. 930-941.

WHO. (2004) Guidelines for drinking-water quality. Vol. 1. World Health Organization.

WHO. (2012) Unsafe drinking-water, sanitation and waste management. World Health Organization.

WHO. (2011) Health care-associated infections.

Wiegand, I., Hilpert, K. and Hancock, R. E. (2008) 'Agar and broth dilution methods to determine the minimal inhibitory concentration (MIC) of antimicrobial substances.' *Nature protocols*, 3(2) p. 163.

Wiegand, P. N., Nathwani, D., Wilcox, M., Stephens, J., Shelbaya, A. and Haider, S. (2012) 'Clinical and economic burden of Clostridium difficile infection in Europe: a systematic review of healthcare-facility-acquired infection.' *Journal of Hospital Infection*, 81(1) pp. 1-14.

Williams, K. L., Butoi, C. I. and Fisher, E. R. (2003) 'Mechanisms for deposition and etching in fluorosilane plasma processing of silicon.' *Journal of Vacuum Science & Technology A: Vacuum, Surfaces, and Films*, 21(5) pp. 1688-1701.

Wise, J. (2012) 'Three babies die in pseudomonas outbreak at Belfast neonatal unit.' *BMJ: British Medical Journal*, e592.

Wu, M. C., Liu, C. T., Chiang, C. Y., Lin, Y. J., Lin, Y. H., Chang, Y. W. and Wu, J. S. (2018) 'Inactivation Effect of Colletotrichum Gloeosporioides by Long-Lived Chemical Species Using Atmospheric-Pressure Corona Plasma-Activated Water.' *IEEE Transactions on Plasma Science*, 47(2) pp. 1100-1104.

Xi, C., Zhang, Y., Marrs, C. F., Ye, W., Simon, C., Foxman, B. and Nriagu, J. (2009) 'Prevalence of antibiotic resistance in drinking water treatment and distribution systems.' *Appl. Environ. Microbiol.,* 75(17) pp. 5714-5718.

Yagub, M. T., Sen, T. K., Afroze, S. and Ang, H. M. (2014) 'Dye and its removal from aqueous solution by adsorption: a review.' *Advances in colloid and interface science*, 209 pp. 172-184.

Yamanishi, Y., Sameshima, S., Kuriki, H., Sakuma, S. and Arai, F. (2013) Transportation of mono-dispersed micro-plasma bubble in microfluidic chip under atmospheric pressure. *IEEE*, pp. 1795-1798.

Yamatake, A. (2007) 'Water purification by atmoshperic DC/pulsed plasmas inside bubbles in water.' *International Journal of Plasma Environmental Science and Technology*, pp. 91-95.

Yamatake, A., Fletcher, J., Yasuoka, K. and Ishii, S. (2006a) 'Water treatment by fast oxygen radical flow with DC-driven microhollow cathode discharge.' *IEEE transactions on plasma science*, 34(4) pp. 1375-1381.

Yamatake, A., Angeloni, D. M., Dickson, S. E., Emelko, M. B., Yasuoka, K. and Chang, J.-S. (2006b) 'Characteristics of pulsed arc electrohydraulic discharge for eccentric electrode cylindrical reactor using phosphate-buffered saline water.' *Japanese journal of applied physics*, 45(10S) p. 8298.

Yang, C., Guangzhou, Q., Tengfei, L., Jiang, N. and Tiecheng, W. (2018) 'Review on reactive species in water treatment using electrical discharge plasma: formation, measurement, mechanisms and mass transfer.' *Plasma Science and Technology*, 20(10) p. 103001.

Yang, D. Z., Wang, W. C., Zhang, S., Tang, K., Liu, Z. J. and Wang, S. (2013) 'Multiple current peaks in room-temperature atmospheric pressure homogenous dielectric barrier discharge plasma excited by high-voltage tunable nanosecond pulse in air.' *Applied Physics Letters*, 102(19) p. 194102.

Yang, X., Bai, M. and Han, F. (2009) 'Treatment of phenol wastewater using hydroxyl radical produced by micro-gap discharge plasma technique.' *Water Environment Research*, 81(4) pp. 450-455.

Yang, X. E., Wu, X., Hao, H. l. and He, Z. l. (2008) 'Mechanisms and assessment of water eutrophication.' *Journal of Zhejiang University Science B*, 9(3) pp. 197-209.

Yanling, C., Yingkuan, W., Chen, P., Deng, S. and Ruan, R. (2014) 'Non-thermal plasma assisted polymer surface modification and synthesis: A review.' *International Journal of Agricultural and Biological Engineering*, 7(2) pp. 1-9.

Yano, T., Shimomura, N., Uchiyama, I., Fukawa, F., Teranishi, K. and Akiyama, H. (2009) 'Decolorization of indigo carmine solution using nanosecond pulsed power.' *IEEE Transactions on Dielectrics and Electrical Insulation*, 16(4).

Yin, H., Xiong, L., Jiang, B., Zheng, J. and Xue, Q. (2014) 'Non-thermal plasma technology for methylene blue decolorization in continuous and circulating system: kinetic model and reactor performance.' *Journal of Advanced Oxidation Technologies*, 17(2) pp. 265-280.

Ying, Z., Risheng, Y., Yuedong, M., Jiaxing, L., Jiang, Y. and Longwei, C. (2017) 'The degradation of oxadiazon by non-thermal plasma with a dielectric barrier configuration.' *Plasma Science and Technology*, 19(3) p. 034001.

Yingguang, C., Ping, Y., Xinpei, L., Zilan, X., Tao, Y., Qing, X. and Ziyong, S., (2011) 'Efficacy of atmospheric pressure plasma as an antibacterial agent against Enterococcus faecalis in vitro.' *Plasma Science and Technology*, 13(1), p.93.

Yoon, S. Y., Jeon, H., Yi, C., Park, S., Ryu, S. and Kim, S. B. (2018) 'Mutual Interaction between Plasma Characteristics and Liquid Properties in AC-driven Pin-to-Liquid Discharge.' *Scientific reports*, 8(1) p. 12037.

Yost, A. D. and Joshi, S. G. (2015) 'Atmospheric nonthermal plasma-treated PBS inactivates Escherichia coli by oxidative DNA damage.' *PloS one*, 10(10) p. e0139903.

Yuan, M. H., Watanabe, T. and Chang, C.-Y. (2010) 'DC water plasma at atmospheric pressure for the treatment of aqueous phenol.' *Environmental science & technology*, 44(12) pp. 4710-4715.

Yuan, X., Tang, J. and Duan, Y. (2011) 'Microplasma technology and its applications in analytical chemistry.' *Applied Spectroscopy Reviews*, 46(7) pp. 581-605.

Xia, H., Tang, Q., Song, J., Ye, J., Wu, H. and Zhang, H., (2017) 'A yigP mutant strain is a small colony variant of E. coli and shows pleiotropic antibiotic resistance.' *Canadian journal of microbiology*, 63(12), pp.961-969.

Zeng, J., Yang, B., Wang, X., Li, Z., Zhang, X. and Lei, L. (2015) 'Degradation of pharmaceutical contaminant ibuprofen in aqueous solution by cylindrical wetted-wall corona discharge.' Chemical Engineering Journal, 267 pp. 282-288.

Zhang, H., Ma, D., Qiu, R., Tang, Y. and Du, C. (2017) 'Non-thermal plasma technology for organic contaminated soil remediation: A review.' *Chemical Engineering Journal*, 313 pp. 157-170.

Zhang, J., Li, W., Chen, J., Qi, W., Wang, F. and Zhou, Y. (2018) 'Impact of biofilm formation and detachment on the transmission of bacterial antibiotic resistance in drinking water distribution systems.' *Chemosphere*, 203 pp. 368-380.

Zhang, M., Ognier, S., Touati, N., Hauner, I., Guyon, C., Binet, L. and Tatoulian, M. (2018) 'A plasma/liquid microreactor for radical reaction chemistry: An experimental and numerical investigation by EPR spin trapping.' *Plasma Processes and Polymers*, 15(6) p. 1700188.

Zhang, Q., Liang, Y., Feng, H., Ma, R., Tian, Y., Zhang, J. and Fang, J. (2013) 'A study of oxidative stress induced by non-thermal plasma-activated water for bacterial damage.' *Applied physics letters*, 102(20) p. 203701.

Zhang, X., Liu, D., Song, Y., Sun, Y. and Yang, S. Z. (2013) 'Atmospheric-pressure air microplasma jets in aqueous media for the inactivation of Pseudomonas fluorescens cells.' *Physics of Plasmas*, 20(5) p. 053501.

Zhang, X., Liu, D., Wang, H., Liu, L., Wang, S. and Yang, S. Z. (2012) 'Highly effective inactivation of Pseudomonas sp HB1 in water by atmospheric pressure microplasma jet array.' Plasma Chemistry and Plasma Processing, 32(5) pp. 949-957.

Zhang, Z., Bai, M., Bai, M., Yang, B. and Bai, X. (2006) 'Killing of red tide organisms in sea enclosure using hydroxyl radical-based micro-gap discharge.' *IEEE transactions on plasma science*, 34(6) pp. 2618-2623.

Zhang, Z., Xu, Z., Cheng, C., Wei, J., Lan, Y., Ni, G., Sun, Q., Qian, S., et al. (2017) 'Bactericidal effects of plasma induced reactive species in dielectric barrier gas–liquid discharge.' *Plasma Chemistry and Plasma Processing*, 37(2) pp. 415-431.

Zhao, Y., Wang, T., MacGregor, S., Wilson, M., Given, M. and Timoshkin, I. (2014) 'Investigation of plasma-induced methylene blue degradation using dielectric barrier discharge.'.

Zhou, R., Zhou, R., Prasad, K., Fang, Z., Speight, R., Bazaka, K. and Ostrikov, K. K. (2018) 'Cold atmospheric plasma activated water as a prospective disinfectant: the crucial role of peroxynitrite.' Green Chemistry, 20(23) pp. 5276-5284.

Zhou, R., Zhou, R., Wang, P., Luan, B., Zhang, X., Fang, Z., Xian, Y., Lu, X., Ostrikov, K. and Bazaka, K., (2019) 'Microplasma Bubbles: Reactive Vehicles for Biofilm Dispersal.' *ACS applied materials & interfaces*.

Ziuzina, D., Patil, S., Cullen, P., Keener, K. and Bourke, P. (2013) 'Atmospheric cold plasma inactivation of E scherichia coli in liquid media inside a sealed package.' *Journal of applied microbiology*, 114(3) pp. 778-787.

Ziuzina, D., Boehm, D., Patil, S., Cullen, P. and Bourke, P. (2015) 'Cold plasma inactivation of bacterial biofilms and reduction of quorum sensing regulated virulence factors.' *PLoS One*, 10(9) p. e0138209.